Supplementary File of "Evolutionary Many-Objective Optimization Based on Adversarial Decomposition"

Mengyuan Wu, Ke Li, Sam Kwong, *Fellow, IEEE*, and Qingfu Zhang, *Fellow, IEEE*

***Abstract*—The paper entitled "Evolutionary Many-Objective Optimization Based on Adversarial Decomposition" develops an adversarial decomposition method that leverages the complementary characteristics of two different scalarizing functions within a single paradigm. More specifically, we maintain two co-evolving populations simultaneously by using different scalarizing functions. In order to avoid allocating redundant computational resources to the same region of the Pareto front, we stably match these two co-evolving populations into one-one solution pairs according to their working regions upon the Pareto front. Then, each solution pair can at most contribute one principal mating parent during the mating selection process. Due to the page limits of the paper, we present some experimental studies in this supplementary file.**

V. Experimental Studies

D. Comparisons on DTLZ and WFG Test Problems under HV Metric with $\mathbf{z}^r = (1.1, \cdots, 1.1)^T$ and IGD Metric

The mean HV metric values with $\mathbf{z}^r = (1.1, \cdots, 1.1)^T$ of different algorithms on DTLZ and WFG test problems are given in Table VII and Table VIII. Generally speaking, the comparisons of HV metric values with $\mathbf{z}^r = (1.1, \cdots, 1.1)^T$ are similar to those with $\mathbf{z}^r = (2, \cdots, 2)^T$. Slight variances can be noticed on some test problems. For example, when using $\mathbf{z}^r = (1.1, \cdots, 1.1)^T$, θ-DEA performs significantly better on DTLZ4 test problem, while MOEA/AD becomes the best algorithm on WFG6 test problem. The IGD results are given in Table IX and Table X. Different from the HV metric values, the comparisons of the IGD metric values vary quite much on different test problems with different number of objectives. On DTLZ test suites, MOEA/AD, θ-DEA, MOEA/D-IPBI and Two_Arch2 perform the best on different problems, whereas on WFG4 to WFG9 test problems, NSGA-III achieves comparable results with MOEA/AD and θ-DEA. Coincident with Table VIII, Two_Arch2 are less competitive on WFG6 to WFG9 test problems with regular PF shapes.

E. Comparisons on DTLZ^{-1} and WFG^{-1} Test Problems under HV Metric with $\mathbf{z}^r = (1.1, \cdots, 1.1)^T$ and IGD Metric

The HV metric values with $\mathbf{z}^r = (1.1, \cdots, 1.1)^T$ on DTLZ^{-1} and WFG^{-1} test problems are presented in Table XI and Table XII. In this case, Two_Arch2 provides the best HV metric values on most of the minus test problems, which is conflict to the HV comparisons using $\mathbf{z}^r = (2, \cdots, 2)^T$ shown in Table IV and Table V. We argue that the worst point $\mathbf{z}^r = (1.1, \cdots, 1.1)^T$ is to close to the inverted PFs of the minus problems. As a result, the HV metric are in favor of the solutions located at the center of the PFs. The mean IGD metric values on DTLZ^{-1} and WFG^{-1} test problems given in Table XIII and Table XIV are coincident with our explanations, where MOEA/D obtains the best mean IGD metric values on 50 out of 55 test problems.

F. Performance Scores under HV Metric with $\mathbf{z}^r = (1.1, \cdots, 1.1)^T$ and IGD Metric

The average performance score of each algorithm on different test problems under HV metric with $\mathbf{z}^r = (1.1, \cdots, 1.1)^T$ are shown in Fig. 6. It can see from Fig. 6(a) that Two_Arch2 obtains the best average performance score on 3-objective test problems. In contrast, when the number of objectives exceeds 5, MOEA/AD becomes the best algorithm, of which the performance score is nearly half of Two_Arch2. As demonstrated in Fig. 6(b), the ranking of the average performance scores on all test problems keeps the same with the case of $\mathbf{z}^r = (2, \cdots, 2)^T$, where MOEA/AD, Two_Arch2 and VaEA are the top three algorithms respectively.

The leading performance of MOEA/AD is more significant under IGD metric. According to Fig. 7(a), the performance score of MOEA/AD keep to be the least on test problems with different number of objectives. As shown in Fig. 7(b), the average number of algorithms that significantly outperforms MOEA/AD is less than 1.

G. Investigation of The Major Components in MOEA/AD

The effectiveness of MOEA/AD on many-objective optimization, regardless of PF orientations, comes from three aspects: 1) the complementary search behaviors induced by two subproblem formulations with different contours; 2) the adversarial search directions due to the use ideal and nadir points in two subproblem formulations respectively; and 3) the sophisticated mating selection process. In this subsection, we investigate the contribution of each component by comparing MOEA/AD with its variants or some similar algorithms.

1) Different Subproblem Formulations: To validate the use of two different subproblem formulations, we compare MOEA/AD with Global WASF-GA, MOEA/D-MR [1] and

M. Wu, S. Kwong and Q. Zhang are with the Department of Computer Science, City University of Hong Kong, Kowloon, Hong Kong SAR (e-mail: mengyuan.wu@my.cityu.edu.hk, cssamk@cityu.edu.hk, qingfu.zhang@cityu.edu.hk).

K. Li is with the College of Engineering, Mathematics and Physical Sciences, University of Exeter, Exeter, EX4 4QF, UK (e-mail: k.li@exeter.ac.uk).

TABLE VII: HV Results of MOEA/AD and 9 Peer Algorithms on DTLZ Test Problems ($\mathbf{z}^r = (1.1, \cdots, 1.1)^T$).

Problem	m	PBI	GWASF	PICEA-g	VaEA	HypE	KnEA	NSGA-III	θ-DEA	TwoArch2	MOEA/AD
DTLZ1	3	1.117e+0†	8.581e-1†	9.017e-1†	1.109e+0†	1.109e+0†	9.942e-1†	1.117e+0	1.106e+0	1.116e+0†	**1.118e+0**
	5	1.578e+0	2.792e-1†	1.537e+0†	1.567e+0†	1.522e+0†	1.301e+0†	1.578e+0†	1.577e+0†	1.571e+0†	**1.578e+0**
	8	2.137e+0†	1.633e-1†	1.758e+0†	2.127e+0†	6.266e-1†	8.459e-1†	2.138e+0†	2.138e+0	2.123e+0†	**2.138e+0**
	10	2.592e+0†	4.692e-1†	2.318e+0†	2.587e+0†	1.118e+0†	1.570e+0†	2.593e+0†	2.593e+0†	2.583e+0†	**2.593e+0**
	15	4.167e+0‡	3.538e-3†	2.235e+0†	4.160e+0‡	0.000e+0†	2.606e+0†	**4.175e+0**‡	4.139e+0‡	4.128e+0	4.077e+0
DTLZ2	3	**7.441e-1**‡	7.001e-1†	7.138e-1†	7.362e-1†	7.199e-1†	7.237e-1†	7.434e-1‡	7.438e-1‡	7.392e-1†	7.428e-1
	5	1.307e+0‡	6.934e-1†	1.290e+0†	1.270e+0†	1.074e+0†	1.274e+0†	1.303e+0†	1.307e+0†	1.240e+0†	**1.307e+0**
	8	1.980e+0†	1.447e+0†	1.904e+0†	1.921e+0†	1.597e+0†	1.898e+0†	1.970e+0†	1.978e+0†	1.698e+0	**1.980e+0**
	10	2.515e+0†	7.301e-1†	2.405e+0†	2.440e+0†	2.231e+0†	2.447e+0†	2.509e+0†	2.514e+0†	2.129e+0†	**2.515e+0**
	15	**4.136e+0**‡	3.796e-1†	3.299e+0†	3.957e+0†	2.707e+0†	4.049e+0†	4.132e+0	4.136e+0‡	3.070e+0†	4.129e+0
DTLZ3	3	7.370e-1‡	4.440e-1†	3.492e-1†	7.324e-1	6.186e-1†	6.705e-1†	7.373e-1	7.343e-1	**7.443e-1**‡	7.339e-1
	5	1.305e+0	1.462e-1†	8.002e-1†	1.279e+0†	0.000e+0†	8.776e-1†	1.301e+0†	1.304e+0†	1.267e+0†	**1.305e+0**
	8	1.829e+0†	1.924e-1†	6.083e-1†	1.419e+0†	0.000e+0†	3.105e-1†	1.951e+0†	1.969e+0†	1.765e+0†	**1.978e+0**
	10	2.515e+0†	2.333e-1†	1.274e+0†	2.075e+0†	0.000e+0†	4.984e-1†	2.508e+0†	2.266e+0†	2.242e+0†	**2.516e+0**
	15	1.924e+0†	3.635e-1†	8.916e-1†	2.526e+0†	0.000e+0†	0.000e+0†	4.124e+0†	1.346e+0†	3.140e+0†	**4.131e+0**
DTLZ4	3	5.060e-1†	6.160e-1†	6.350e-1†	7.391e-1†	7.338e-1‡	7.265e-1†	6.419e-1	7.135e-1‡	6.791e-1†	**7.426e-1**
	5	1.123e+0†	5.835e-1†	1.226e+0†	1.276e+0†	1.171e+0†	1.279e+0†	1.308e+0‡	**1.309e+0**‡	1.232e+0†	1.305e+0
	8	1.839e+0†	5.077e-1†	1.872e+0†	1.937e+0†	1.375e+0†	1.904e+0†	1.980e+0‡	**1.981e+0**‡	1.663e+0†	1.974e+0
	10	2.437e+0†	9.981e-1†	2.436e+0†	2.457e+0†	2.178e+0†	2.491e+0†	2.515e+0‡	**2.516e+0**‡	2.124e+0†	2.511e+0
	15	3.994e+0†	3.731e-1†	3.477e+0†	4.012e+0†	3.155e+0†	4.088e+0†	4.136e+0‡	**4.137e+0**‡	3.335e+0†	4.113e+0

According to Wilcoxon's rank sum test, † and ‡ indicates whether the corresponding algorithm is significantly worse or better than MOEA/AD respectively.

TABLE VIII: HV Results of MOEA/AD and 9 Peer Algorithms on WFG Test Problems ($\mathbf{z}^r = (1.1, \cdots, 1.1)^T$).

Problem	m	PBI	GWASF	PICEA-g	VaEA	HypE	KnEA	NSGA-III	θ-DEA	TwoArch2	MOEA/AD
WFG1	3	5.952e-1†	7.281e-1†	5.299e-1†	5.556e-1†	1.834e-1†	5.601e-1†	3.507e-1†	5.531e-1†	7.967e-1	**8.104e-1**
	5	1.232e+0†	1.173e+0†	9.693e-1†	6.328e-1†	3.492e-1†	6.758e-1†	4.583e-1†	1.009e+0†	1.099e+0†	**1.404e+0**
	8	1.569e+0†	6.613e-1†	1.580e+0†	1.570e+0†	4.535e-1†	1.008e+0†	5.024e-1†	1.773e+0	**1.970e+0**‡	1.785e+0
	10	1.797e+0†	1.156e+0†	2.359e+0‡	2.224e+0†	5.638e-1†	1.453e+0†	6.904e-1†	2.284e+0†	**2.486e+0**‡	2.304e+0
	15	1.649e+0†	5.886e-1†	3.022e+0‡	3.636e+0‡	7.368e-1†	2.392e+0†	1.610e+0†	2.067e+0†	**3.934e+0**‡	2.726e+0
WFG2	3	9.627e-1†	1.096e+0	1.150e+0‡	1.122e+0‡	1.017e+0†	1.144e+0‡	1.116e+0‡	1.155e+0‡	**1.174e+0**‡	1.057e+0
	5	1.276e+0†	1.439e+0	**1.589e+0**‡	1.546e+0‡	1.458e+0	1.575e+0‡	1.541e+0‡	1.509e+0	1.588e+0‡	1.384e+0
	8	1.655e+0†	2.311e-1†	2.038e+0‡	2.057e+0‡	1.882e+0†	2.115e+0‡	2.006e+0‡	1.836e+0†	**2.137e+0**‡	1.948e+0
	10	2.140e+0†	2.759e-1†	2.521e+0‡	2.569e+0‡	2.388e+0†	2.569e+0‡	2.530e+0‡	2.294e+0†	**2.590e+0**‡	2.410e+0
	15	3.428e+0†	3.777e-1†	3.761e+0	3.988e+0‡	3.522e+0†	3.877e+0†	3.623e+0†	2.585e+0†	**4.172e+0**‡	3.818e+0
WFG3	3	7.389e-1†	8.357e-1‡	8.382e-1‡	7.882e-1†	7.070e-1†	8.256e-1	8.102e-1‡	8.136e-1	**8.392e-1**‡	7.998e-1
	5	9.002e-1†	9.424e-1†	**1.075e+0**‡	9.259e-1†	9.037e-1†	9.784e-1†	9.949e-1†	1.027e+0†	1.063e+0‡	1.048e+0
	8	7.509e-1†	1.940e-1†	1.362e+0‡	1.251e+0†	1.182e+0†	1.305e+0†	7.936e-1†	5.730e-1†	**1.398e+0**‡	1.319e+0
	10	5.762e-1†	2.351e-1†	1.697e+0‡	1.499e+0†	1.500e+0†	1.620e+0	8.666e-1†	6.490e-1†	**1.710e+0**‡	1.598e+0
	15	5.831e-1†	3.774e-1†	2.452e+0	2.332e+0	2.213e+0†	1.763e+0†	1.100e+0†	8.203e-1†	**2.628e+0**‡	2.416e+0
WFG4	3	6.647e-1†	6.918e-1†	7.102e-1†	6.946e-1†	6.367e-1†	7.093e-1†	7.120e-1†	7.136e-1†	7.248e-1	**7.253e-1**
	5	1.104e+0†	6.751e-1†	1.248e+0†	1.163e+0†	8.697e-1†	1.240e+0†	1.235e+0†	1.238e+0†	1.190e+0†	**1.280e+0**
	8	9.375e-1†	2.008e-1†	1.245e+0†	1.808e+0†	9.238e-1†	1.928e+0†	1.889e+0†	1.900e+0†	1.702e+0†	**1.953e+0**
	10	1.094e+0†	2.396e-1†	1.662e+0†	2.284e+0†	1.243e+0†	2.480e+0†	2.426e+0†	2.442e+0†	2.204e+0†	**2.496e+0**
	15	1.315e+0†	3.797e-1†	2.150e+0†	3.731e+0†	1.612e+0†	**4.069e+0**	3.849e+0†	3.677e+0†	3.607e+0†	4.040e+0
WFG5	3	6.457e-1†	6.425e-1†	6.564e-1†	6.644e-1†	5.994e-1†	6.710e-1	6.677e-1†	6.690e-1†	6.720e-1	**6.741e-1**
	5	1.098e+0†	6.071e-1†	1.174e+0†	1.132e+0†	9.194e-1†	1.188e+0†	1.189e+0†	1.195e+0†	1.136e+0†	**1.215e+0**
	8	1.115e+0†	7.679e-1†	1.427e+0†	1.758e+0†	8.618e-1†	1.826e+0	1.818e+0†	1.817e+0†	1.581e+0†	**1.828e+0**
	10	1.173e+0†	2.052e-1†	1.772e+0†	2.221e+0†	1.314e+0†	2.329e+0†	2.317e+0†	2.313e+0†	2.013e+0†	**2.332e+0**
	15	1.195e+0†	3.303e-1†	2.252e+0†	3.622e+0†	1.614e+0†	3.796e+0	3.775e+0†	3.141e+0†	2.947e+0†	**3.808e+0**
WFG6	3	6.309e-1‡	6.588e-1†	6.768e-1	6.613e-1†	5.784e-1†	6.719e-1†	6.716e-1†	6.754e-1	**6.862e-1**‡	6.781e-1
	5	9.557e-1†	6.134e-1†	1.210e+0	1.137e+0†	9.133e-1†	1.193e+0†	1.202e+0†	1.203e+0†	1.157e+0†	**1.217e+0**
	8	6.678e-1†	1.473e+0†	1.700e+0†	1.807e+0†	1.078e+0†	1.774e+0†	1.838e+0†	1.847e+0	1.625e+0†	**1.856e+0**
	10	7.357e-1†	8.631e-1†	2.163e+0†	2.281e+0†	1.399e+0†	2.344e+0†	2.342e+0†	2.354e+0†	2.085e+0†	**2.375e+0**
	15	5.326e-1†	3.691e-1†	2.692e+0†	3.699e+0†	1.724e+0†	3.833e+0†	3.809e+0†	3.145e+0†	3.403e+0†	**3.866e+0**
WFG7	3	6.331e-1†	7.011e-1†	7.226e-1†	7.138e-1	5.961e-1†	7.260e-1	7.239e-1	7.278e-1	**7.341e-1**‡	7.314e-1
	5	1.046e+0†	6.998e-1†	1.275e+0†	1.219e+0†	8.475e-1†	1.278e+0†	1.273e+0†	1.283e+0†	1.234e+0†	**1.298e+0**
	8	7.670e-1†	8.813e-1†	1.547e+0†	1.906e+0†	9.386e-1†	1.966e+0†	1.938e+0†	1.949e+0†	1.748e+0†	**1.973e+0**
	10	9.040e-1†	2.358e-1†	2.005e+0†	2.409e+0†	1.413e+0†	2.509e+0	2.472e+0†	2.484e+0†	2.258e+0†	**2.509e+0**
	15	6.801e-1†	3.797e-1†	2.605e+0†	3.930e+0†	1.741e+0†	3.915e+0†	3.586e+0†	2.966e+0†	3.701e+0†	**4.132e+0**
WFG8	3	5.754e-1†	6.029e-1†	5.960e-1†	5.900e-1†	5.100e-1†	6.069e-1†	6.100e-1†	6.115e-1	**6.266e-1**‡	6.144e-1
	5	8.994e-1†	5.745e-1†	1.071e+0†	9.771e-1†	7.440e-1†	1.061e+0†	1.079e+0†	1.086e+0†	1.024e+0†	**1.136e+0**
	8	1.463e-1†	3.350e-1†	1.497e+0†	1.390e+0†	9.597e-1†	1.634e+0†	1.610e+0†	1.628e+0†	1.317e+0†	**1.736e+0**
	10	1.593e-1†	2.639e-1†	1.902e+0†	1.858e+0†	1.392e+0†	2.252e+0†	2.140e+0	2.171e+0	1.861e+0†	**2.313e+0**
	15	5.861e-1†	4.281e-1†	2.499e+0†	3.293e+0†	1.825e+0†	3.054e+0†	**3.648e+0**‡	2.255e+0†	2.950e+0†	3.640e+0
WFG9	3	5.681e-1†	5.865e-1†	6.200e-1†	6.471e-1	5.036e-1†	6.456e-1	6.394e-1	6.441e-1	6.485e-1	**6.488e-1**
	5	9.927e-1†	5.576e-1†	1.063e+0†	1.028e+0†	6.233e-1†	**1.123e+0**	1.078e+0†	1.090e+0	1.062e+0	1.085e+0
	8	8.282e-1†	1.261e+0†	1.457e+0†	1.507e+0†	6.032e-1†	**1.672e+0**‡	1.555e+0	1.595e+0	1.400e+0†	1.562e+0
	10	7.097e-1†	5.503e-1†	1.841e+0†	1.888e+0†	8.118e-1†	**2.174e+0**‡	2.003e+0†	2.009e+0†	1.754e+0†	2.003e+0
	15	5.673e-1†	3.209e-1†	2.598e+0†	2.851e+0†	1.211e+0†	**3.363e+0**‡	3.013e+0†	3.079e+0	2.211e+0†	3.111e+0

According to Wilcoxon's rank sum test, † and ‡ indicates whether the corresponding algorithm is significantly worse or better than MOEA/AD respectively.

TABLE IX: IGD Results of MOEA/AD and 9 Peer Algorithms on DTLZ Test Problems.

Problem	m	IPBI	GWASF	PICEA-g	VaEA	HypE	KnEA	NSGA-III	θ-DEA	TwoArch2	MOEA/AD
DTLZ1	3	4.182e-2	2.735e-1†	2.009e-1†	4.508e-2†	5.945e-2†	1.001e-1†	4.204e-2	4.596e-2	4.435e-2†	**4.162e-2**
	5	1.082e-1	8.712e-1†	2.003e-1†	1.065e-1‡	1.804e-1†	2.333e-1†	1.080e-1	1.101e-1‡	**1.030e-1**‡	1.081e-1
	8	1.880e-1	2.165e+0†	5.522e-1†	2.003e-1†	4.899e-1†	6.845e-1†	1.896e-1†	1.891e-1†	1.902e-1†	**1.879e-1**
	10	2.047e-1‡	1.322e+0†	5.410e-1†	2.156e-1†	6.737e-1†	5.920e-1†	2.064e-1†	2.050e-1	**2.024e-1**‡	2.054e-1
	15	**3.126e-1**‡	7.219e+0†	7.887e-1†	3.164e-1‡	5.522e+0†	5.094e-1†	3.303e-1‡	3.217e-1‡	3.205e-1‡	3.874e-1
DTLZ2	3	**5.479e-2**‡	8.329e-2†	7.123e-2†	5.818e-2†	6.745e-2†	6.524e-2†	5.485e-2‡	5.481e-2‡	6.033e-2†	5.489e-2
	5	1.709e-1	5.516e-1†	1.719e-1†	1.700e-1‡	2.874e-1†	1.840e-1†	1.711e-1†	1.707e-1‡	**1.676e-1**‡	1.709e-1
	8	**3.377e-1**‡	6.502e-1†	3.954e-1†	3.694e-1†	5.419e-1†	3.969e-1†	3.396e-1†	3.381e-1‡	3.601e-1†	3.382e-1
	10	4.030e-1†	1.086e+0†	5.017e-1†	4.157e-1†	4.486e-1†	4.568e-1†	4.031e-1†	**4.020e-1**‡	4.284e-1†	4.025e-1
	15	**5.615e-1**‡	1.299e+0†	9.214e-1†	6.079e-1†	9.663e-1†	6.297e-1†	5.693e-1‡	5.687e-1‡	6.225e-1†	5.769e-1
DTLZ3	3	5.532e-2‡	4.570e-1†	3.439e-1†	5.797e-2†	8.536e-2†	9.912e-2†	**5.523e-2**‡	5.792e-2	5.956e-2†	5.566e-2
	5	1.712e-1†	1.104e+0†	4.700e-1†	**1.679e-1**‡	1.131e+0†	4.241e-1†	1.712e-1	1.711e-1	1.680e-1‡	1.711e-1
	8	3.878e-1	1.205e+0†	9.357e-1†	6.911e-1†	4.899e+0†	1.090e+0†	3.444e-1†	3.401e-1†	3.571e-1†	**3.393e-1**
	10	4.028e-1†	1.242e+0†	8.961e-1†	7.157e-1†	2.751e+0†	1.097e+0†	4.036e-1†	4.670e-1†	4.087e-1†	**4.018e-1**
	15	9.236e-1†	1.301e+0†	1.180e+0†	1.215e+0†	5.721e+0†	3.134e+1†	5.750e-1†	1.029e+0†	6.693e-1†	**5.685e-1**
DTLZ4	3	4.321e-1	2.396e-1†	2.290e-1†	5.834e-2	7.693e-2‡	6.559e-2†	2.254e-1	9.936e-2‡	1.477e-1†	**5.757e-2**
	5	3.976e-1†	7.153e-1†	2.688e-1	1.700e-1‡	2.659e-1†	1.823e-1	1.710e-1‡	1.709e-1‡	**1.683e-1**‡	1.811e-1
	8	5.136e-1†	1.070e+0†	4.596e-1†	3.667e-1†	7.771e-1†	3.951e-1†	3.380e-1‡	**3.378e-1**‡	3.636e-1†	3.504e-1
	10	5.175e-1†	1.003e+0†	4.835e-1†	4.145e-1†	6.589e-1†	4.309e-1†	4.030e-1†	4.029e-1†	4.297e-1†	**3.990e-1**
	15	6.989e-1†	1.300e+0†	8.841e-1†	6.068e-1†	8.256e-1†	6.203e-1†	5.615e-1‡	**5.612e-1**‡	6.252e-1†	5.825e-1

According to Wilcoxon's rank sum test, † and ‡ indicates whether the corresponding algorithm is significantly worse or better than MOEA/AD respectively.

TABLE X: IGD Results of MOEA/AD and 9 Peer Algorithms on WFG Test Problems.

Problem	m	IPBI	GWASF	PICEA-g	VaEA	HypE	KnEA	NSGA-III	θ-DEA	TwoArch2	MOEA/AD
WFG4	3	7.432e-2†	8.249e-2†	6.238e-2†	6.136e-2†	1.390e-1†	5.986e-2†	5.592e-2‡	**5.564e-2**‡	5.984e-2†	5.619e-2
	5	2.975e-1†	5.154e-1†	1.869e-1†	**1.653e-1**‡	4.188e-1†	1.716e-1†	1.662e-1‡	1.660e-1‡	1.679e-1‡	1.686e-1
	8	7.592e-1†	1.201e+0†	7.428e-1†	3.508e-1†	7.731e-1†	4.177e-1†	3.358e-1‡	**3.358e-1**‡	3.563e-1†	3.387e-1
	10	8.809e-1†	1.239e+0†	8.187e-1†	**3.950e-1**‡	8.581e-1†	4.513e-1†	3.965e-1‡	3.968e-1‡	4.138e-1†	3.997e-1
	15	1.075e+0†	1.299e+0†	1.032e+0†	5.930e-1†	1.035e+0†	6.436e-1†	7.017e-1†	7.913e-1†	6.089e-1†	**5.679e-1**
WFG5	3	7.358e-2†	8.529e-2†	6.859e-2†	6.432e-2†	1.468e-1†	6.347e-2†	6.123e-2	6.093e-2	6.550e-2†	**0.0609**
	5	2.568e-1†	5.446e-1†	1.704e-1†	1.657e-1†	3.656e-1†	1.689e-1†	**1.637e-1**‡	1.640e-1‡	1.686e-1†	1.649e-1
	8	6.611e-1†	8.882e-1†	5.850e-1†	3.534e-1†	7.124e-1†	3.677e-1†	**3.328e-1**‡	3.329e-1‡	3.583e-1†	3.340e-1
	10	8.280e-1†	1.218e+0†	6.861e-1†	3.986e-1†	7.161e-1†	4.146e-1†	3.927e-1	3.925e-1	4.150e-1†	**0.3925**
	15	1.071e+0†	1.283e+0†	9.386e-1†	5.956e-1†	1.003e+0†	5.847e-1†	5.716e-1†	7.825e-1†	6.080e-1†	**5.587e-1**
WFG6	3	8.255e-2†	8.495e-2†	6.781e-2†	6.759e-2†	1.369e-1†	6.667e-2†	6.160e-2‡	**6.086e-2**‡	6.471e-2†	6.327e-2
	5	3.413e-1†	5.620e-1†	1.769e-1†	1.704e-1†	3.403e-1†	1.787e-1†	1.657e-1‡	**1.656e-1**‡	1.693e-1†	1.672e-1
	8	8.537e-1†	5.539e-1†	4.480e-1†	3.599e-1†	6.002e-1†	3.925e-1†	**3.351e-1**‡	3.353e-1‡	3.633e-1†	3.389e-1
	10	9.717e-1†	1.011e+0†	5.641e-1†	4.021e-1†	6.510e-1†	4.262e-1†	**3.959e-1**‡	3.965e-1‡	4.210e-1†	3.988e-1
	15	1.210e+0†	1.287e+0†	8.969e-1†	5.983e-1†	9.056e-1†	6.141e-1†	6.162e-1†	8.442e-1†	6.113e-1†	**5.634e-1**
WFG7	3	8.425e-2†	8.235e-2†	6.120e-2†	5.871e-2†	1.723e-1†	6.066e-2†	5.506e-2‡	**5.475e-2**‡	5.935e-2†	5.587e-2
	5	3.331e-1†	5.724e-1†	1.779e-1†	**1.655e-1**‡	4.428e-1†	1.744e-1†	1.676e-1‡	1.683e-1‡	1.659e-1‡	1.700e-1
	8	8.453e-1†	9.065e-1†	6.065e-1†	3.611e-1†	7.454e-1†	3.744e-1†	3.380e-1‡	**3.376e-1**‡	3.569e-1†	3.396e-1
	10	9.434e-1†	1.241e+0†	7.031e-1†	4.000e-1‡	7.389e-1†	4.182e-1†	**3.983e-1**‡	3.995e-1‡	4.130e-1†	4.027e-1
	15	1.194e+0†	1.299e+0†	9.653e-1†	5.957e-1†	1.029e+0†	6.292e-1†	8.423e-1†	9.356e-1†	6.033e-1†	**5.676e-1**
WFG8	3	1.007e-1†	1.084e-1†	9.900e-2†	9.684e-2†	1.611e-1†	9.082e-2†	8.796e-2†	8.643e-2†	8.977e-2†	**8.501e-2**
	5	2.909e-1†	4.750e-1†	2.166e-1†	2.142e-1†	5.167e-1†	2.037e-1†	1.977e-1†	1.928e-1†	2.123e-1†	**1.885e-1**
	8	9.056e-1†	1.098e+0†	6.272e-1†	4.220e-1†	7.378e-1†	4.224e-1†	4.026e-1†	3.920e-1†	4.289e-1†	**3.634e-1**
	10	1.018e+0†	1.195e+0†	7.213e-1†	4.794e-1†	8.036e-1†	4.472e-1†	4.680e-1†	4.566e-1†	4.822e-1†	**4.032e-1**
	15	1.110e+0†	1.274e+0†	9.587e-1†	6.788e-1‡	1.025e+0†	6.958e-1‡	7.631e-1†	1.017e+0†	**6.745e-1**‡	7.216e-1
WFG9	3	9.313e-2†	9.443e-2†	7.368e-2†	6.434e-2	1.951e-1†	7.479e-2†	6.484e-2	6.350e-2	**6.827e-2**†	6.352e-2
	5	2.379e-1†	4.832e-1†	1.687e-1†	1.657e-1†	4.427e-1†	1.622e-1†	1.585e-1	**1.576e-1**	1.689e-1†	1.581e-1
	8	6.806e-1†	5.250e-1†	4.585e-1†	3.409e-1†	8.203e-1†	3.908e-1†	3.262e-1	**3.243e-1**‡	3.557e-1†	3.260e-1
	10	8.368e-1†	1.064e+0†	5.627e-1†	3.892e-1†	8.584e-1†	4.211e-1†	3.744e-1†	3.734e-1	4.173e-1†	**3.725e-1**
	15	1.021e+0†	1.283e+0†	8.751e-1†	5.816e-1†	1.023e+0†	6.061e-1†	5.488e-1†	5.494e-1	6.260e-1†	**5.466e-1**

According to Wilcoxon's rank sum test, † and ‡ indicates whether the corresponding algorithm is significantly worse or better than MOEA/AD respectively.

DBEA-DS [2] on DTLZ and DTLZ^{-1} test problems. These four algorithms use both the ideal and nadir points to guide the search directions. In particular, MOEA/AD and DBEA-DS co-evolve two populations, while Global GASF-GA and MOEA/D-MR maintain a single population, half of which are evolved toward ideal point while the others are evolved backward from the nadir point. Among them, only MOEA/AD employs different subproblem formulations for two populations that follow adversarial search directions. As a consequence, two populations are expected to have complementary search behaviors, i.e., one is diversity-oriented and the other is convergence-oriented. The comparison results under HV metric with $\mathbf{z}^r = (2, \cdots, 2)^T$ are shown in Table XV and Table XVI. Due to limitation of the mechanism used to maintain the external population [3], MOEA/D-MR is only run on 3-objective test problems. For DTLZ1 to DTLZ4 test problems, MOEA/AD performs significantly better in 43 out of 44 comparisons. DBEA-DS, which co-evolves two populations using the same subproblem formulations, only outperforms MOEA/AD on 3-objective DTLZ1 test problem. The HV re-

TABLE XI: HV Results of MOEA/AD and 9 Peer Algorithms on DTLZ^{-1} Test Problems ($\mathbf{z}^r = (1.1, \cdots, 1.1)^T$).

Problem	m	IPBI	GWASF	PICEA-g	VaEA	HypE	KnEA	NSGA-III	θ-DEA	TwoArch2	MOEA/AD
DTLZ1^{-1}	3	1.718e-1†	2.682e-1†	2.032e-1†	2.768e-1†	2.182e-1†	2.209e-1†	2.627e-1†	2.415e-1†	2.815e-1†	**2.844e-1**
	5	6.455e-3†	1.542e-2†	9.732e-3†	1.766e-2†	5.834e-3†	1.057e-2†	1.010e-2†	8.392e-3†	**2.022e-2‡**	1.955e-2
	8	3.190e-5†	5.471e-5†	1.445e-5†	5.125e-5†	1.550e-5†	1.154e-5†	2.577e-5†	4.252e-6†	**7.437e-5‡**	6.548e-5
	10	6.196e-7†	1.126e-6†	2.240e-7†	1.118e-6†	2.071e-7†	2.515e-7†	4.493e-7†	4.526e-8†	1.373e-6	**1.377e-6**
	15	0.000e+0	0.000e+0	0.000e+0	0.000e+0	0.000e+0	0.000e+0	0.000e+0	0.000e+0	0.000e+0	0.000e+0
DTLZ2^{-1}	3	7.065e-1†	6.820e-1†	5.007e-1†	6.966e-1†	3.097e-1†	6.412e-1†	6.905e-1†	6.912e-1†	**7.157e-1‡**	7.114e-1
	5	1.490e-1†	9.354e-2†	1.311e-1†	1.812e-1†	7.719e-3†	1.006e-1†	1.376e-1†	1.374e-1†	**2.121e-1‡**	1.898e-1
	8	3.046e-3†	6.955e-3‡	2.640e-3†	4.678e-3†	7.249e-5†	6.401e-4†	4.017e-3†	3.206e-3†	**8.873e-3‡**	5.832e-3
	10	2.084e-4†	5.382e-4‡	2.724e-5†	4.249e-4‡	1.316e-6†	2.170e-5†	2.473e-4†	1.679e-4†	**1.017e-3‡**	3.581e-4
	15	1.976e-7	4.278e-7‡	3.650E-10†	**4.493e-7‡**	1.000E-10†	1.000E-10†	5.625e-9†	2.641e-8†	9.479e-8†	1.865e-7
DTLZ3^{-1}	3	6.326e-1†	6.104e-1†	4.736e-1†	6.256e-1†	6.139e-1†	5.601e-1†	6.192e-1†	6.218e-1†	**6.392e-1‡**	6.353e-1
	5	1.262e-1†	7.867e-2†	1.153e-1†	1.453e-1†	1.292e-1†	6.086e-2†	1.070e-1†	1.193e-1†	**1.751e-1‡**	1.546e-1
	8	2.380e-3†	5.272e-3‡	2.007e-3†	3.557e-3†	1.658e-3†	1.521e-4†	2.613e-3†	2.009e-3†	**6.397e-3‡**	3.986e-3
	10	1.547e-4†	3.576e-4‡	5.375e-5†	3.080e-4‡	1.341e-4†	5.109e-6†	1.640e-4†	9.882e-5†	**6.864e-4‡**	2.450e-4
	15	1.288e-7	**3.544e-7‡**	3.950E-10†	2.804e-7‡	5.500e-9†	9.350E-10†	8.315e-9†	1.513e-8†	8.242e-8†	1.296e-7
DTLZ4^{-1}	3	6.761e-1†	6.818e-1†	2.689e-1†	6.977e-1†	2.296e-1†	6.442e-1†	6.943e-1†	6.953e-1†	**7.154e-1‡**	7.092e-1
	5	1.432e-1†	9.217e-2†	5.261e-2†	1.764e-1†	6.639e-3†	1.015e-1†	1.210e-1†	1.112e-1†	**2.118e-1‡**	1.797e-1
	8	2.758e-3†	5.328e-3‡	1.179e-4†	4.627e-3‡	2.157e-5†	5.138e-4†	1.678e-3†	1.799e-3†	**8.886e-3‡**	4.267e-3
	10	2.090e-4†	5.395e-4‡	6.990e-6†	4.093e-4‡	2.277e-7†	2.125e-5†	7.024e-5†	1.194e-4†	**1.021e-3‡**	2.714e-4
	15	1.466e-7†	3.419e-7‡	2.550E-10†	**4.574e-7‡**	0.000e+0†	1.100E-10†	5.500E-11†	1.385e-7†	1.080e-7†	2.065e-7

According to Wilcoxon's rank sum test, † and ‡ indicates whether the corresponding algorithm is significantly worse or better than MOEA/AD respectively.

TABLE XII: HV Results of MOEA/AD and 9 Peer Algorithms on WFG^{-1} Test Problems ($\mathbf{z}^r = (1.1, \cdots, 1.1)^T$).

Problem	m	IPBI	GWASF	PICEA-g	VaEA	HypE	KnEA	NSGA-III	θ-DEA	TwoArch2	MOEA/AD
WFG1^{-1}	3	6.492e-2†	**1.237e-1**	5.995e-2†	8.172e-2†	3.060e-2†	1.205e-1‡	7.661e-2†	7.590e-2†	1.165e-1	1.205e-1
	5	1.196e-3†	2.259e-3†	1.474e-3†	2.600e-3†	4.412e-4†	2.123e-3†	1.017e-3†	1.411e-3†	9.856e-4†	**3.715e-3**
	8	1.625e-6	9.462e-7†	2.186e-6†	**3.714e-6‡**	5.152e-7†	1.803e-6	1.000e-6†	1.195e-6†	6.075e-7†	1.585e-6
	10	2.432e-8‡	1.161e-8†	3.916e-8‡	**5.775e-8‡**	4.700e-9†	2.712e-8‡	9.630e-9†	1.407e-8	4.875e-9†	1.371e-8
	15	0.000e+0	0.000e+0	0.000e+0	0.000e+0	0.000e+0	0.000e+0	0.000e+0	0.000e+0	0.000e+0	0.000e+0
WFG2^{-1}	3	3.183e-1†	3.672e-1†	2.819e-1†	3.778e-1†	3.163e-1†	3.469e-1†	3.817e-1†	3.811e-1†	3.802e-1†	**3.839e-1**
	5	4.495e-3†	6.125e-3†	3.696e-3†	1.280e-2†	4.145e-3†	3.229e-3†	9.060e-3†	8.126e-3†	7.142e-3†	**1.492e-2**
	8	7.901e-6†	6.955e-6†	8.057e-7†	2.185e-5†	3.219e-6†	2.333e-6†	6.176e-6†	7.211e-6†	2.591e-7†	**3.177e-5**
	10	9.818e-8†	8.333e-8†	4.290e-9†	3.394e-7†	3.620e-8†	4.377e-8†	6.536e-8†	7.181e-8†	2.530e-9†	**5.861e-7**
	15	0.000e+0	0.000e+0	0.000e+0	0.000e+0	0.000e+0	0.000e+0	0.000e+0	0.000e+0	0.000e+0	0.000e+0
WFG3^{-1}	3	1.169e-1†	2.777e-1†	1.893e-1†	2.833e-1†	8.383e-2†	1.876e-1†	2.635e-1†	2.496e-1†	2.910e-1†	**2.928e-1**
	5	2.858e-3†	1.635e-2†	8.276e-3†	1.980e-2†	2.093e-3†	8.877e-3†	1.016e-2†	8.649e-3†	**2.080e-2‡**	2.025e-2
	8	3.171e-6†	5.460e-5†	5.315e-6†	5.012e-5†	3.994e-6†	3.146e-5†	7.647e-6†	3.944e-6†	2.429e-5†	**5.843e-5**
	10	5.136e-8†	1.059e-6‡	5.336e-8†	**1.073e-6‡**	1.540e-8†	8.863e-7†	9.689e-8†	5.079e-8†	2.680e-7†	9.985e-7
	15	0.000e+0	0.000e+0	0.000e+0	0.000e+0	0.000e+0	0.000e+0	0.000e+0	0.000e+0	0.000e+0	0.000e+0
WFG4^{-1}	3	6.914e-1†	6.810e-1†	5.979e-1†	6.764e-1†	3.736e-1†	5.117e-1†	6.498e-1†	6.791e-1†	**7.165e-1‡**	7.071e-1
	5	1.210e-1†	9.821e-2†	1.814e-1	1.632e-1†	3.627e-2†	8.291e-3†	1.230e-1†	1.498e-1†	**2.150e-1‡**	1.816e-1
	8	2.296e-3†	7.713e-3‡	3.471e-3	4.464e-3‡	2.007e-4†	3.214e-7†	6.660e-4†	2.108e-3†	**8.376e-3‡**	3.923e-3
	10	1.375e-4†	6.289e-4‡	1.911e-4	4.012e-4‡	7.782e-6†	3.135e-9†	6.023e-5†	4.332e-5†	**7.269e-4‡**	2.060e-4
	15	3.605e-8†	**5.053e-7‡**	0.000e+0†	4.330e-7‡	8.000E-10†	0.000e+0†	3.080e-9†	0.000e+0†	3.550E-10†	7.919e-8
WFG5^{-1}	3	6.907e-1†	6.804e-1†	5.975e-1†	6.769e-1†	3.136e-1†	5.465e-1†	6.570e-1†	6.818e-1†	**7.114e-1‡**	7.061e-1
	5	1.235e-1†	9.791e-2†	1.700e-1†	1.765e-1†	2.825e-2†	8.366e-3†	1.352e-1†	1.388e-1†	**2.037e-1‡**	1.820e-1
	8	2.341e-3†	**7.282e-3‡**	3.687e-3	3.985e-3‡	1.759e-4†	9.516e-7†	1.222e-3†	1.628e-3†	6.788e-3‡	3.778e-3
	10	1.457e-4†	5.103e-4‡	1.390e-4†	3.783e-4‡	6.639e-6†	3.745e-9†	5.835e-5†	1.937e-5†	**5.726e-4‡**	2.214e-4
	15	3.685e-8†	3.708e-7‡	2.795e-8†	**3.987e-7‡**	7.000E-10†	0.000e+0†	4.170e-9†	0.000e+0†	6.950E-10†	1.239e-7
WFG6^{-1}	3	6.914e-1†	6.808e-1†	6.092e-1†	6.915e-1†	2.210e-1†	5.867e-1†	6.769e-1†	6.890e-1†	**7.142e-1‡**	7.083e-1
	5	1.218e-1†	9.401e-2†	1.781e-1†	1.835e-1	1.513e-2†	1.175e-2†	1.195e-1†	1.326e-1†	**2.099e-1‡**	1.821e-1
	8	2.346e-3†	7.291e-3‡	4.679e-3‡	3.811e-3†	1.003e-4†	3.204e-7†	1.083e-3†	1.543e-3†	**7.812e-3‡**	4.114e-3
	10	1.440e-4†	5.874e-4‡	2.349e-4	3.742e-4‡	2.687e-6†	9.500E-11†	6.655e-5†	7.982e-6†	**7.460e-4‡**	2.450e-4
	15	3.082e-8†	2.329e-7‡	1.930e-9†	**4.012e-7‡**	2.000E-10†	0.000e+0†	7.460e-9†	0.000e+0†	1.447e-8†	1.572e-7
WFG7^{-1}	3	6.914e-1†	6.780e-1†	6.297e-1†	6.762e-1†	4.346e-1†	4.558e-1†	6.543e-1†	6.810e-1†	**7.158e-1‡**	7.032e-1
	5	1.206e-1†	9.498e-2†	1.844e-1‡	1.717e-1†	2.337e-2†	6.369e-3†	1.337e-1†	1.343e-1†	**2.113e-1‡**	1.793e-1
	8	2.340e-3†	6.671e-3‡	4.010e-3‡	3.776e-3‡	1.716e-4†	1.656e-7†	9.156e-4†	1.676e-3†	**7.281e-3‡**	3.235e-3
	10	1.423e-4†	**6.491e-4‡**	1.597e-4	3.570e-4‡	5.329e-6†	6.650E-10†	5.868e-5†	2.298e-5†	6.435e-4‡	1.874e-4
	15	5.932e-8†	2.245e-7	0.000e+0†	**3.772e-7‡**	1.000e-8†	0.000e+0†	2.670e-9†	0.000e+0†	8.495e-9†	1.051e-7
WFG8^{-1}	3	6.914e-1†	6.812e-1†	6.547e-1†	6.938e-1†	4.982e-1†	6.196e-1†	6.879e-1†	6.914e-1†	**7.131e-1‡**	7.097e-1
	5	1.213e-1†	9.547e-2†	1.932e-1‡	1.900e-1‡	1.218e-2†	4.276e-2†	1.506e-1†	1.437e-1†	**2.074e-1‡**	1.834e-1
	8	2.489e-3†	7.210e-3‡	6.919e-3‡	4.534e-3‡	1.040e-4†	2.363e-4†	1.511e-3†	1.828e-3†	**7.902e-3‡**	3.760e-3
	10	1.575e-4†	4.764e-4‡	5.333e-4‡	4.101e-4‡	4.569e-6†	4.081e-5†	8.888e-5†	1.976e-5†	**8.376e-4‡**	2.297e-4
	15	4.377e-8†	3.202e-7‡	1.418e-8†	**4.204e-7‡**	5.000E-10†	2.725e-9†	1.030e-8†	0.000e+0†	1.004e-7	1.420e-7
WFG9^{-1}	3	6.877e-1†	6.720e-1†	6.805e-1†	6.851e-1†	2.888e-1†	5.939e-1†	6.725e-1†	6.838e-1†	**7.094e-1‡**	6.981e-1
	5	1.319e-1†	1.029e-1†	1.989e-1‡	1.876e-1‡	3.676e-2†	1.021e-1†	1.367e-1†	1.356e-1†	**2.082e-1‡**	1.814e-1
	8	2.260e-3†	**7.265e-3‡**	6.083e-3‡	4.894e-3‡	7.330e-4†	1.825e-4†	1.692e-3†	1.083e-3†	7.205e-3‡	3.967e-3
	10	1.404e-4†	**7.781e-4‡**	4.202e-4‡	4.283e-4‡	1.573e-5†	1.132e-5†	1.143e-4†	2.729e-6†	6.904e-4‡	2.336e-4
	15	3.691e-8†	3.693e-7‡	1.138e-8†	**4.514e-7‡**	2.100e-9†	4.000E-11†	2.163e-8†	0.000e+0†	8.776e-8	9.345e-8

According to Wilcoxon's rank sum test, † and ‡ indicates whether the corresponding algorithm is significantly worse or better than MOEA/AD respectively.

TABLE XIII: IGD Results of MOEA/AD and 9 Peer Algorithms on DTLZ^{-1} Test Problems.

Problem	m	IPBI	GWASF	PICEA-g	VaEA	HypE	KnEA	NSGA-III	θ-DEA	TwoArch2	MOEA/AD
DTLZ1^{-1}	3	1.465e-1†	5.655e-2†	1.178e-1†	4.580e-2†	1.030e-1†	7.955e-2†	6.049e-2†	7.970e-2†	4.350e-2†	**4.160e-2**
	5	2.398e-1†	1.305e-1†	1.771e-1†	1.082e-1†	2.512e-1†	1.374e-1†	1.774e-1†	2.146e-1†	**9.956e-2**‡	1.057e-1
	8	2.518e-1†	2.251e-1†	2.754e-1†	2.034e-1†	3.195e-1†	2.692e-1†	2.612e-1†	4.265e-1†	2.003e-1†	**1.834e-1**
	10	2.640e-1†	2.411e-1†	3.011e-1†	2.182e-1†	3.480e-1†	2.528e-1†	2.781e-1†	4.536e-1†	2.271e-1†	**2.028e-1**
	15	3.572e-1†	4.187e-1†	3.879e-1†	3.432e-1†	6.719e-1†	3.443e-1†	4.300e-1†	5.215e-1†	3.187e-1†	**3.061e-1**
DTLZ2^{-1}	3	**5.477e-2**‡	7.917e-2†	2.974e-1†	7.093e-2†	2.241e-1†	7.118e-2†	7.161e-2†	7.655e-2†	5.951e-2†	5.770e-2
	5	1.707e-1†	3.165e-1†	3.866e-1†	1.777e-1†	4.714e-1†	2.141e-1†	1.952e-1†	2.377e-1†	1.689e-1†	**1.529e-1**
	8	3.375e-1†	5.103e-1†	5.146e-1†	3.621e-1†	5.175e-1†	4.096e-1†	5.664e-1†	6.463e-1†	3.663e-1†	**3.079e-1**
	10	4.024e-1†	7.193e-1†	5.654e-1†	4.101e-1†	5.669e-1†	4.238e-1†	5.651e-1†	8.210e-1†	4.297e-1†	**3.524e-1**
	15	5.620e-1†	9.300e-1†	7.398e-1†	6.065e-1†	6.457e-1†	5.903e-1†	8.847e-1†	1.022e+0†	6.058e-1†	**5.241e-1**
DTLZ3^{-1}	3	**6.957e-2**‡	8.979e-2†	2.598e-1†	8.526e-2†	1.584e-1†	1.015e-1†	8.629e-2†	8.641e-2†	7.360e-2†	7.129e-2
	5	1.731e-1†	3.134e-1†	3.586e-1†	1.879e-1†	4.270e-1†	2.731e-1†	2.079e-1†	2.416e-1†	1.725e-1†	**1.536e-1**
	8	3.332e-1†	4.933e-1†	5.231e-1†	3.580e-1†	4.852e-1†	5.536e-1†	5.351e-1†	6.621e-1†	3.644e-1†	**3.029e-1**
	10	3.968e-1†	7.131e-1†	5.630e-1†	4.051e-1†	5.484e-1†	5.437e-1†	5.407e-1†	8.270e-1†	4.246e-1†	**3.476e-1**
	15	5.506e-1†	9.001e-1†	7.399e-1†	5.940e-1†	7.798e-1†	6.935e-1†	7.829e-1†	1.005e+0†	6.033e-1†	**5.157e-1**
DTLZ4^{-1}	3	7.711e-2‡	7.893e-2†	3.614e-1†	7.185e-2†	2.770e-1†	7.055e-2†	7.286e-2†	7.161e-2†	5.979e-2†	**5.676e-2**
	5	1.827e-1†	3.176e-1†	4.381e-1†	1.781e-1†	4.804e-1†	2.109e-1†	1.995e-1†	2.510e-1†	1.685e-1†	**1.486e-1**
	8	3.528e-1†	4.450e-1†	5.521e-1†	3.644e-1†	5.663e-1†	4.080e-1†	4.232e-1†	7.681e-1†	3.684e-1†	**3.066e-1**
	10	4.029e-1†	5.014e-1†	5.719e-1†	4.128e-1†	6.288e-1†	4.176e-1†	4.615e-1†	8.496e-1†	4.318e-1†	**3.525e-1**
	15	5.778e-1†	9.475e-1†	7.251e-1†	6.107e-1†	6.966e-1†	5.958e-1†	7.555e-1†	9.690e-1†	6.068e-1†	**5.252e-1**

According to Wilcoxon's rank sum test, † and ‡ indicates whether the corresponding algorithm is significantly worse or better than MOEA/AD respectively.

TABLE XIV: IGD Results of MOEA/AD and 9 Peer Algorithms on WFG^{-1} Test Problems.

Problem	m	IPBI	GWASF	PICEA-g	VaEA	HypE	KnEA	NSGA-III	θ-DEA	TwoArch2	MOEA/AD
WFG3^{-1}	3	2.488e-1†	5.639e-2†	1.415e-1†	4.356e-2†	3.187e-1†	1.111e-1†	5.935e-2†	7.966e-2†	4.246e-2†	**4.063e-2**
	5	2.488e-1†	5.639e-2†	1.415e-1†	4.356e-2‡	3.187e-1†	1.111e-1†	5.935e-2†	7.966e-2†	4.246e-2‡	**4.063e-2**
	8	4.830e-1†	2.238e-1†	4.073e-1†	2.103e-1†	4.720e-1†	2.093e-1†	4.374e-1†	4.672e-1†	2.407e-1†	**1.949e-1**
	10	4.829e-1†	2.415e-1†	4.329e-1†	2.251e-1†	6.816e-1†	**2.065e-1**‡	4.701e-1†	5.323e-1†	2.752e-1†	2.220e-1
	15	5.174e-1†	4.316e-1†	5.492e-1†	3.754e-1†	5.567e-1†	**3.059e-1**‡	5.613e-1†	7.217e-1†	3.102e-1‡	3.369e-1
WFG4^{-1}	3	6.258e-2†	7.867e-2†	1.975e-1†	7.514e-2†	1.957e-1†	1.258e-1†	7.771e-2†	7.825e-2†	5.904e-2†	**5.808e-2**
	5	6.258e-2†	7.867e-2†	1.975e-1†	7.514e-2†	1.957e-1†	1.258e-1†	7.771e-2†	7.825e-2†	5.904e-2†	**5.808e-2**
	8	3.758e-1†	5.210e-1†	5.952e-1†	3.525e-1†	5.883e-1†	6.092e-1†	5.968e-1†	6.296e-1†	3.585e-1†	**3.141e-1**
	10	4.251e-1†	7.089e-1†	6.885e-1†	4.001e-1†	6.332e-1†	6.301e-1†	6.482e-1†	8.905e-1†	4.189e-1†	**3.606e-1**
	15	5.911e-1†	9.231e-1†	1.085e+0†	6.092e-1†	7.029e-1†	9.063e-1†	9.064e-1†	1.227e+0†	6.963e-1†	**5.344e-1**
WFG5^{-1}	3	6.265e-2†	7.830e-2†	1.795e-1†	7.362e-2†	2.364e-1†	1.083e-1†	7.528e-2†	7.501e-2†	5.892e-2†	**5.710e-2**
	5	6.265e-2†	7.830e-2†	1.795e-1†	7.362e-2†	2.364e-1†	1.083e-1†	7.528e-2†	7.501e-2†	5.892e-2†	**5.710e-2**
	8	3.730e-1†	4.852e-1†	5.114e-1†	3.589e-1†	5.394e-1†	6.114e-1†	5.660e-1†	6.667e-1†	3.551e-1†	**3.078e-1**
	10	4.223e-1†	7.420e-1†	6.000e-1†	4.011e-1†	5.858e-1†	6.753e-1†	6.426e-1†	9.028e-1†	4.165e-1†	**3.530e-1**
	15	5.881e-1†	9.388e-1†	8.144e-1†	5.976e-1†	6.854e-1†	8.783e-1†	8.979e-1†	1.161e+0†	6.848e-1†	**5.227e-1**
WFG6^{-1}	3	6.264e-2†	7.857e-2†	1.693e-1†	7.082e-2†	2.938e-1†	8.949e-2†	7.086e-2†	7.438e-2†	5.881e-2†	**5.739e-2**
	5	6.264e-2†	7.857e-2†	1.693e-1†	7.082e-2†	2.938e-1†	8.949e-2†	7.086e-2†	7.438e-2†	5.881e-2†	**5.739e-2**
	8	3.761e-1†	4.960e-1†	4.886e-1†	3.674e-1†	5.648e-1†	6.062e-1†	5.669e-1†	6.909e-1†	3.607e-1†	**3.064e-1**
	10	4.257e-1†	6.932e-1†	5.699e-1†	4.066e-1†	6.048e-1†	7.282e-1†	6.428e-1†	9.255e-1†	4.203e-1†	**3.530e-1**
	15	5.918e-1†	9.544e-1†	8.470e-1†	6.036e-1†	7.033e-1†	9.309e-1†	8.981e-1†	1.125e+0†	6.403e-1†	**5.231e-1**
WFG7^{-1}	3	6.274e-2†	7.880e-2†	1.441e-1†	7.326e-2†	1.847e-1†	1.592e-1†	7.388e-2†	7.380e-2†	5.861e-2†	**5.753e-2**
	5	6.274e-2†	7.880e-2†	1.441e-1†	7.326e-2†	1.847e-1†	1.592e-1†	7.388e-2†	7.380e-2†	5.861e-2†	**5.753e-2**
	8	3.760e-1†	4.780e-1†	5.329e-1†	3.655e-1†	5.965e-1†	6.175e-1†	5.916e-1†	6.647e-1†	3.590e-1†	**3.109e-1**
	10	4.254e-1†	5.925e-1†	6.377e-1†	4.063e-1†	6.319e-1†	6.790e-1†	6.626e-1†	8.966e-1†	4.217e-1†	**3.538e-1**
	15	5.921e-1†	1.002e+0†	9.819e-1†	6.016e-1†	7.050e-1†	9.885e-1†	9.153e-1†	1.186e+0†	6.471e-1†	**5.248e-1**
WFG8^{-1}	3	6.297e-2†	7.852e-2†	1.403e-1†	7.377e-2†	1.634e-1†	7.794e-2†	7.144e-2†	7.763e-2†	6.033e-2†	**5.798e-2**
	5	6.297e-2†	7.852e-2†	1.403e-1†	7.377e-2†	1.634e-1†	7.794e-2†	7.144e-2†	7.763e-2†	6.033e-2†	**5.798e-2**
	8	3.765e-1†	4.806e-1†	4.892e-1†	3.572e-1†	5.557e-1†	5.476e-1†	5.642e-1†	6.770e-1†	3.672e-1†	**3.083e-1**
	10	4.259e-1†	7.356e-1†	5.773e-1†	4.051e-1†	6.032e-1†	5.116e-1†	6.412e-1†	8.915e-1†	4.276e-1†	**3.534e-1**
	15	5.921e-1†	9.473e-1†	8.799e-1†	6.037e-1†	6.939e-1†	7.903e-1†	9.030e-1†	1.132e+0†	6.309e-1†	**5.232e-1**
WFG9^{-1}	3	6.045e-2†	7.827e-2†	9.412e-2†	7.023e-2†	2.575e-1†	8.675e-2†	7.051e-2†	7.199e-2†	5.783e-2	**5.783e-2**
	5	6.045e-2†	7.827e-2†	9.412e-2†	7.023e-2†	2.575e-1†	8.675e-2†	7.051e-2†	7.199e-2†	5.783e-2†	**5.783e-2**
	8	3.648e-1†	4.841e-1†	4.782e-1†	3.496e-1†	5.289e-1†	5.561e-1†	5.395e-1†	7.487e-1†	3.631e-1†	**3.099e-1**
	10	4.124e-1†	5.989e-1†	5.627e-1†	3.984e-1†	6.197e-1†	5.797e-1†	6.210e-1†	9.255e-1†	4.258e-1†	**3.543e-1**
	15	5.737e-1†	9.294e-1†	8.185e-1†	5.928e-1†	7.028e-1†	7.260e-1†	8.725e-1†	1.113e+0†	6.405e-1†	**5.234e-1**

According to Wilcoxon's rank sum test, † and ‡ indicates whether the corresponding algorithm is significantly worse or better than MOEA/AD respectively.

sults on DTLZ^{-1} test problems are similar. Although DBEA-DS obtains better mean metric values on 3 3-objective test problems, its superiority is only significant on 3-objective DTLZ4^{-1} test problem. When the number of objectives is more that 3, MOEA/AD remains the best algorithms on all test problems.

2) Adversarial Search Directions: The adversarial search directions of the two populations in MOEA/AD make it adapt to problems with inverted PFs. In addition, they different search directions also add diversity to the mating process. In this experiment, we develop a variant of MOEA/AD, denoted by MOEA/D-2P, of which both the two populations are

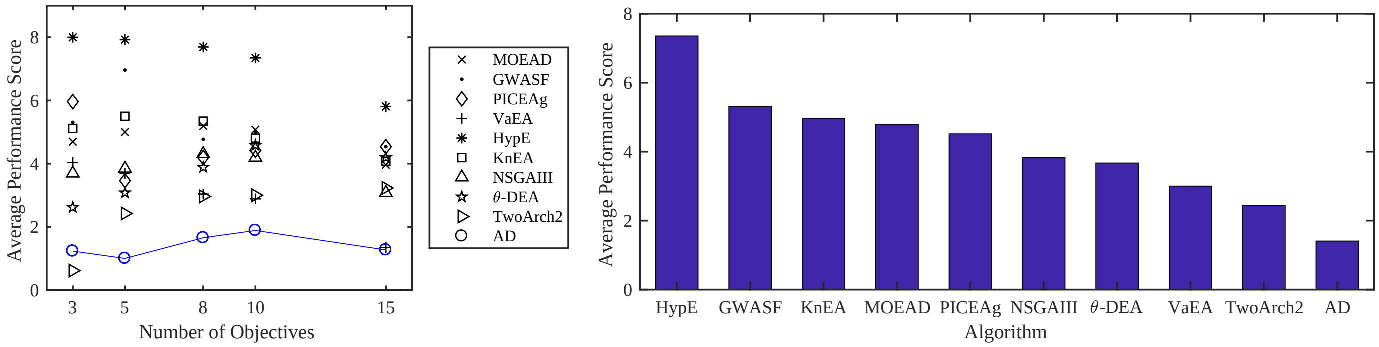

(a) (b)

Fig. 6: Average performance scores under HV metric with $\mathbf{z}^r = (1.1, \cdots, 1.1)^T$: (a) on test problems with different number of objectives; (b) over all test problems.

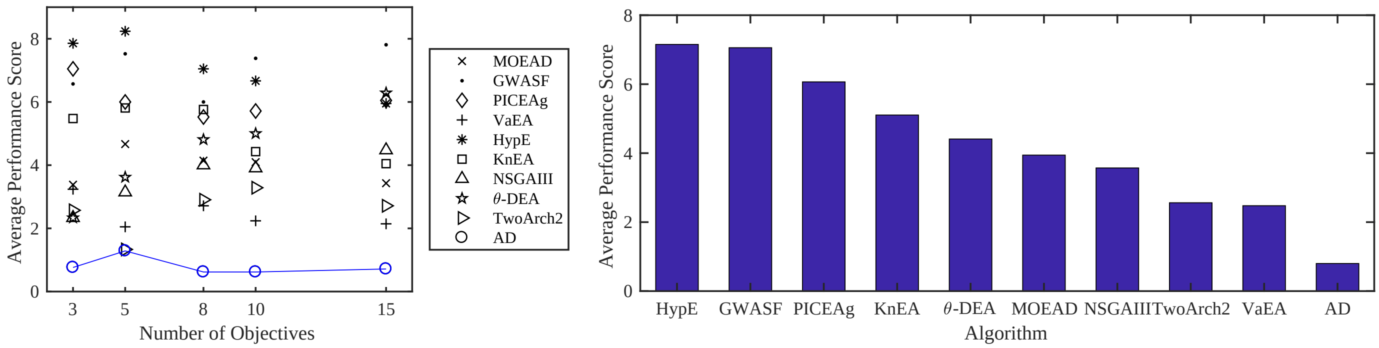

(a) (b)

Fig. 7: Average performance scores under IGD metric: (a) on test problems with different number of objectives; (b) over all test problems.

TABLE XV: HV Results of Global WASF-GA, MOEA/D-MR, DBEA-DS and MOEA/AD on DTLZ Test Problems ($\mathbf{z}^r = (2, \cdots, 2)^T$).

Problem	m	GWASF	MR	DBEA-DS	MOEA/AD
DTLZ1	3	7.134e+0†	4.562e+0†	**7.788e+0**‡	7.787e+0
	5	1.965e+1†	–	3.088e+1†	**3.197e+1**
	8	7.026e+1†	–	0.000e+0†	**2.560e+2**
	10	4.761e+2†	–	0.000e+0†	**1.024e+3**
	15	1.092e+3†	–	0.000e+0†	**3.270e+4**
DTLZ2	3	7.301e+0†	7.321e+0†	7.404e+0†	**7.412e+0**
	5	3.037e+1†	–	3.110e+1†	**3.170e+1**
	8	2.423e+2†	–	2.549e+2†	**2.558e+2**
	10	6.398e+2†	–	8.505e+2†	**1.024e+3**
	15	1.638e+4†	–	1.426e+4†	**3.276e+4**
DTLZ3	3	6.504e+0†	1.109e+0†	7.374e+0†	**7.403e+0**
	5	1.600e+1†	–	0.000e+0†	**3.169e+1**
	8	1.278e+2†	–	0.000e+0†	**2.558e+2**
	10	5.115e+2†	–	0.000e+0†	**1.024e+3**
	15	1.631e+4†	–	0.000e+0†	**3.276e+4**
DTLZ4	3	6.961e+0†	7.343e+0†	7.376e+0†	**7.412e+0**
	5	2.710e+1†	–	2.742e+1†	**3.169e+1**
	8	1.575e+2†	–	7.228e+0†	**2.558e+2**
	10	7.165e+2†	–	2.611e+1†	**1.024e+3**
	15	1.636e+4†	–	5.815e+2†	**3.276e+4**

According to Wilcoxon's rank sum test, † and ‡ indicates whether the corresponding algorithm is significantly worse or better than MOEA/AD respectively.

TABLE XVI: HV Results of Global WASF-GA, MOEA/D-MR, DBEA-DS and MOEA/AD on DTLZ^{-1} Test Problems ($\mathbf{z}^r = (2, \cdots, 2)^T$).

Problem	m	GWASF	MR	DBEA-DS	MOEA/AD
DTLZ1^{-1}	3	5.357e+0†	5.140e+0†	5.377e+0†	**5.394e+0**
	5	1.021e+1†	–	7.887e+0†	**1.088e+1**
	8	8.880e+0†	–	5.361e+0†	**1.949e+1**
	10	1.119e+1†	–	6.610e+0†	**2.946e+1**
	15	6.379e+0†	–	4.880e+0†	**4.151e+1**
DTLZ2^{-1}	3	6.622e+0†	6.653e+0†	**6.690e+0**	6.689e+0
	5	1.356e+1†	–	1.604e+1†	**1.774e+1**
	8	2.981e+1†	–	1.764e+1†	**4.941e+1**
	10	3.308e+1†	–	2.533e+1†	**9.045e+1**
	15	4.900e+1†	–	3.283e+1†	**1.492e+2**
DTLZ3^{-1}	3	6.266e+0†	6.006e+0†	**6.338e+0**	6.328e+0
	5	1.261e+1†	–	1.390e+1†	**1.636e+1**
	8	2.725e+1†	–	1.038e+1†	**4.415e+1**
	10	2.844e+1†	–	1.449e+1†	**8.018e+1**
	15	4.581e+1†	–	1.647e+1†	**1.312e+2**
DTLZ4^{-1}	3	6.623e+0†	6.666e+0†	**6.714e+0**‡	6.694e+0
	5	1.355e+1†	–	1.729e+1†	**1.777e+1**
	8	3.225e+1†	–	2.061e+1†	**4.856e+1**
	10	5.378e+1†	–	3.958e+1†	**8.781e+1**
	15	4.730e+1†	–	6.916e+1†	**1.463e+2**

According to Wilcoxon's rank sum test, † and ‡ indicates whether the corresponding algorithm is significantly worse or better than MOEA/AD respectively.

evolved following search directions toward the ideal point. The HV results are presented in Table XVII and Table XVIII. As

TABLE XVII: HV Results of MOEA/D-2P and MOEA/AD on DTLZ Test Problems ($\mathbf{z}^r = (2, \cdots, 2)^T$).

Problem	m	MOEA/D-2P	MOEA/AD
DTLZ1	3	7.593e+0†	**7.787e+0**
	5	3.080e+1†	**3.197e+1**
	8	2.499e+2†	**2.560e+2**
	10	9.893e+2†	**1.024e+3**
	15	3.125e+4	**3.270e+4**
DTLZ2	3	**7.412e+0**‡	7.412e+0
	5	**3.170e+1**‡	3.170e+1
	8	2.558e+2†	**2.558e+2**
	10	1.024e+3†	**1.024e+3**
	15	**3.276e+4**‡	3.276e+4
DTLZ3	3	7.100e+0	**7.403e+0**
	5	2.946e+1†	**3.169e+1**
	8	2.313e+2†	**2.558e+2**
	10	8.389e+2†	**1.024e+3**
	15	2.729e+4†	**3.276e+4**
DTLZ4	3	7.410e+0	**7.412e+0**
	5	3.169e+1†	**3.169e+1**
	8	**2.558e+2**	2.558e+2
	10	**1.024e+3**‡	1.024e+3
	15	**3.276e+4**	3.276e+4

According to Wilcoxon's rank sum test, † and ‡ indicates whether the corresponding algorithm is significantly worse or better than MOEA/AD respectively.

TABLE XVIII: HV Results of MOEA/D-2P and MOEA/AD on DTLZ^{-1} Test Problems ($\mathbf{z}^r = (2, \cdots, 2)^T$).

Problem	m	MOEA/D-2P	MOEA/AD
DTLZ1^{-1}	3	5.341e+0†	**5.394e+0**
	5	8.714e+0†	**1.088e+1**
	8	5.053e+0†	**1.949e+1**
	10	4.665e+0†	**2.946e+1**
	15	3.419e+0†	**4.151e+1**
DTLZ2^{-1}	3	6.525e+0†	**6.689e+0**
	5	1.329e+1†	**1.774e+1**
	8	2.180e+1†	**4.941e+1**
	10	3.025e+1†	**9.045e+1**
	15	4.376e+1†	**1.492e+2**
DTLZ3^{-1}	3	6.173e+0†	**6.328e+0**
	5	1.238e+1†	**1.636e+1**
	8	1.925e+1†	**4.415e+1**
	10	2.681e+1†	**8.018e+1**
	15	3.858e+1†	**1.312e+2**
DTLZ4^{-1}	3	6.523e+0†	**6.694e+0**
	5	1.328e+1†	**1.777e+1**
	8	1.959e+1†	**4.856e+1**
	10	2.707e+1†	**8.781e+1**
	15	5.053e+1†	**1.463e+2**

According to Wilcoxon's rank sum test, † and ‡ indicates whether the corresponding algorithm is significantly worse or better than MOEA/AD respectively.

can be seen from Table XVIII, thanks to the search directions backward from the nadir point, the HV metric values obtained by MOEA/AD are significantly better than those of MOEA/D-2P on all DTLZ^{-1} test problems. When it comes to DTLZ test problems with regular PF orientation, MOEA/AD still performs better than MOEA/D-2P in 16 out of 20 comparisons and obtains comparable results on the remaining test problems, which can be owed to the additional diversity provided by the adversarial search directions.

3) Sophisticated Mating Selection: To further investigate the effectiveness of the sophisticated mating selection process, we design the following three variants to validate its three major components, i.e., the pairing step, the mating selection step and the principal parent selection.

Algorithm 6: MatingSelectionV2($S_c, S_d, i, M, R, C, W, B$)

Input: S_c, S_d, W, matching array M and the subproblem index i, sentinel array R, neighborhood structure B
Output: mating parents $\overline{S}$

```
pop ← PopSelection(S_c, S_d, i, M, W);
if rand < δ then
    S_p ← ∅;
    if pop == 1 then
        for j ← 1 to T do
            S_p ← S_p ∪ {x_d^{B[i][j]}};
        x^r ← Randomly select a solution from S_p;
        S̄ ← {x_d^i, x^r};
    else
        for j ← 1 to T do
            S_p ← S_p ∪ {x_c^{B[M[i]][j]}};
        x^r ← Randomly select a solution from S_p;
        S̄ ← {x_c^{M[i]}, x^r};
else
    if pop == 1 then
        x^r ← Randomly select a solution from S_d;
        S̄ ← {x_d^i, x^r};
    else
        x^r ← Randomly select a solution from S_c;
        S̄ ← {x_c^{M[i]}, x^r};
return S̄
```

- MOEA/AD-$v1$: it replaces the two-level stable matching in line 13 of Algorithm 1. with random matching. In particular, M is set as a random permutation of 1 to N and $R[i] = 1$ for all $i \in \{1, \cdots, N\}$.
- MOEA/AD-$v2$: it does not consider the collaboration between S_d and S_c in the mating selection step. In particular, it randomly selects the mating parents from S_d or S_c depending on the principal parent. The pseudo code is given in Algorithm 6.
- MOEA/AD-$v3$: it only considers one primary criteria, i.e., subproblem's relative improvement, to select the principal parent solution. In short, line 6 to line 11 of Algorithm 4 are replaced by $pop \leftarrow$ *Randomly select from* $\{1, 2\}$.

The comparison results between MOEA/AD and its three variants under HV metric with $\mathbf{z}^r = (2, \cdots, 2)^T$ are presented in Table XIX. We find that our proposed MOEA/AD is still the best candidate where it obtains the best mean HV values on 16 out of 20 test problems. In particular, its better HV values are with statistical significance on almost all DTLZ1 and DTLZ3 test problems. Although MOEA/AD is outperformed by its variants on some test problems, the differences to the best results are quite small. We have the following three assertions from the comparison results.

- The stable matching procedure divides solutions of two populations into different pairs according to their working regions upon the PF. It facilitates the mating selection

TABLE XIX: HV Results of MOEA/AD and its Three Variants on DTLZ Test Problems ($\mathbf{z}^r = (2, \cdots, 2)^T$).

Problem	m	AD-$v1$	AD-$v2$	AD-$v3$	MOEA/AD
DTLZ1	3	7.785e+0†	7.785e+0†	7.777e+0†	**7.787e+0**
	5	3.197e+1†	3.196e+1†	3.191e+1†	**3.197e+1**
	8	2.560e+2†	2.491e+2†	2.499e+2†	**2.560e+2**
	10	1.008e+3†	9.767e+2†	1.006e+3†	**1.024e+3**
	15	3.055e+4†	3.186e+4†	3.098e+4†	**3.270e+4**
DTLZ2	3	7.412e+0	7.412e+0	7.411e+0†	**7.412e+0**
	5	3.170e+1	**3.170e+1**	3.170e+1†	3.170e+1
	8	2.558e+2†	2.558e+2†	2.558e+2†	**2.558e+2**
	10	1.024e+3†	1.024e+3†	1.024e+3	**1.024e+3**
	15	**3.276e+4**	3.276e+4	3.276e+4	3.276e+4
DTLZ3	3	**7.405e+0**	7.239e+0	7.405e+0	7.403e+0
	5	3.097e+1†	2.877e+1†	3.092e+1†	**3.169e+1**
	8	2.125e+2†	2.330e+2†	2.058e+2†	**2.558e+2**
	10	8.783e+2†	8.356e+2†	6.739e+2†	**1.024e+3**
	15	2.761e+4†	2.574e+4†	2.681e+4†	**3.276e+4**
DTLZ4	3	7.410e+0†	7.411e+0	7.410e+0†	**7.412e+0**
	5	3.169e+1	3.169e+1	3.169e+1	**3.169e+1**
	8	2.558e+2	2.558e+2	**2.558e+2**	2.558e+2
	10	1.024e+3	1.024e+3	1.024e+3	**1.024e+3**
	15	3.276e+4	3.276e+4†	3.276e+4	**3.276e+4**

According to Wilcoxon's rank sum test, † and ‡ indicates whether the corresponding algorithm is significantly worse or better than MOEA/AD respectively.

process and helps spread the search efforts upon the entire PF. In the meanwhile, the two-level stable matching also provides addition information on whether a solution pair work on similar regions upon the PF.

- The collaboration between two populations help strengthen their complementary behaviors, i.e., one is diversity-oriented and the other is convergence-oriented.
- The three criteria together help to select a promising principal parent solution from a matching pair, which makes the reproduction more efficient.

H. Online Comparisons of Two Populations

In this subsection, we study the different properties of the two populations during the optimization of 3-objective DTLZ1 and DTLZ1^{-1} test problems. According to [4], the $g(\mathbf{x})$ of the DTLZ test problem is adopted to assess the convergence of the two populations. A smaller $g(\mathbf{x})$ indicates better convergence of a population for a DTLZ test problem. As shown in Fig. 8(a), the mean $g(\mathbf{x})$ of P_c decreases much earlier than P_d, indicating the better convergence ability of the AASF subproblem formulation. Similar trends of $g(\mathbf{x})$ can be seen in Fig. 8(b). A difference between Fig. 8(a) and Fig. 8(b) is that the convergence of P_c can be as good as P_d on DTLZ1 test problem but not on DTLZ1^{-1} test problem, which is caused by the limited convergence ability of the PBI subproblem formulation when the search directions are not suitable for the inverted PF. As for the diversity of the two populations, it is not only affected by the subproblem formulations but mainly depends on the search directions. Typically, the population that follows search directions suitable for the orientation of the PF is expected to achieve better diversity, which can be seen in Fig. 9. Note that the diversity measure in Fig. 9 is defined as the mean value of the angle between each reference direction and its closest objective vector in the solution set.

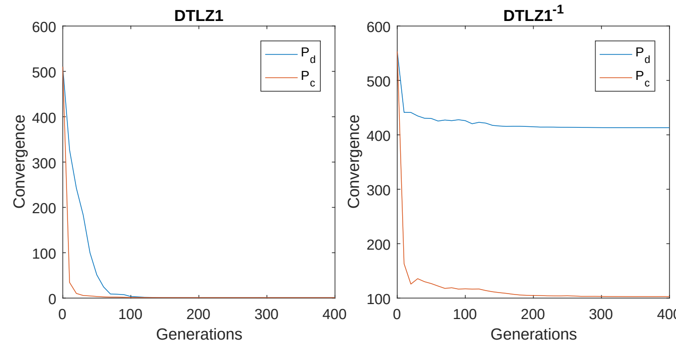

Fig. 8: Online convergence comparisons of two populations.

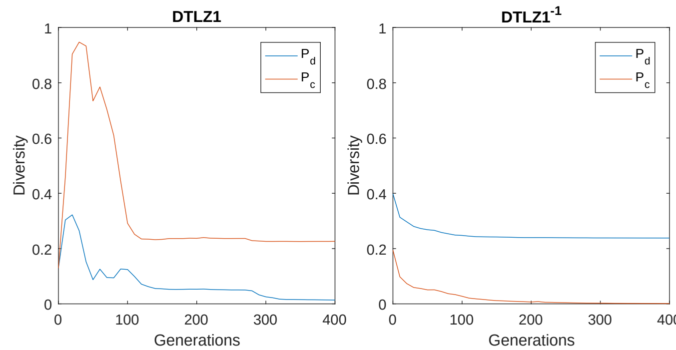

Fig. 9: Online diversity comparisons of two populations.

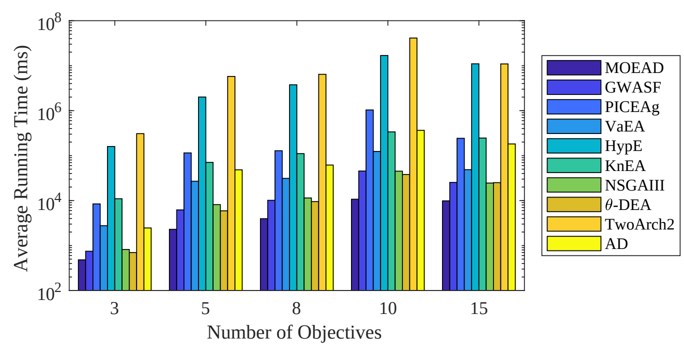

Fig. 10: Comparisons on average running time on WFG and WFG^{-1} test problems.

I. Comparisons on Time Complexity

The average running times of different algorithms on WFG and WFG^{-1} test problems are presented in Fig. 10. Generally speaking, the average running times of different algorithms increase with the number of objectives and the population size. It can be seen from Fig. 10 that the deposition-based EMO algorithms tend to have lower running times than other types of algorithms. Compared with other deposition-based algorithms, the time complexity of the proposed MOEA/AD is moderately higher, which mainly comes from three factors: 1) two populations need to be maintained simultaneously; 2) the estimation of the nadir point requires to compute the current non-dominated solutions in each generation; and 3) the time complexity of the two-level one-one stable matching is $\mathcal{O}(N^2 \log N)$ [5].

J. Demonstration of Final Solution Sets

The final solution sets obtained by different algorithms in the run of median HV metric values with $\mathbf{z}^r = (2, \cdots, 2)^T$ on each test instance are demonstrated in Fig. 11 to Fig. 140. It can be seen from the figures that MOEA/AD is very competitive on regular PF shapes such as hyperplanes and hyperspheres due to the evenly distributed weight vectors. Thanks to the complementary effects of the two subproblem formulations, it can achieve better convergence and diversity on other decomposition-based EMO algorithms, e.g., on 3-objective WFG8 test problem shown in Fig. 22. In contrast, the distribution of the final solution sets obtained by other types of EMO algorithms, e.g., Two_Arch2, VaEA and PICEA-g, are less uniform. However, MOEA/AD still suffers from a common issue of decomposition-based methods, i.e., the irregular PF shapes. The dealing with irregular PF shapes is out of the scope of this paper. Another strength of MOEA/AD is shown on problems with inverted PFs, which can be owed to the adversarial search directions of the two populations.

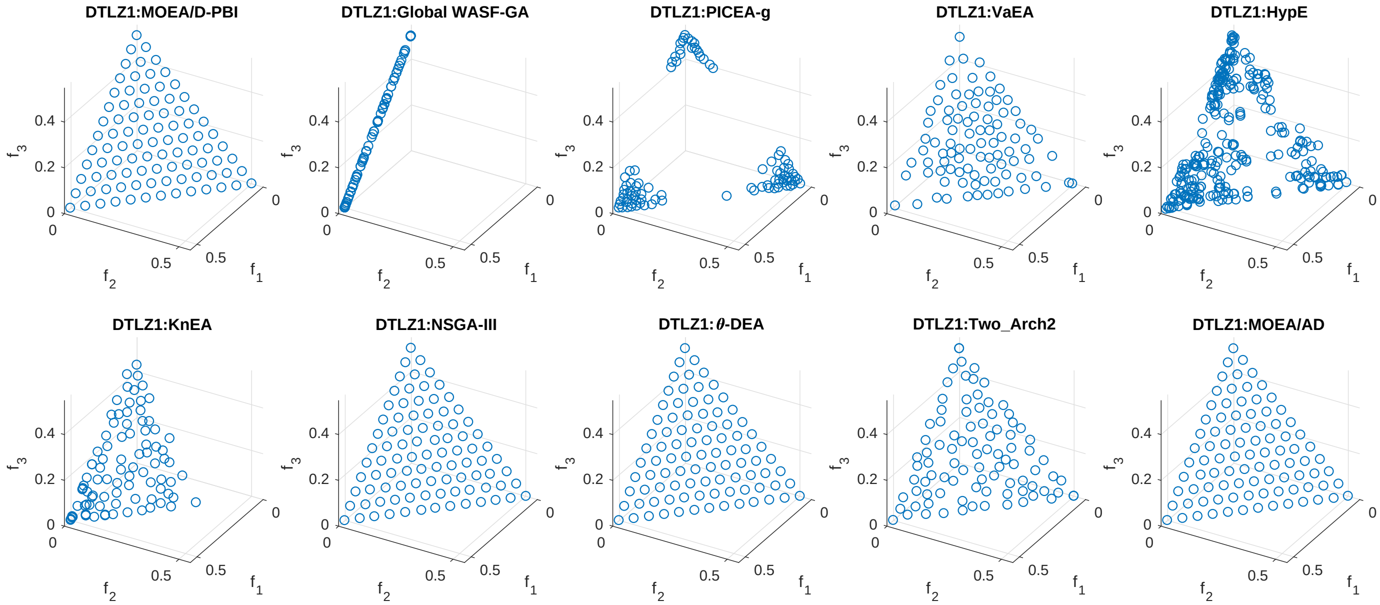

Fig. 11: Final solution sets on 3-objective DTLZ1 test problem obtained by 10 algorithms in the run of median HV metric values with $\mathbf{z}^r = (2, \cdots, 2)^T$.

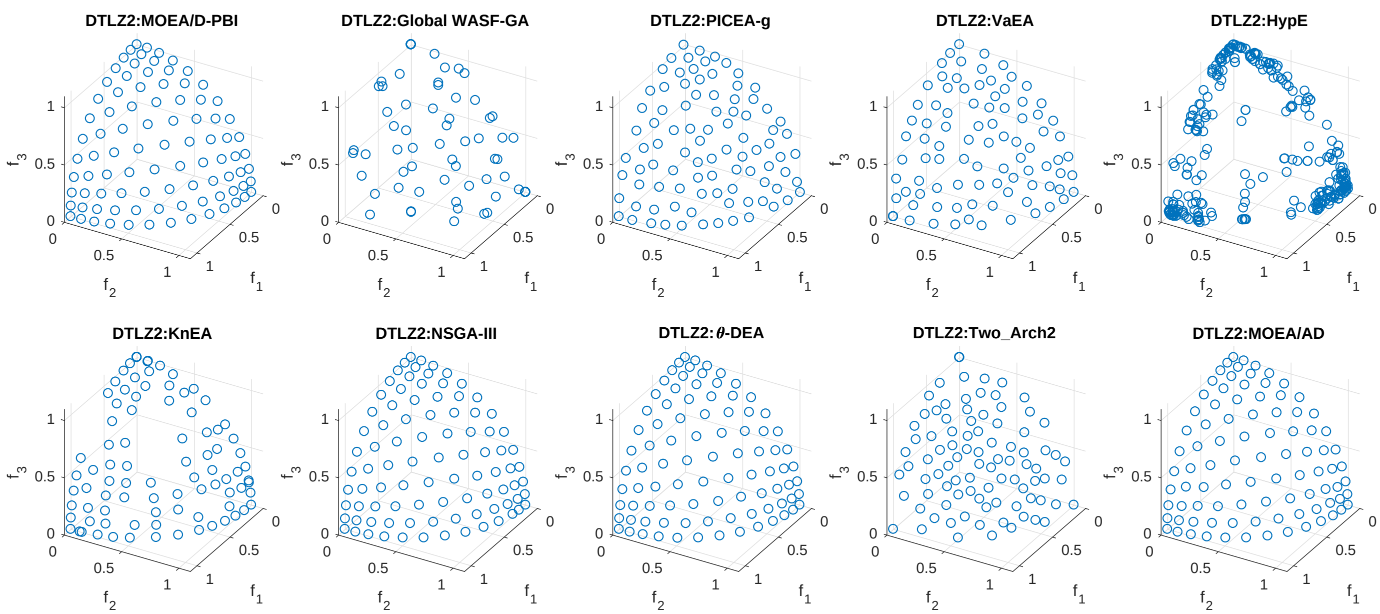

Fig. 12: Final solution sets on 3-objective DTLZ2 test problem obtained by 10 algorithms in the run of median HV metric values with $\mathbf{z}^r = (2, \cdots, 2)^T$.

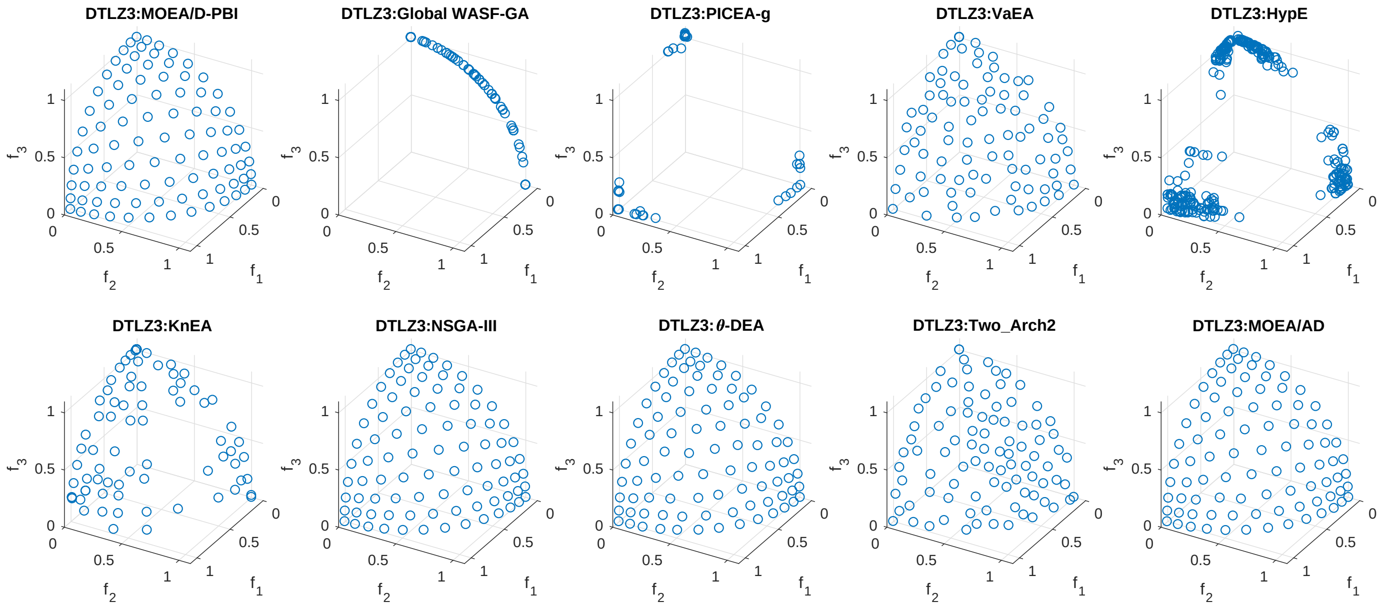

Fig. 13: Final solution sets on 3-objective DTLZ3 test problem obtained by 10 algorithms in the run of median HV metric values with $\mathbf{z}^r = (2, \cdots, 2)^T$.

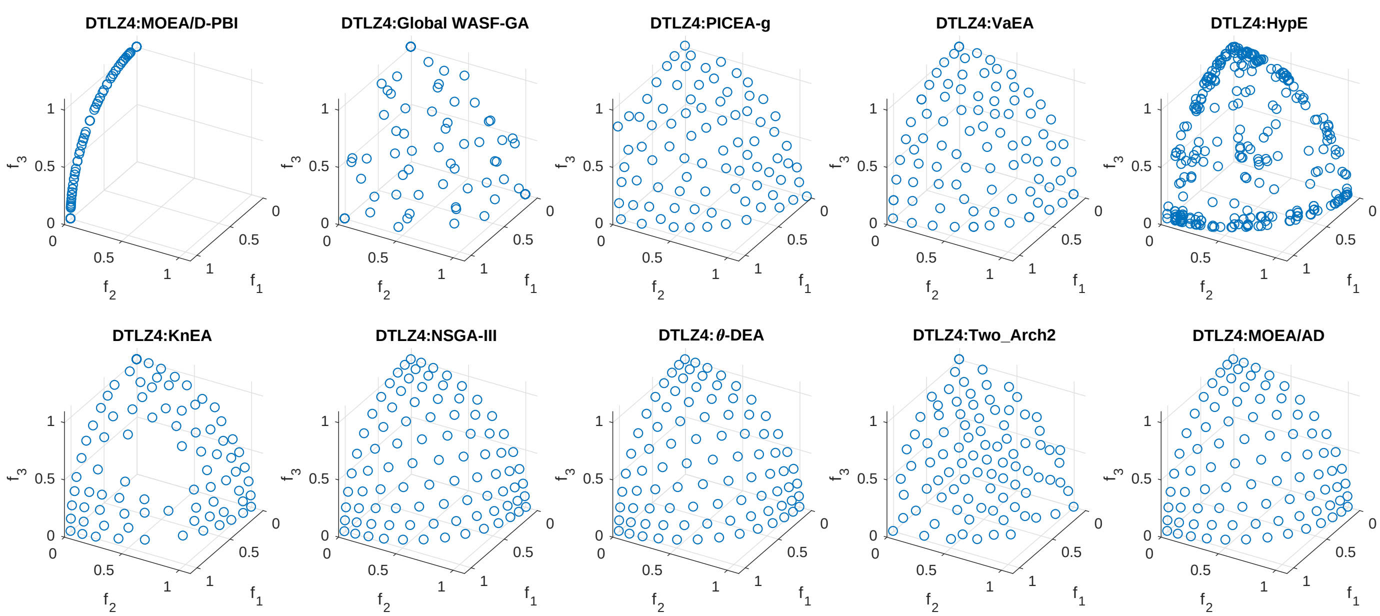

Fig. 14: Final solution sets on 3-objective DTLZ4 test problem obtained by 10 algorithms in the run of median HV metric values with $\mathbf{z}^r = (2, \cdots, 2)^T$.

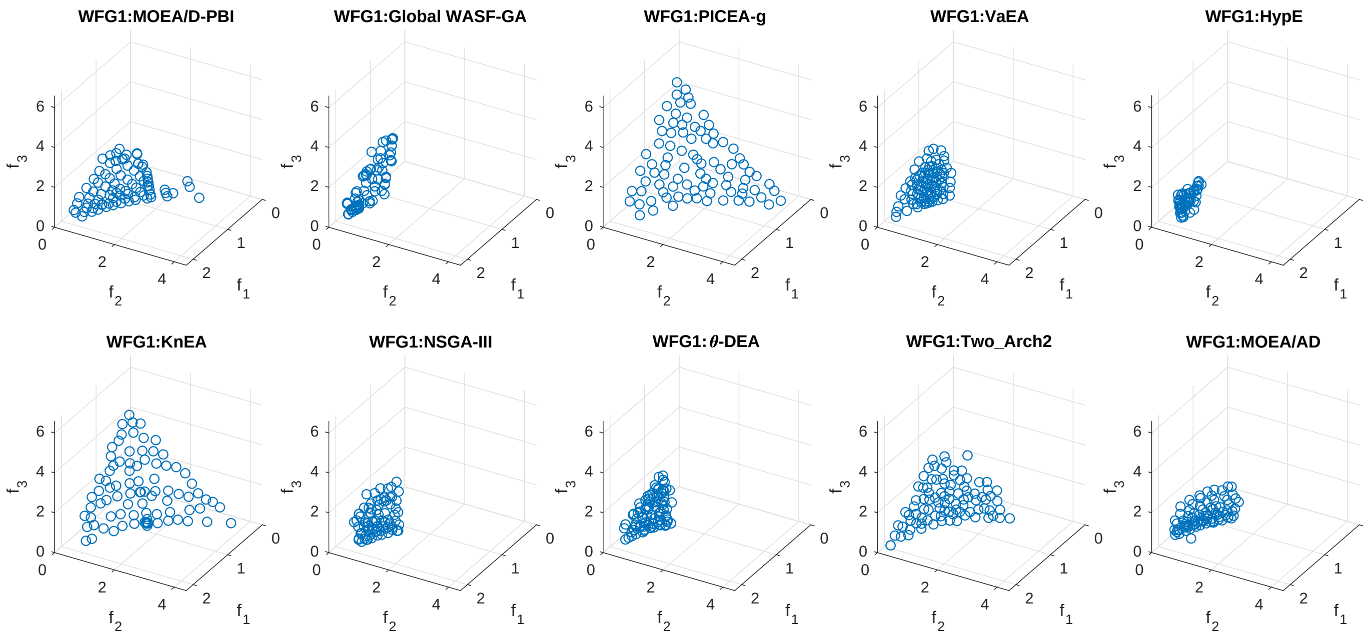

Fig. 15: Final solution sets on 3-objective WFG1 test problem obtained by 10 algorithms in the run of median HV metric values with $\mathbf{z}^r = (2, \cdots, 2)^T$.

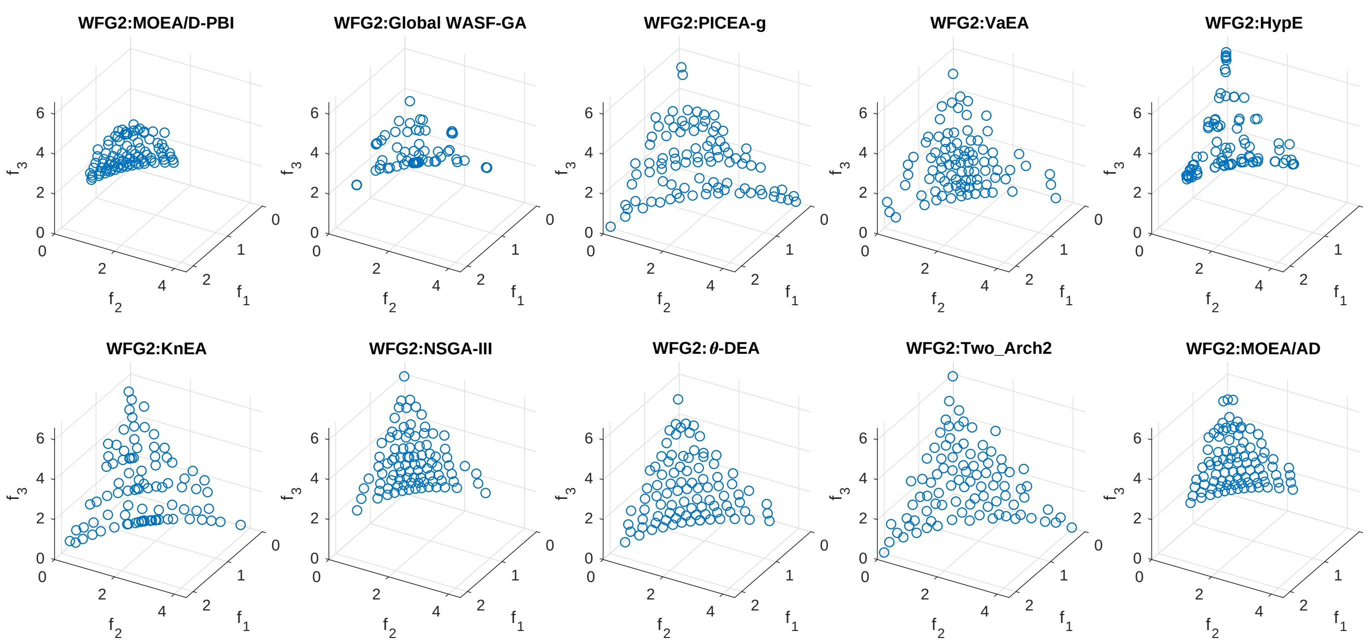

Fig. 16: Final solution sets on 3-objective WFG2 test problem obtained by 10 algorithms in the run of median HV metric values with $\mathbf{z}^r = (2, \cdots, 2)^T$.

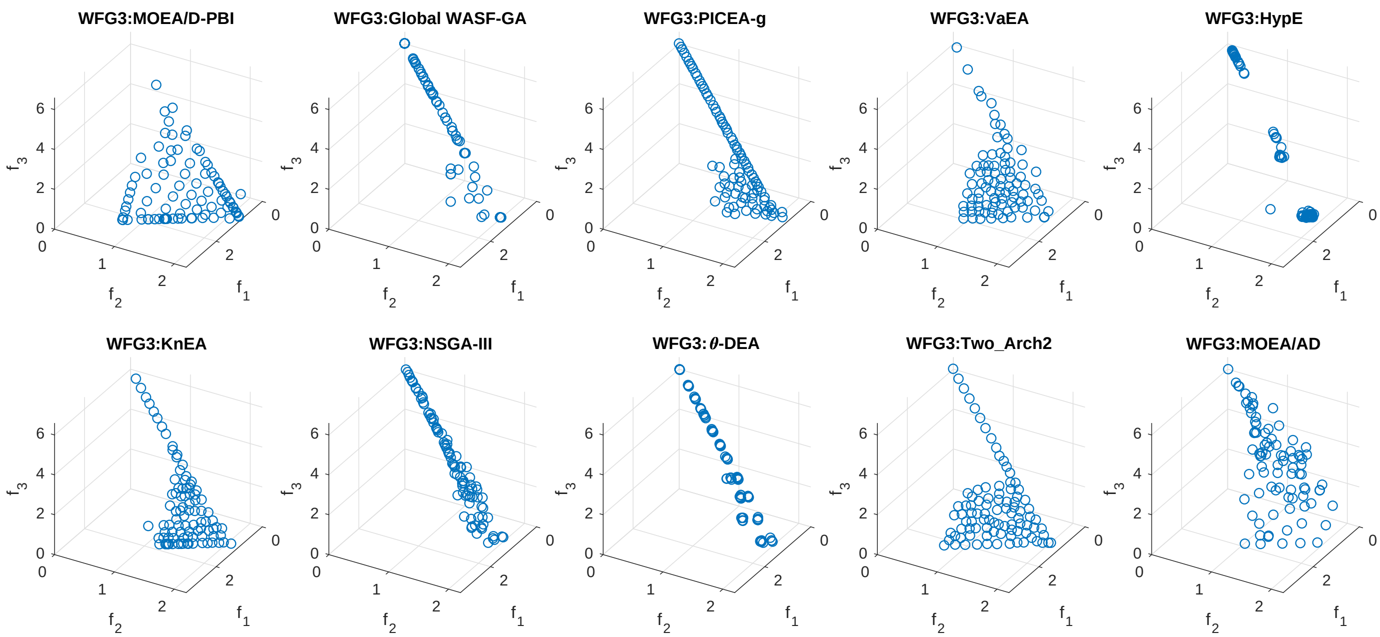

Fig. 17: Final solution sets on 3-objective WFG3 test problem obtained by 10 algorithms in the run of median HV metric values with $\mathbf{z}^r = (2, \cdots, 2)^T$.

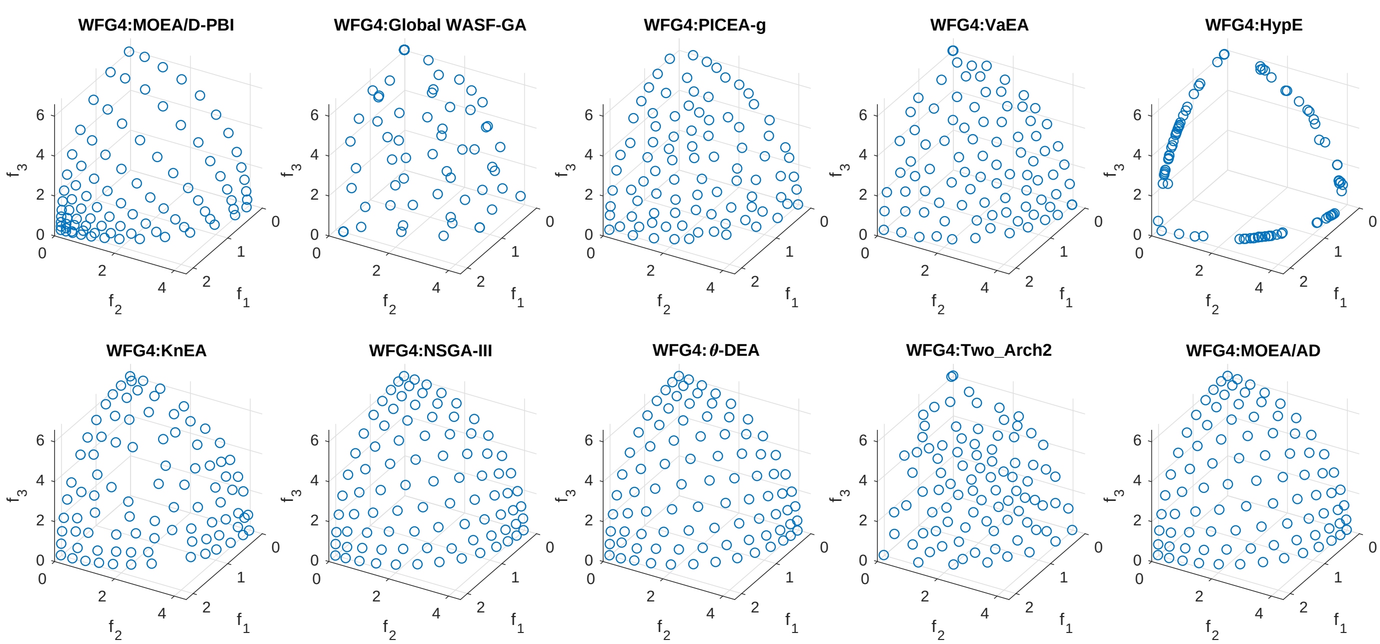

Fig. 18: Final solution sets on 3-objective WFG4 test problem obtained by 10 algorithms in the run of median HV metric values with $\mathbf{z}^r = (2, \cdots, 2)^T$.

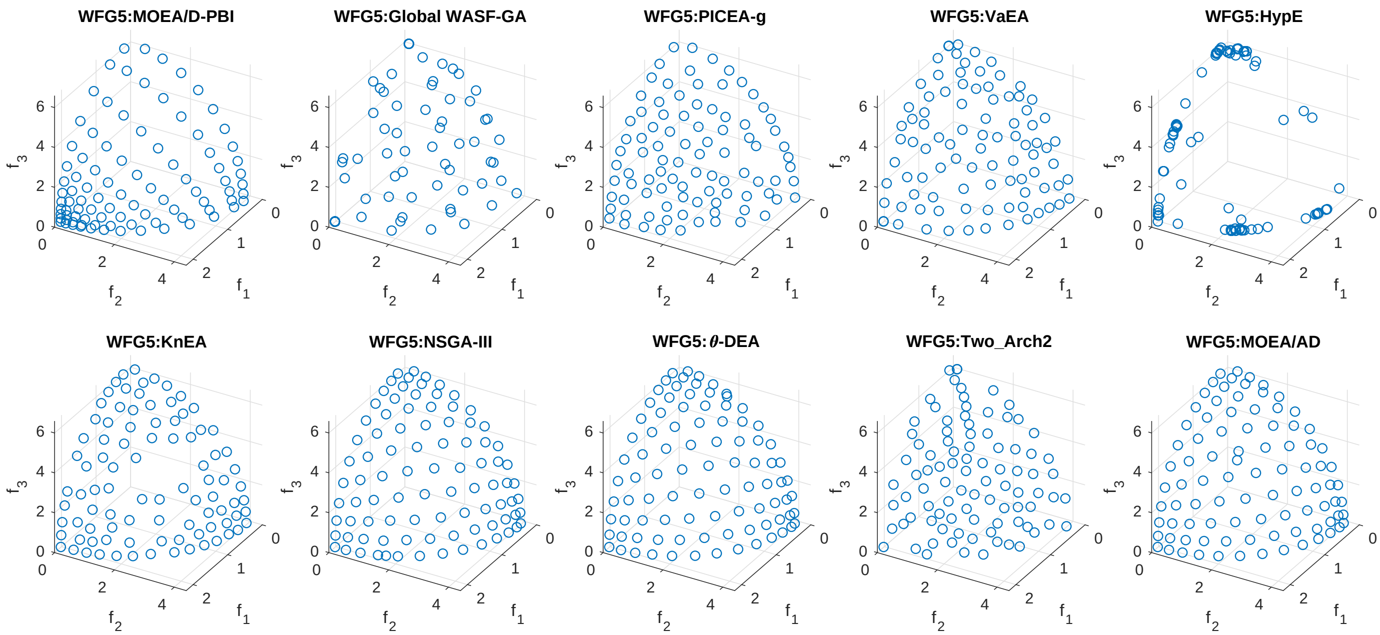

Fig. 19: Final solution sets on 3-objective WFG5 test problem obtained by 10 algorithms in the run of median HV metric values with $\mathbf{z}^r = (2, \cdots, 2)^T$.

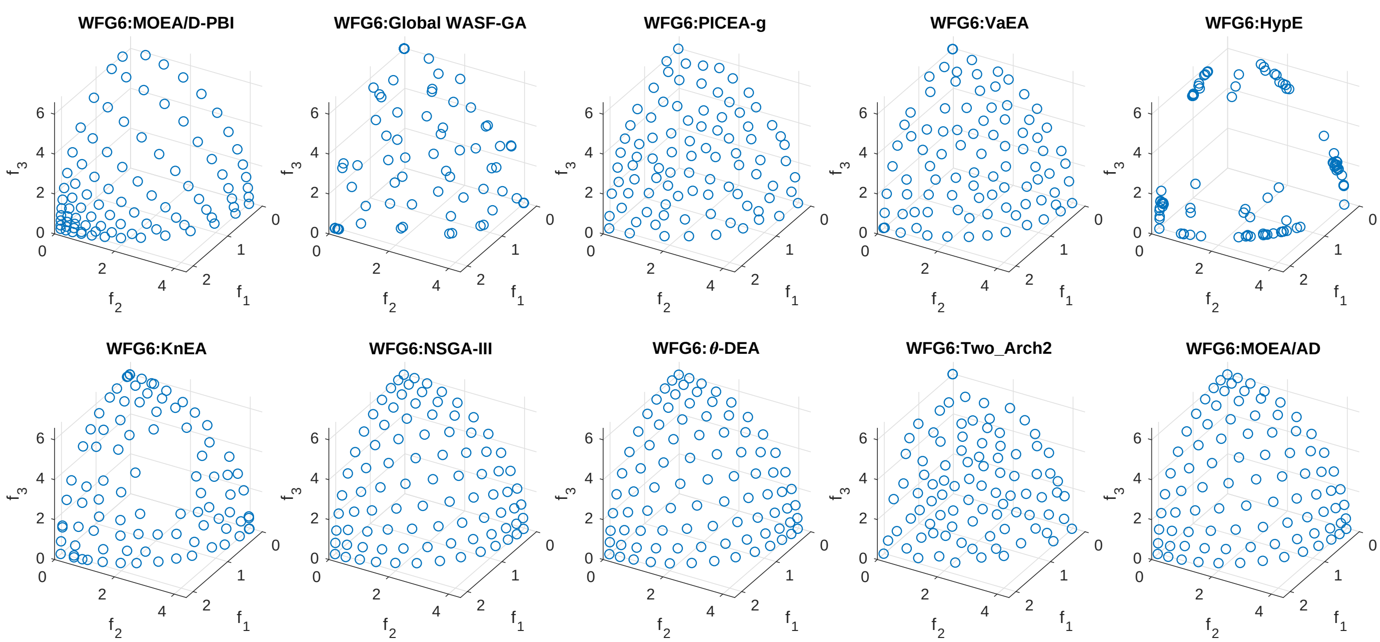

Fig. 20: Final solution sets on 3-objective WFG6 test problem obtained by 10 algorithms in the run of median HV metric values with $\mathbf{z}^r = (2, \cdots, 2)^T$.

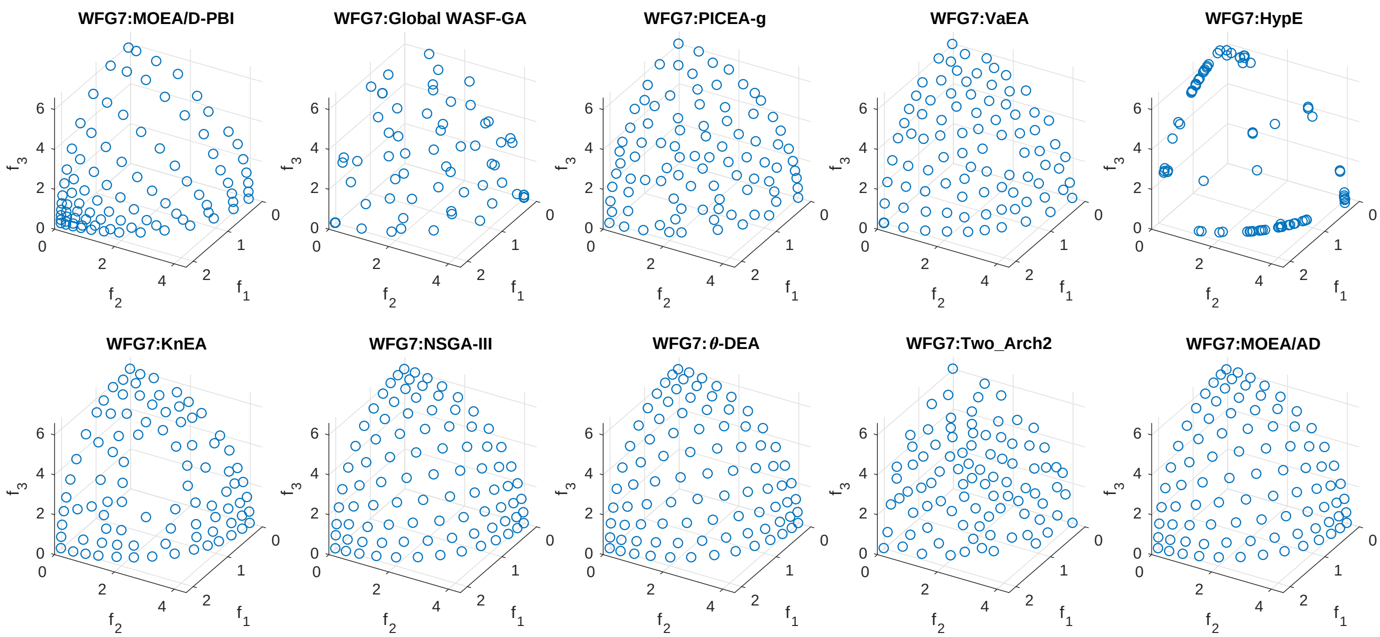

Fig. 21: Final solution sets on 3-objective WFG7 test problem obtained by 10 algorithms in the run of median HV metric values with $\mathbf{z}^r = (2, \cdots, 2)^T$.

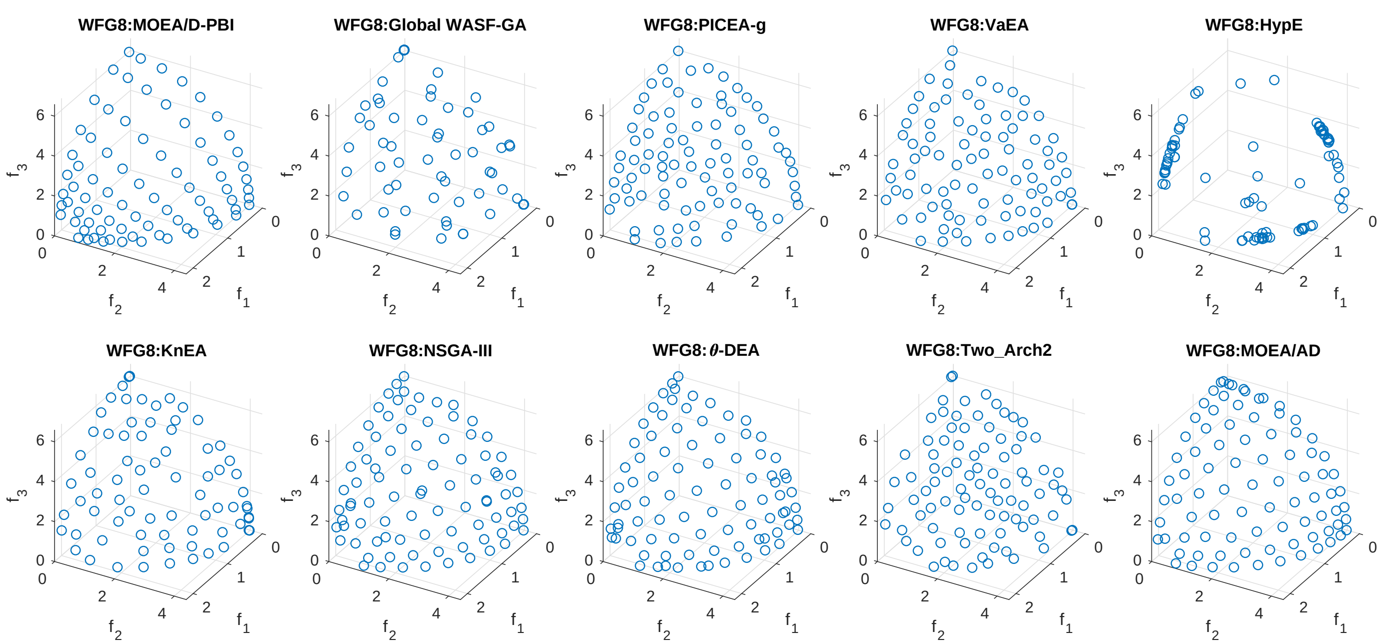

Fig. 22: Final solution sets on 3-objective WFG8 test problem obtained by 10 algorithms in the run of median HV metric values with $\mathbf{z}^r = (2, \cdots, 2)^T$.

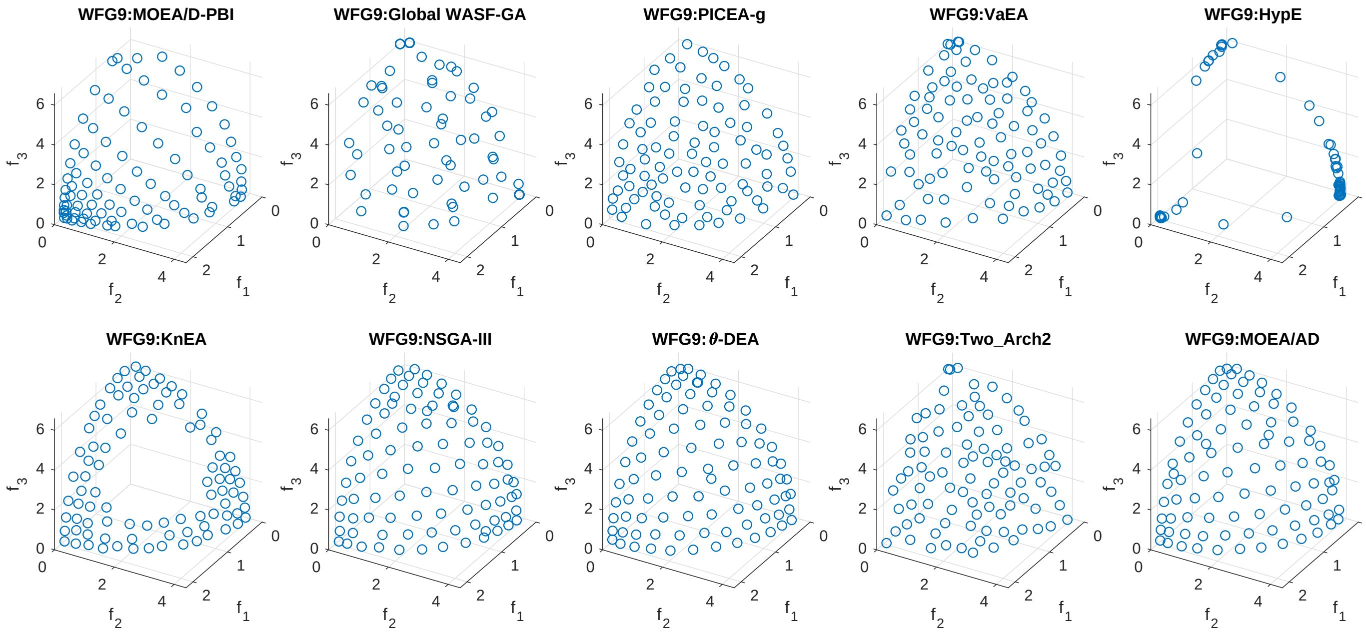

Fig. 23: Final solution sets on 3-objective WFG9 test problem obtained by 10 algorithms in the run of median HV metric values with $\mathbf{z}^r = (2, \cdots, 2)^T$.

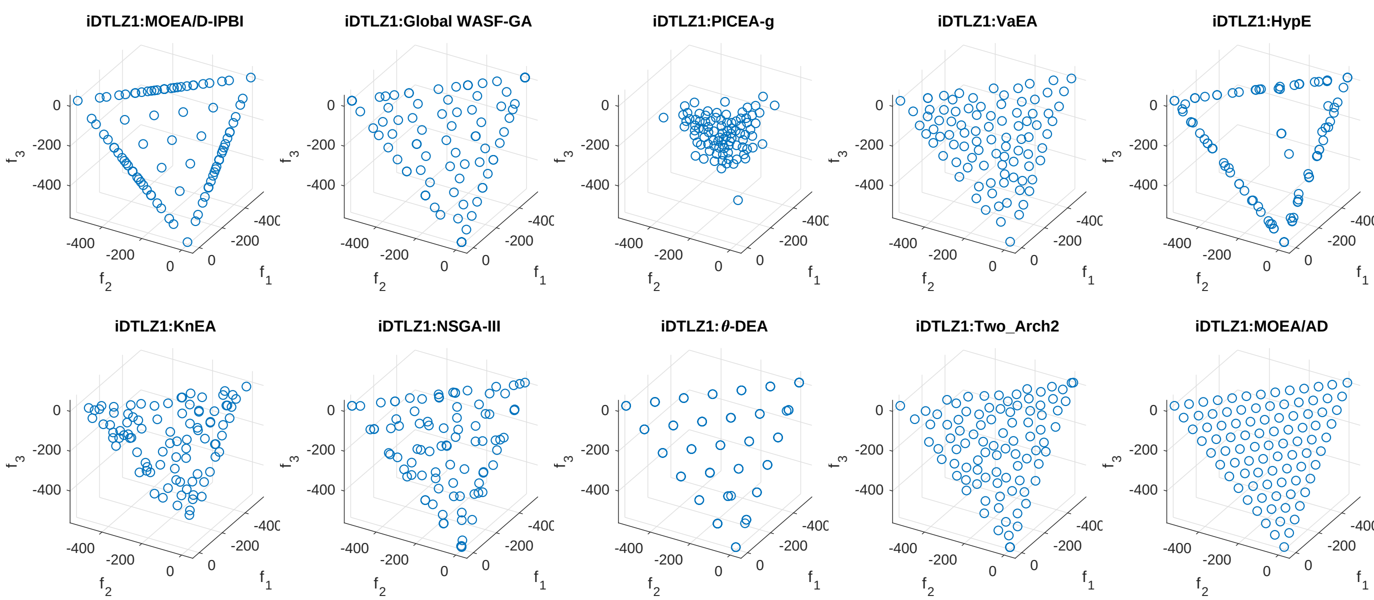

Fig. 24: Final solution sets on 3-objective DTLZ1^{-1} test problem obtained by 10 algorithms in the run of median HV metric values with $\mathbf{z}^r = (2, \cdots, 2)^T$.

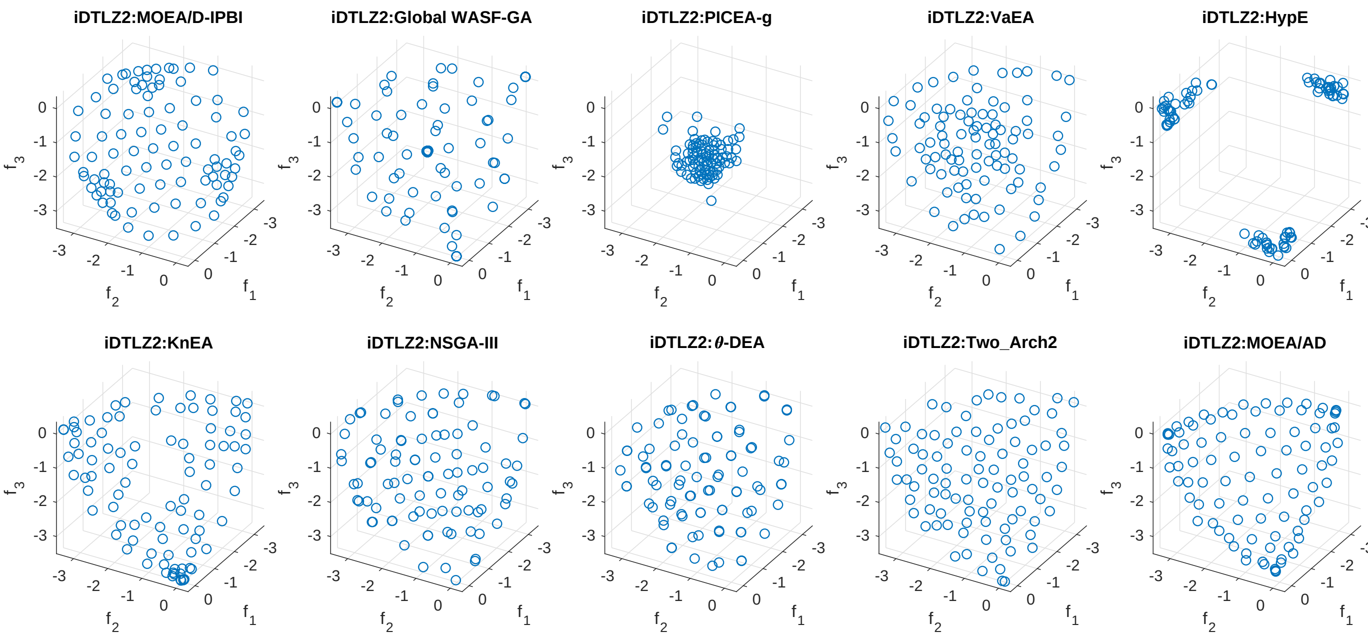

Fig. 25: Final solution sets on 3-objective DTLZ2^{-1} test problem obtained by 10 algorithms in the run of median HV metric values with $\mathbf{z}^r = (2, \cdots, 2)^T$.

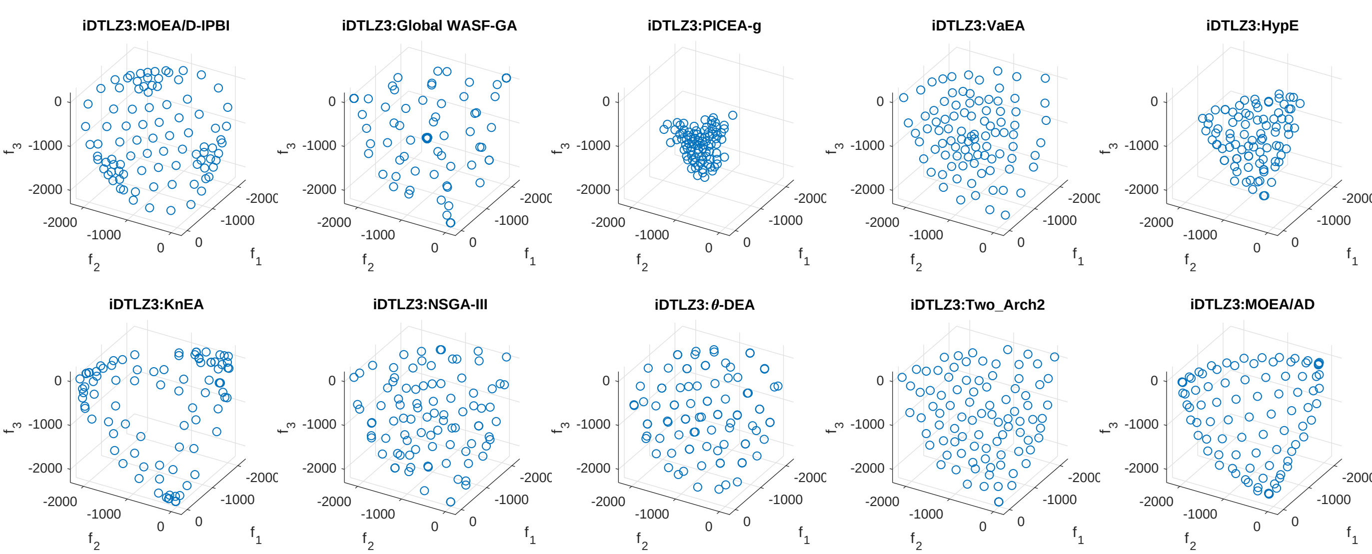

Fig. 26: Final solution sets on 3-objective DTLZ3^{-1} test problem obtained by 10 algorithms in the run of median HV metric values with $\mathbf{z}^r = (2, \cdots, 2)^T$.

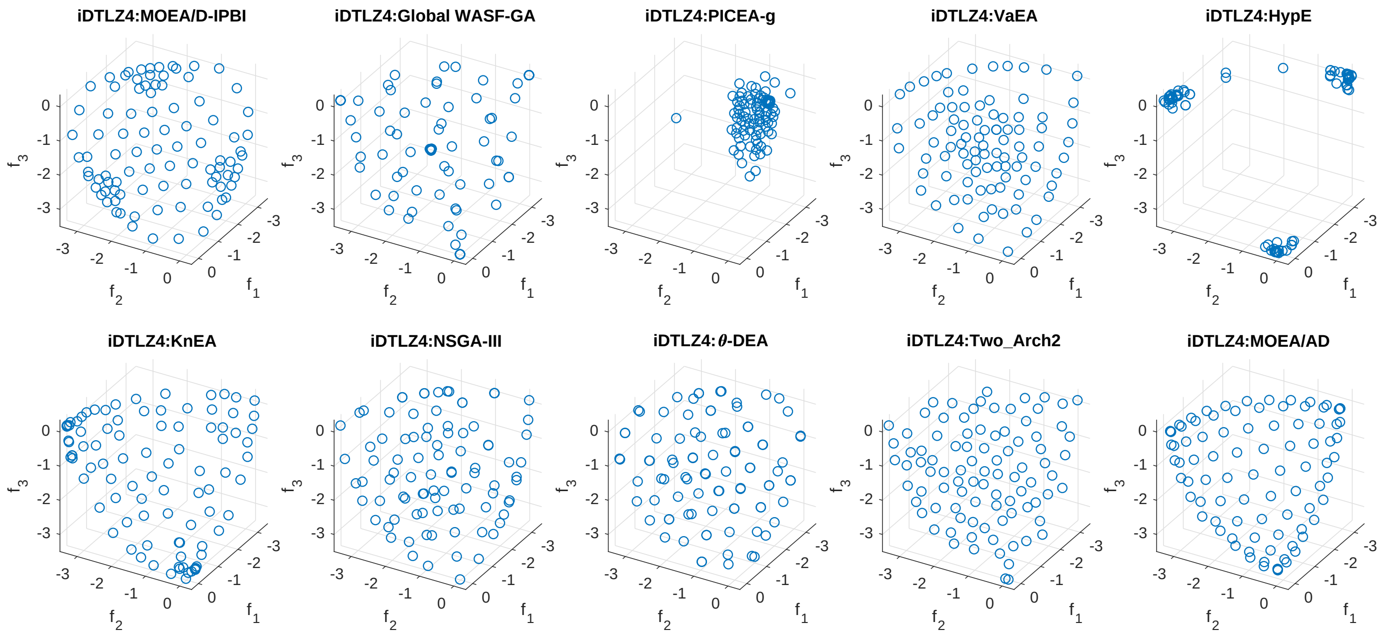

Fig. 27: Final solution sets on 3-objective DTLZ4^{-1} test problem obtained by 10 algorithms in the run of median HV metric values with $\mathbf{z}^r = (2, \cdots, 2)^T$.

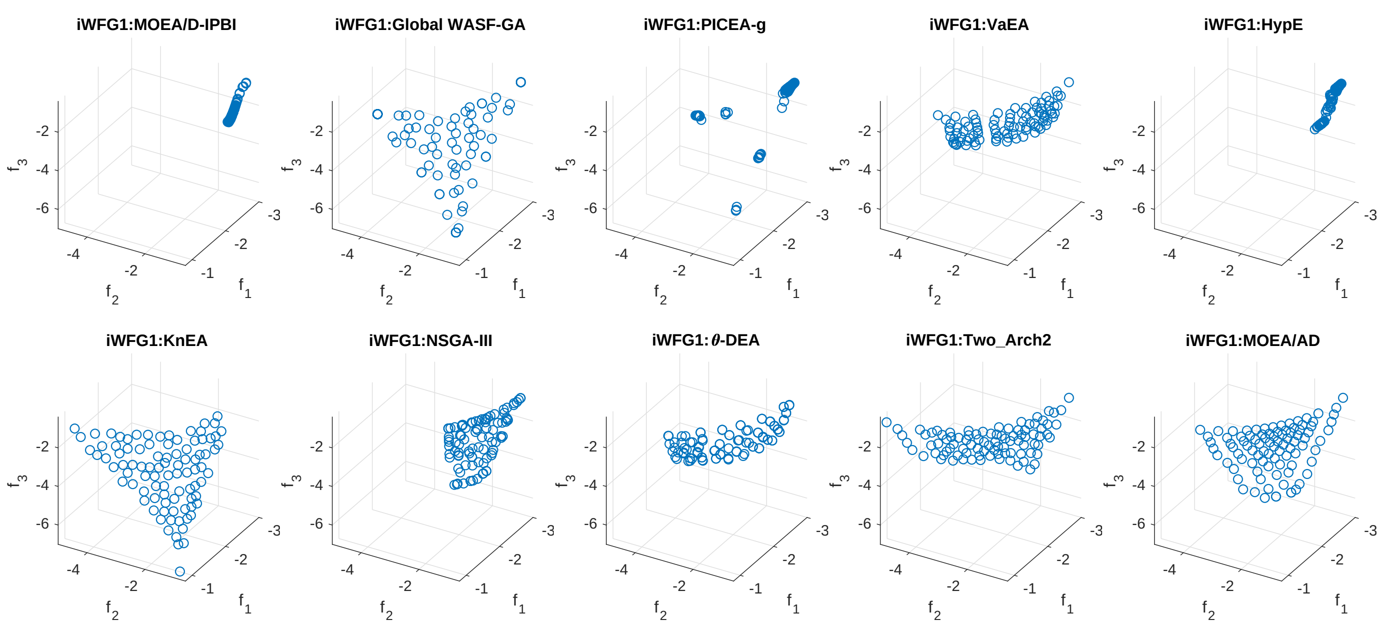

Fig. 28: Final solution sets on 3-objective WFG1^{-1} test problem obtained by 10 algorithms in the run of median HV metric values with $\mathbf{z}^r = (2, \cdots, 2)^T$.

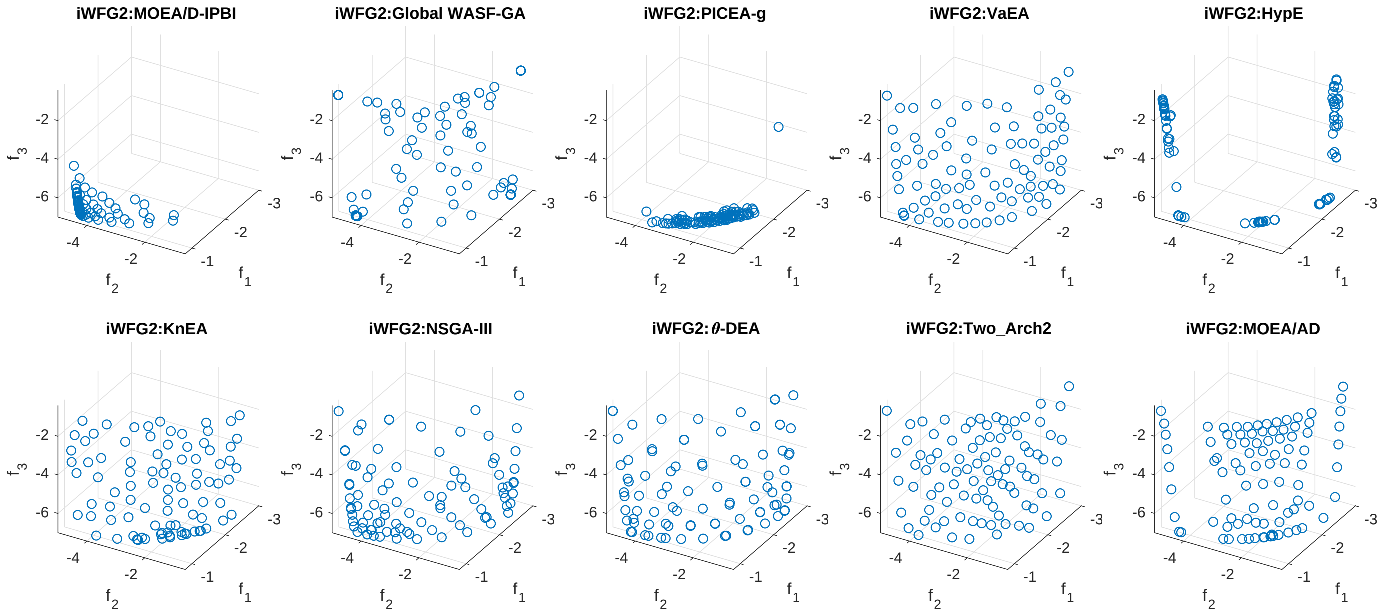

Fig. 29: Final solution sets on 3-objective WFG2^{-1} test problem obtained by 10 algorithms in the run of median HV metric values with $\mathbf{z}^r = (2, \cdots, 2)^T$.

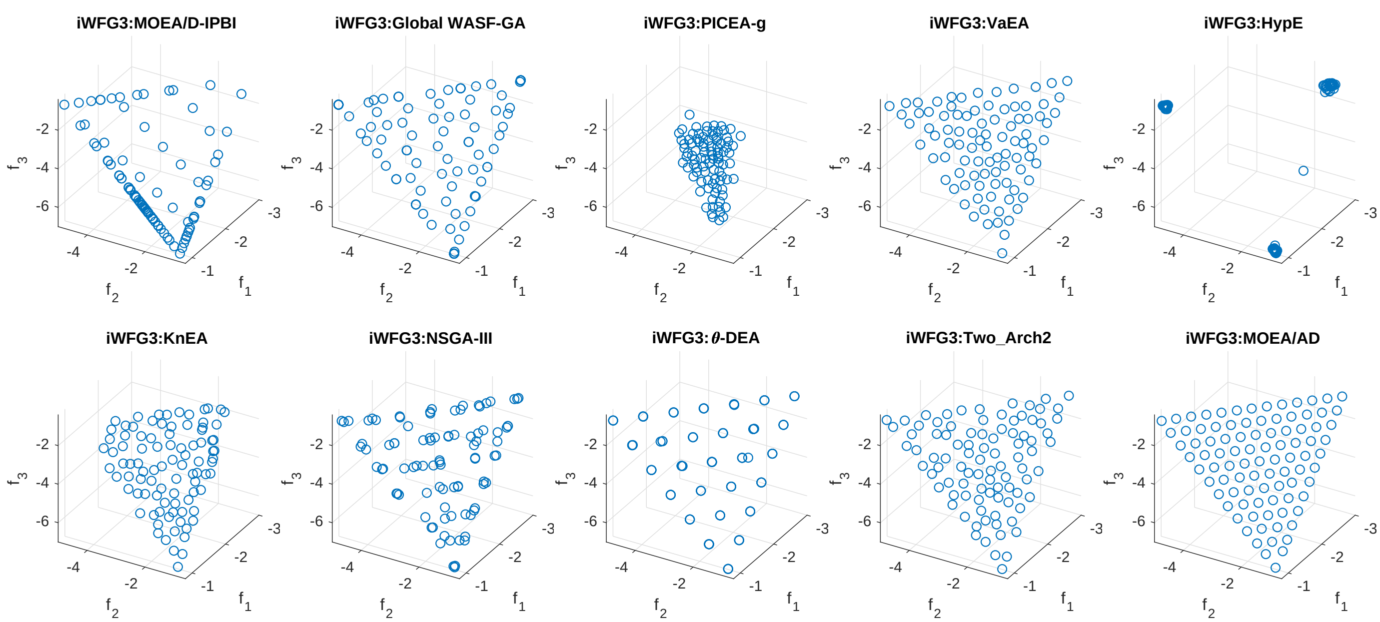

Fig. 30: Final solution sets on 3-objective WFG3^{-1} test problem obtained by 10 algorithms in the run of median HV metric values with $\mathbf{z}^r = (2, \cdots, 2)^T$.

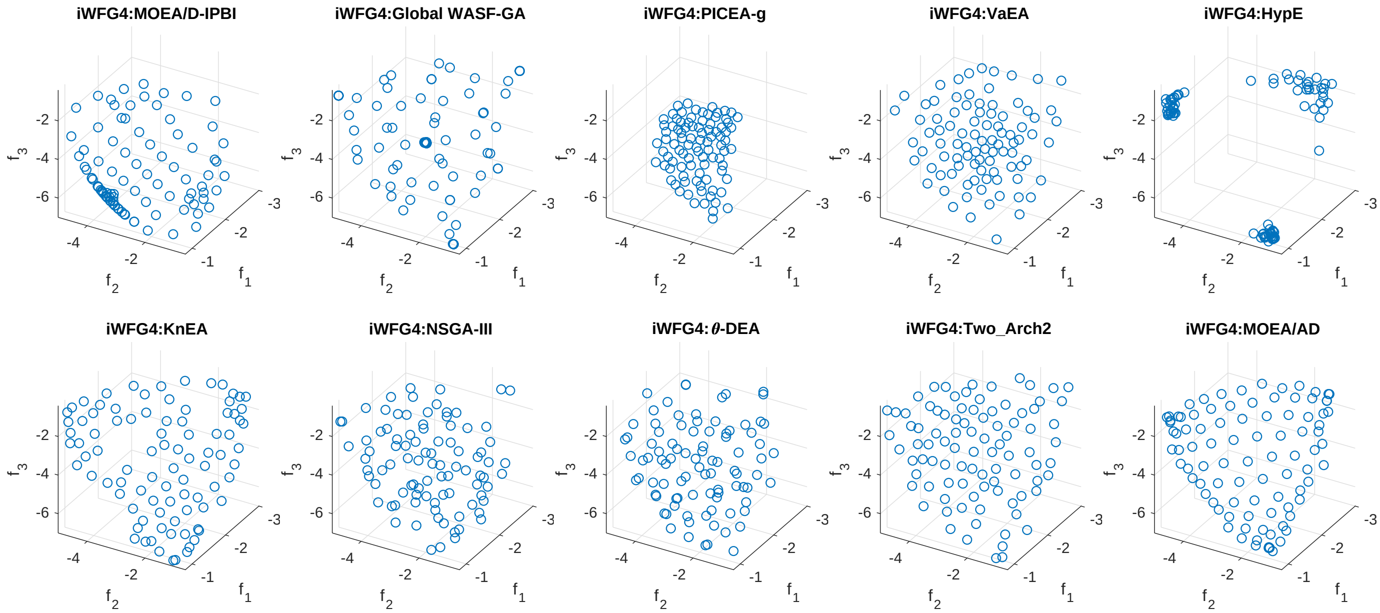

Fig. 31: Final solution sets on 3-objective WFG4^{-1} test problem obtained by 10 algorithms in the run of median HV metric values with $\mathbf{z}^r = (2, \cdots, 2)^T$.

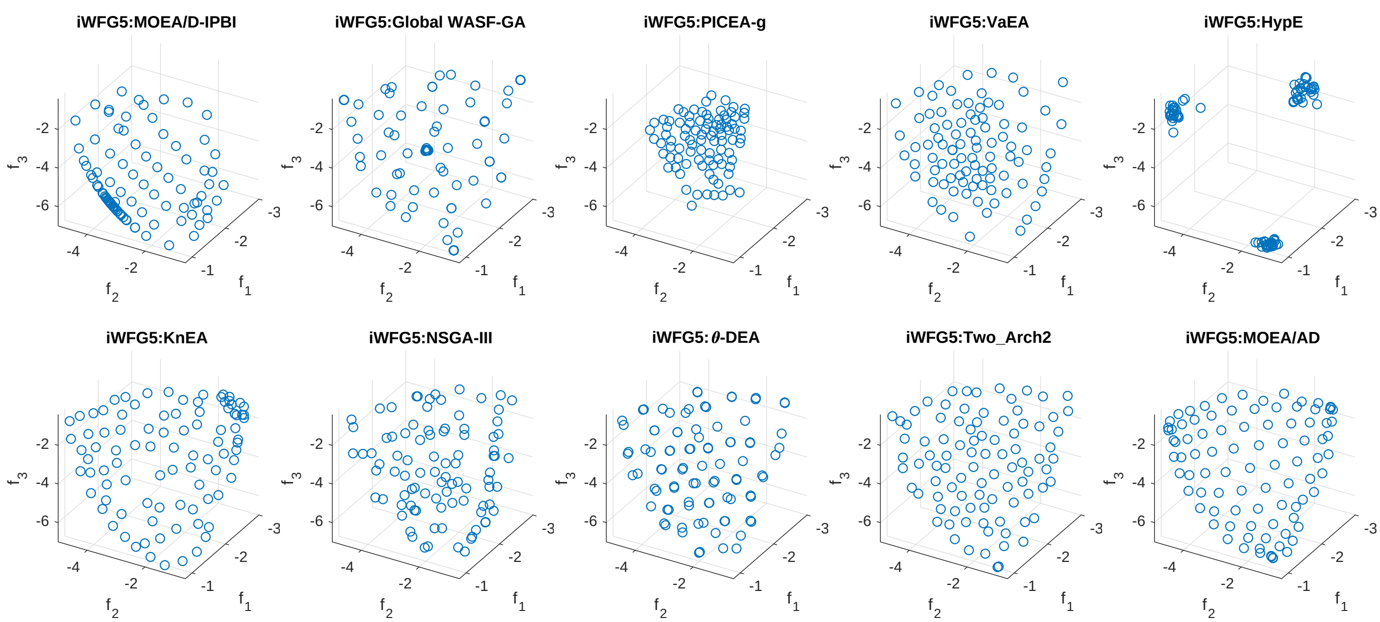

Fig. 32: Final solution sets on 3-objective WFG5^{-1} test problem obtained by 10 algorithms in the run of median HV metric values with $\mathbf{z}^r = (2, \cdots, 2)^T$.

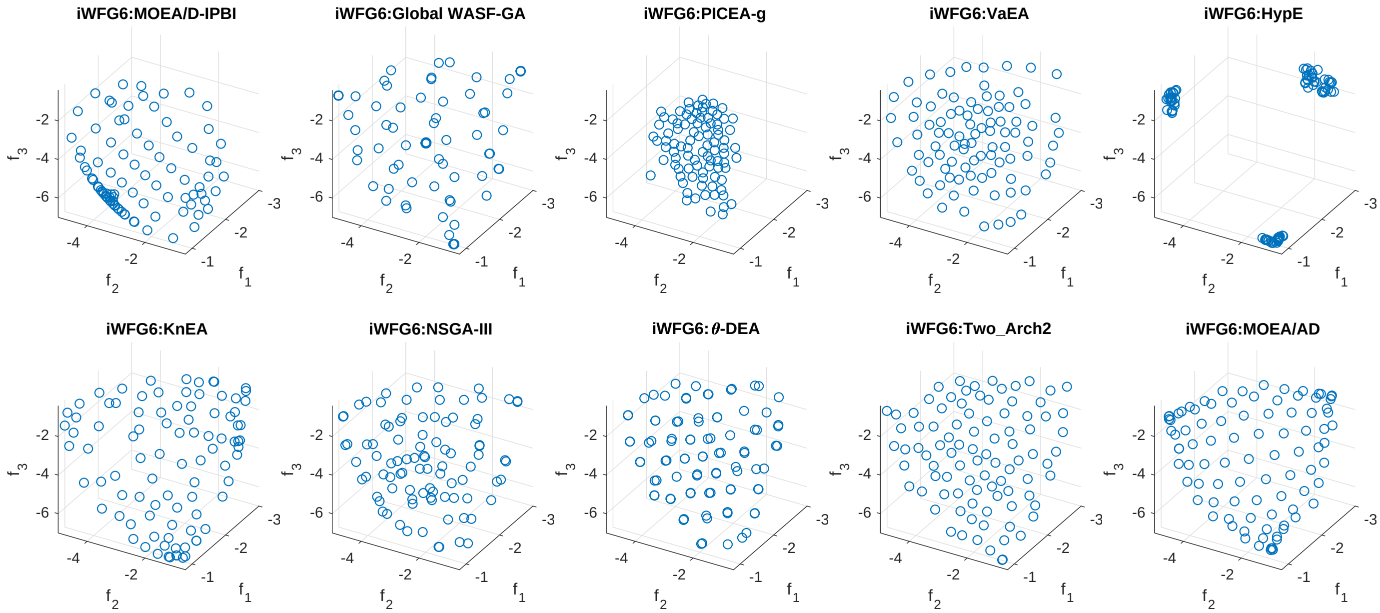

Fig. 33: Final solution sets on 3-objective WFG6^{-1} test problem obtained by 10 algorithms in the run of median HV metric values with $\mathbf{z}^r = (2, \cdots, 2)^T$.

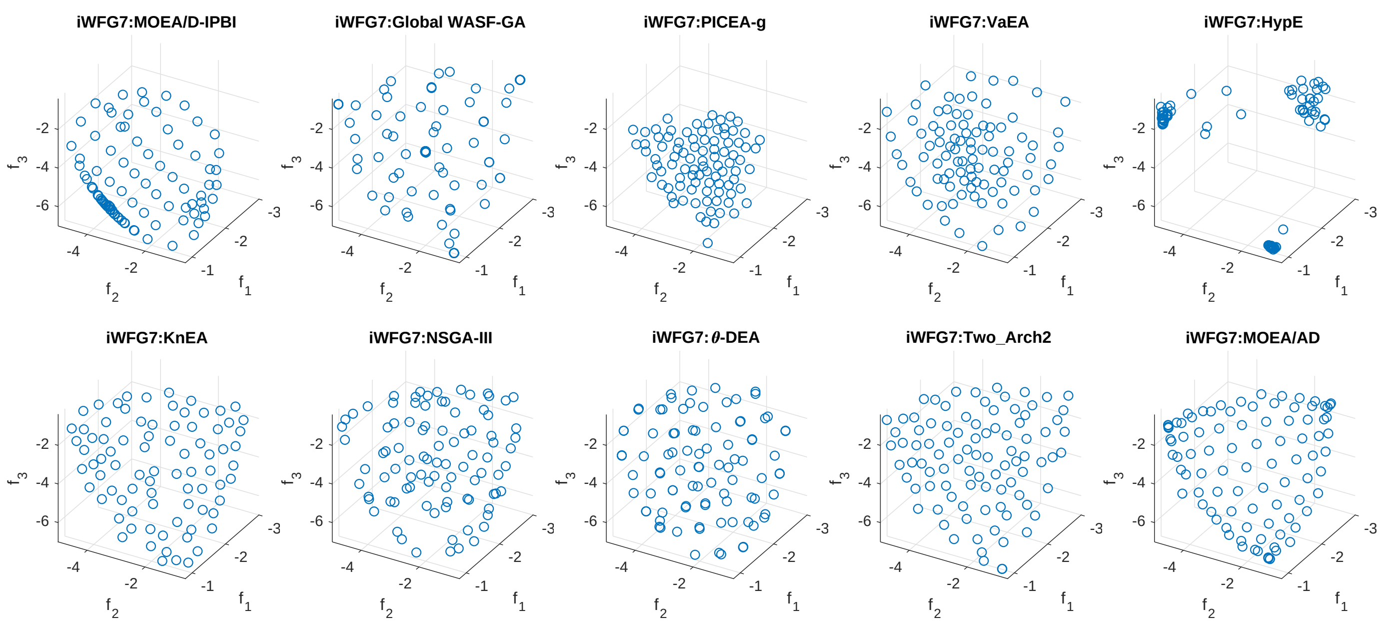

Fig. 34: Final solution sets on 3-objective WFG7^{-1} test problem obtained by 10 algorithms in the run of median HV metric values with $\mathbf{z}^r = (2, \cdots, 2)^T$.

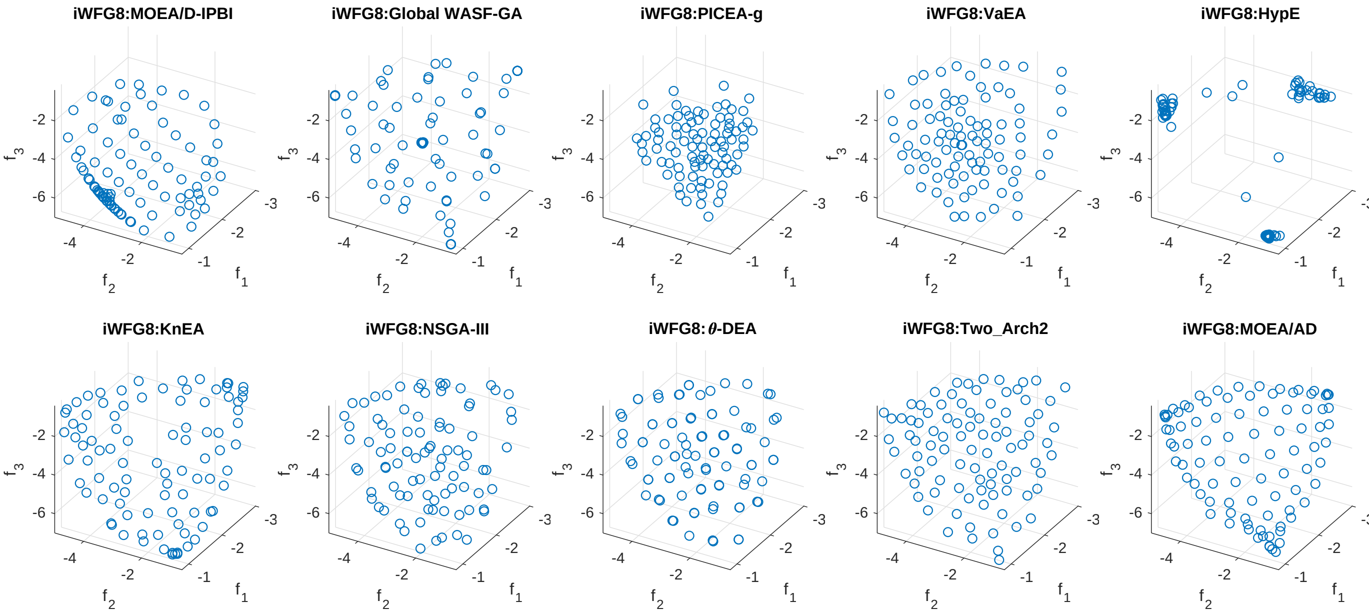

Fig. 35: Final solution sets on 3-objective WFG8^{-1} test problem obtained by 10 algorithms in the run of median HV metric values with $\mathbf{z}^r = (2, \cdots, 2)^T$.

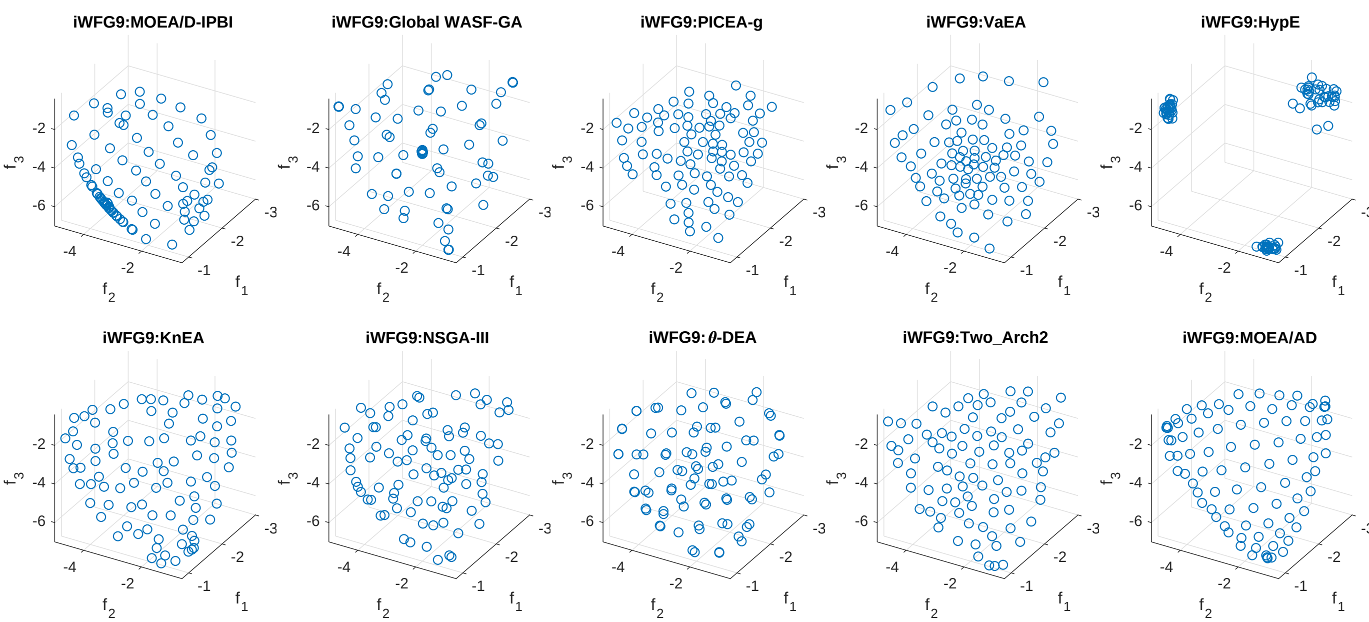

Fig. 36: Final solution sets on 3-objective WFG9^{-1} test problem obtained by 10 algorithms in the run of median HV metric values with $\mathbf{z}^r = (2, \cdots, 2)^T$.

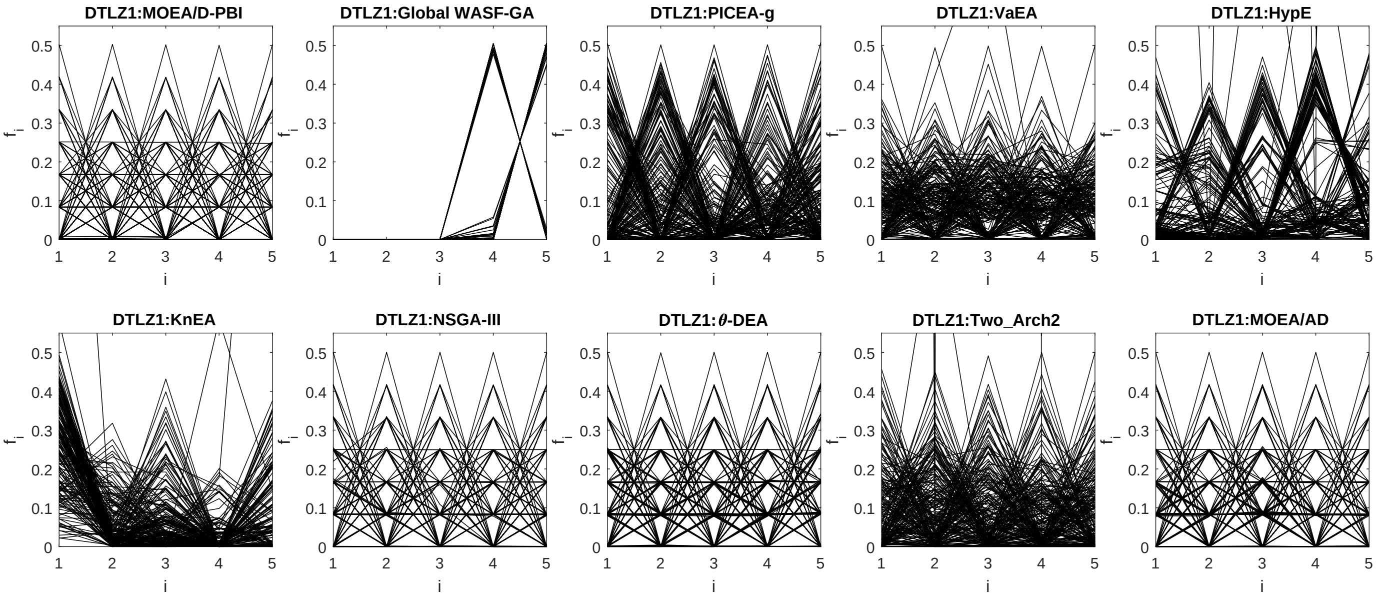

Fig. 37: Final solution sets on 5-objective DTLZ1 test problem obtained by 10 algorithms in the run of median HV metric values with $\mathbf{z}^r = (2, \cdots, 2)^T$.

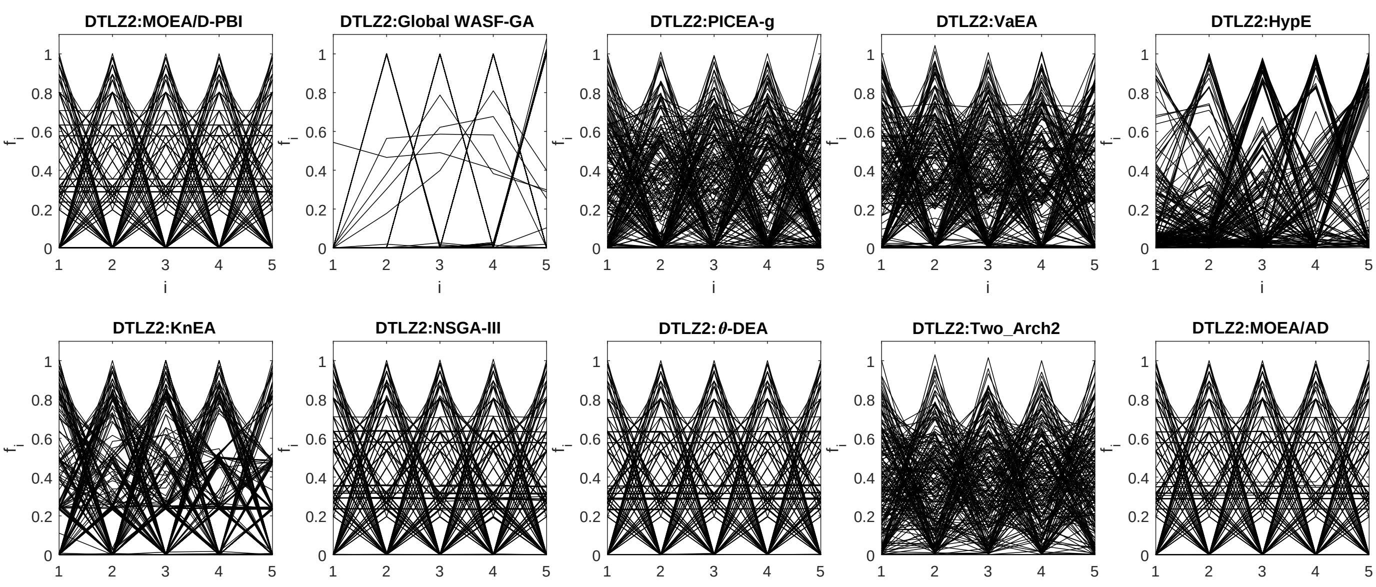

Fig. 38: Final solution sets on 5-objective DTLZ2 test problem obtained by 10 algorithms in the run of median HV metric values with $\mathbf{z}^r = (2, \cdots, 2)^T$.

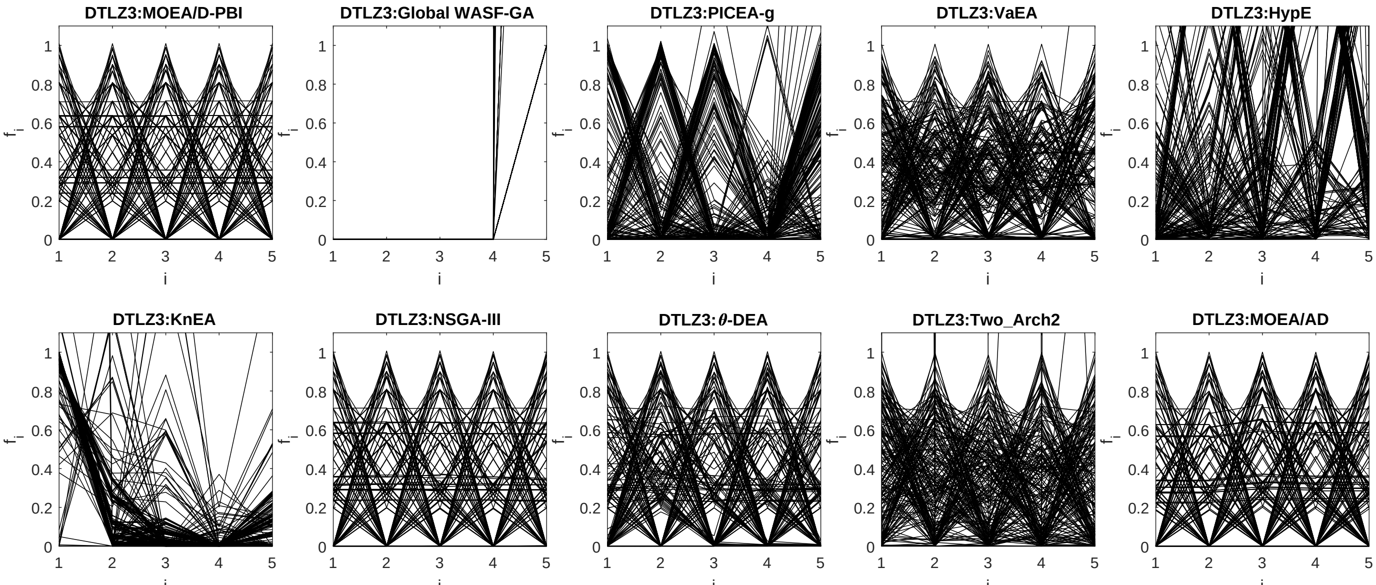

Fig. 39: Final solution sets on 5-objective DTLZ3 test problem obtained by 10 algorithms in the run of median HV metric values with $\mathbf{z}^r = (2, \cdots, 2)^T$.

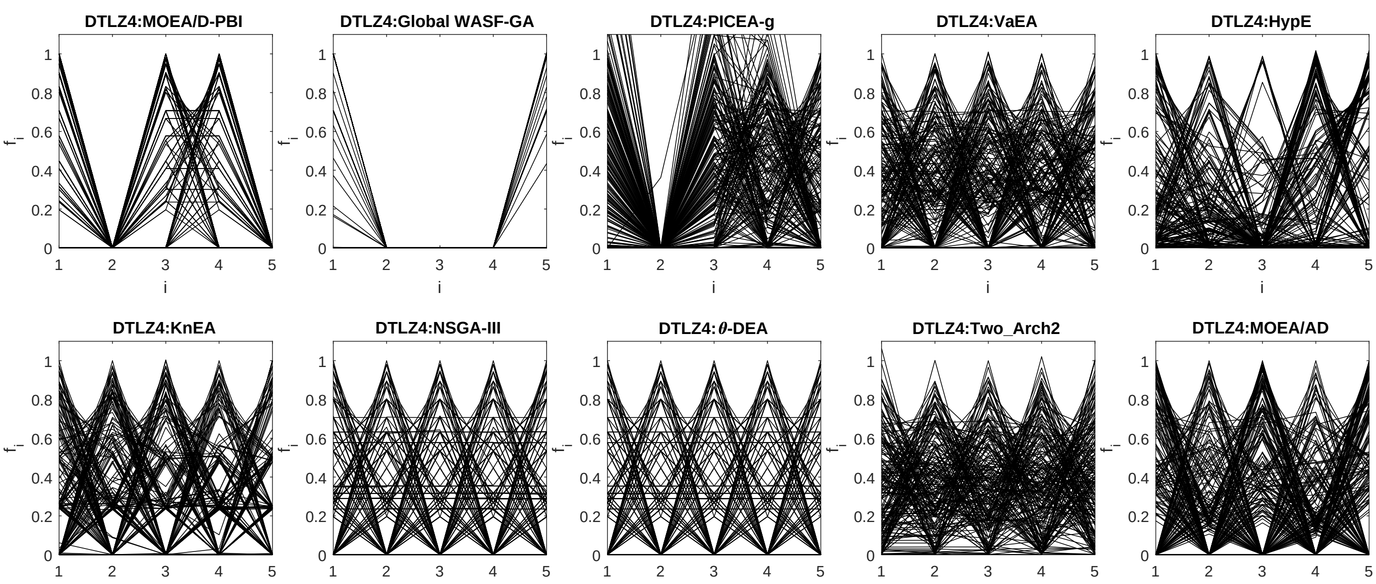

Fig. 40: Final solution sets on 5-objective DTLZ4 test problem obtained by 10 algorithms in the run of median HV metric values with $\mathbf{z}^r = (2, \cdots, 2)^T$.

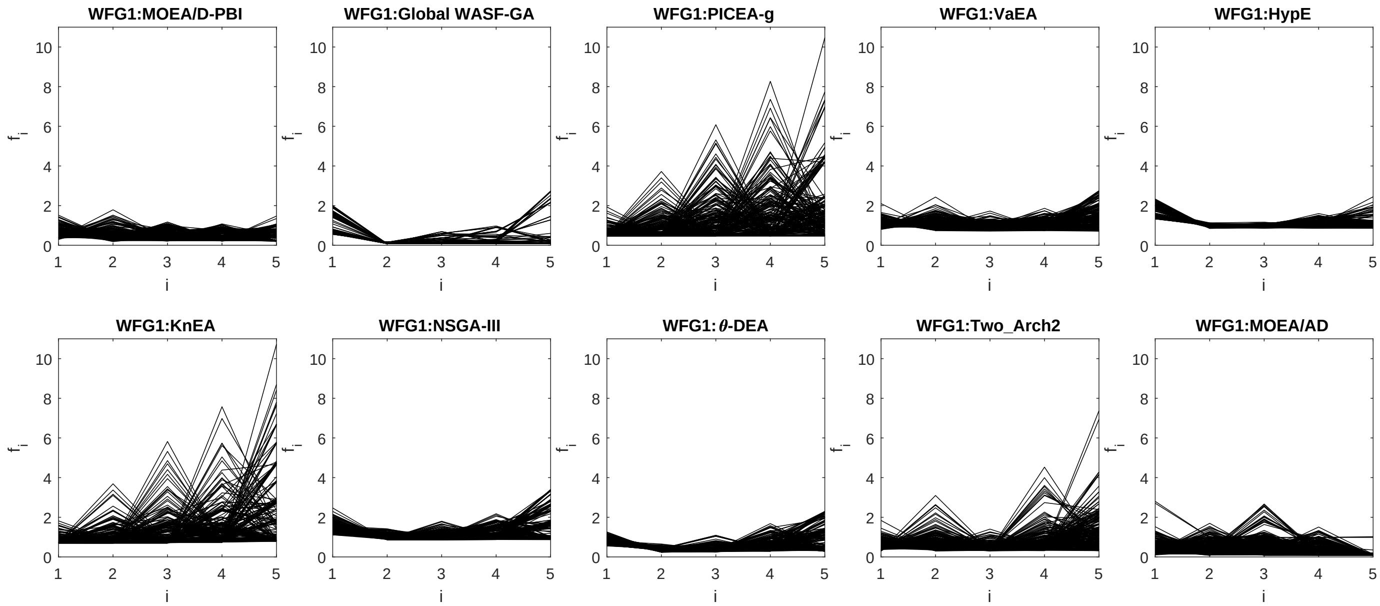

Fig. 41: Final solution sets on 5-objective WFG1 test problem obtained by 10 algorithms in the run of median HV metric values with $\mathbf{z}^r = (2, \cdots, 2)^T$.

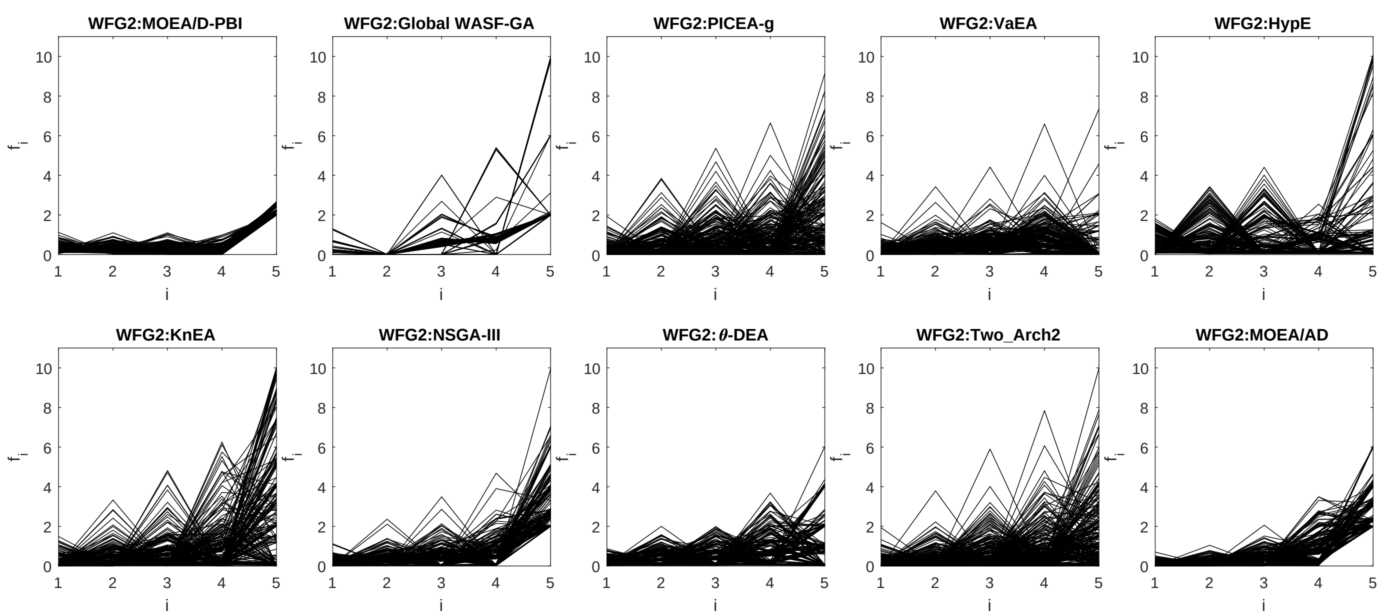

Fig. 42: Final solution sets on 5-objective WFG2 test problem obtained by 10 algorithms in the run of median HV metric values with $\mathbf{z}^r = (2, \cdots, 2)^T$.

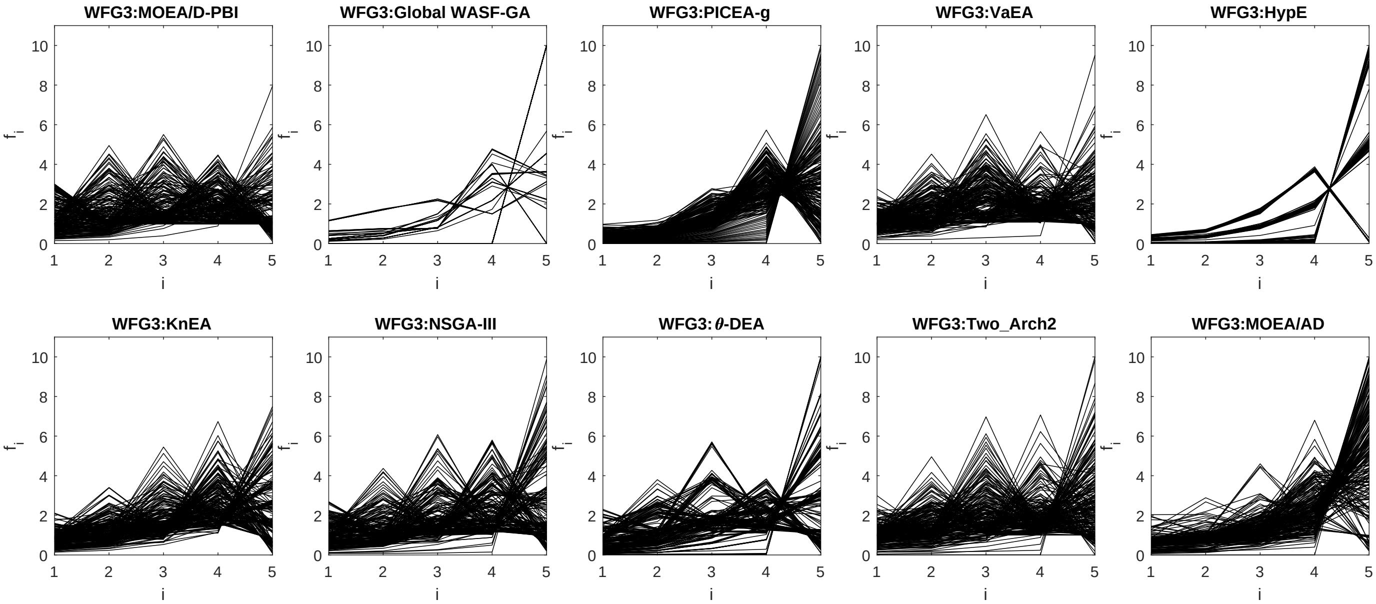

Fig. 43: Final solution sets on 5-objective WFG3 test problem obtained by 10 algorithms in the run of median HV metric values with $\mathbf{z}^r = (2, \cdots, 2)^T$.

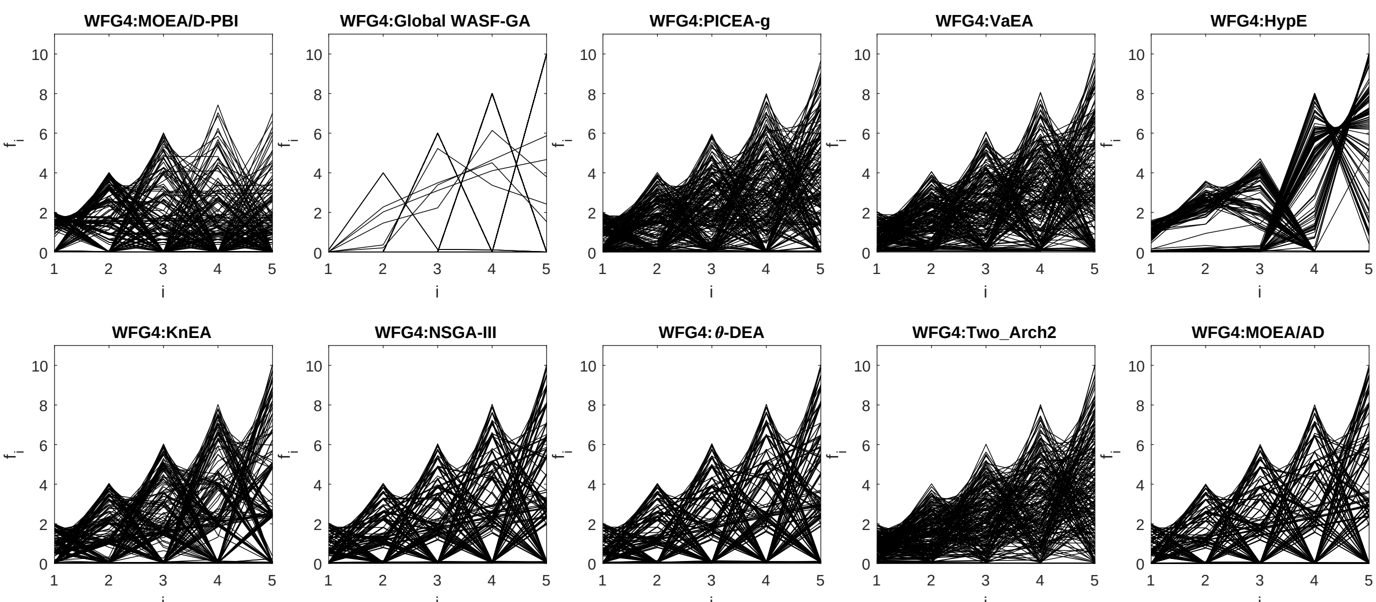

Fig. 44: Final solution sets on 5-objective WFG4 test problem obtained by 10 algorithms in the run of median HV metric values with $\mathbf{z}^r = (2, \cdots, 2)^T$.

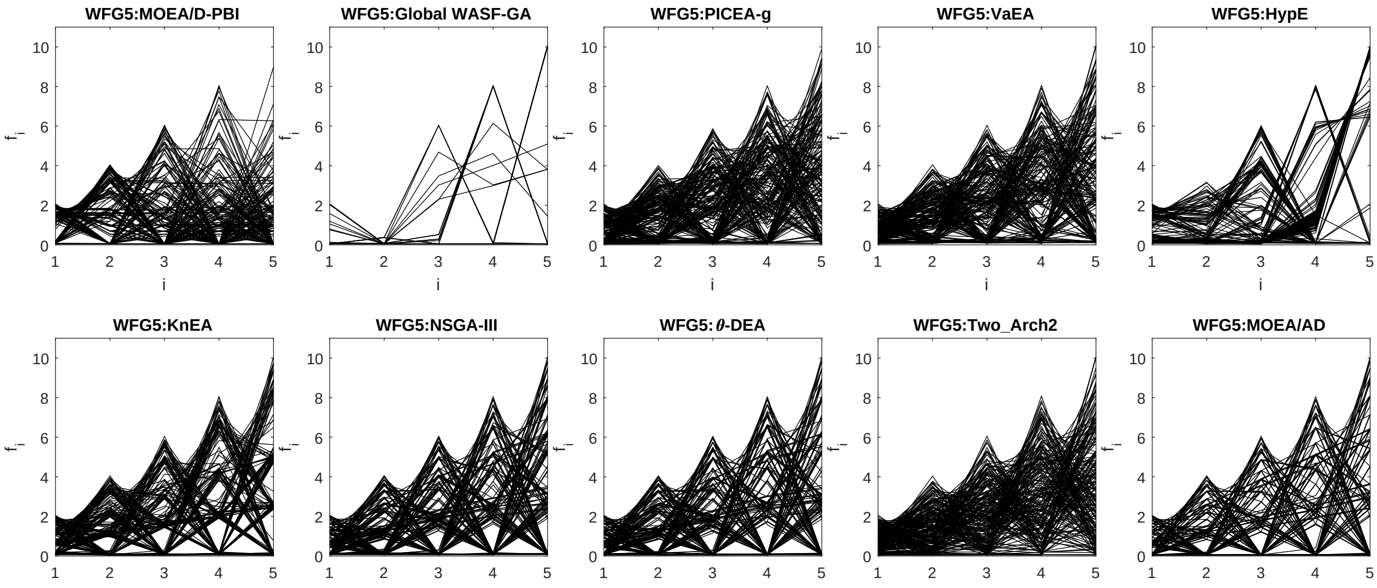

Fig. 45: Final solution sets on 5-objective WFG5 test problem obtained by 10 algorithms in the run of median HV metric values with $\mathbf{z}^r = (2, \cdots, 2)^T$.

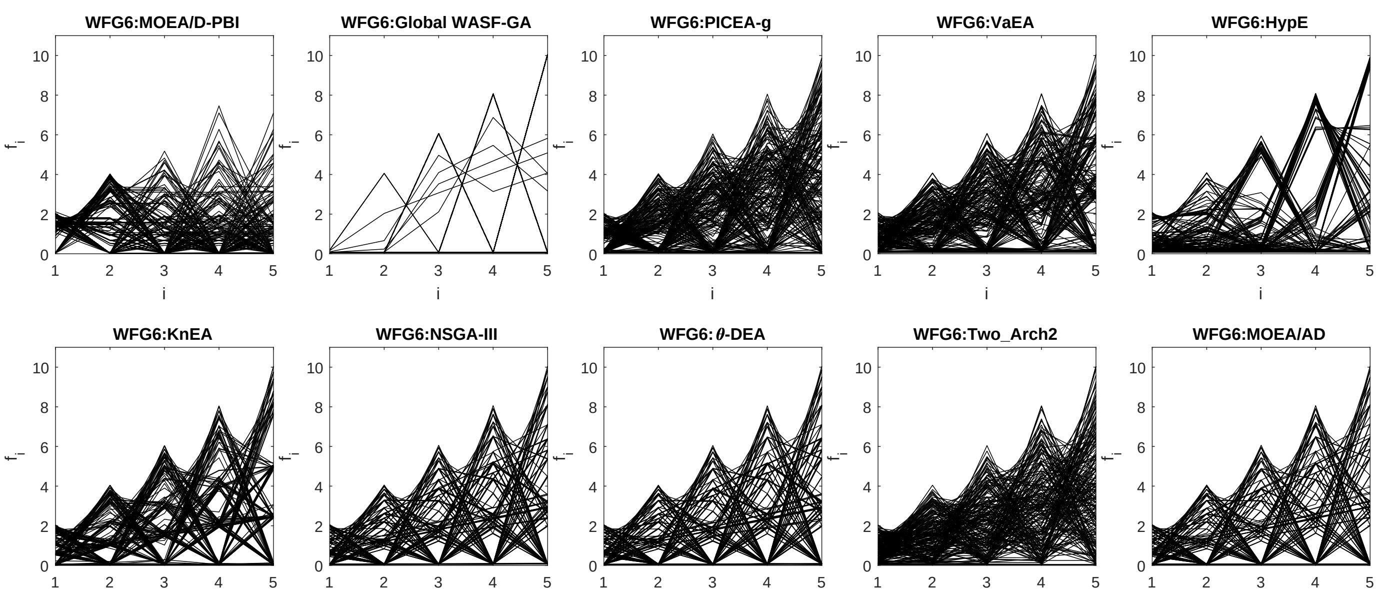

Fig. 46: Final solution sets on 5-objective WFG6 test problem obtained by 10 algorithms in the run of median HV metric values with $\mathbf{z}^r = (2, \cdots, 2)^T$.

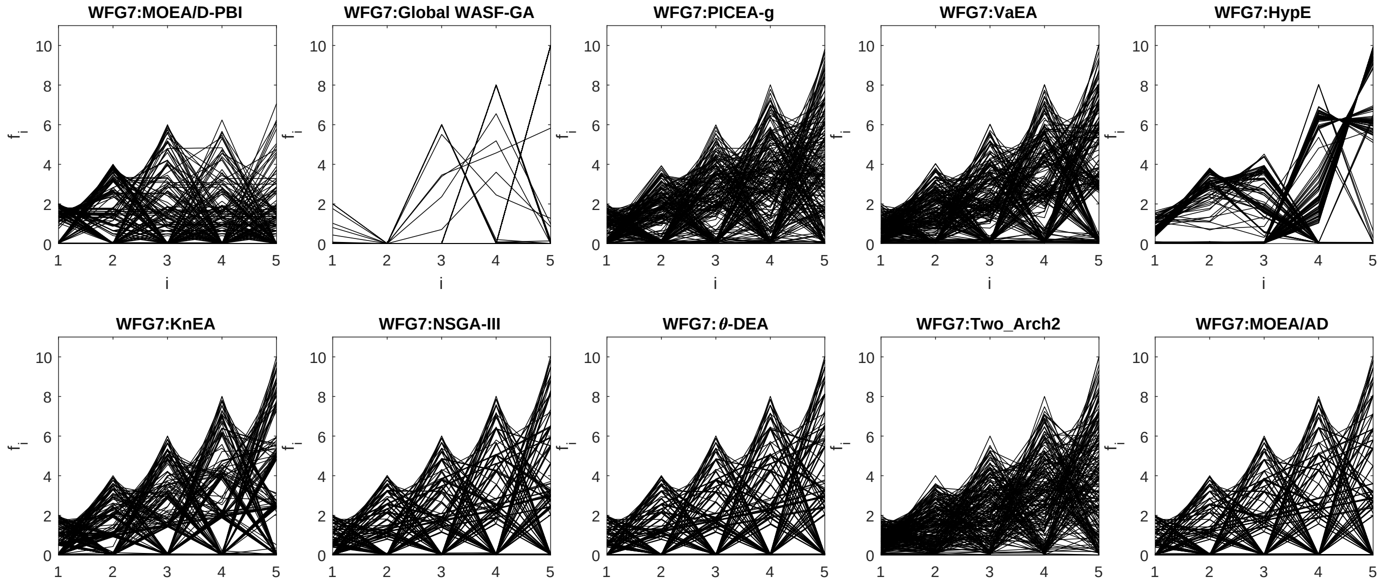

Fig. 47: Final solution sets on 5-objective WFG7 test problem obtained by 10 algorithms in the run of median HV metric values with $\mathbf{z}^r = (2, \cdots, 2)^T$.

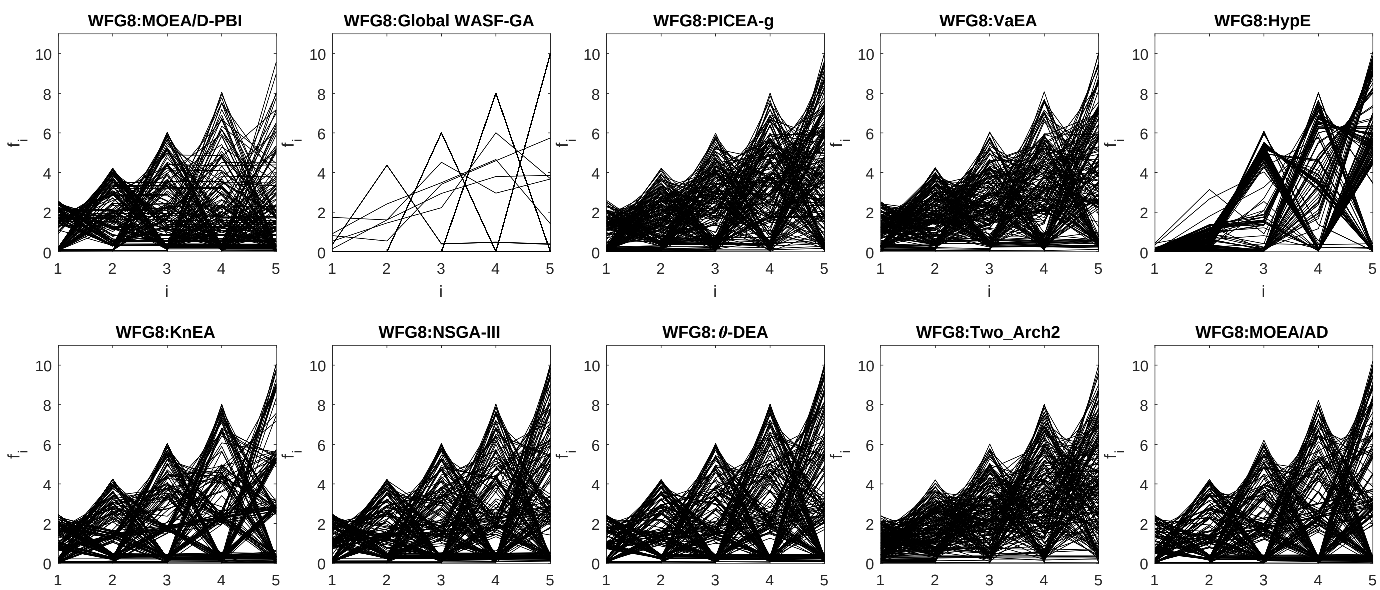

Fig. 48: Final solution sets on 5-objective WFG8 test problem obtained by 10 algorithms in the run of median HV metric values with $\mathbf{z}^r = (2, \cdots, 2)^T$.

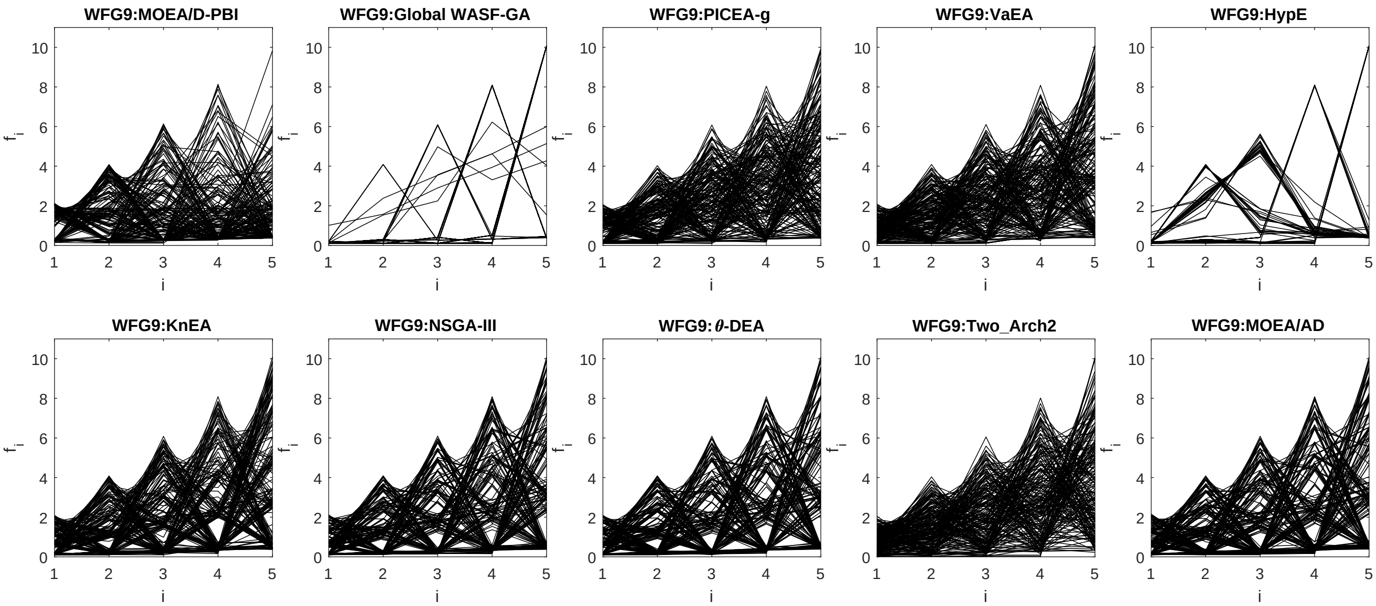

Fig. 49: Final solution sets on 5-objective WFG9 test problem obtained by 10 algorithms in the run of median HV metric values with $\mathbf{z}^r = (2, \cdots, 2)^T$.

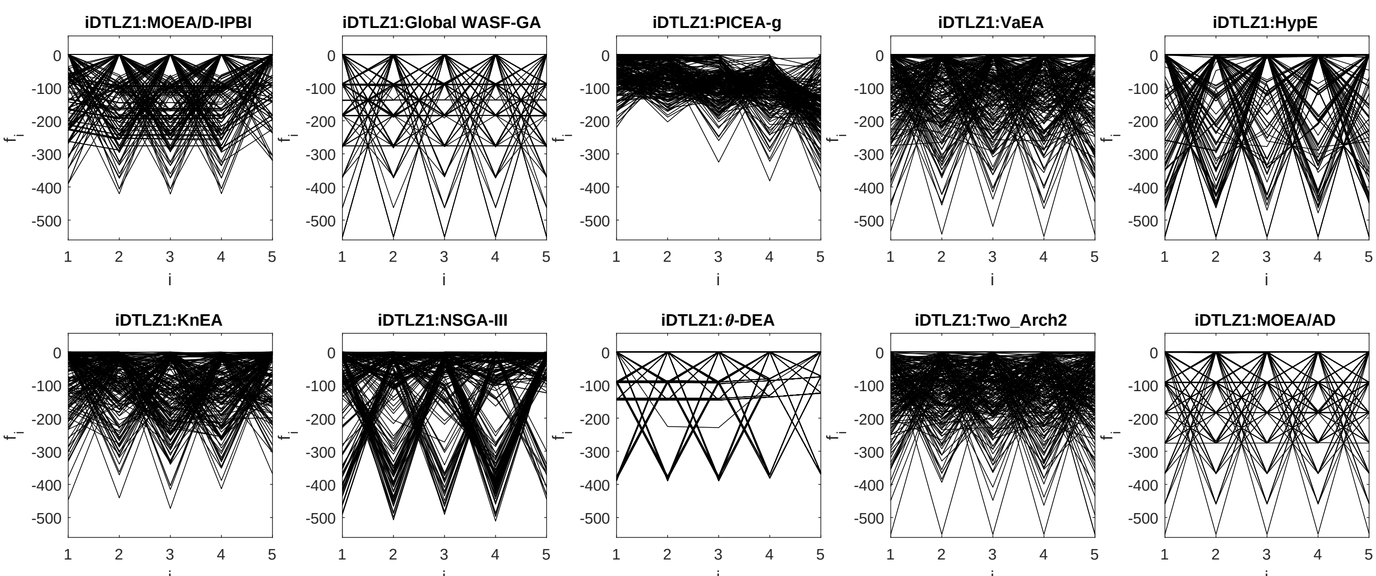

Fig. 50: Final solution sets on 5-objective DTLZ1^{-1} test problem obtained by 10 algorithms in the run of median HV metric values with $\mathbf{z}^r = (2, \cdots, 2)^T$.

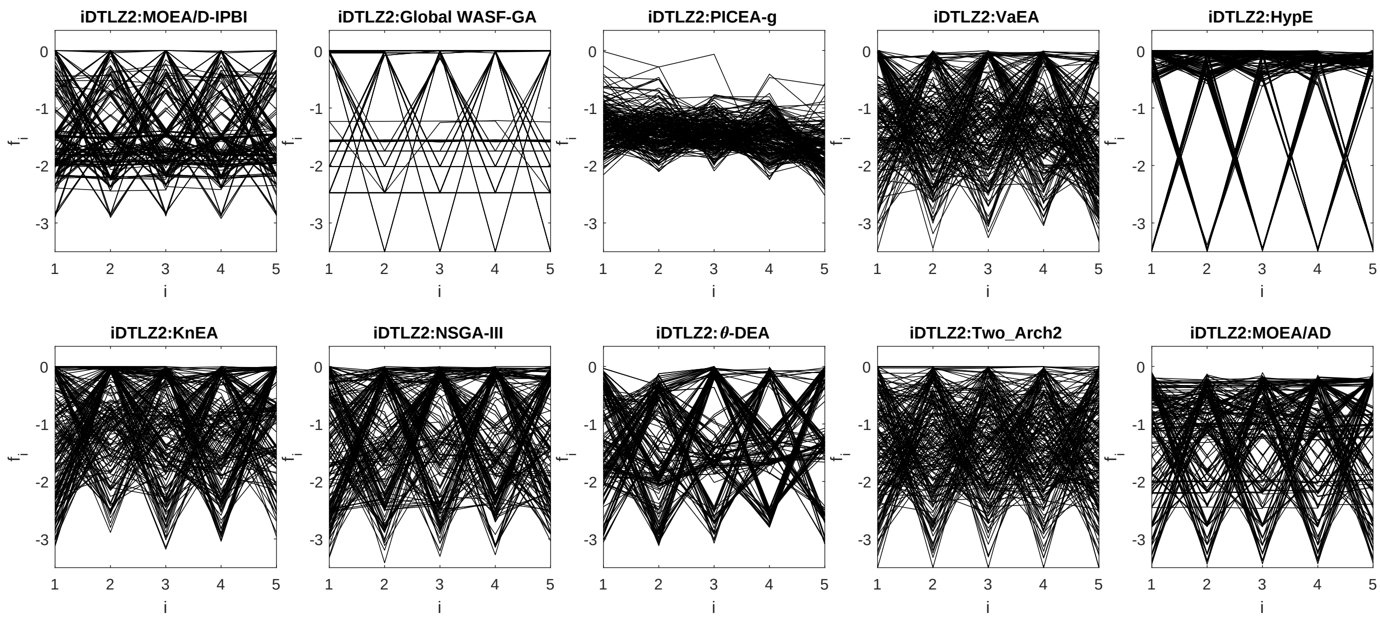

Fig. 51: Final solution sets on 5-objective DTLZ2^{-1} test problem obtained by 10 algorithms in the run of median HV metric values with $\mathbf{z}^r = (2, \cdots, 2)^T$.

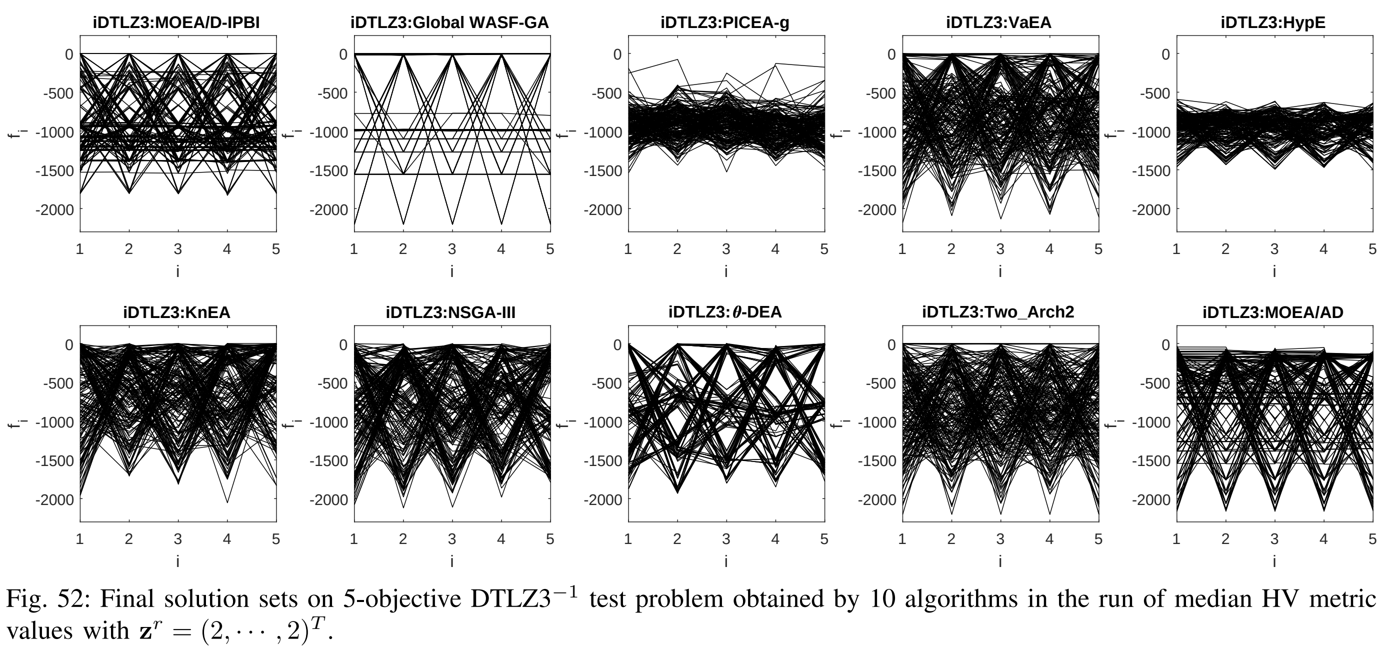

Fig. 52: Final solution sets on 5-objective DTLZ3^{-1} test problem obtained by 10 algorithms in the run of median HV metric values with $\mathbf{z}^r = (2, \cdots, 2)^T$.

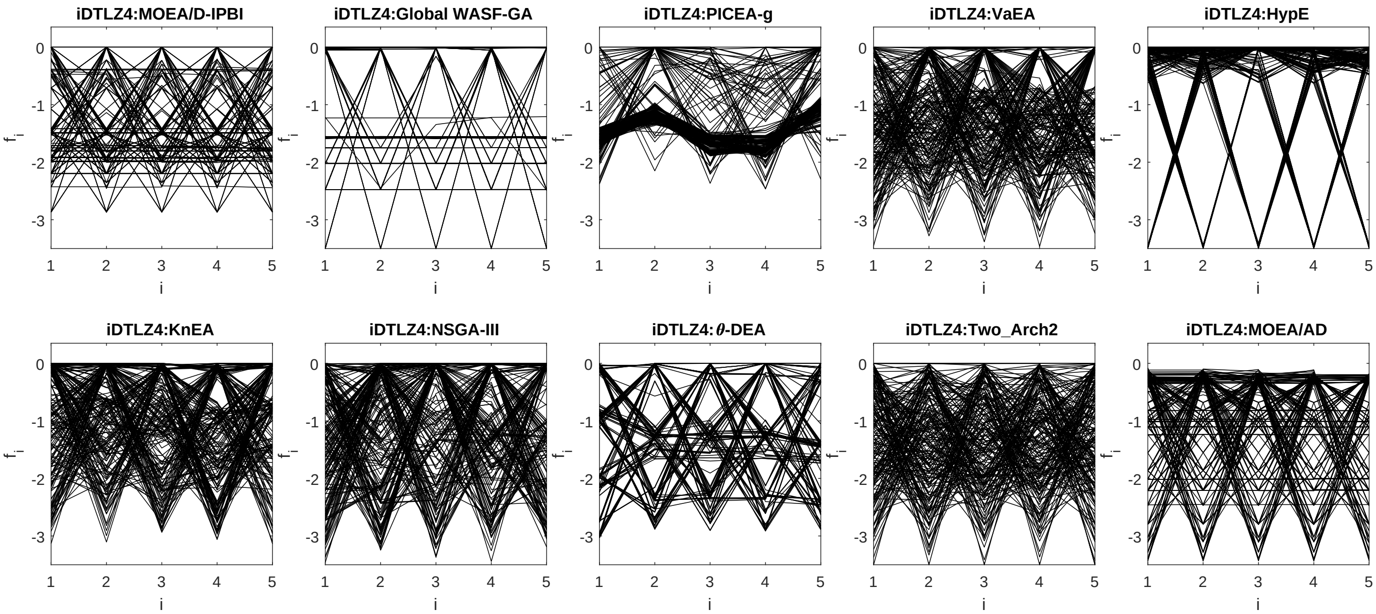

Fig. 53: Final solution sets on 5-objective DTLZ4^{-1} test problem obtained by 10 algorithms in the run of median HV metric values with $\mathbf{z}^r = (2, \cdots, 2)^T$.

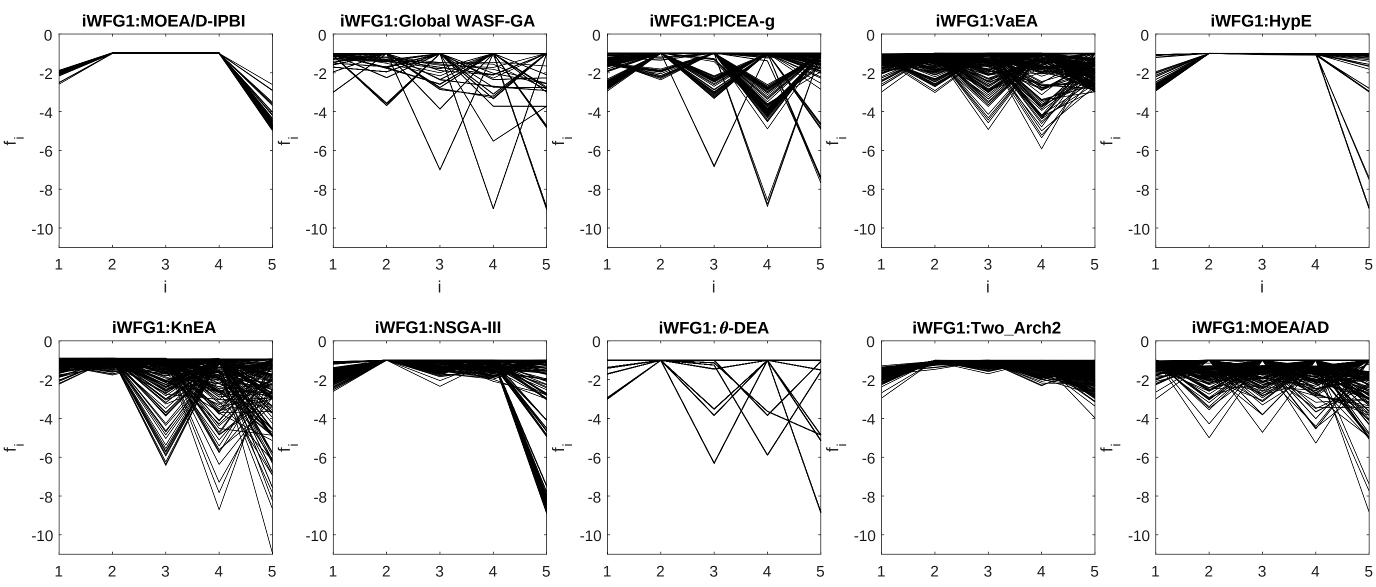

Fig. 54: Final solution sets on 5-objective WFG1^{-1} test problem obtained by 10 algorithms in the run of median HV metric values with $\mathbf{z}^r = (2, \cdots, 2)^T$.

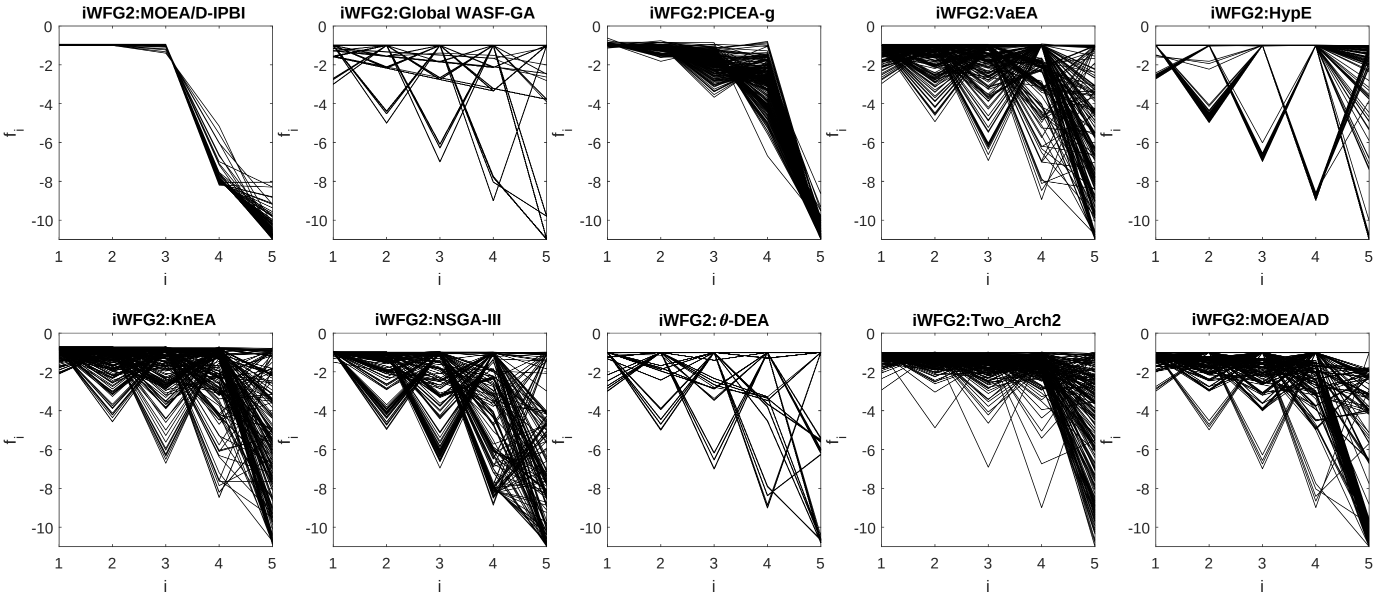

Fig. 55: Final solution sets on 5-objective WFG2^{-1} test problem obtained by 10 algorithms in the run of median HV metric values with $\mathbf{z}^r = (2, \cdots, 2)^T$.

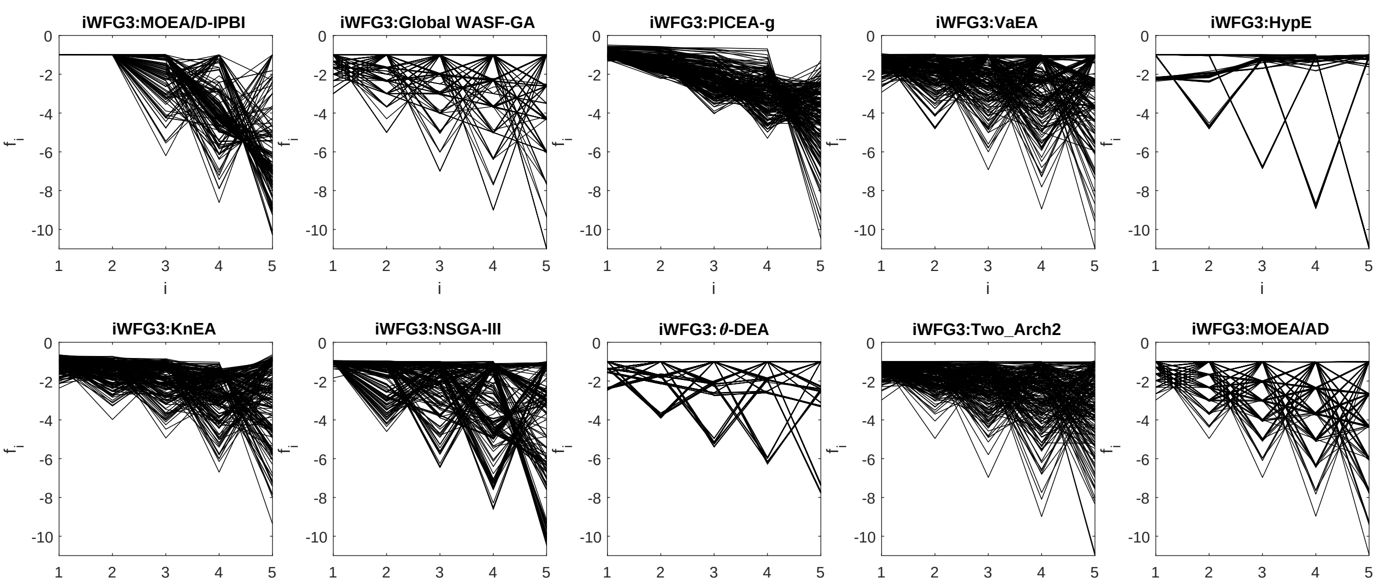

Fig. 56: Final solution sets on 5-objective WFG3^{-1} test problem obtained by 10 algorithms in the run of median HV metric values with $\mathbf{z}^r = (2, \cdots, 2)^T$.

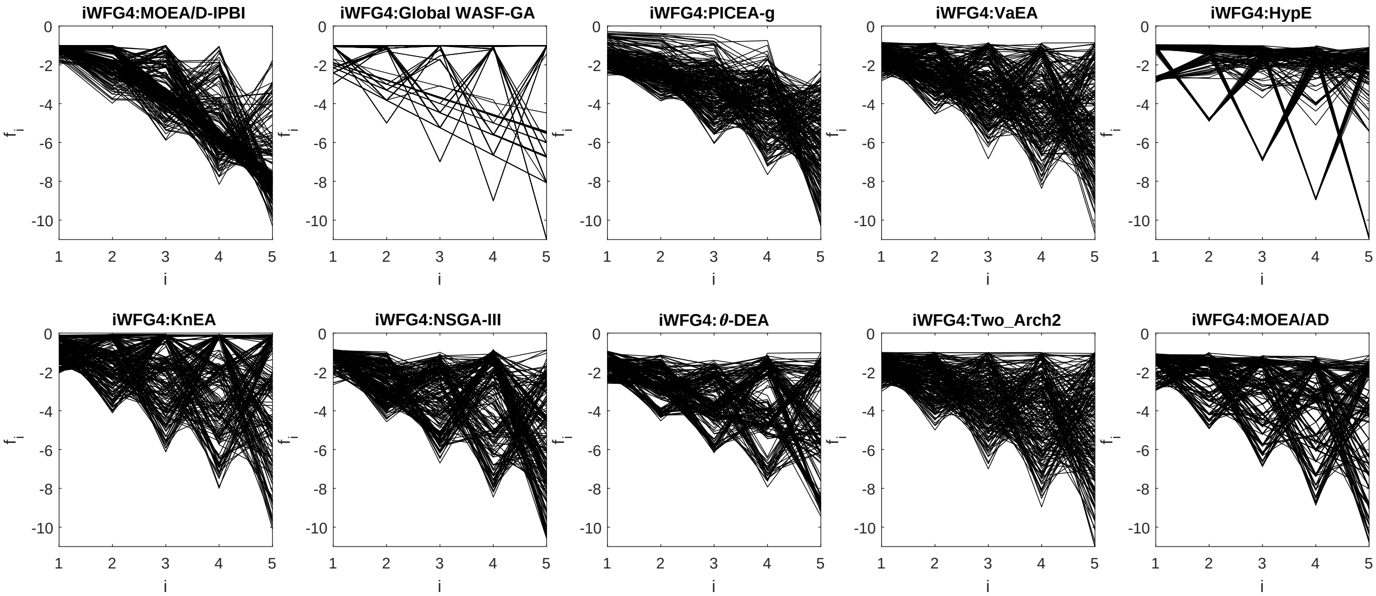

Fig. 57: Final solution sets on 5-objective WFG4^{-1} test problem obtained by 10 algorithms in the run of median HV metric values with $\mathbf{z}^r = (2, \cdots, 2)^T$.

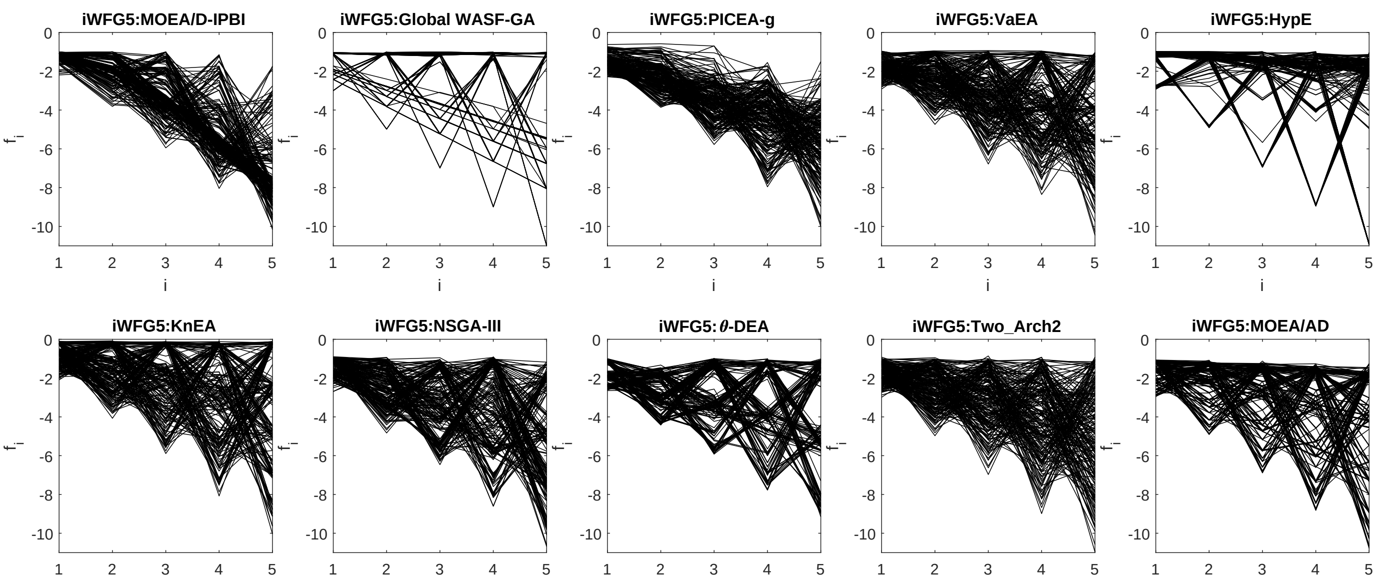

Fig. 58: Final solution sets on 5-objective WFG5^{-1} test problem obtained by 10 algorithms in the run of median HV metric values with $\mathbf{z}^r = (2, \cdots, 2)^T$.

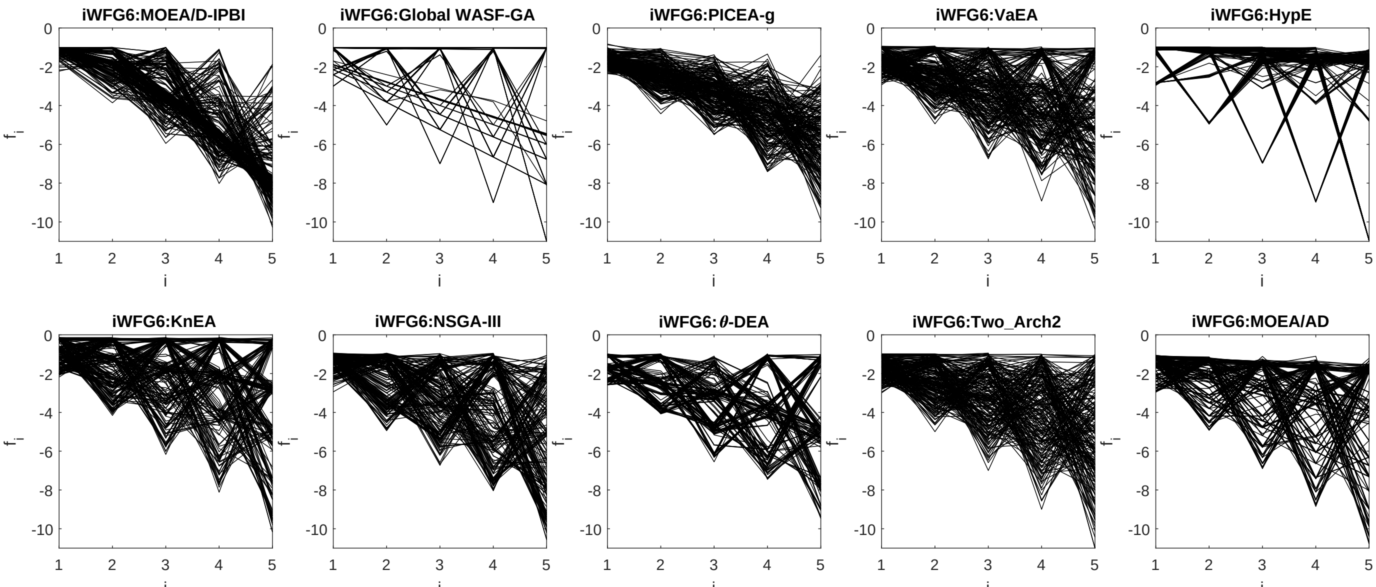

Fig. 59: Final solution sets on 5-objective WFG6^{-1} test problem obtained by 10 algorithms in the run of median HV metric values with $\mathbf{z}^r = (2, \cdots, 2)^T$.

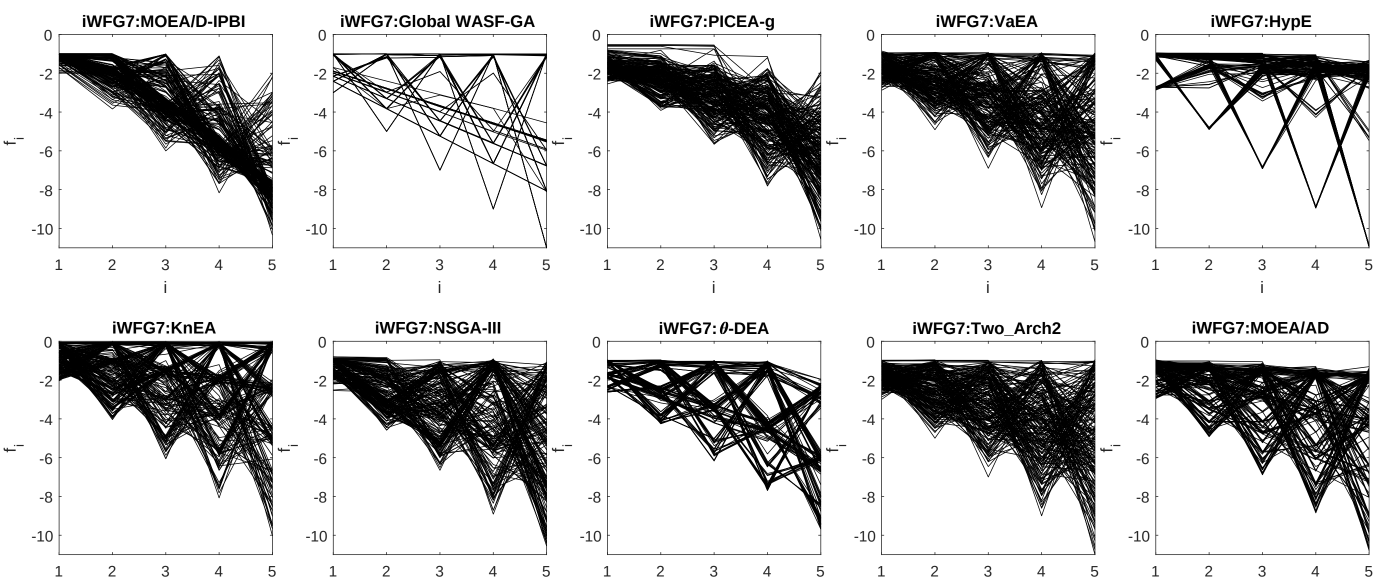

Fig. 60: Final solution sets on 5-objective WFG7^{-1} test problem obtained by 10 algorithms in the run of median HV metric values with $\mathbf{z}^r = (2, \cdots, 2)^T$.

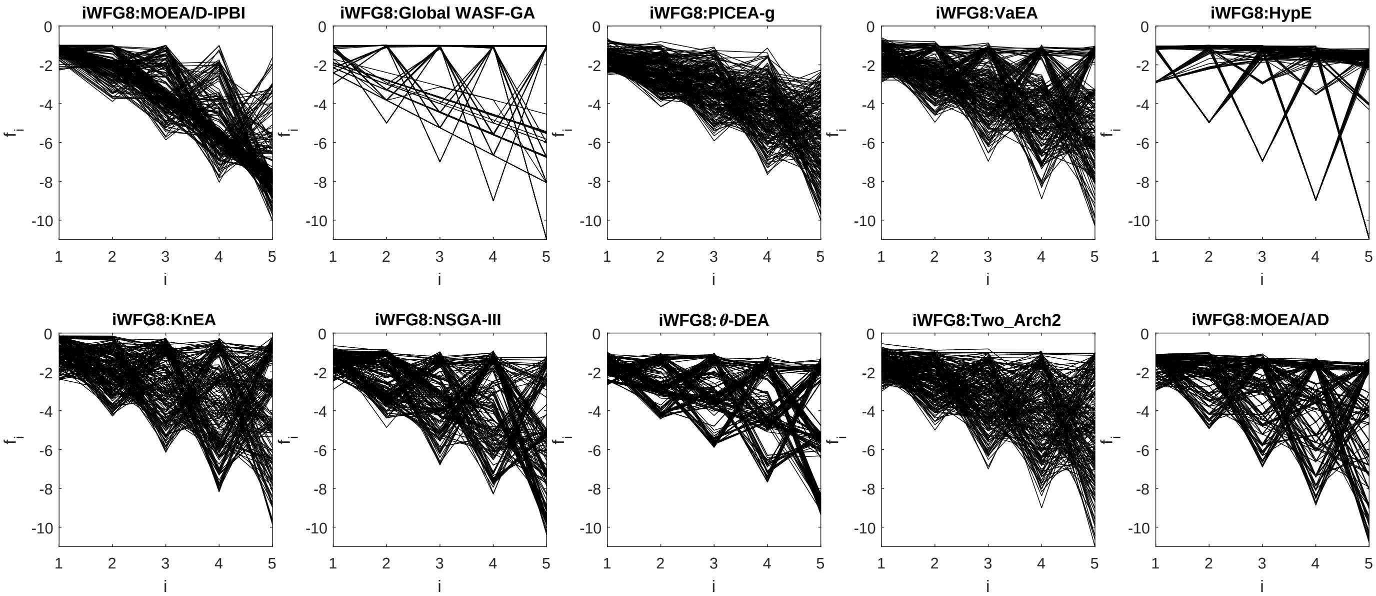

Fig. 61: Final solution sets on 5-objective WFG8^{-1} test problem obtained by 10 algorithms in the run of median HV metric values with $\mathbf{z}^r = (2, \cdots, 2)^T$.

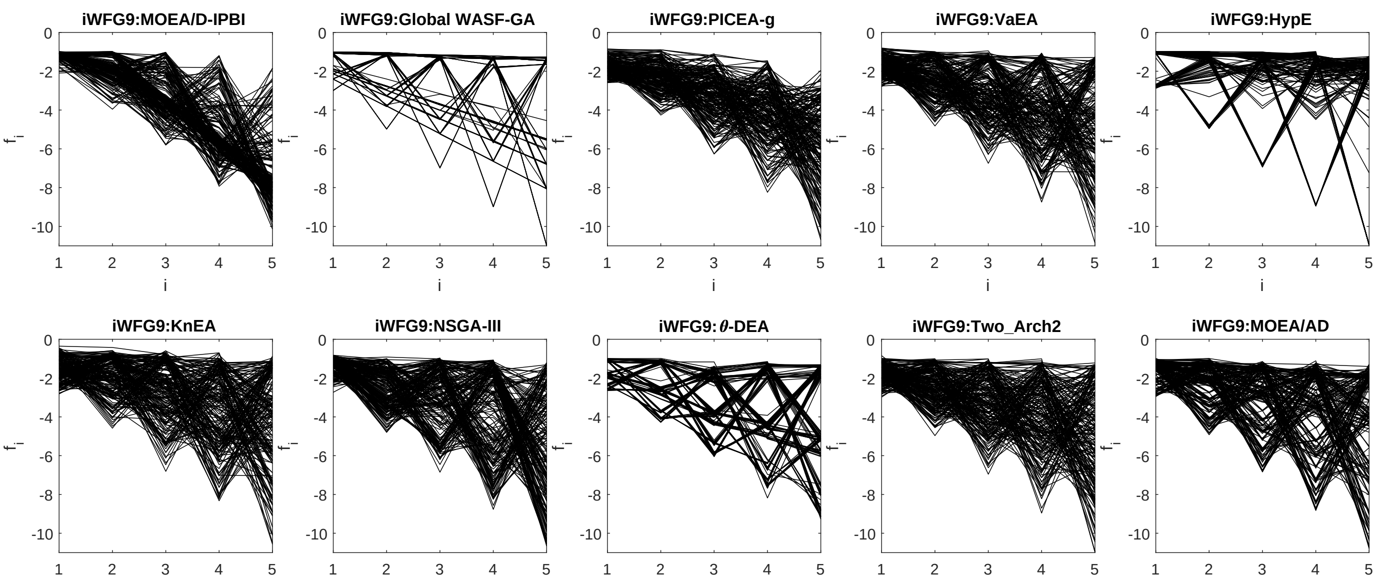

Fig. 62: Final solution sets on 5-objective WFG9^{-1} test problem obtained by 10 algorithms in the run of median HV metric values with $\mathbf{z}^r = (2, \cdots, 2)^T$.

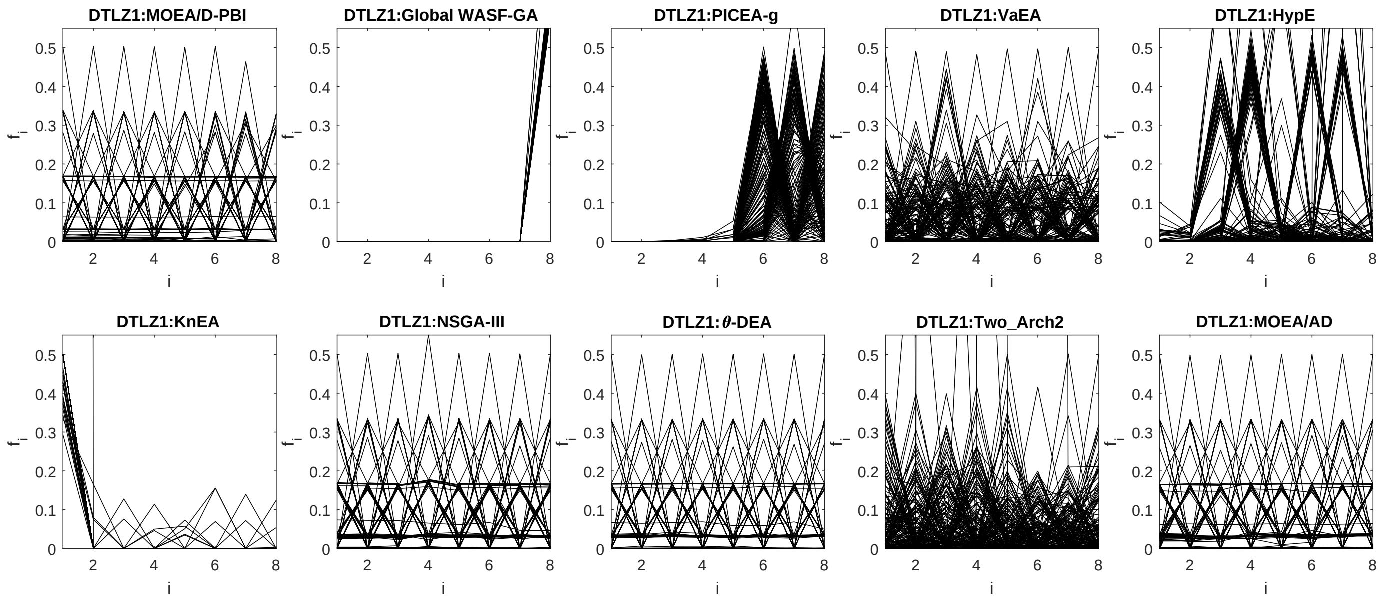

Fig. 63: Final solution sets on 8-objective DTLZ1 test problem obtained by 10 algorithms in the run of median HV metric values with $\mathbf{z}^r = (2, \cdots, 2)^T$.

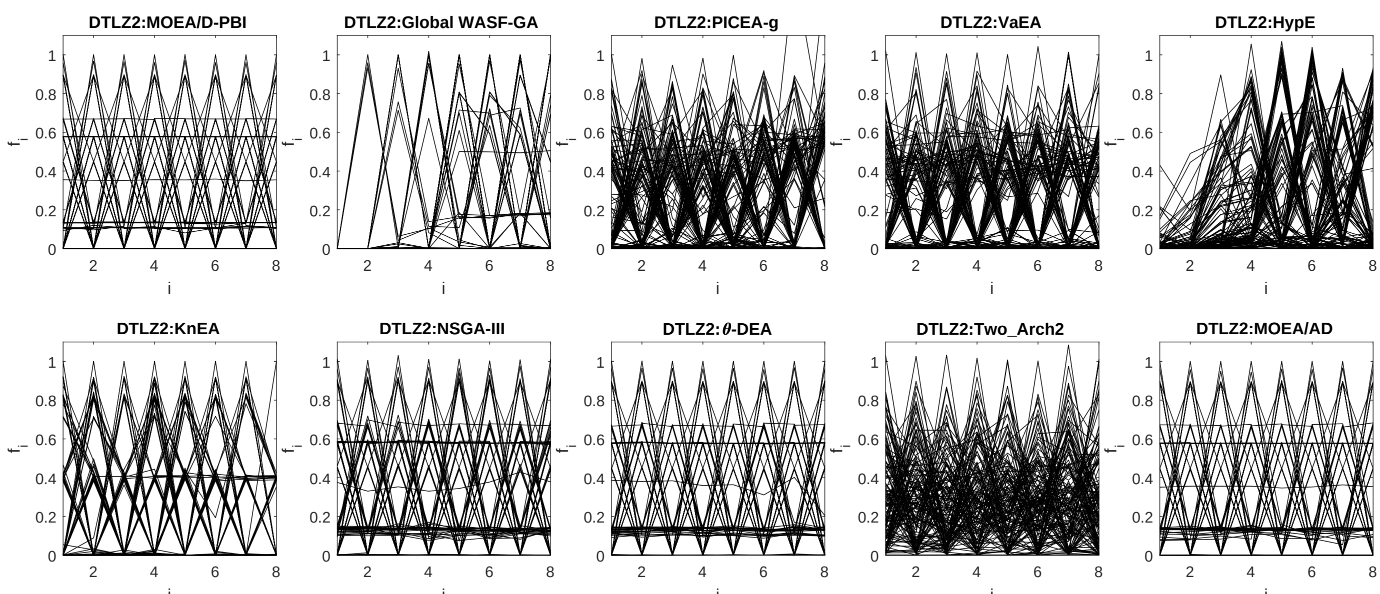

Fig. 64: Final solution sets on 8-objective DTLZ2 test problem obtained by 10 algorithms in the run of median HV metric values with $\mathbf{z}^r = (2, \cdots, 2)^T$.

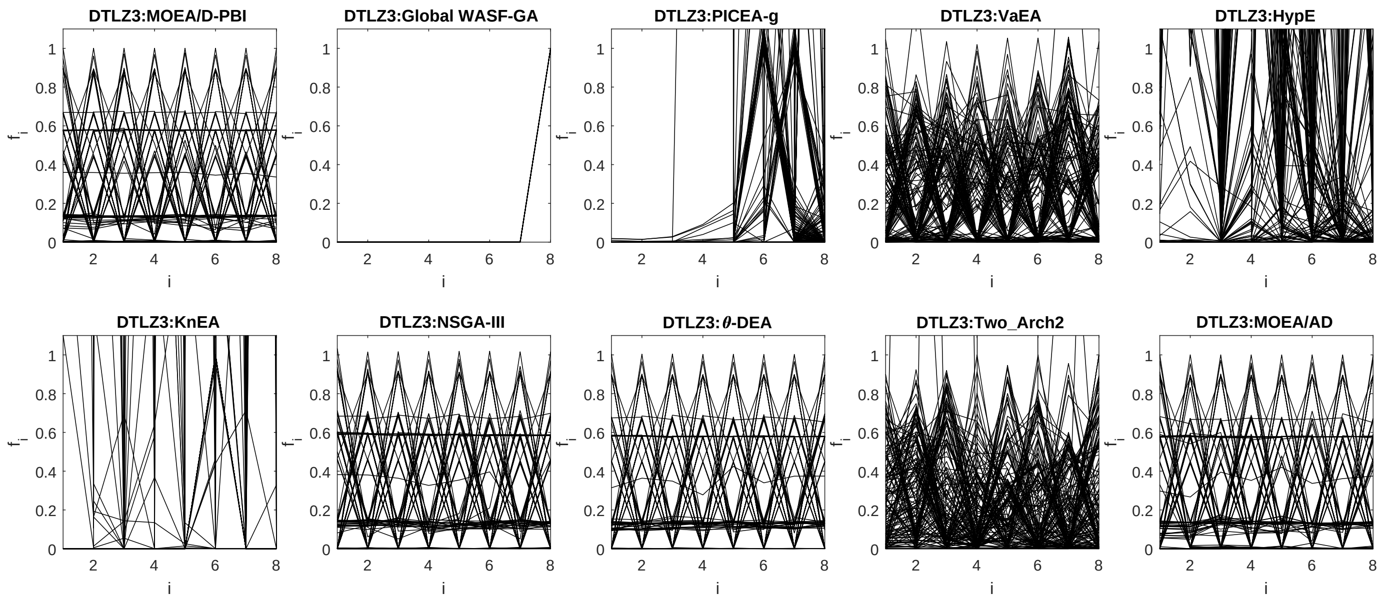

Fig. 65: Final solution sets on 8-objective DTLZ3 test problem obtained by 10 algorithms in the run of median HV metric values with $\mathbf{z}^r = (2, \cdots, 2)^T$.

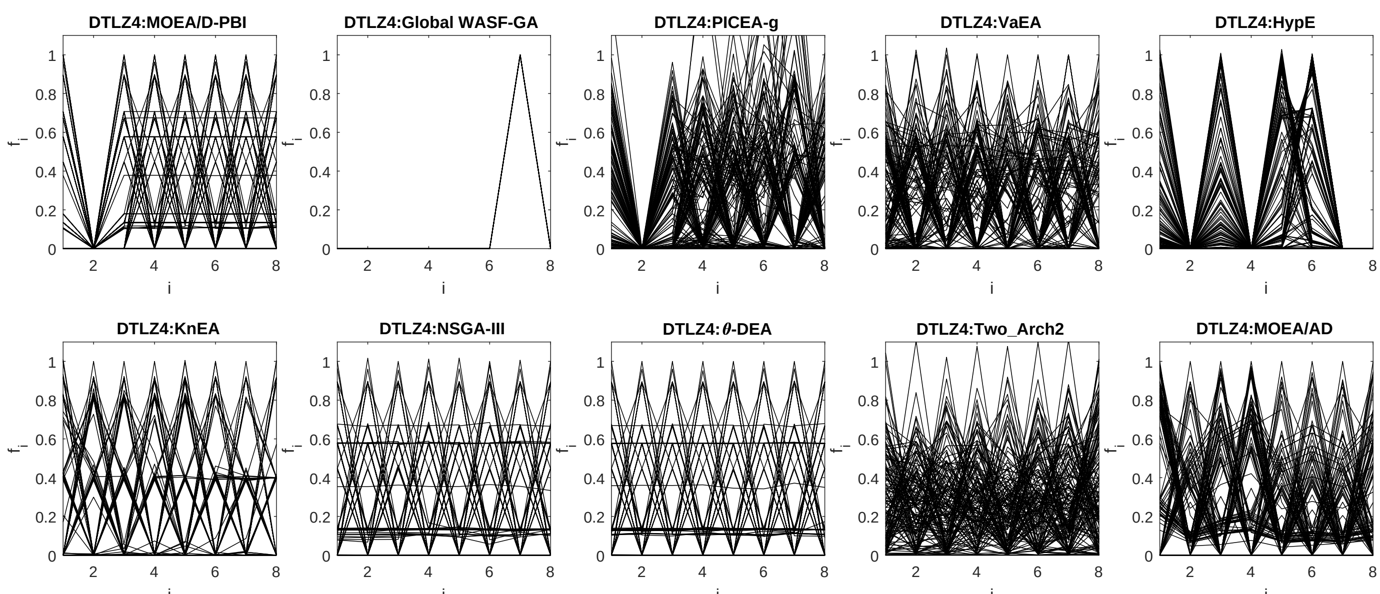

Fig. 66: Final solution sets on 8-objective DTLZ4 test problem obtained by 10 algorithms in the run of median HV metric values with $\mathbf{z}^r = (2, \cdots, 2)^T$.

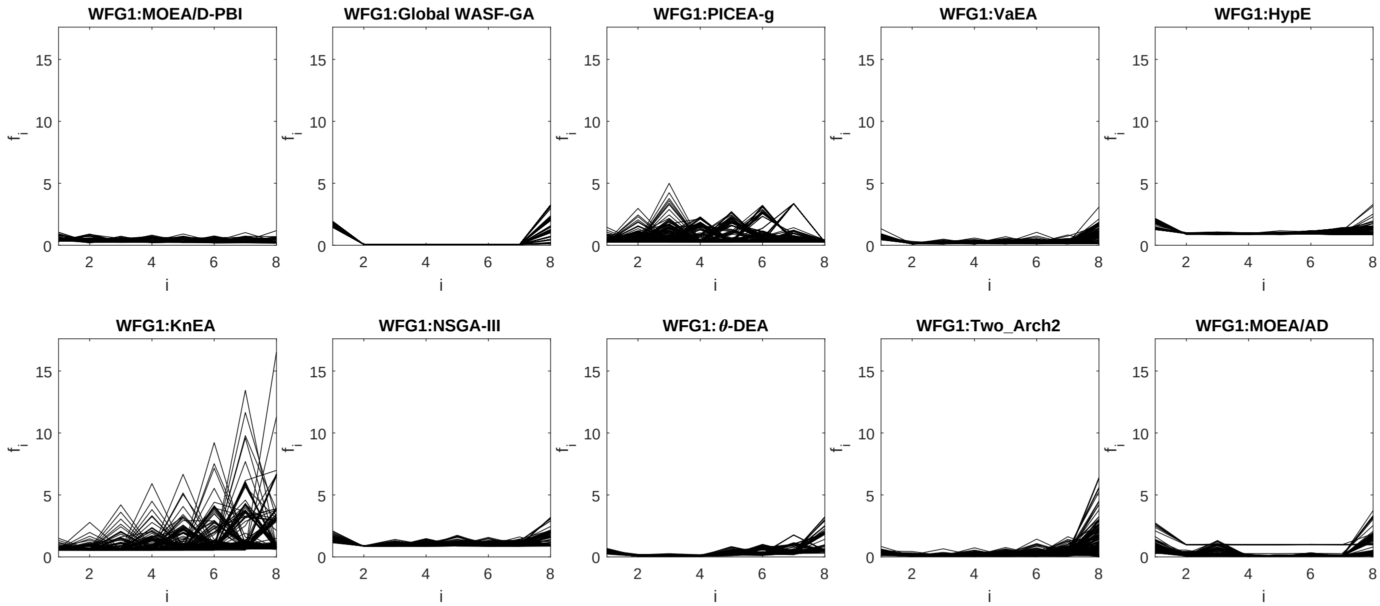

Fig. 67: Final solution sets on 8-objective WFG1 test problem obtained by 10 algorithms in the run of median HV metric values with $\mathbf{z}^r = (2, \cdots, 2)^T$.

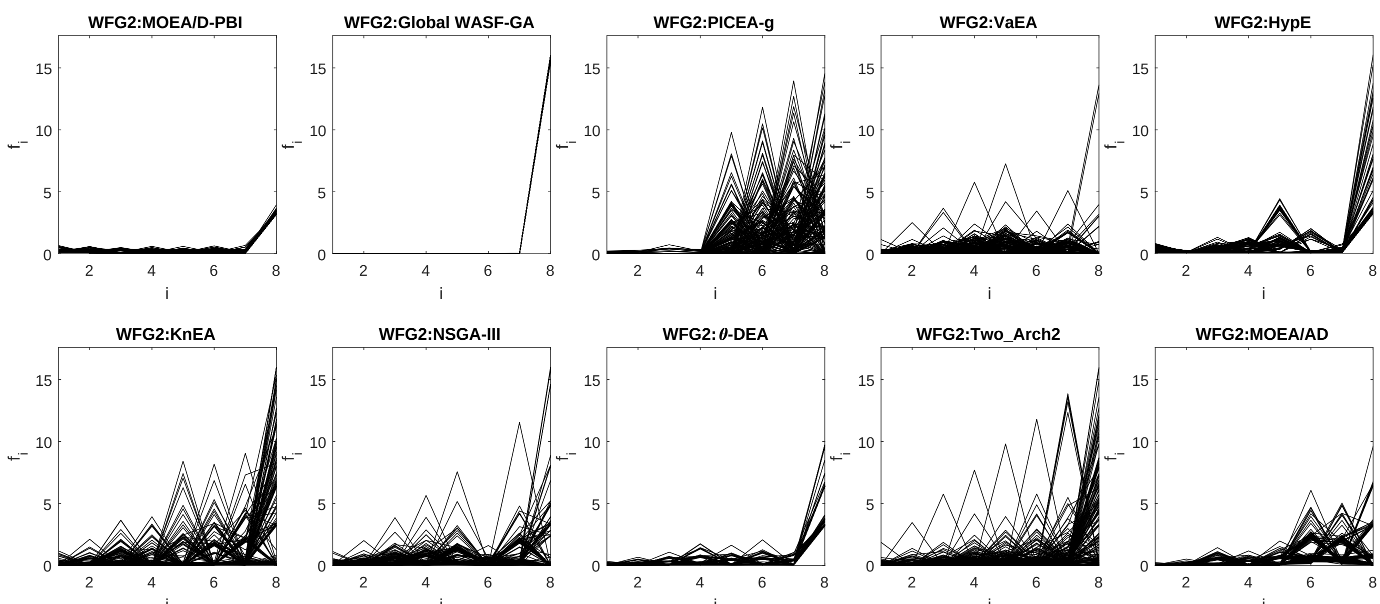

Fig. 68: Final solution sets on 8-objective WFG2 test problem obtained by 10 algorithms in the run of median HV metric values with $\mathbf{z}^r = (2, \cdots, 2)^T$.

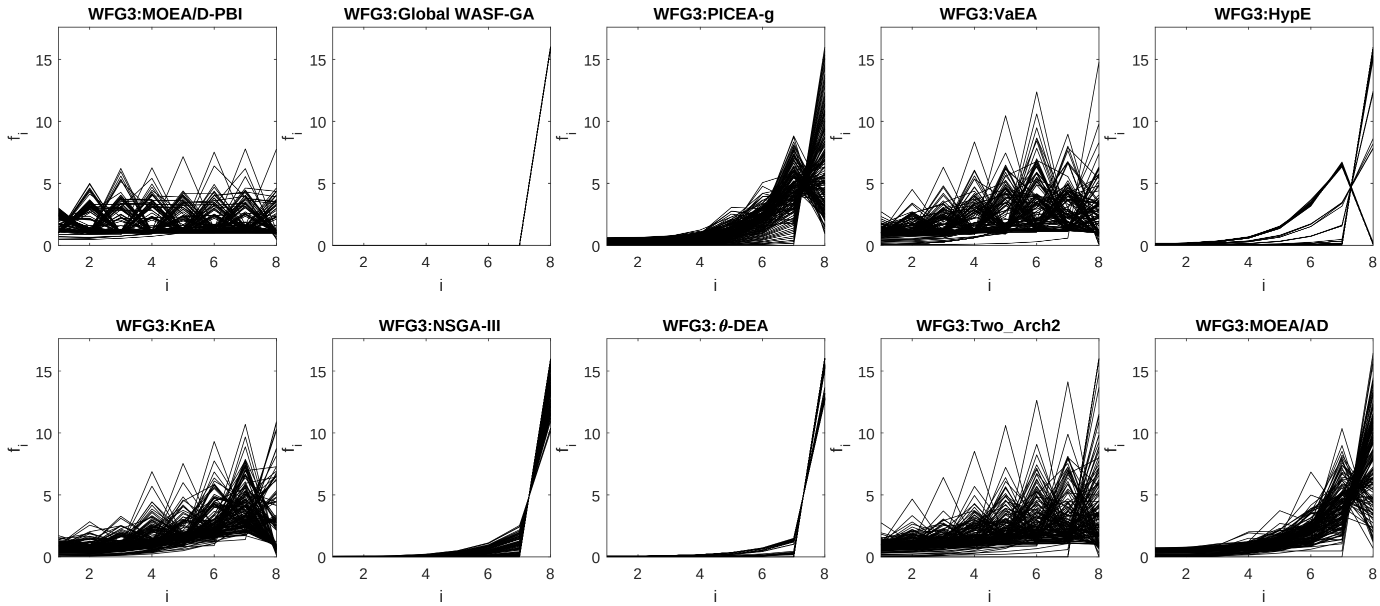

Fig. 69: Final solution sets on 8-objective WFG3 test problem obtained by 10 algorithms in the run of median HV metric values with $\mathbf{z}^r = (2, \cdots, 2)^T$.

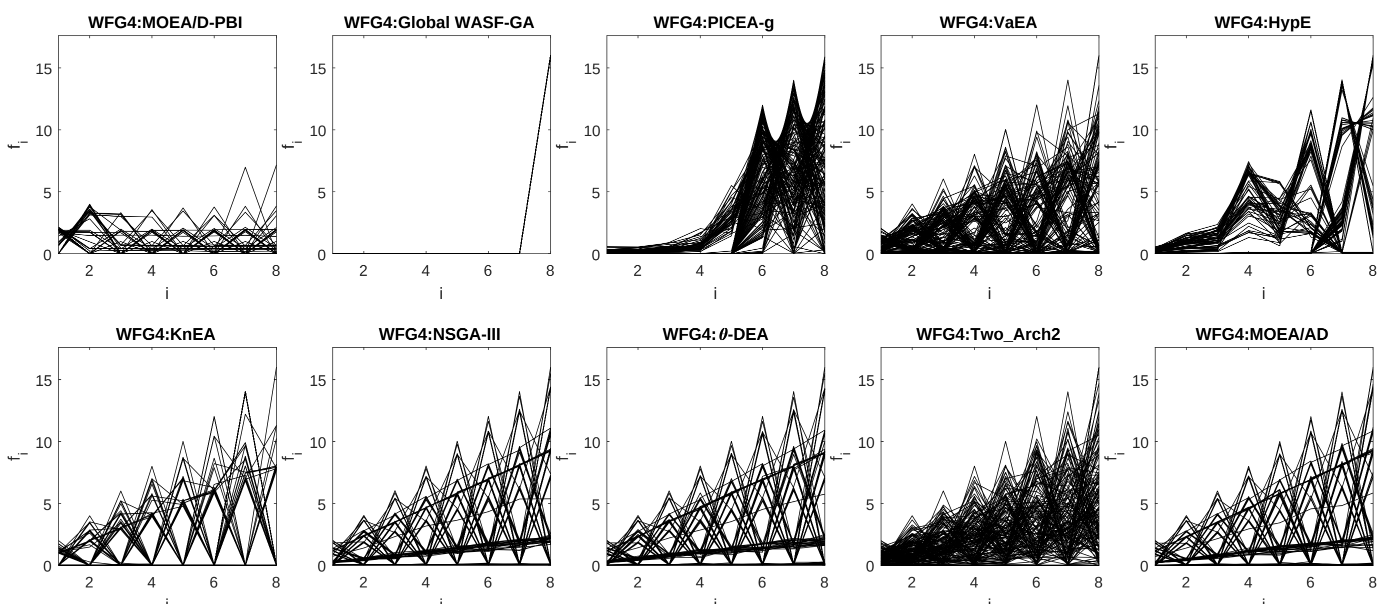

Fig. 70: Final solution sets on 8-objective WFG4 test problem obtained by 10 algorithms in the run of median HV metric values with $\mathbf{z}^r = (2, \cdots, 2)^T$.

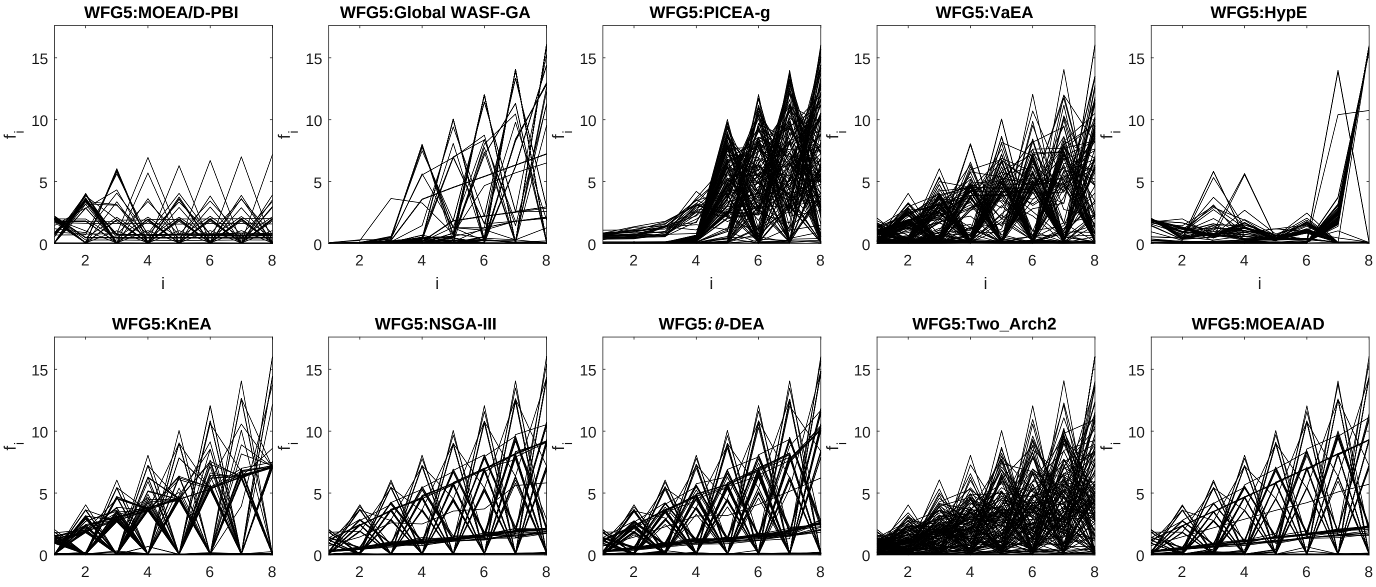

Fig. 71: Final solution sets on 8-objective WFG5 test problem obtained by 10 algorithms in the run of median HV metric values with $\mathbf{z}^r = (2, \cdots, 2)^T$.

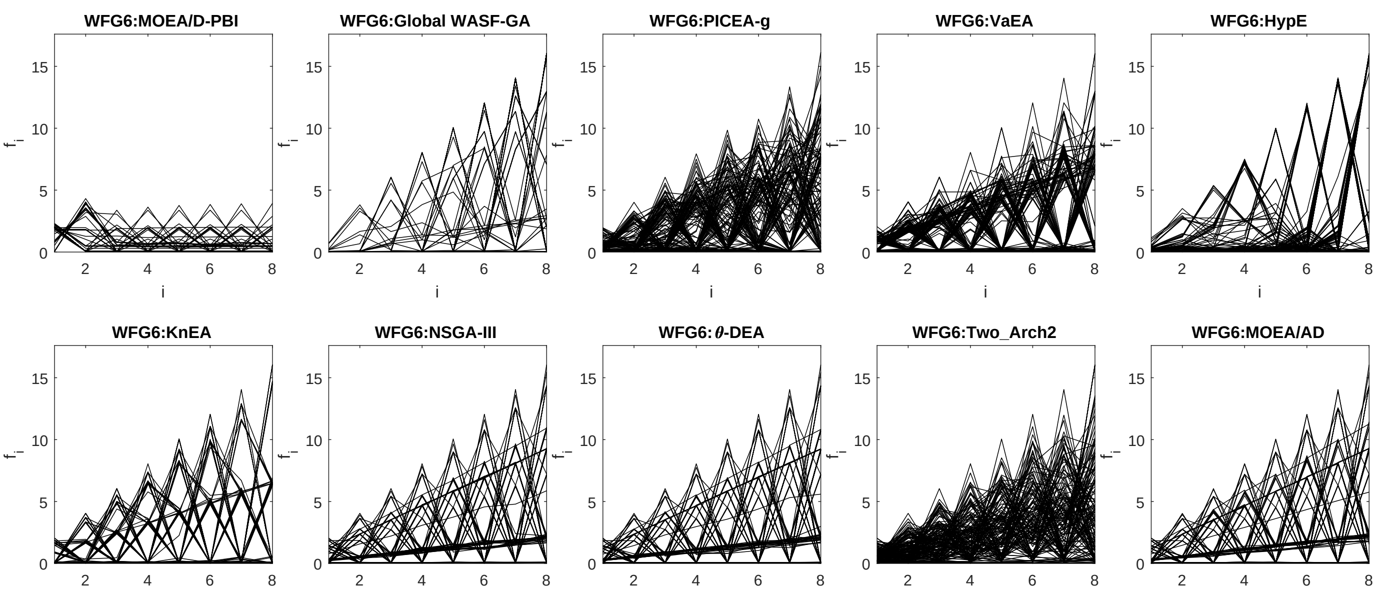

Fig. 72: Final solution sets on 8-objective WFG6 test problem obtained by 10 algorithms in the run of median HV metric values with $\mathbf{z}^r = (2, \cdots, 2)^T$.

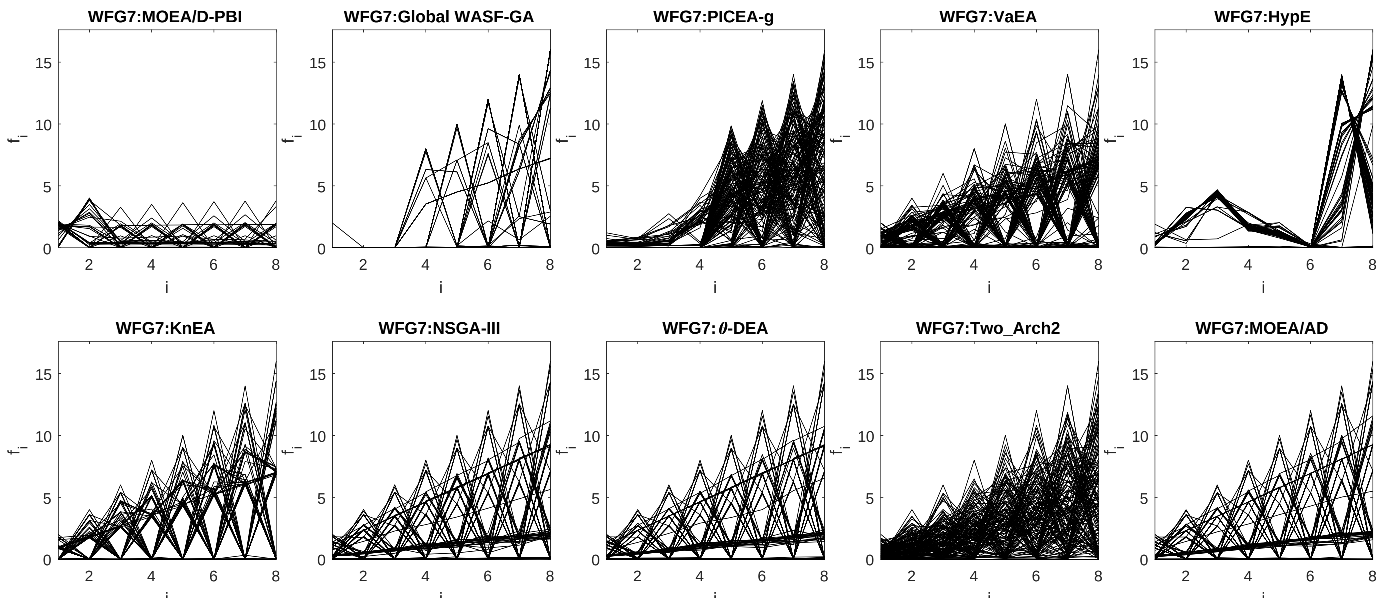

Fig. 73: Final solution sets on 8-objective WFG7 test problem obtained by 10 algorithms in the run of median HV metric values with $\mathbf{z}^r = (2, \cdots, 2)^T$.

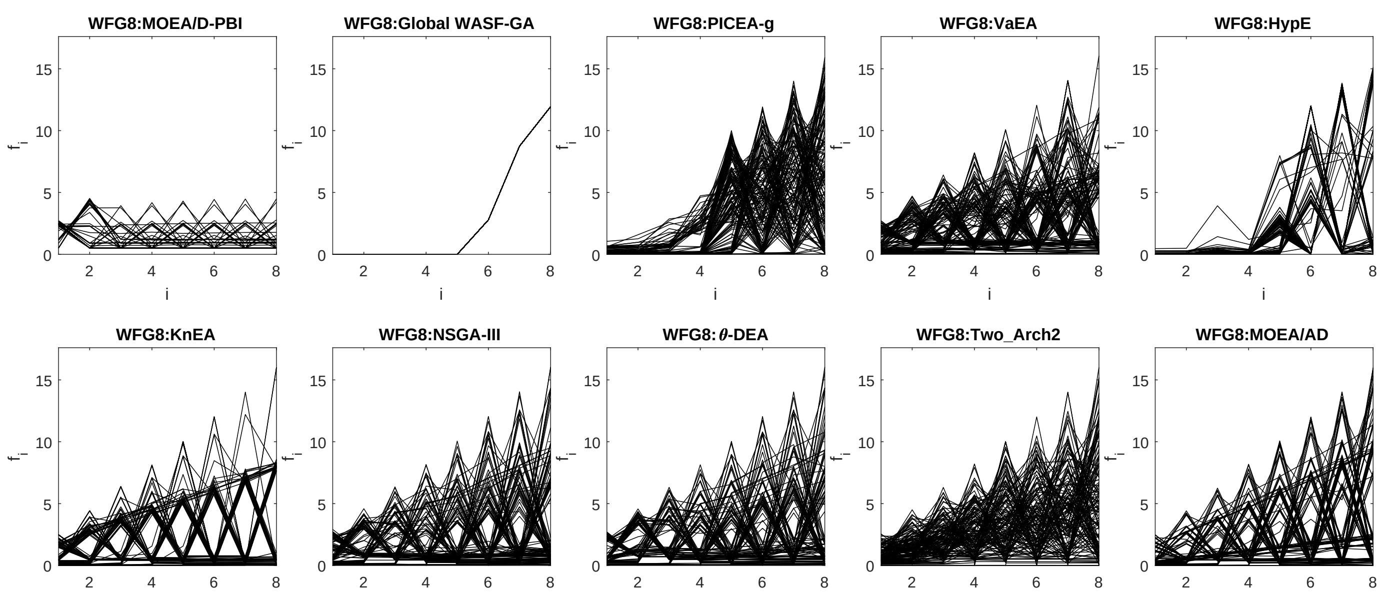

Fig. 74: Final solution sets on 8-objective WFG8 test problem obtained by 10 algorithms in the run of median HV metric values with $\mathbf{z}^r = (2, \cdots, 2)^T$.

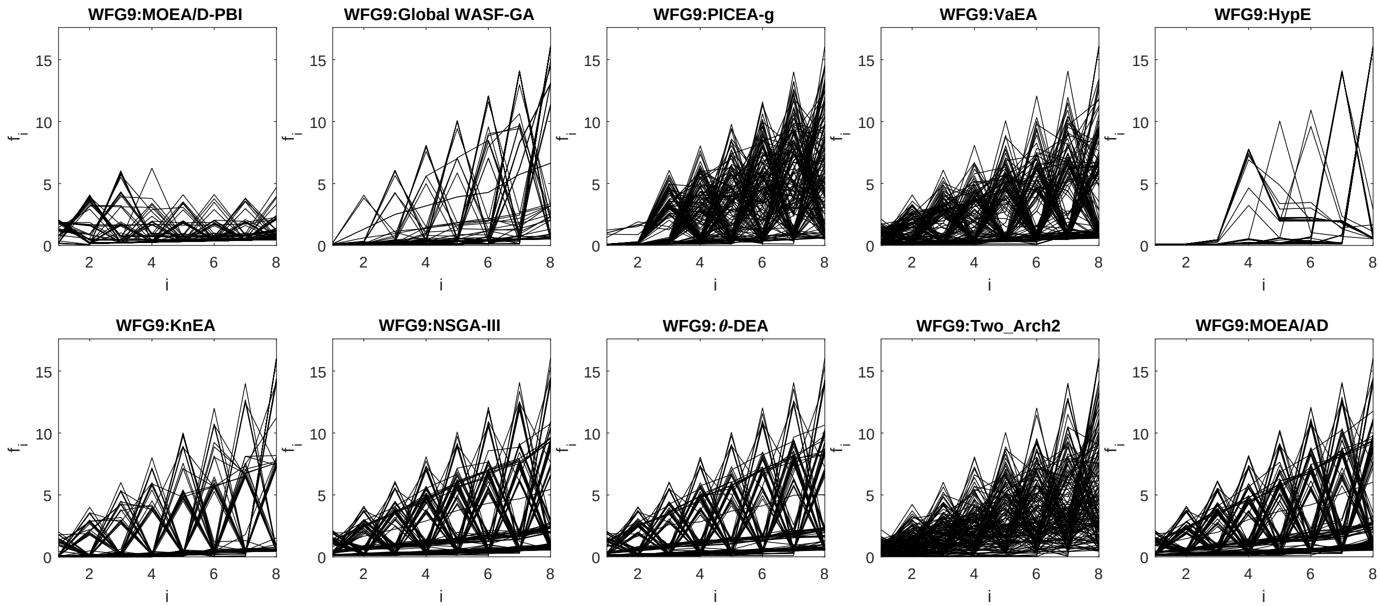

Fig. 75: Final solution sets on 8-objective WFG9 test problem obtained by 10 algorithms in the run of median HV metric values with $\mathbf{z}^r = (2, \cdots, 2)^T$.

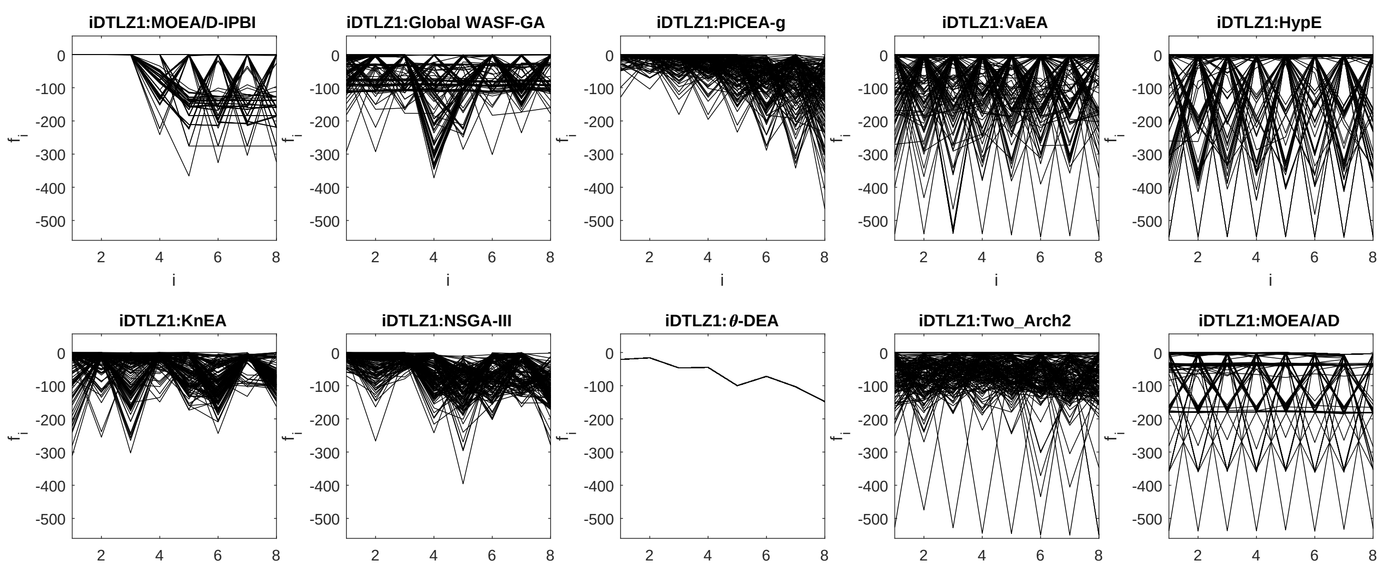

Fig. 76: Final solution sets on 8-objective DTLZ1^{-1} test problem obtained by 10 algorithms in the run of median HV metric values with $\mathbf{z}^r = (2, \cdots, 2)^T$.

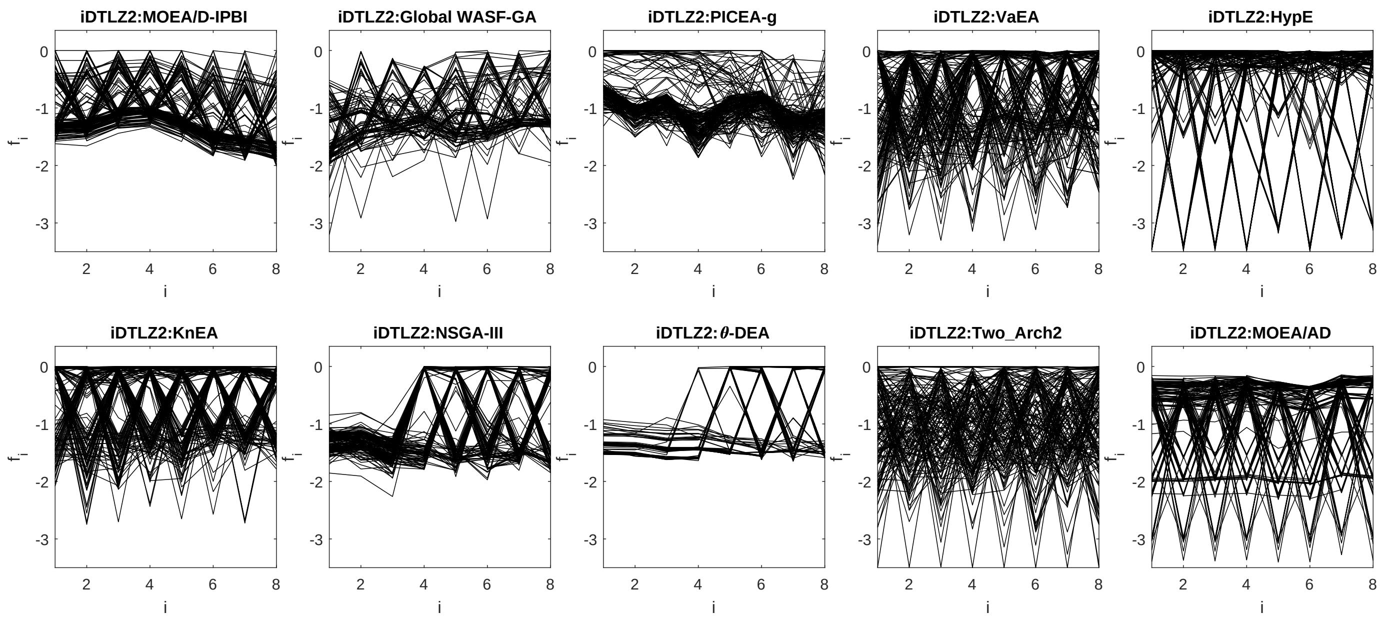

Fig. 77: Final solution sets on 8-objective DTLZ2^{-1} test problem obtained by 10 algorithms in the run of median HV metric values with $\mathbf{z}^r = (2, \cdots, 2)^T$.

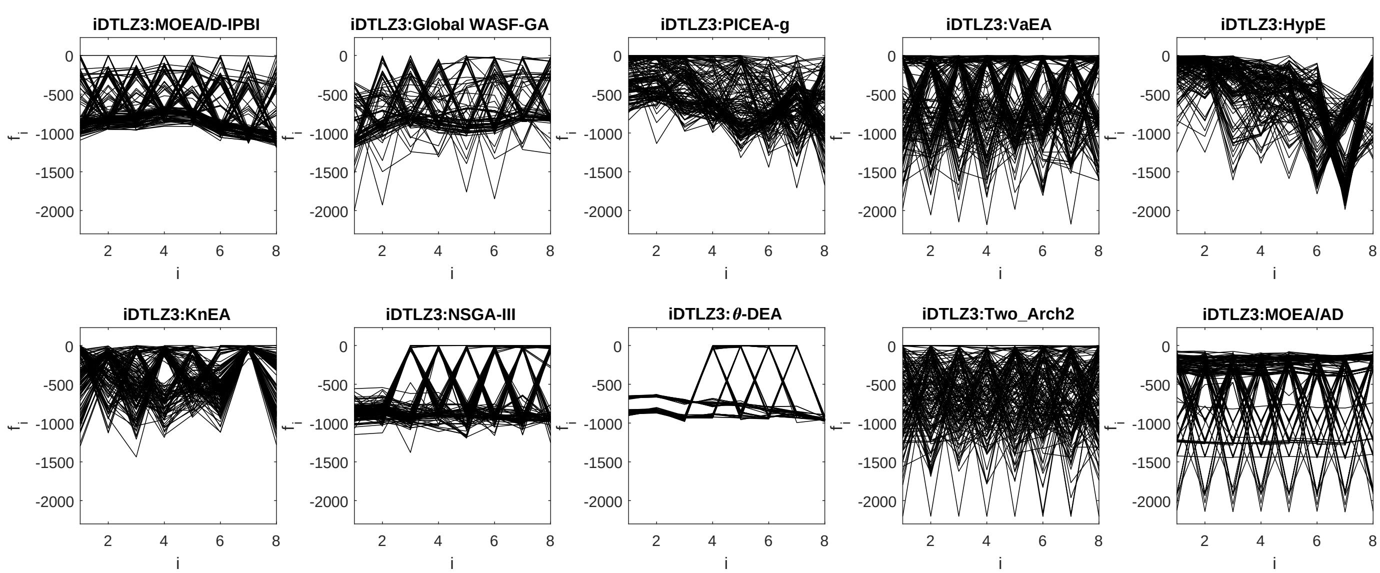

Fig. 78: Final solution sets on 8-objective DTLZ3^{-1} test problem obtained by 10 algorithms in the run of median HV metric values with $\mathbf{z}^r = (2, \cdots, 2)^T$.

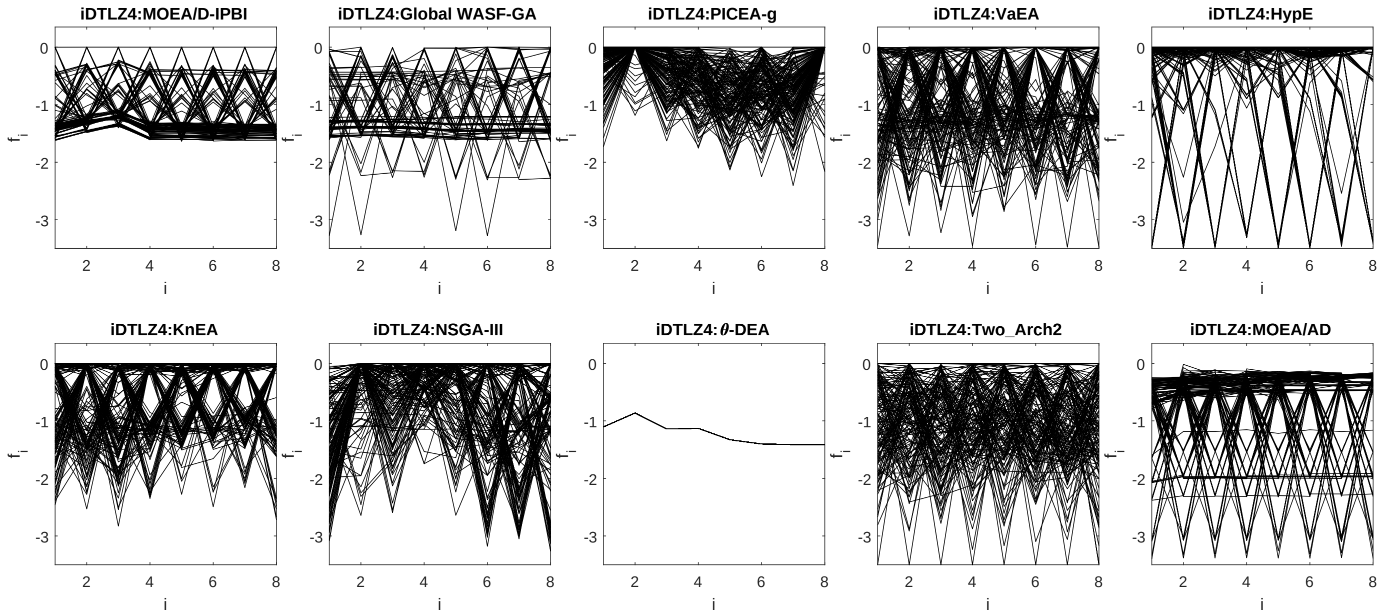

Fig. 79: Final solution sets on 8-objective DTLZ4^{-1} test problem obtained by 10 algorithms in the run of median HV metric values with $\mathbf{z}^r = (2, \cdots, 2)^T$.

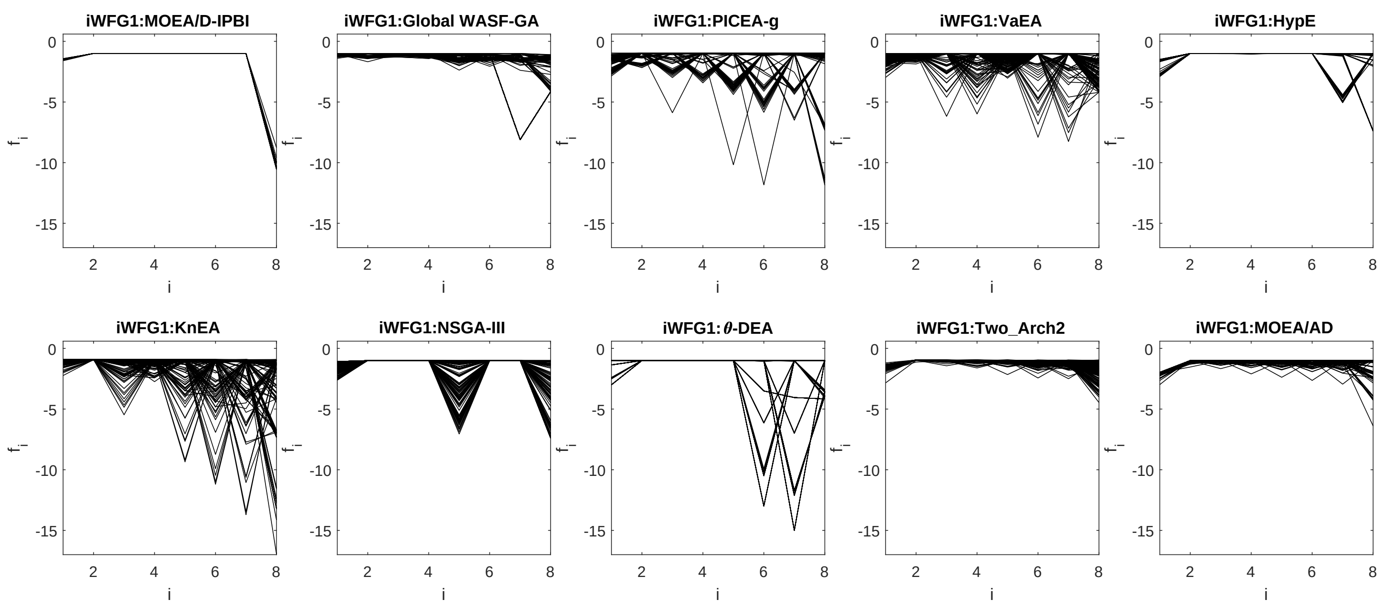

Fig. 80: Final solution sets on 8-objective WFG1^{-1} test problem obtained by 10 algorithms in the run of median HV metric values with $\mathbf{z}^r = (2, \cdots, 2)^T$.

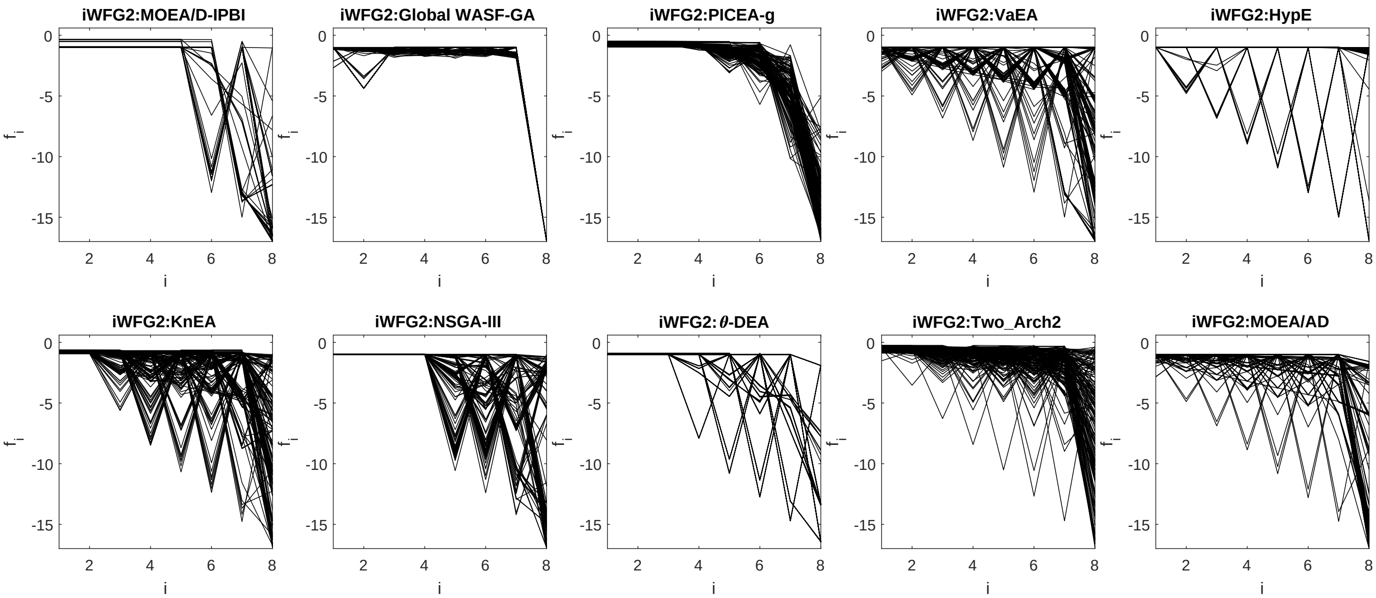

Fig. 81: Final solution sets on 8-objective WFG2^{-1} test problem obtained by 10 algorithms in the run of median HV metric values with $\mathbf{z}^r = (2, \cdots, 2)^T$.

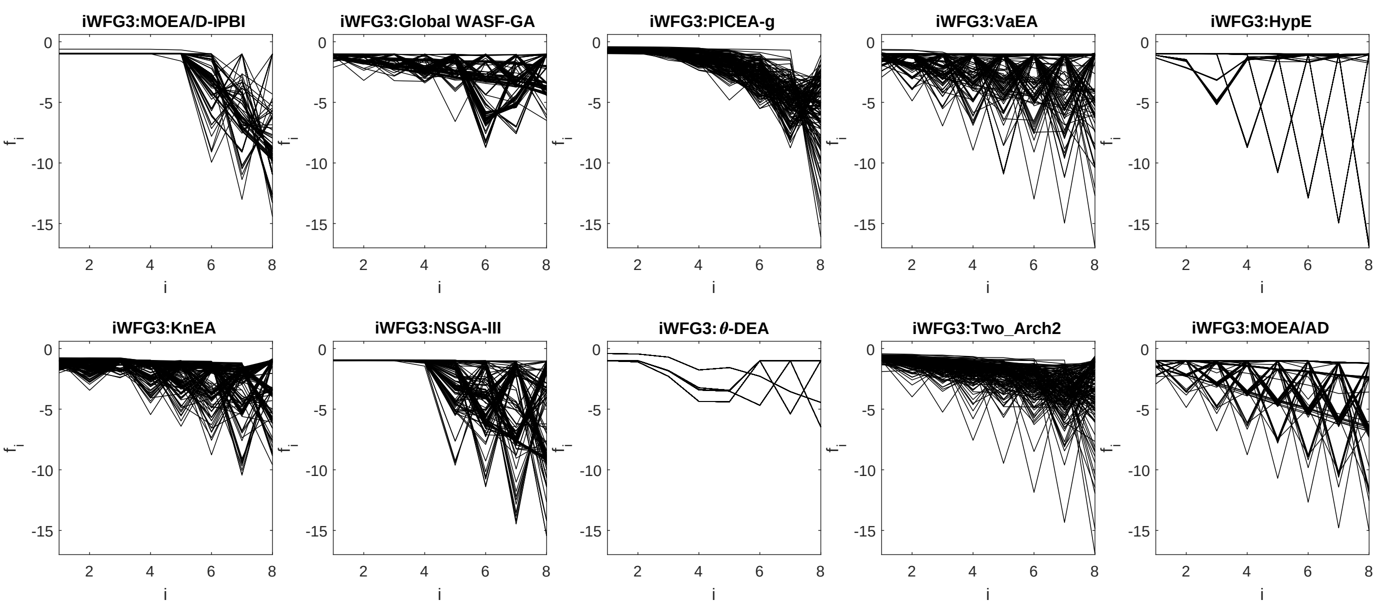

Fig. 82: Final solution sets on 8-objective WFG3^{-1} test problem obtained by 10 algorithms in the run of median HV metric values with $\mathbf{z}^r = (2, \cdots, 2)^T$.

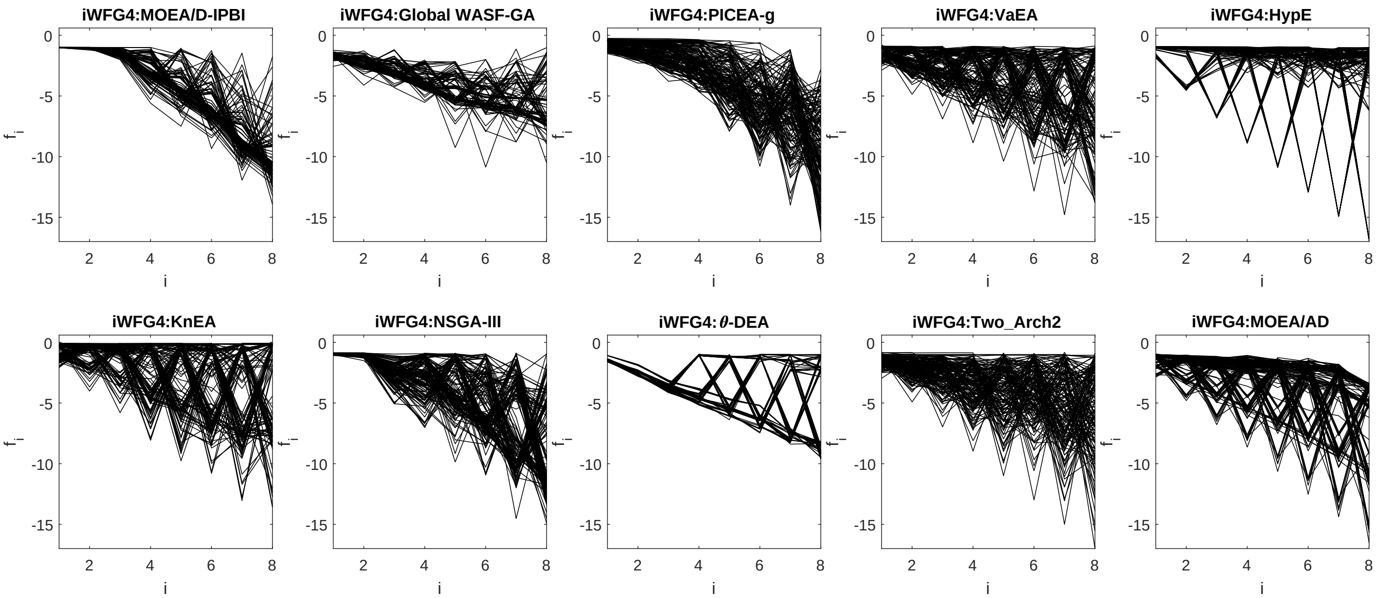

Fig. 83: Final solution sets on 8-objective WFG4^{-1} test problem obtained by 10 algorithms in the run of median HV metric values with $\mathbf{z}^r = (2, \cdots, 2)^T$.

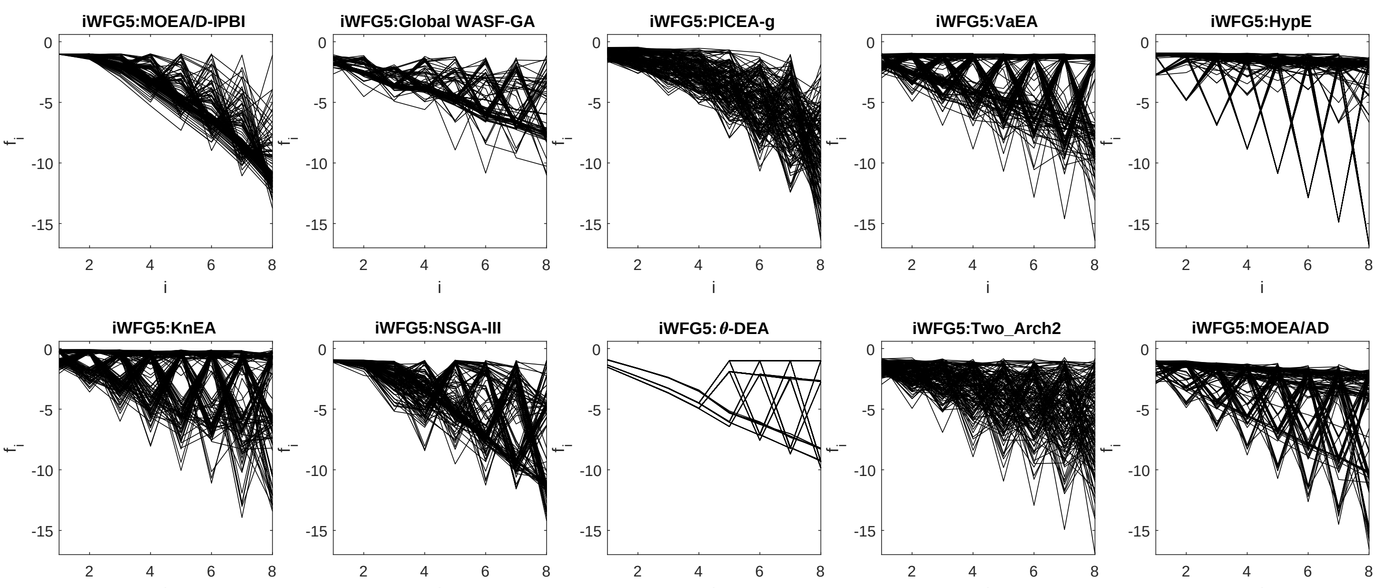

Fig. 84: Final solution sets on 8-objective WFG5^{-1} test problem obtained by 10 algorithms in the run of median HV metric values with $\mathbf{z}^r = (2, \cdots, 2)^T$.

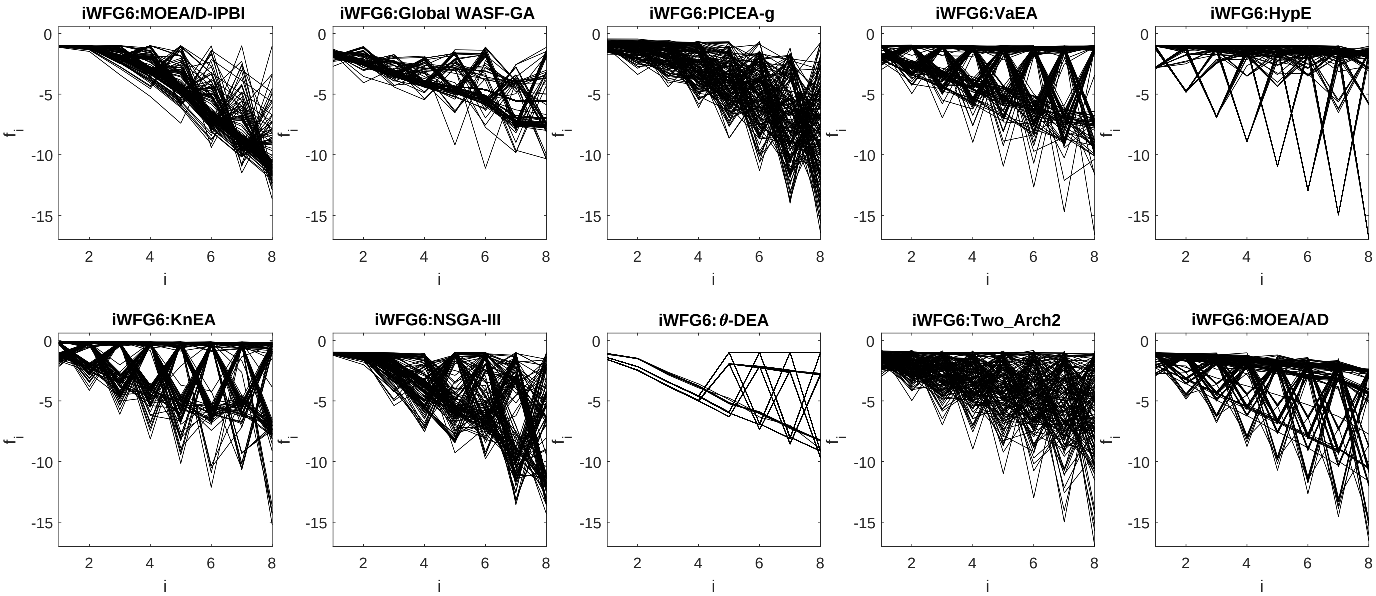

Fig. 85: Final solution sets on 8-objective WFG6^{-1} test problem obtained by 10 algorithms in the run of median HV metric values with $\mathbf{z}^r = (2, \cdots, 2)^T$.

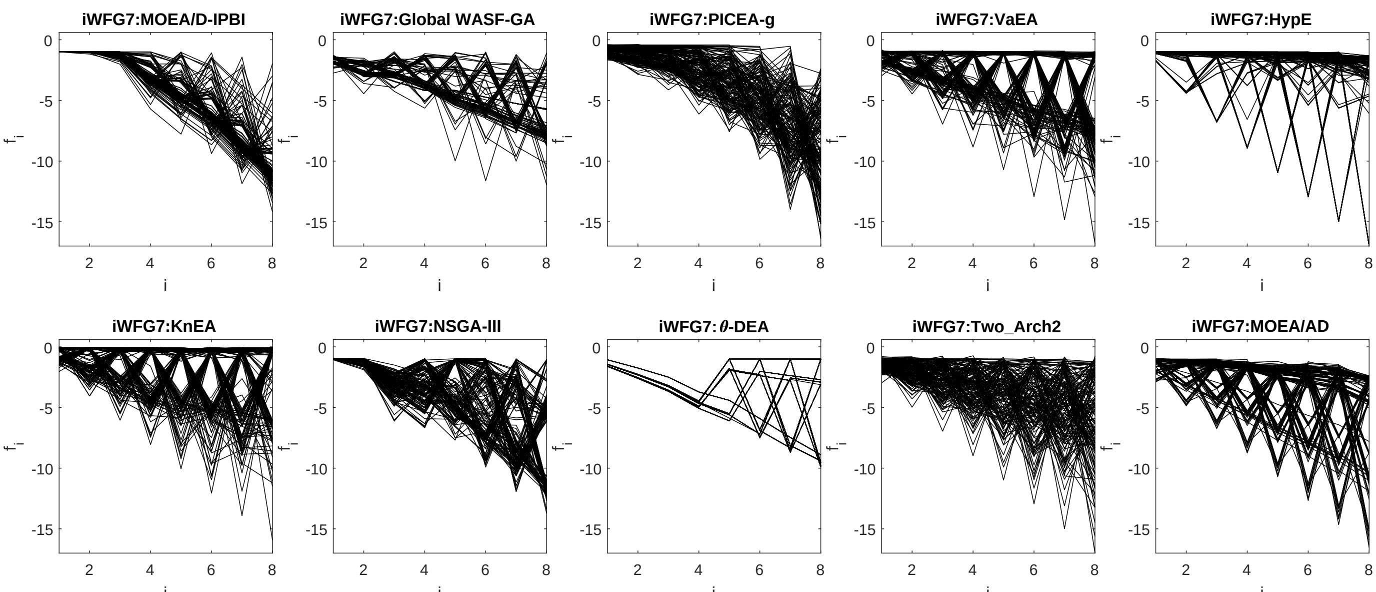

Fig. 86: Final solution sets on 8-objective WFG7^{-1} test problem obtained by 10 algorithms in the run of median HV metric values with $\mathbf{z}^r = (2, \cdots, 2)^T$.

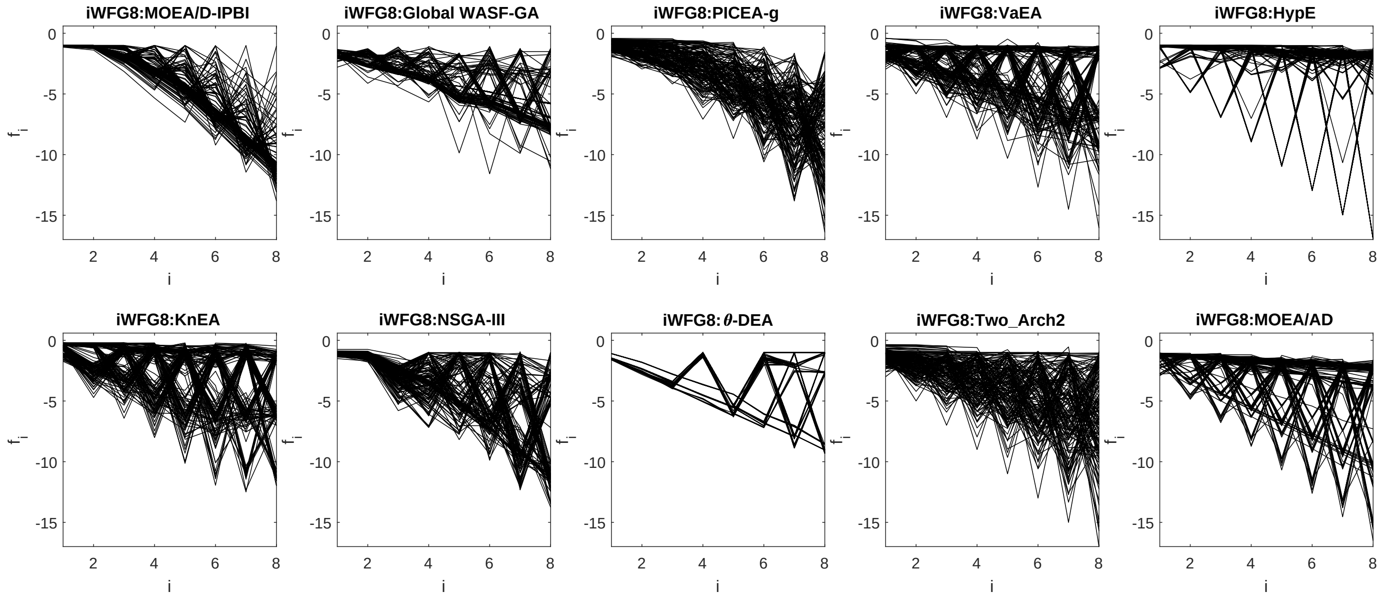

Fig. 87: Final solution sets on 8-objective WFG8^{-1} test problem obtained by 10 algorithms in the run of median HV metric values with $\mathbf{z}^r = (2, \cdots, 2)^T$.

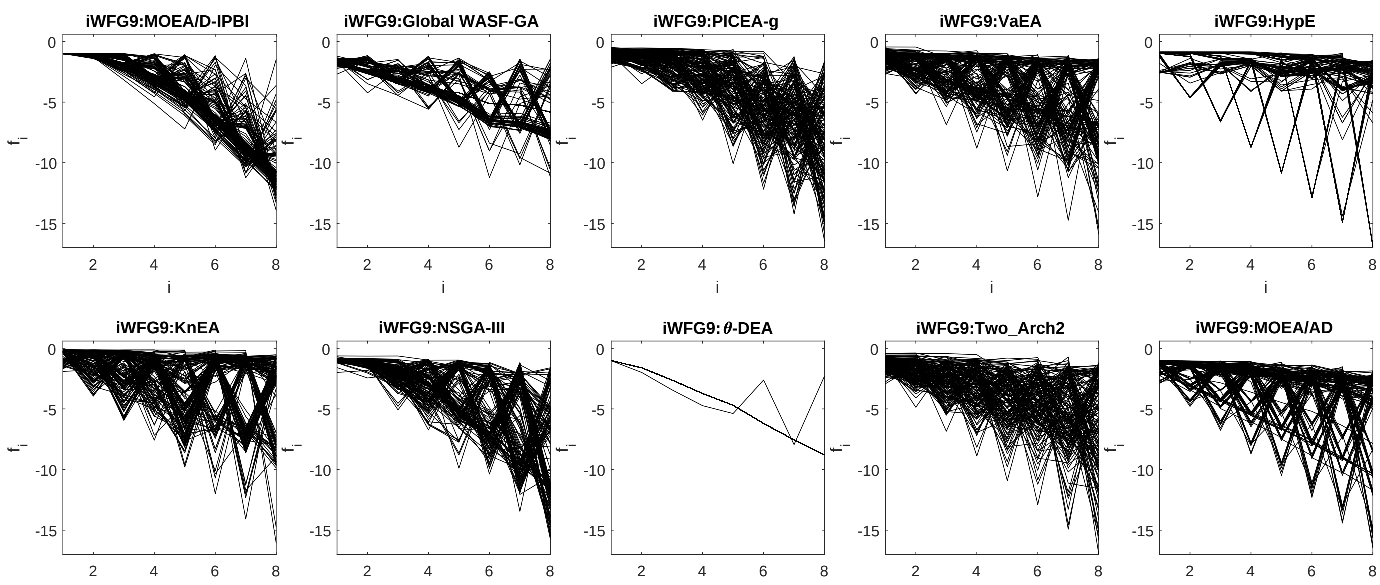

Fig. 88: Final solution sets on 8-objective WFG9^{-1} test problem obtained by 10 algorithms in the run of median HV metric values with $\mathbf{z}^r = (2, \cdots, 2)^T$.

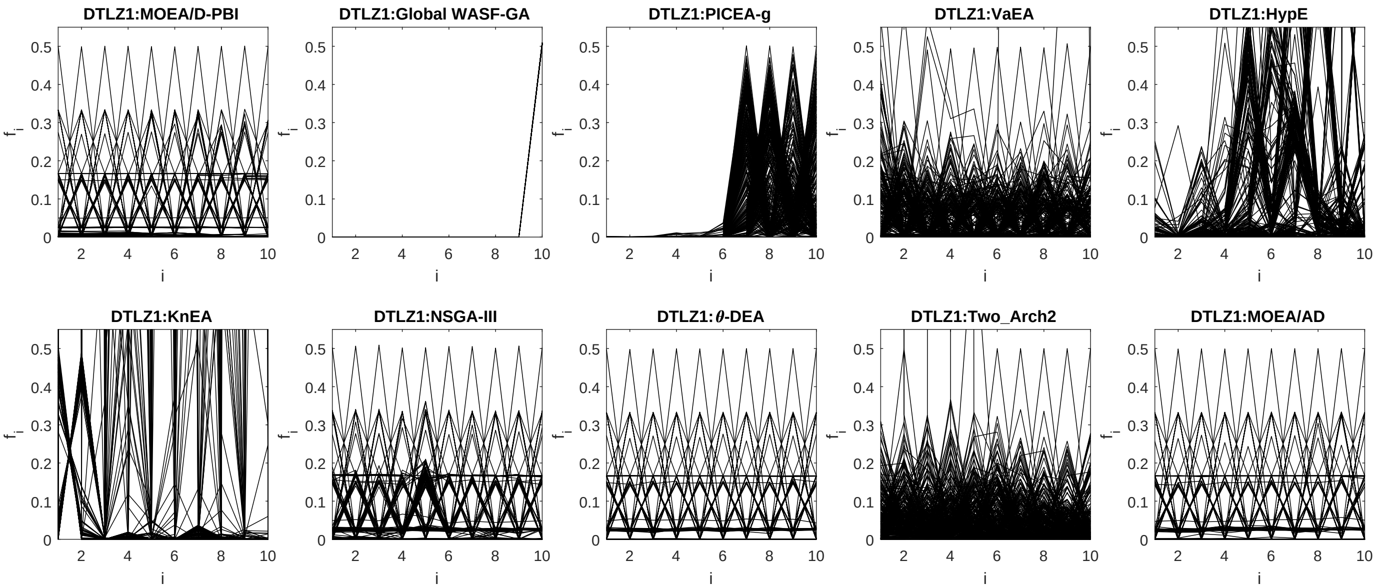

Fig. 89: Final solution sets on 10-objective DTLZ1 test problem obtained by 10 algorithms in the run of median HV metric values with $\mathbf{z}^r = (2, \cdots, 2)^T$.

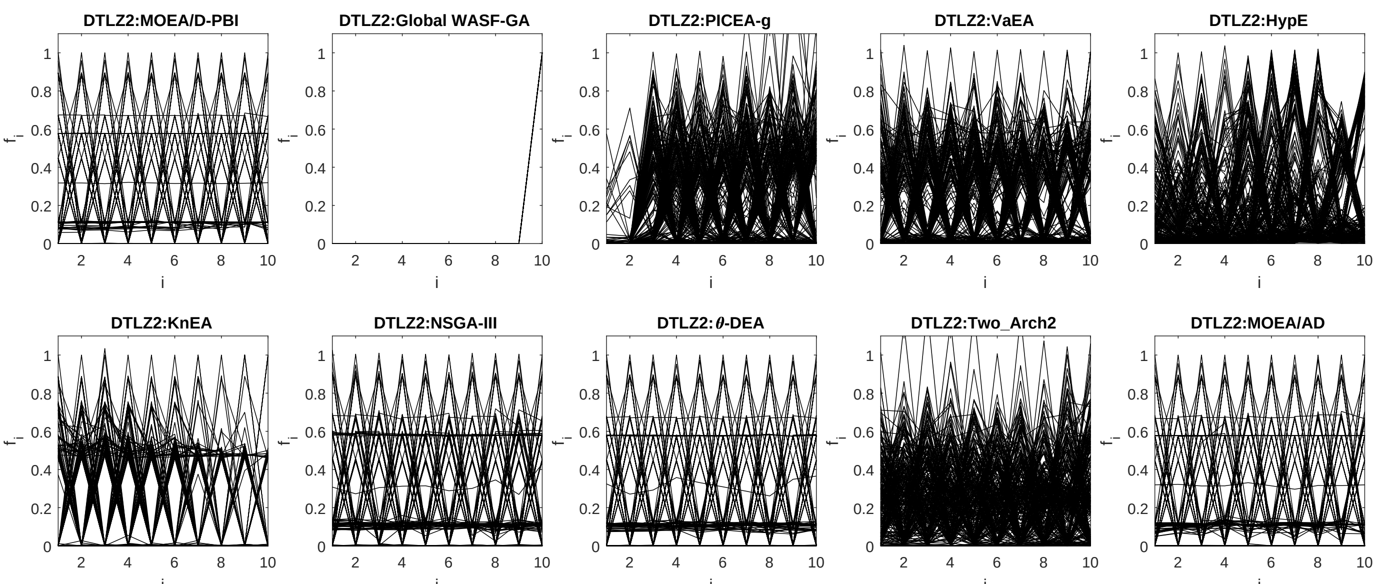

Fig. 90: Final solution sets on 10-objective DTLZ2 test problem obtained by 10 algorithms in the run of median HV metric values with $\mathbf{z}^r = (2, \cdots, 2)^T$.

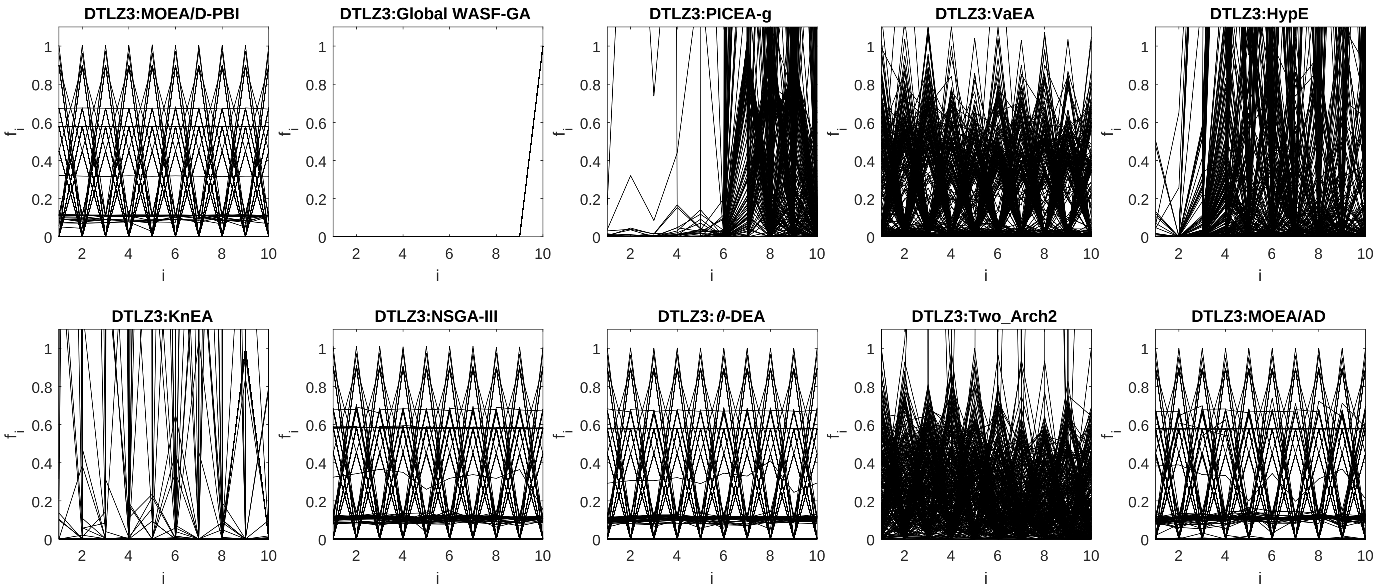

Fig. 91: Final solution sets on 10-objective DTLZ3 test problem obtained by 10 algorithms in the run of median HV metric values with $\mathbf{z}^r = (2, \cdots, 2)^T$.

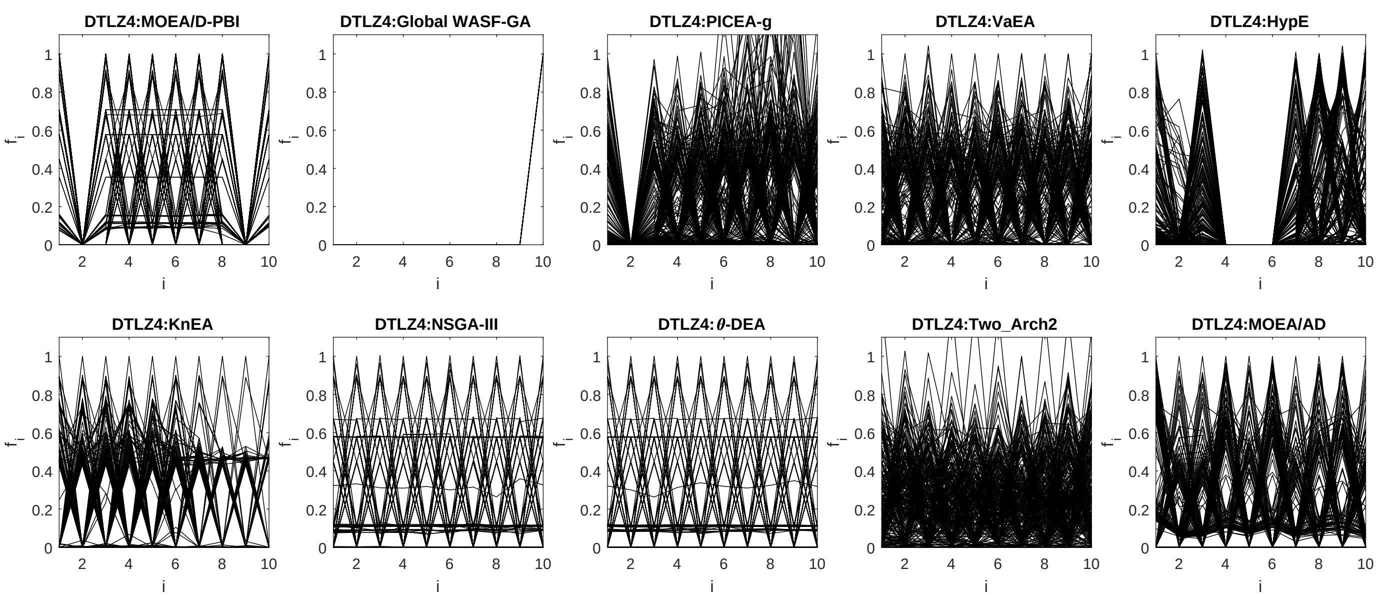

Fig. 92: Final solution sets on 10-objective DTLZ4 test problem obtained by 10 algorithms in the run of median HV metric values with $\mathbf{z}^r = (2, \cdots, 2)^T$.

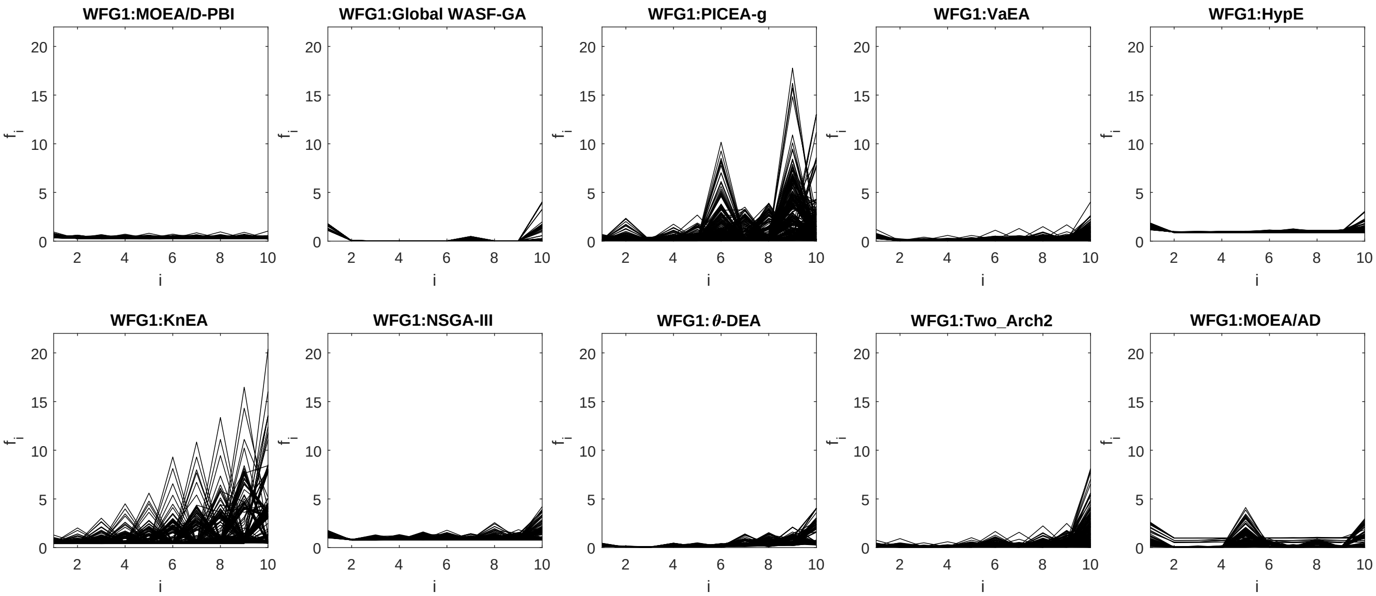

Fig. 93: Final solution sets on 10-objective WFG1 test problem obtained by 10 algorithms in the run of median HV metric values with $\mathbf{z}^r = (2, \cdots, 2)^T$.

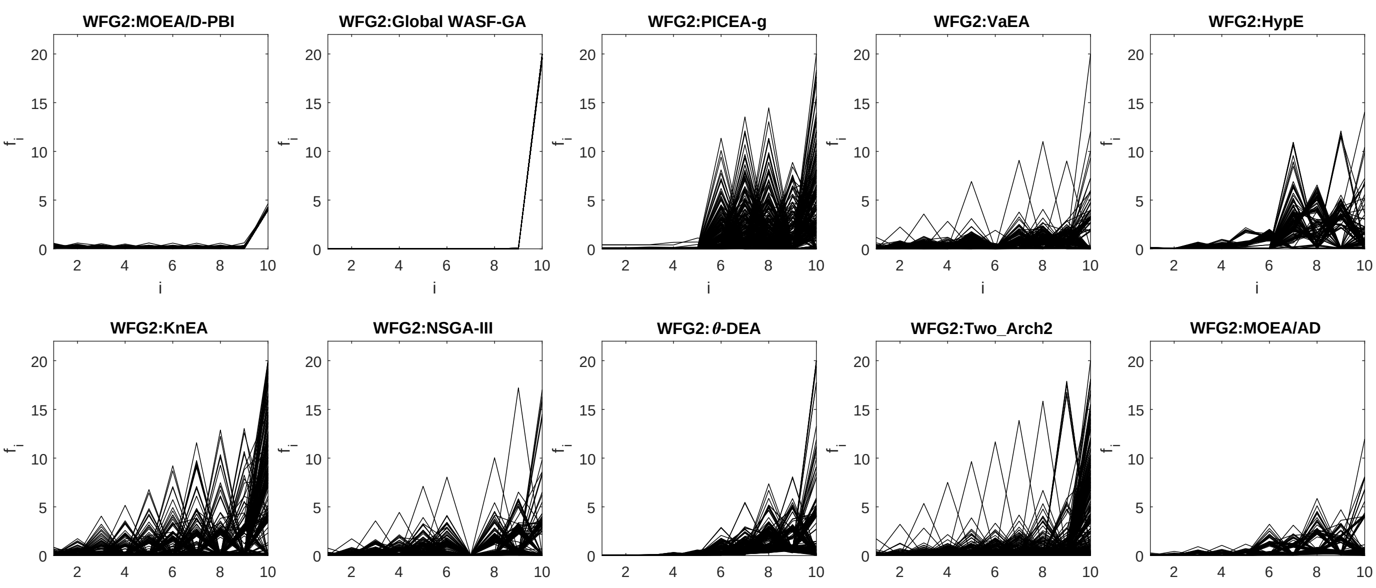

Fig. 94: Final solution sets on 10-objective WFG2 test problem obtained by 10 algorithms in the run of median HV metric values with $\mathbf{z}^r = (2, \cdots, 2)^T$.

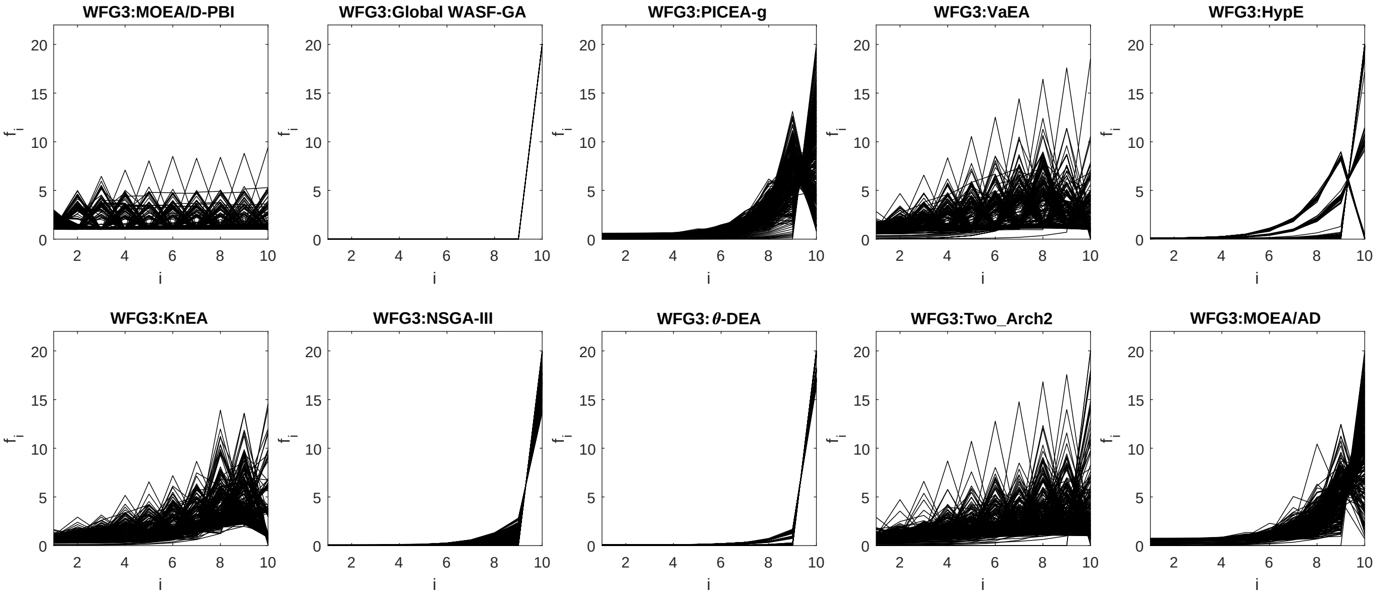

Fig. 95: Final solution sets on 10-objective WFG3 test problem obtained by 10 algorithms in the run of median HV metric values with $\mathbf{z}^r = (2, \cdots, 2)^T$.

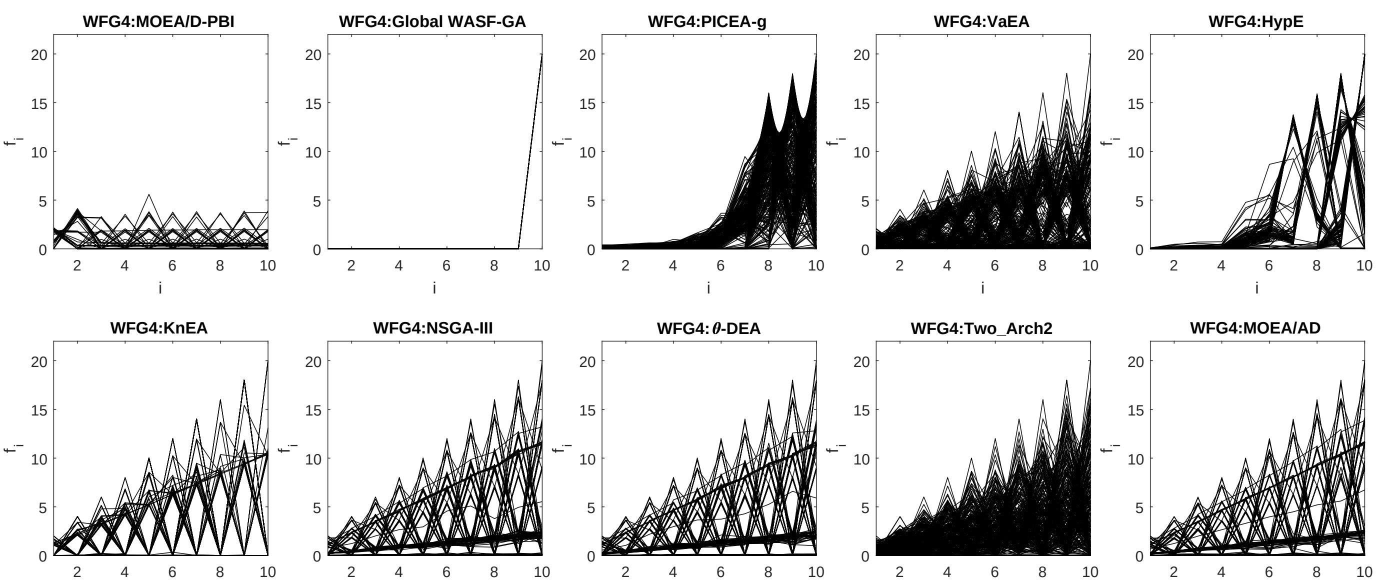

Fig. 96: Final solution sets on 10-objective WFG4 test problem obtained by 10 algorithms in the run of median HV metric values with $\mathbf{z}^r = (2, \cdots, 2)^T$.

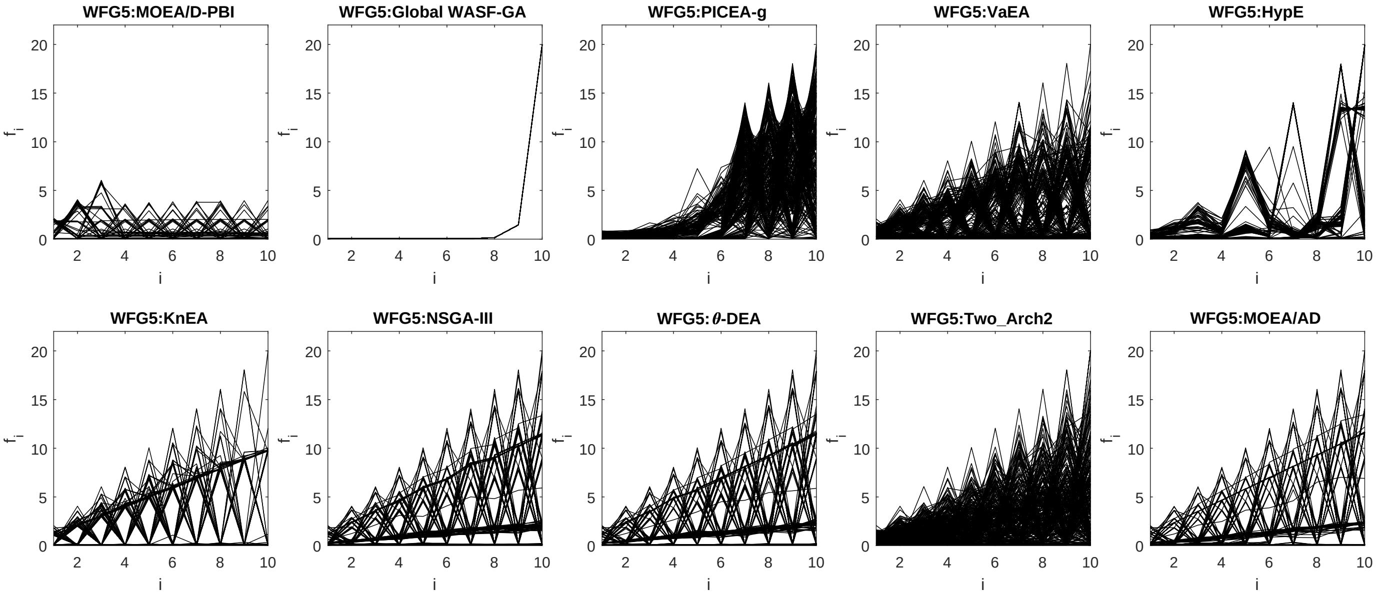

Fig. 97: Final solution sets on 10-objective WFG5 test problem obtained by 10 algorithms in the run of median HV metric values with $\mathbf{z}^r = (2, \cdots, 2)^T$.

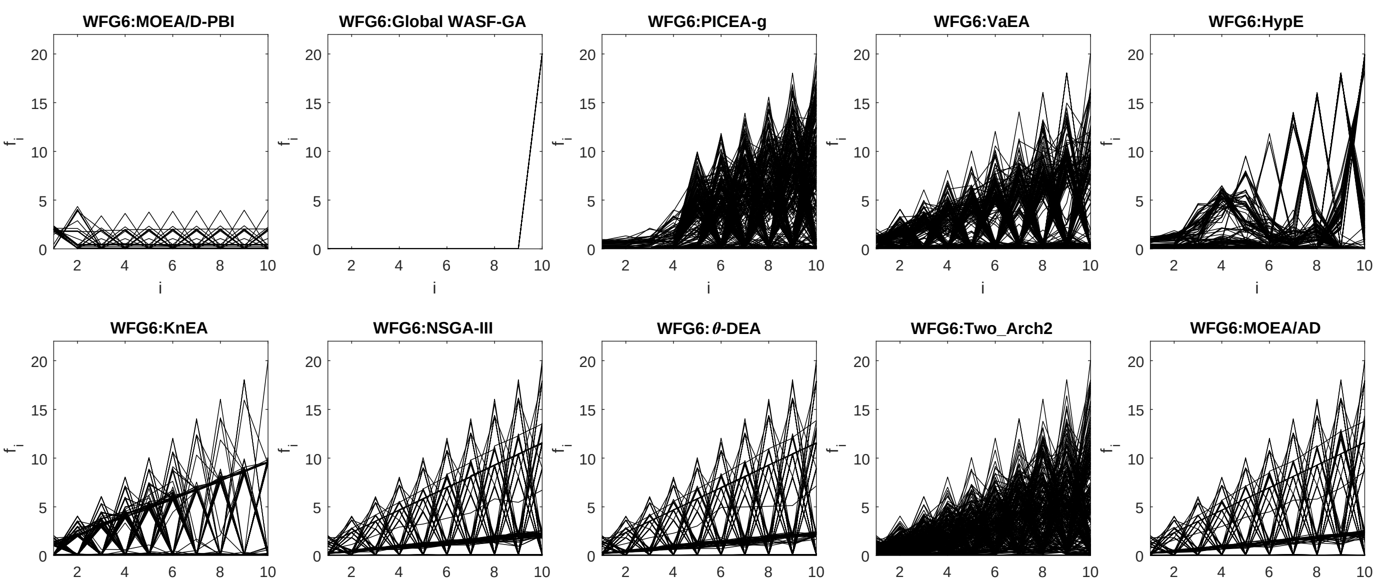

Fig. 98: Final solution sets on 10-objective WFG6 test problem obtained by 10 algorithms in the run of median HV metric values with $\mathbf{z}^r = (2, \cdots, 2)^T$.

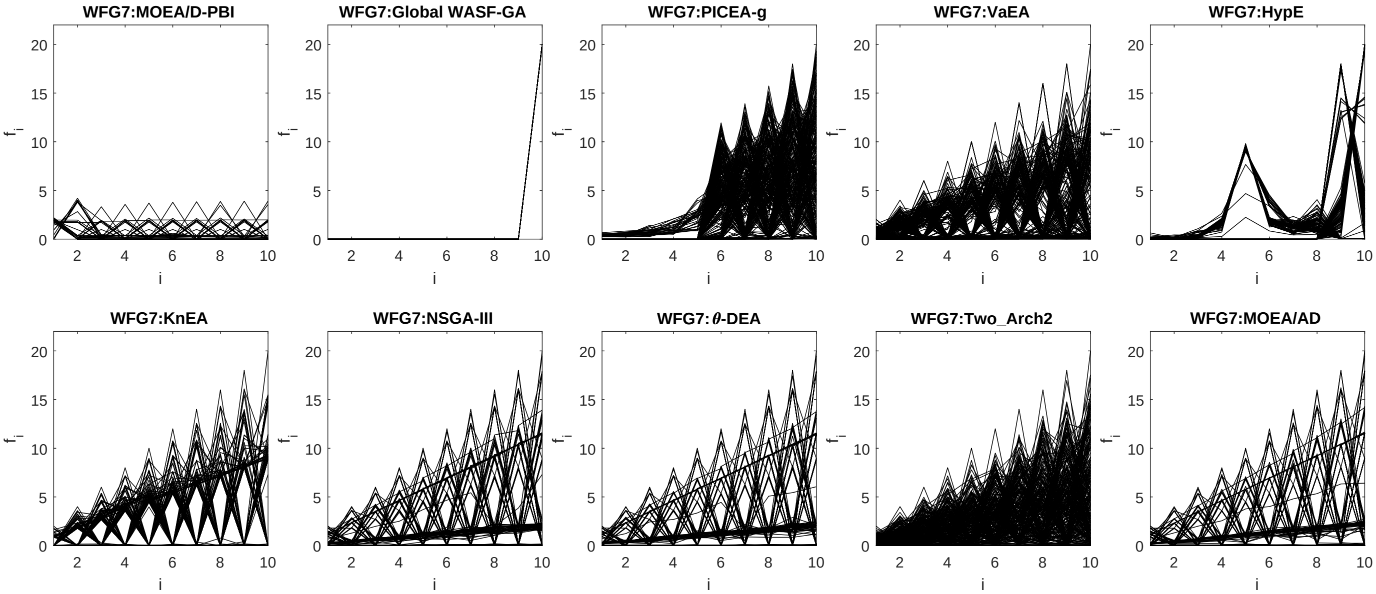

Fig. 99: Final solution sets on 10-objective WFG7 test problem obtained by 10 algorithms in the run of median HV metric values with $\mathbf{z}^r = (2, \cdots, 2)^T$.

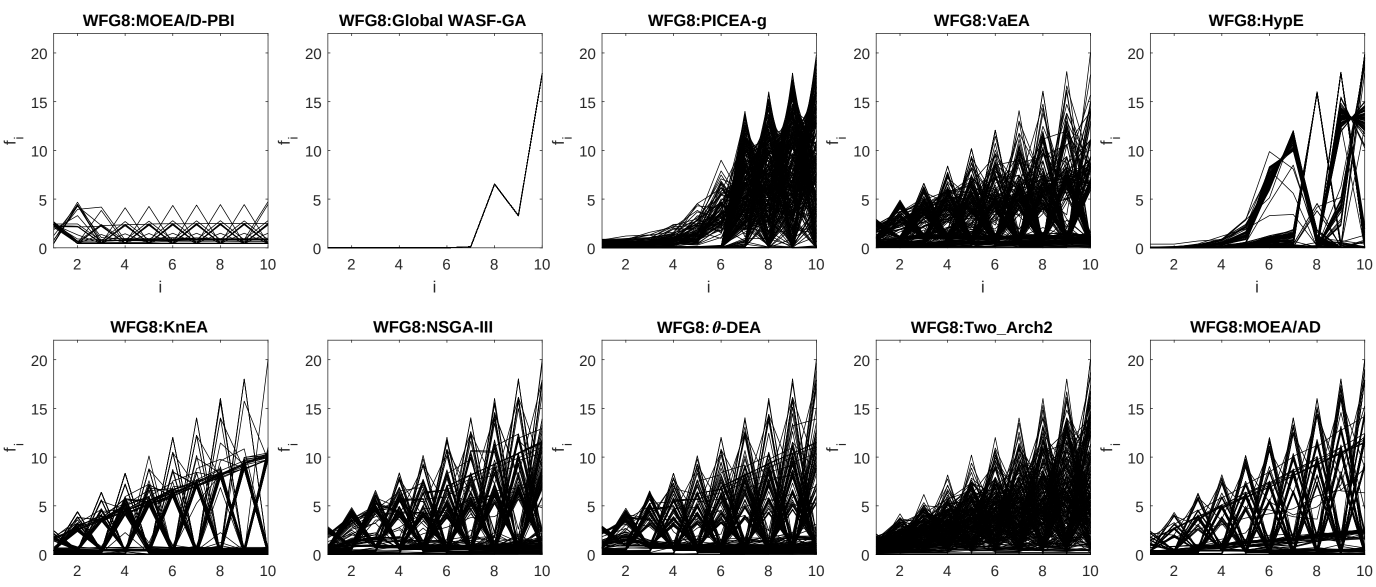

Fig. 100: Final solution sets on 10-objective WFG8 test problem obtained by 10 algorithms in the run of median HV metric values with $\mathbf{z}^r = (2, \cdots, 2)^T$.

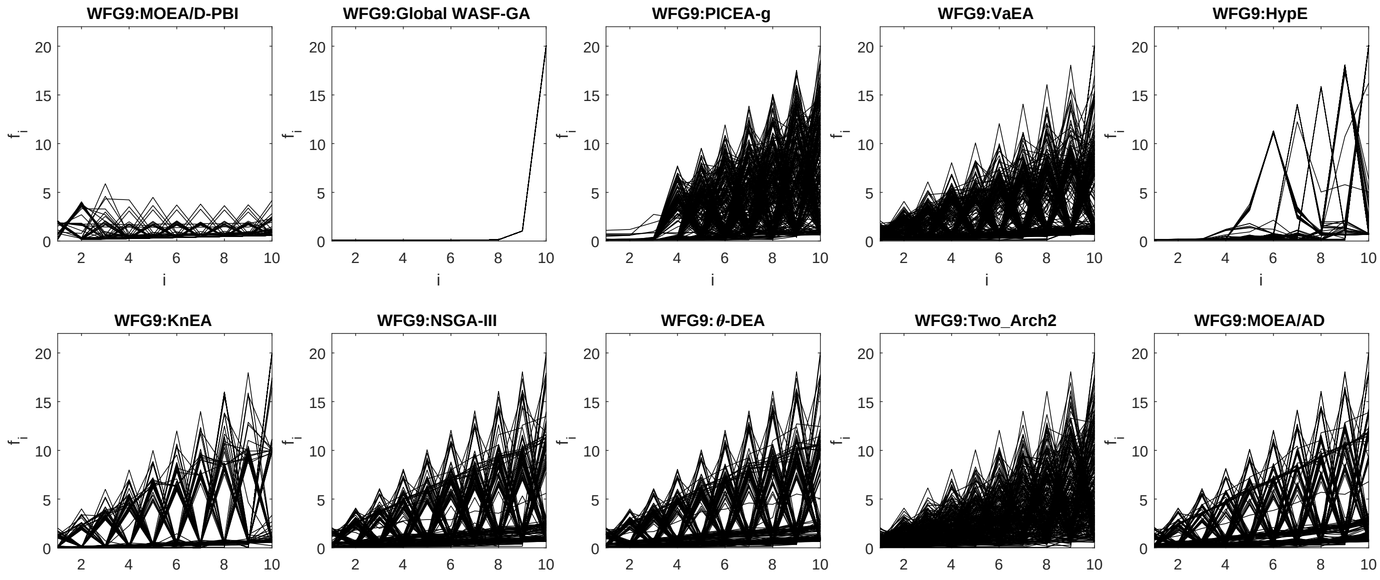

Fig. 101: Final solution sets on 10-objective WFG9 test problem obtained by 10 algorithms in the run of median HV metric values with $\mathbf{z}^r = (2, \cdots, 2)^T$.

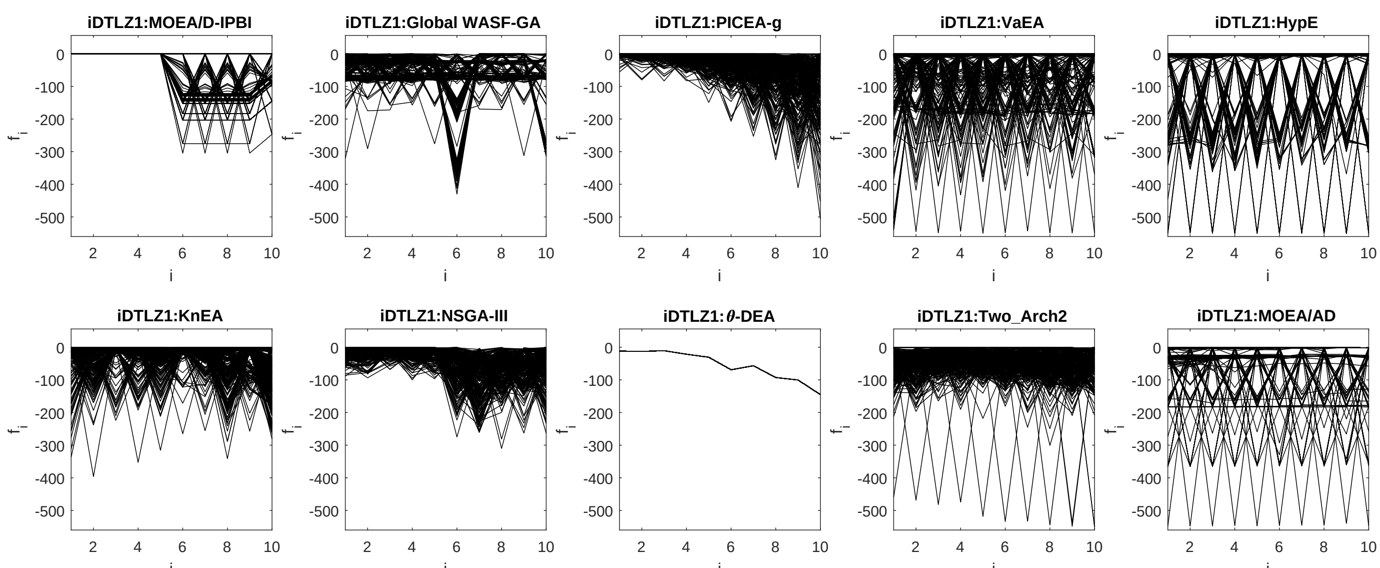

Fig. 102: Final solution sets on 10-objective DTLZ1^{-1} test problem obtained by 10 algorithms in the run of median HV metric values with $\mathbf{z}^r = (2, \cdots, 2)^T$.

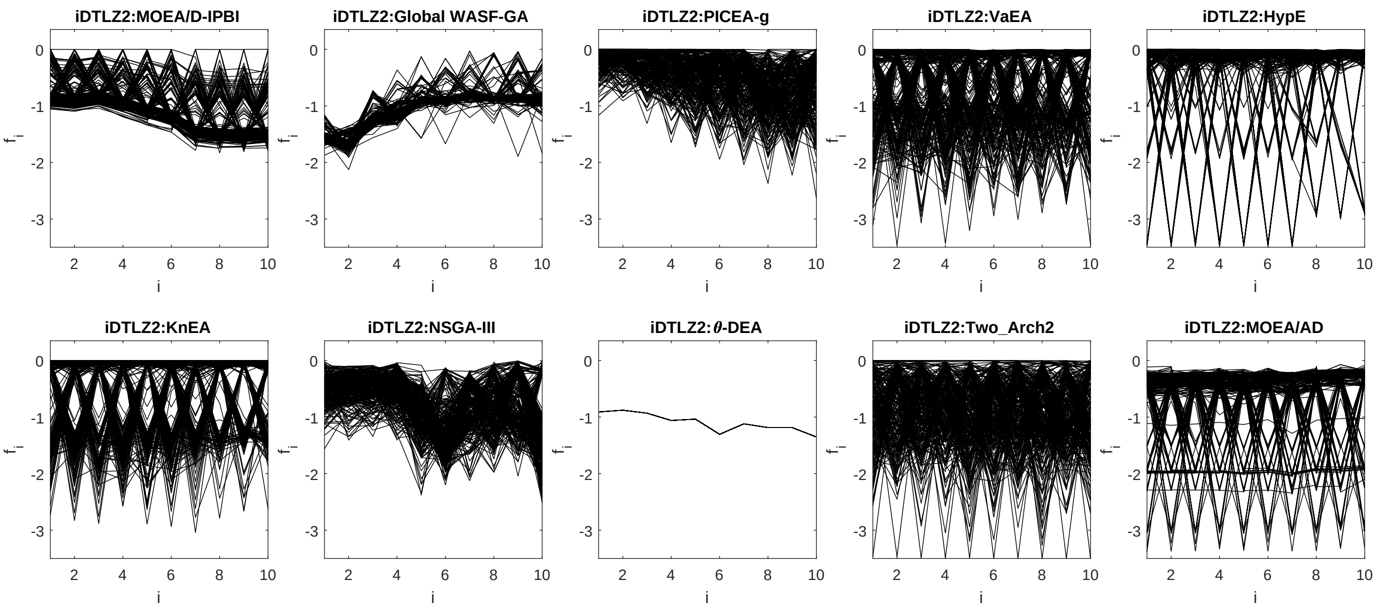

Fig. 103: Final solution sets on 10-objective DTLZ2^{-1} test problem obtained by 10 algorithms in the run of median HV metric values with $\mathbf{z}^r = (2, \cdots, 2)^T$.

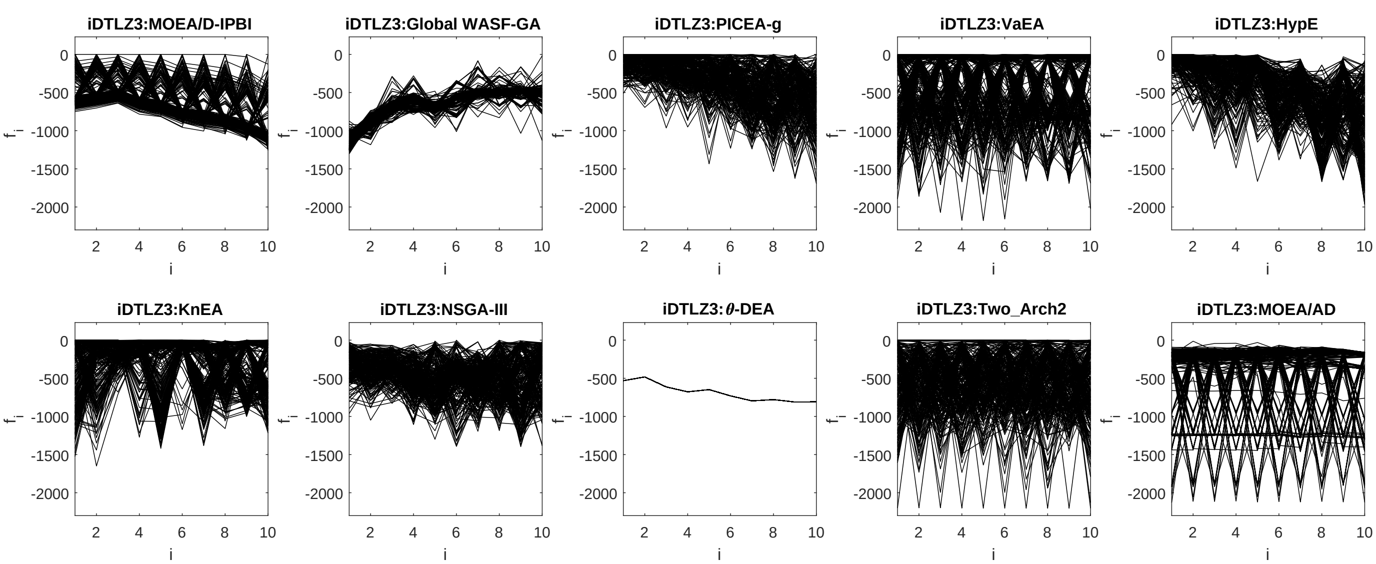

Fig. 104: Final solution sets on 10-objective DTLZ3^{-1} test problem obtained by 10 algorithms in the run of median HV metric values with $\mathbf{z}^r = (2, \cdots, 2)^T$.

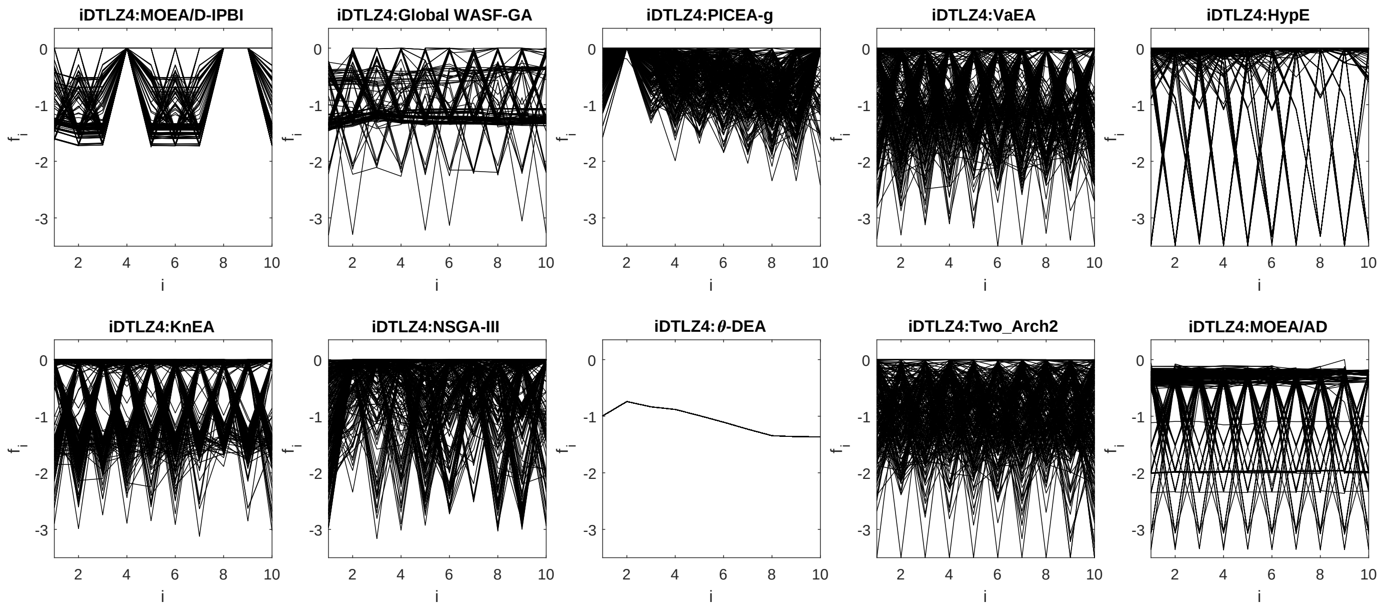

Fig. 105: Final solution sets on 10-objective DTLZ4^{-1} test problem obtained by 10 algorithms in the run of median HV metric values with $\mathbf{z}^r = (2, \cdots, 2)^T$.

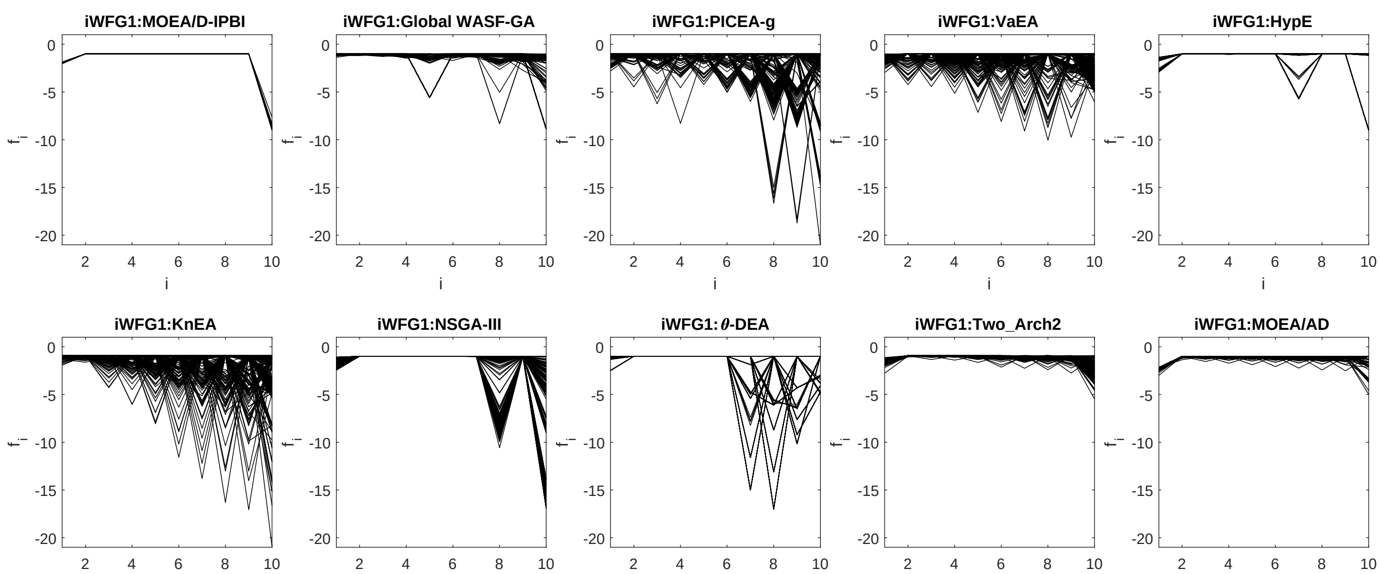

Fig. 106: Final solution sets on 10-objective WFG1^{-1} test problem obtained by 10 algorithms in the run of median HV metric values with $\mathbf{z}^r = (2, \cdots, 2)^T$.

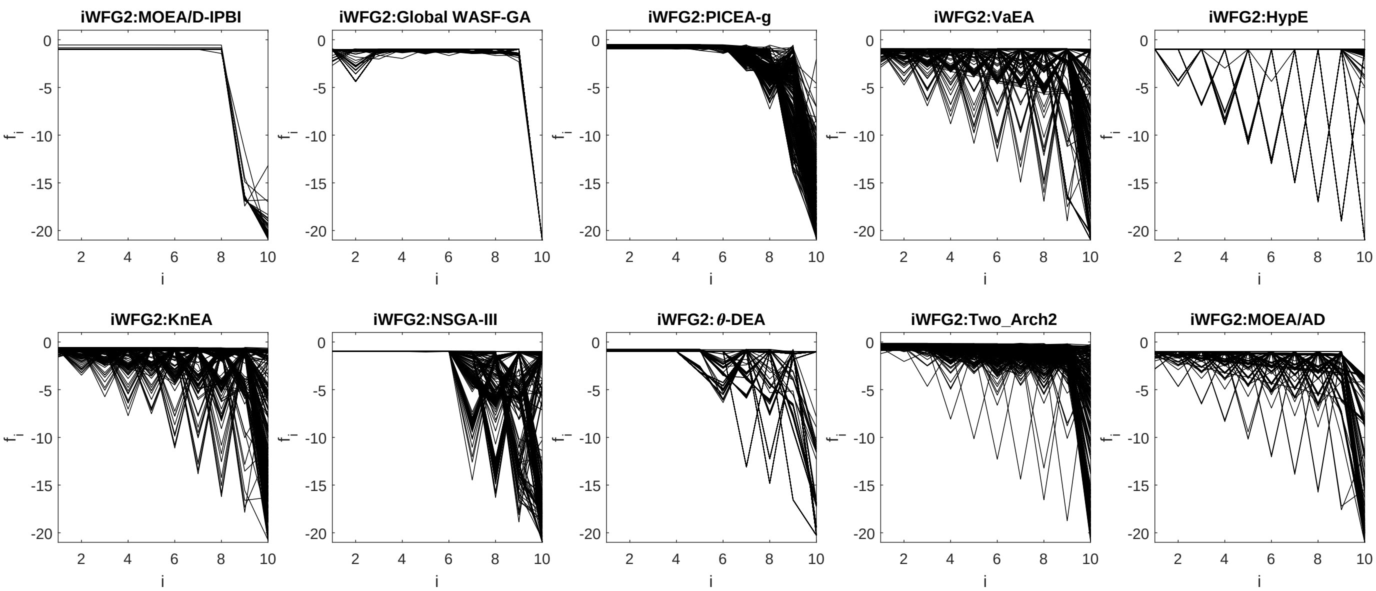

Fig. 107: Final solution sets on 10-objective WFG2^{-1} test problem obtained by 10 algorithms in the run of median HV metric values with $\mathbf{z}^r = (2, \cdots, 2)^T$.

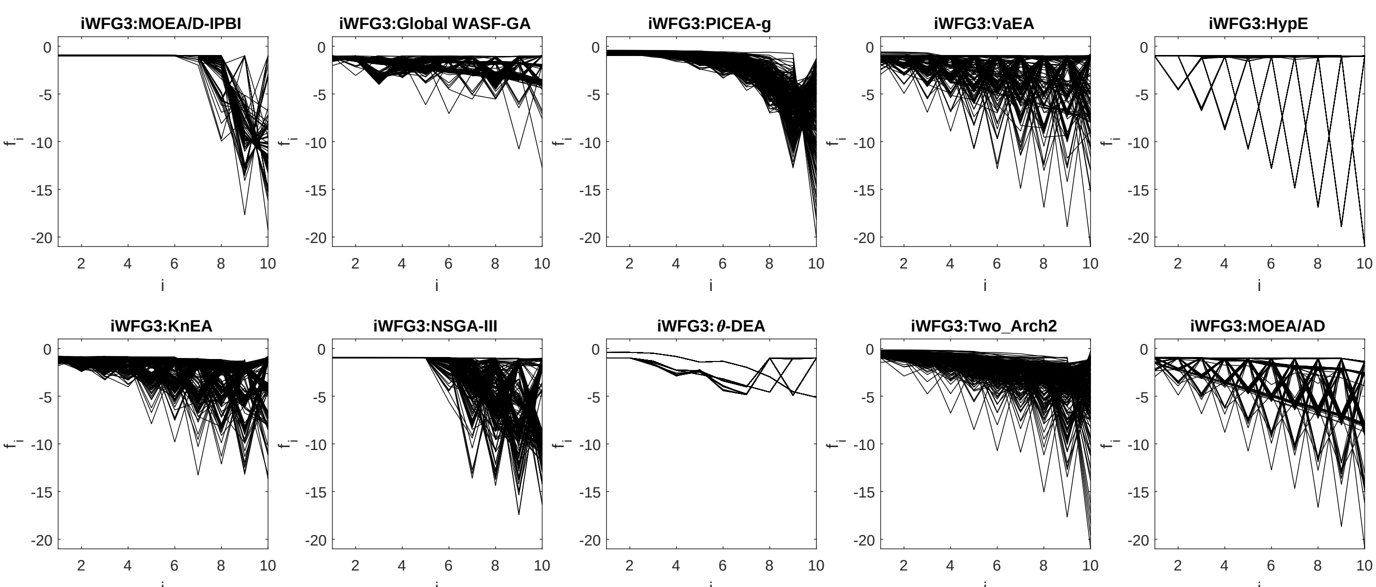

Fig. 108: Final solution sets on 10-objective WFG3^{-1} test problem obtained by 10 algorithms in the run of median HV metric values with $\mathbf{z}^r = (2, \cdots, 2)^T$.

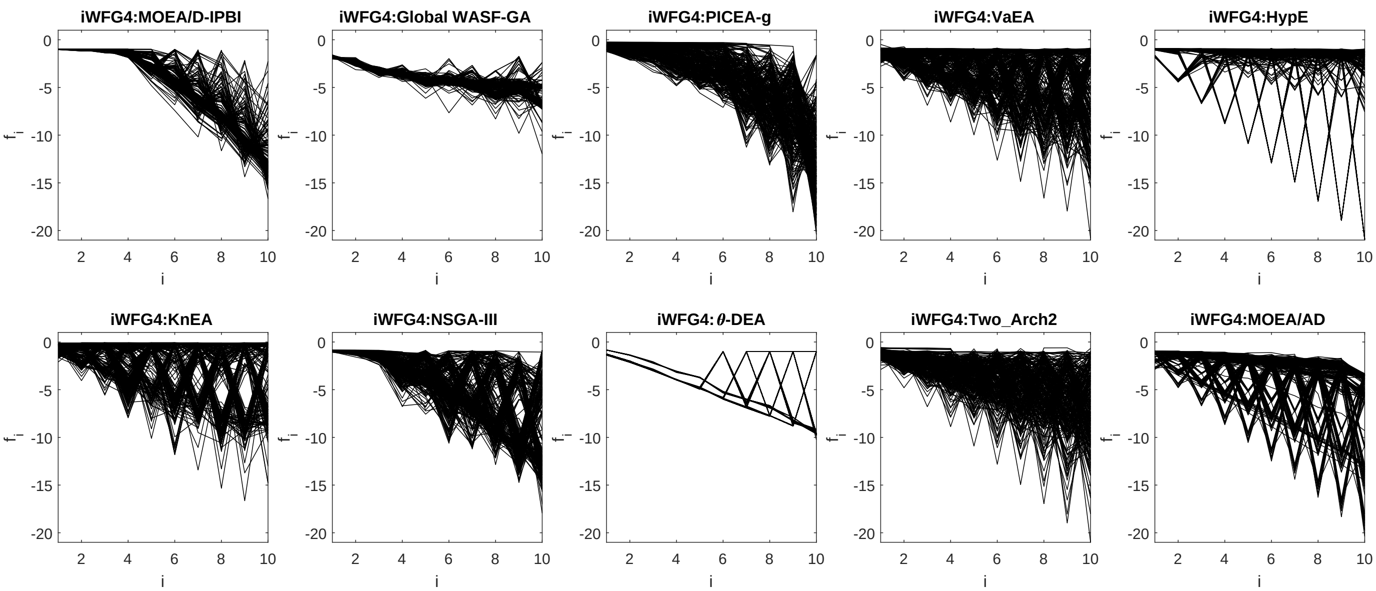

Fig. 109: Final solution sets on 10-objective WFG4^{-1} test problem obtained by 10 algorithms in the run of median HV metric values with $\mathbf{z}^r = (2, \cdots, 2)^T$.

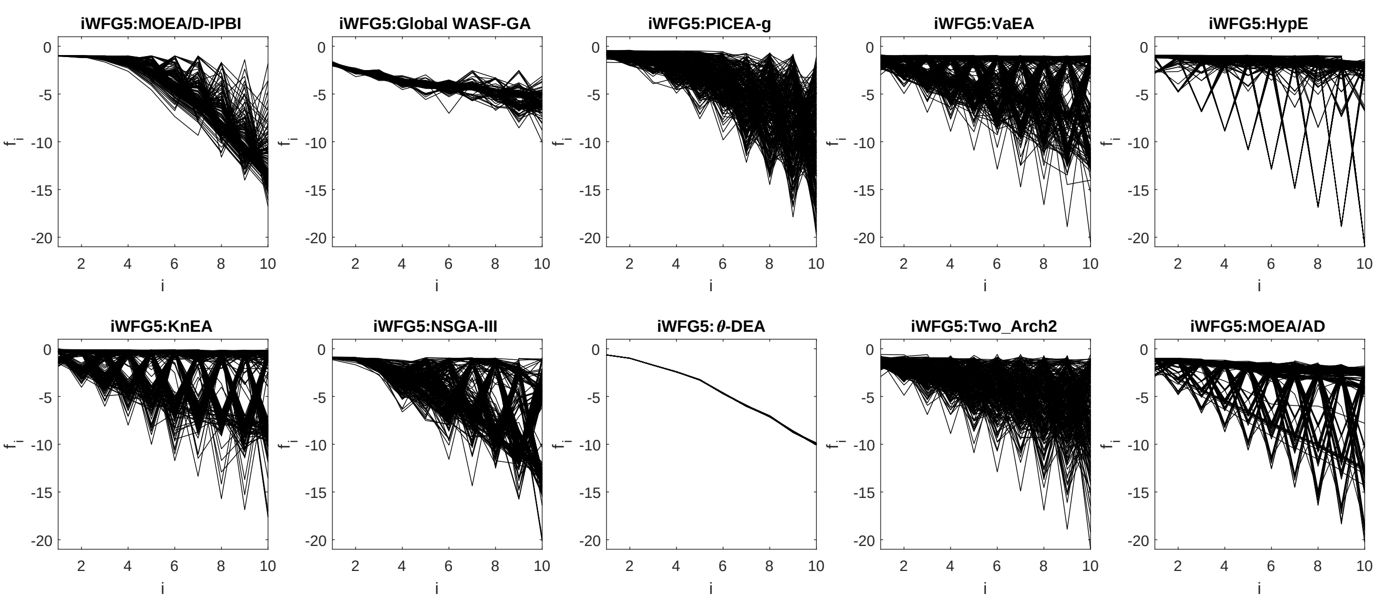

Fig. 110: Final solution sets on 10-objective WFG5^{-1} test problem obtained by 10 algorithms in the run of median HV metric values with $\mathbf{z}^r = (2, \cdots, 2)^T$.

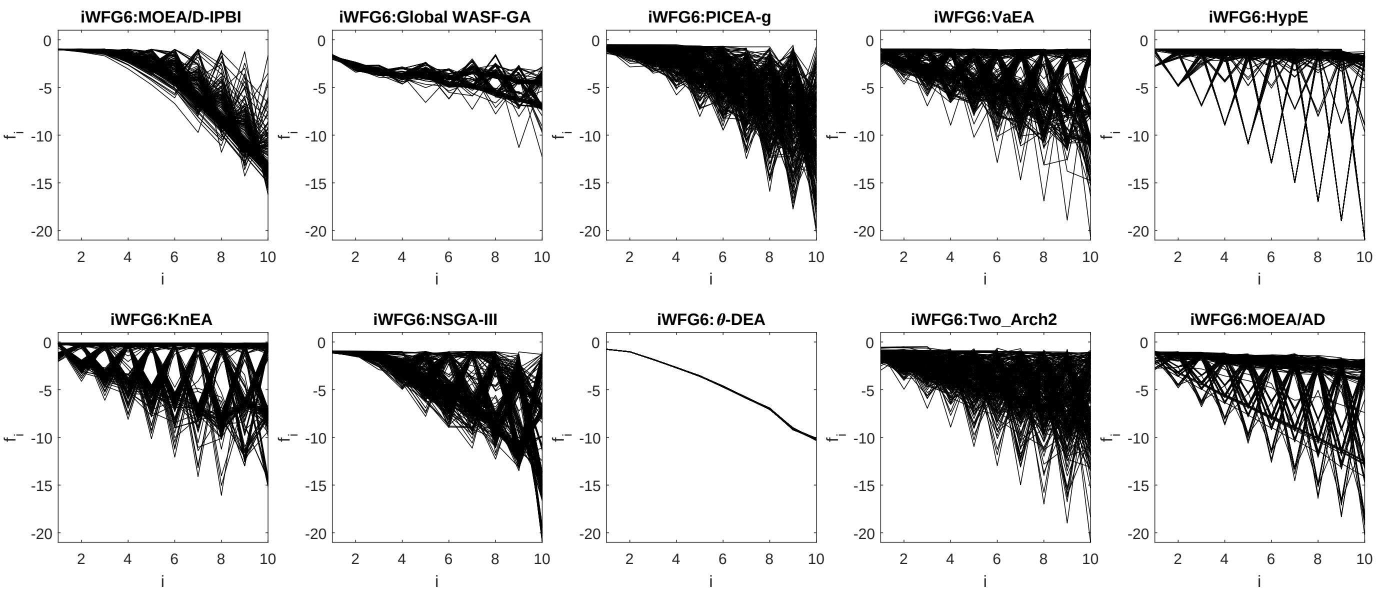

Fig. 111: Final solution sets on 10-objective WFG6^{-1} test problem obtained by 10 algorithms in the run of median HV metric values with $\mathbf{z}^r = (2, \cdots, 2)^T$.

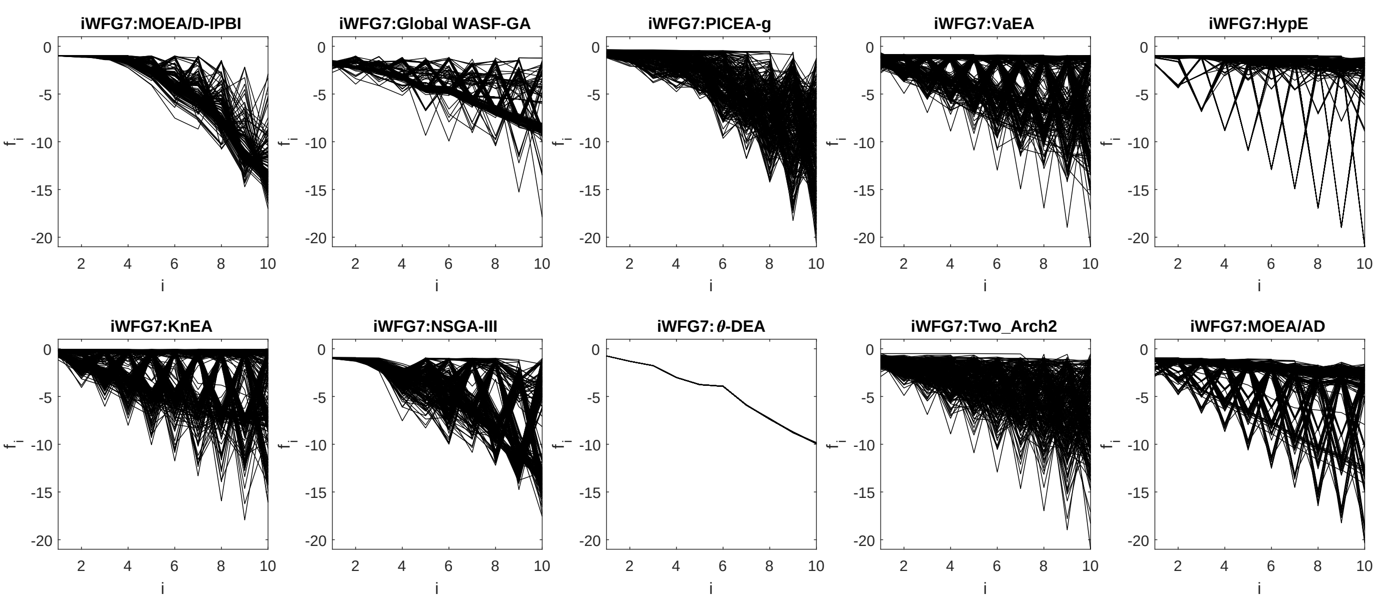

Fig. 112: Final solution sets on 10-objective WFG7^{-1} test problem obtained by 10 algorithms in the run of median HV metric values with $\mathbf{z}^r = (2, \cdots, 2)^T$.

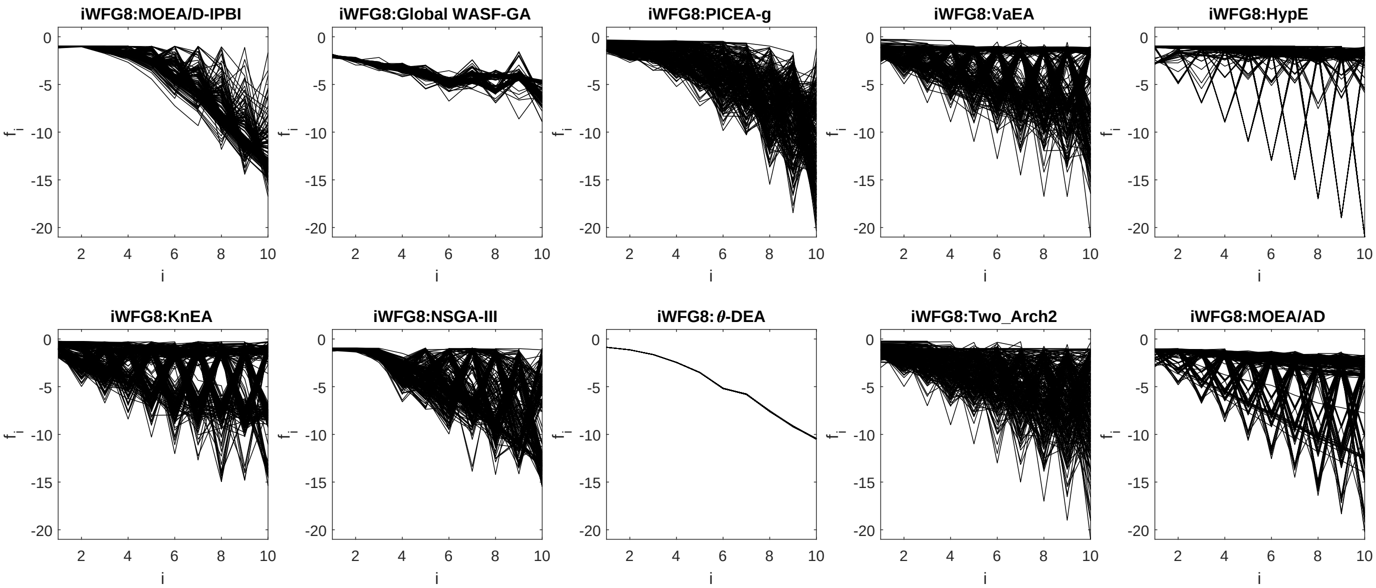

Fig. 113: Final solution sets on 10-objective WFG8^{-1} test problem obtained by 10 algorithms in the run of median HV metric values with $\mathbf{z}^r = (2, \cdots, 2)^T$.

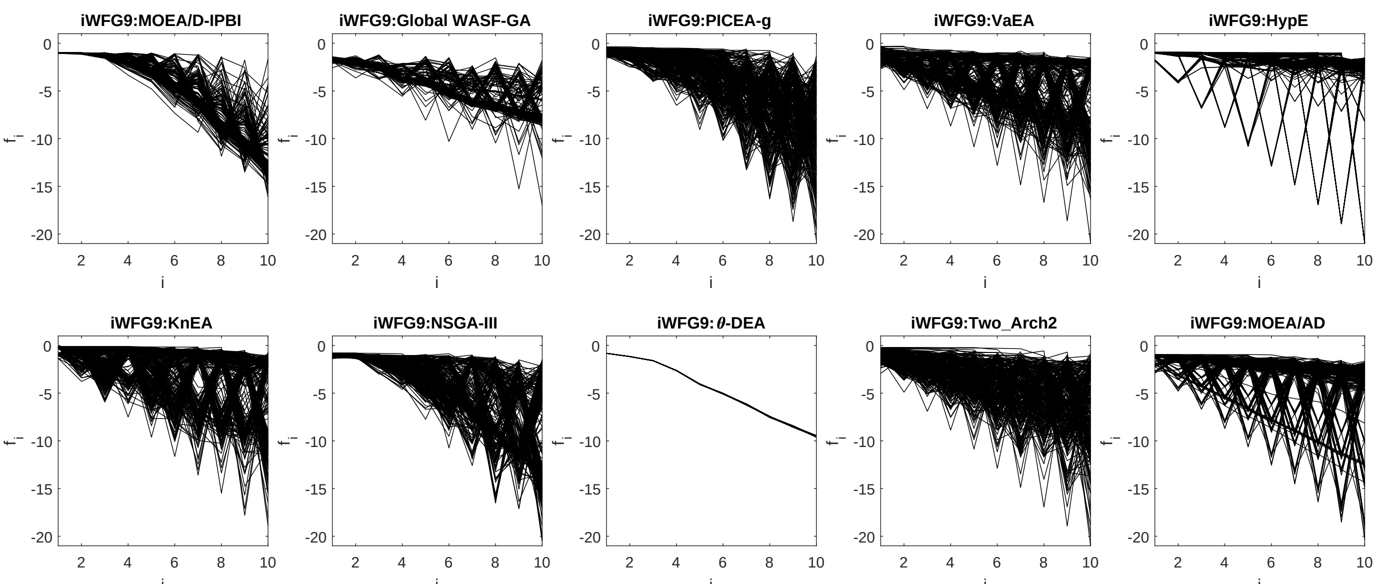

Fig. 114: Final solution sets on 10-objective WFG9^{-1} test problem obtained by 10 algorithms in the run of median HV metric values with $\mathbf{z}^r = (2, \cdots, 2)^T$.

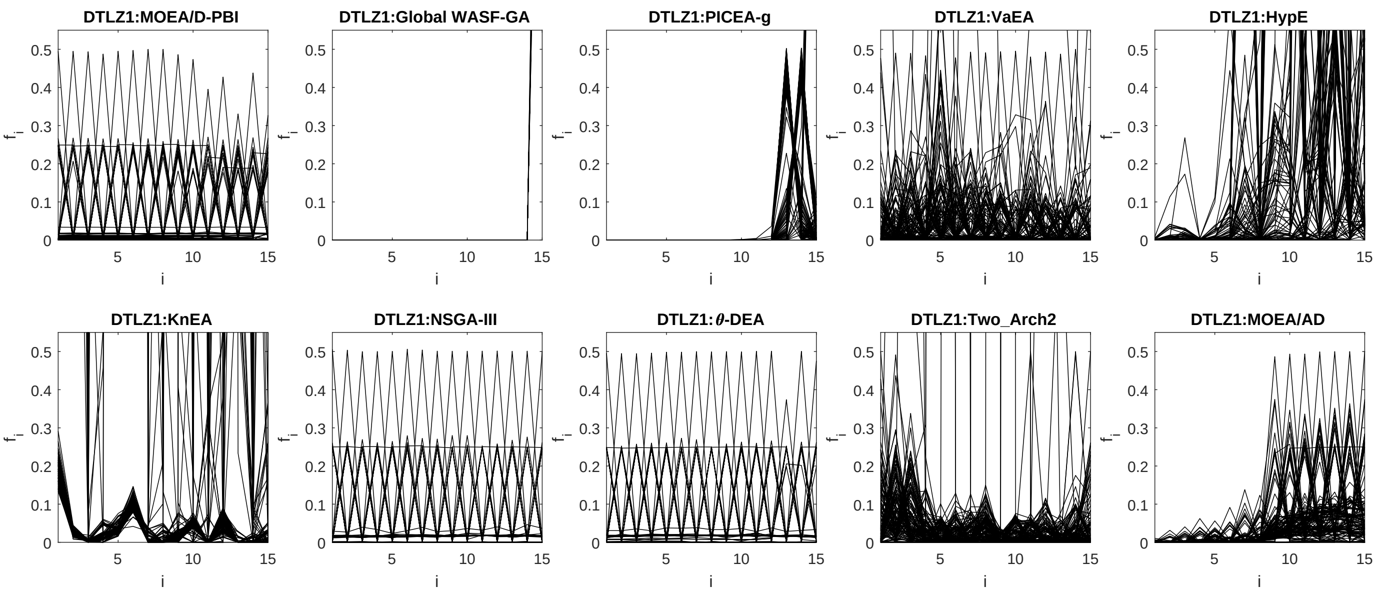

Fig. 115: Final solution sets on 15-objective DTLZ1 test problem obtained by 10 algorithms in the run of median HV metric values with $\mathbf{z}^r = (2, \cdots, 2)^T$.

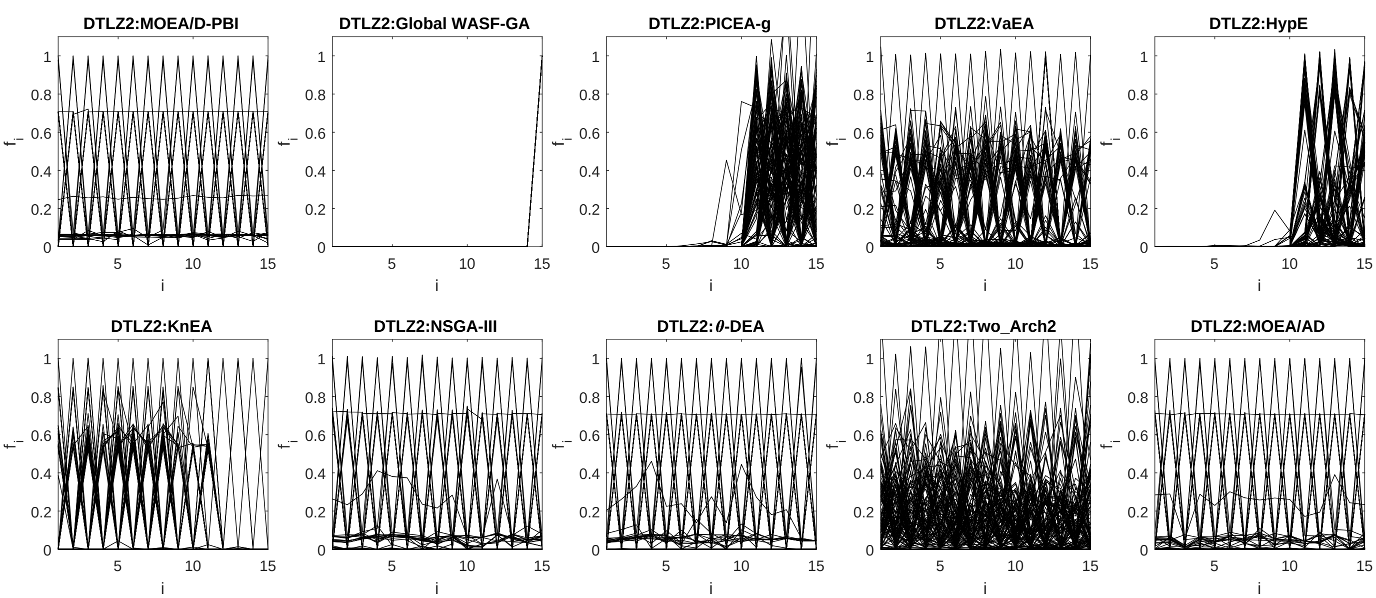

Fig. 116: Final solution sets on 15-objective DTLZ2 test problem obtained by 10 algorithms in the run of median HV metric values with $\mathbf{z}^r = (2, \cdots, 2)^T$.

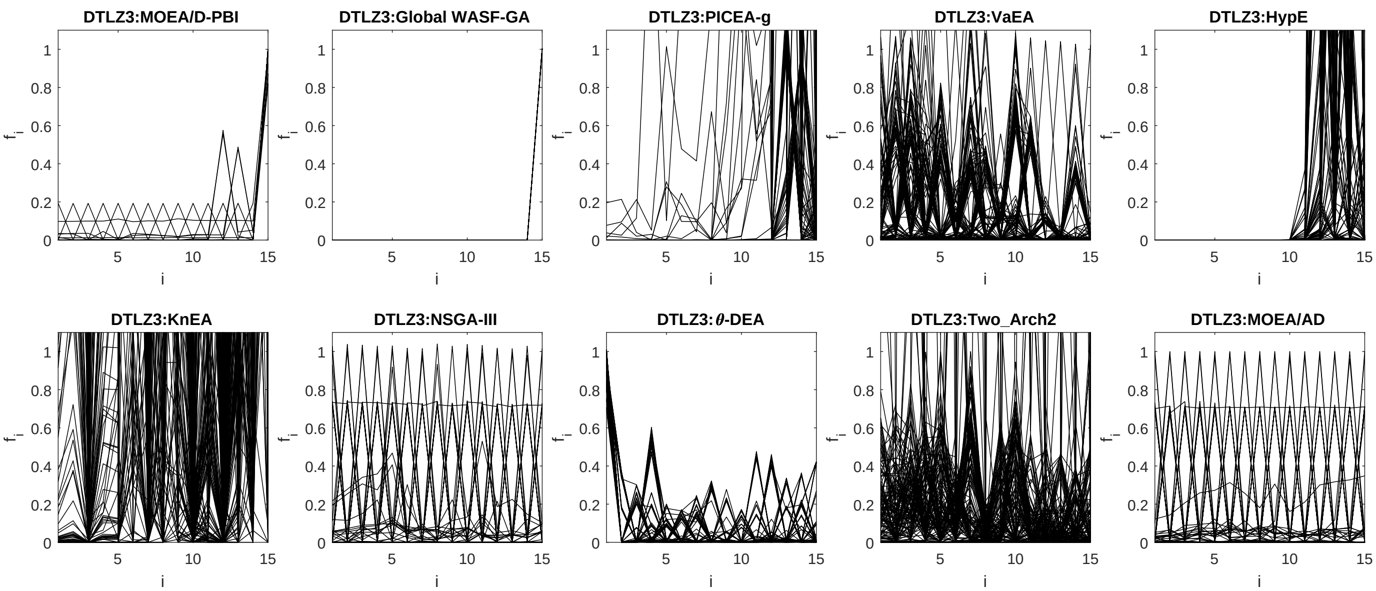

Fig. 117: Final solution sets on 15-objective DTLZ3 test problem obtained by 10 algorithms in the run of median HV metric values with $\mathbf{z}^r = (2, \cdots, 2)^T$.

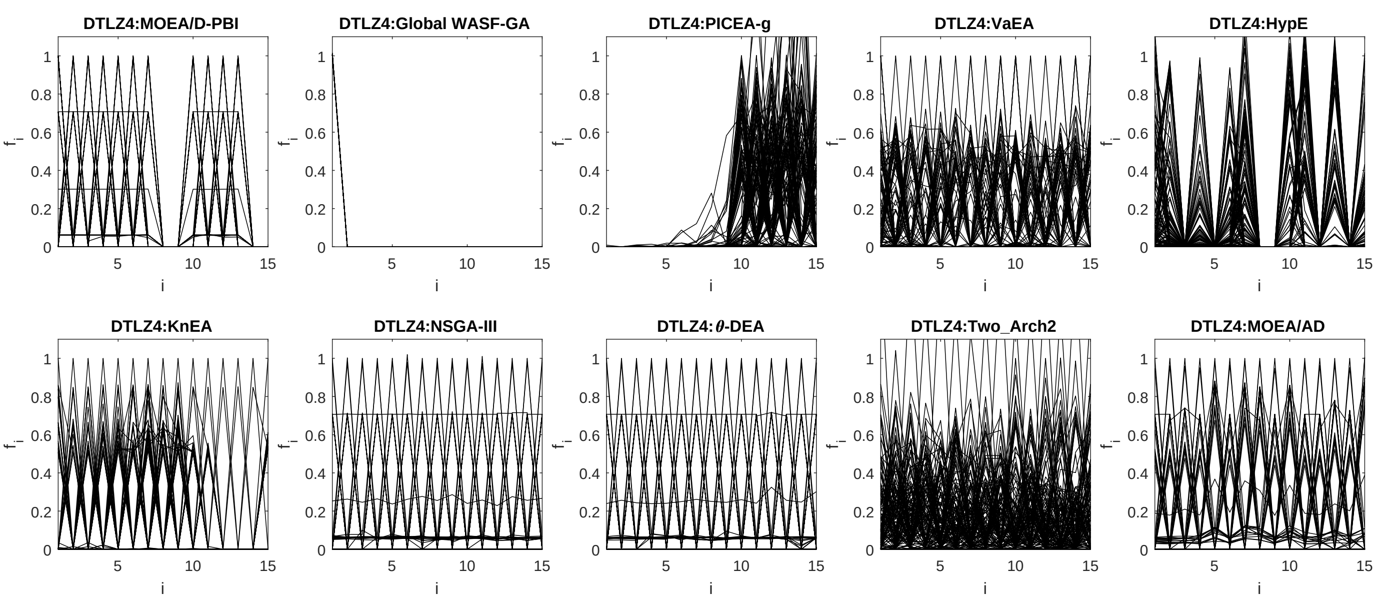

Fig. 118: Final solution sets on 15-objective DTLZ4 test problem obtained by 10 algorithms in the run of median HV metric values with $\mathbf{z}^r = (2, \cdots, 2)^T$.

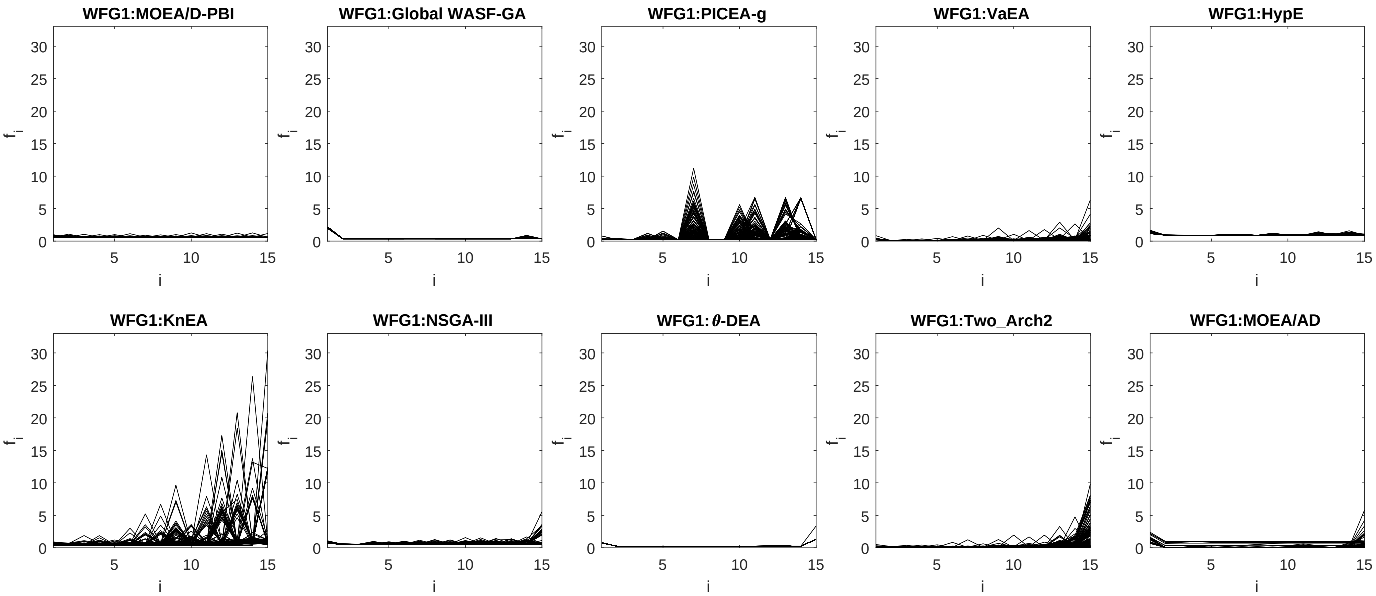

Fig. 119: Final solution sets on 15-objective WFG1 test problem obtained by 10 algorithms in the run of median HV metric values with $\mathbf{z}^r = (2, \cdots, 2)^T$.

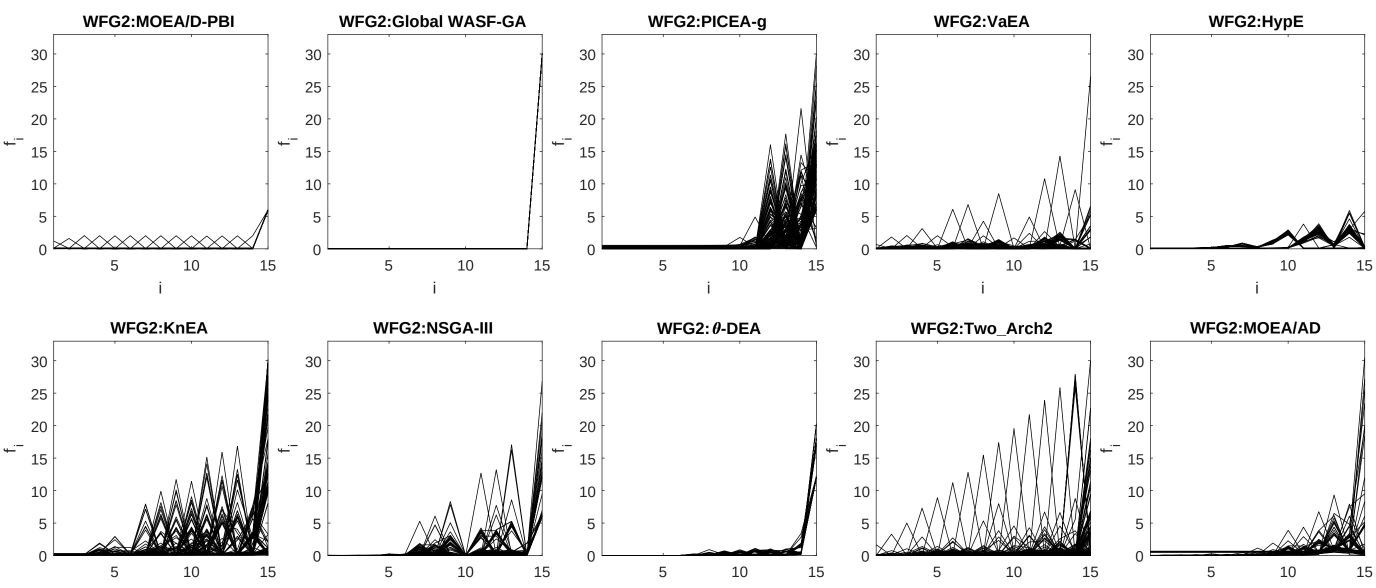

Fig. 120: Final solution sets on 15-objective WFG2 test problem obtained by 10 algorithms in the run of median HV metric values with $\mathbf{z}^r = (2, \cdots, 2)^T$.

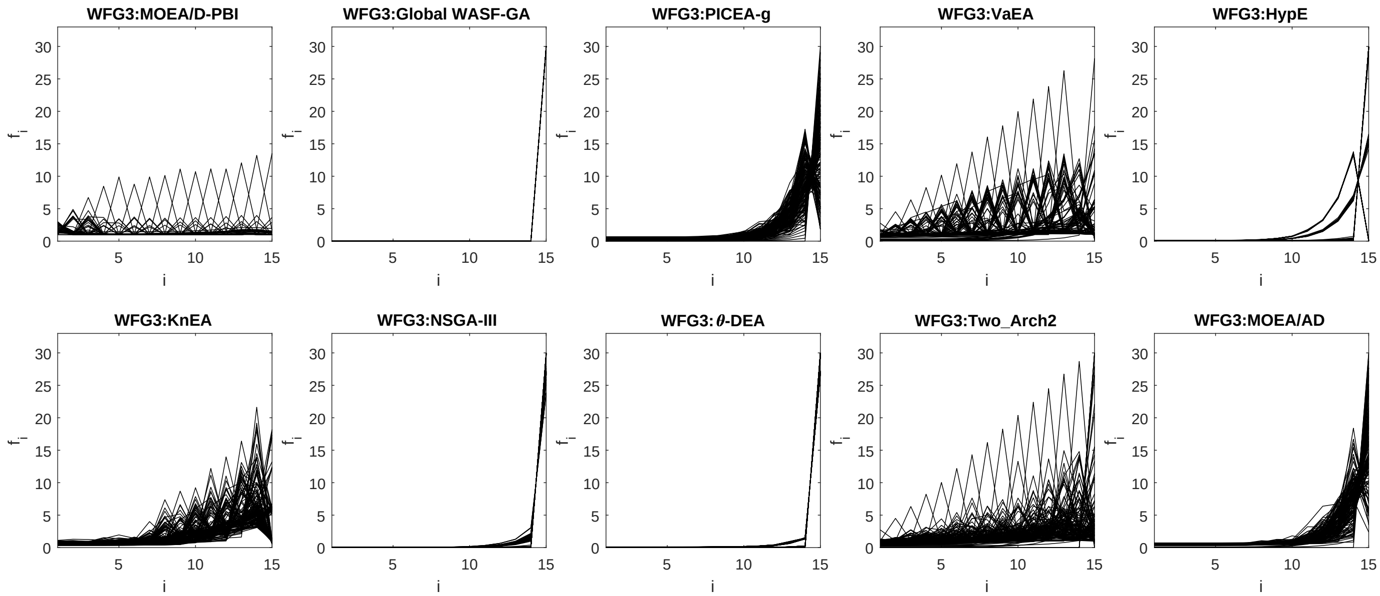

Fig. 121: Final solution sets on 15-objective WFG3 test problem obtained by 10 algorithms in the run of median HV metric values with $\mathbf{z}^r = (2, \cdots, 2)^T$.

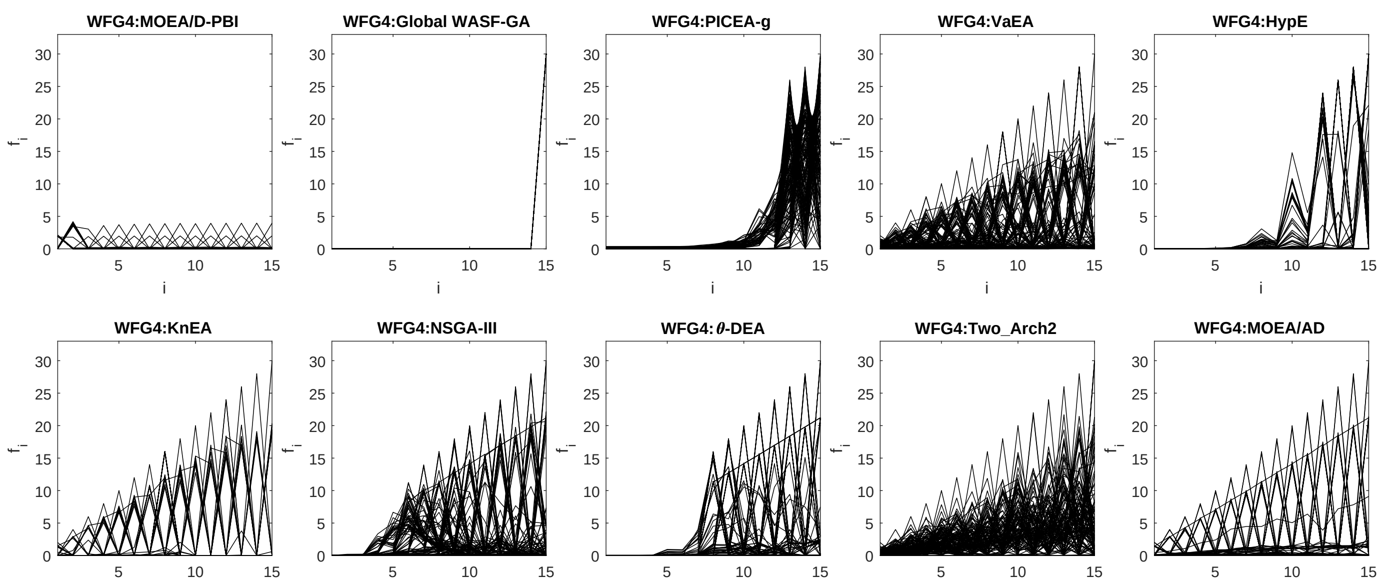

Fig. 122: Final solution sets on 15-objective WFG4 test problem obtained by 10 algorithms in the run of median HV metric values with $\mathbf{z}^r = (2, \cdots, 2)^T$.

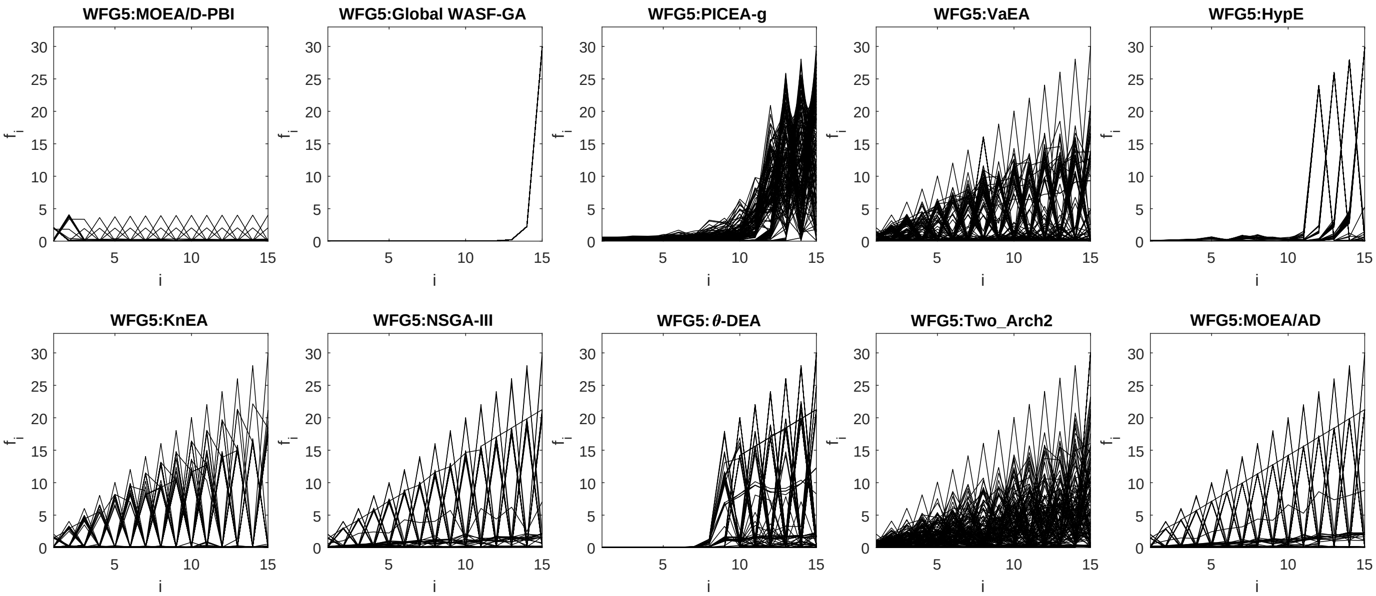

Fig. 123: Final solution sets on 15-objective WFG5 test problem obtained by 10 algorithms in the run of median HV metric values with $\mathbf{z}^r = (2, \cdots, 2)^T$.

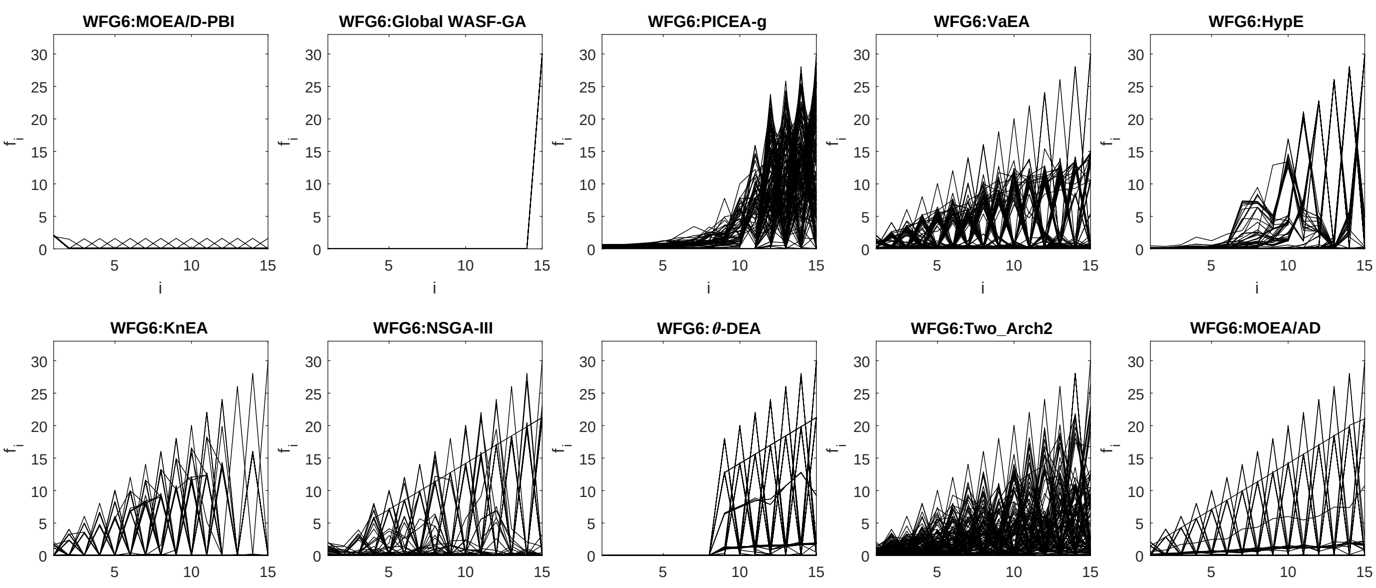

Fig. 124: Final solution sets on 15-objective WFG6 test problem obtained by 10 algorithms in the run of median HV metric values with $\mathbf{z}^r = (2, \cdots, 2)^T$.

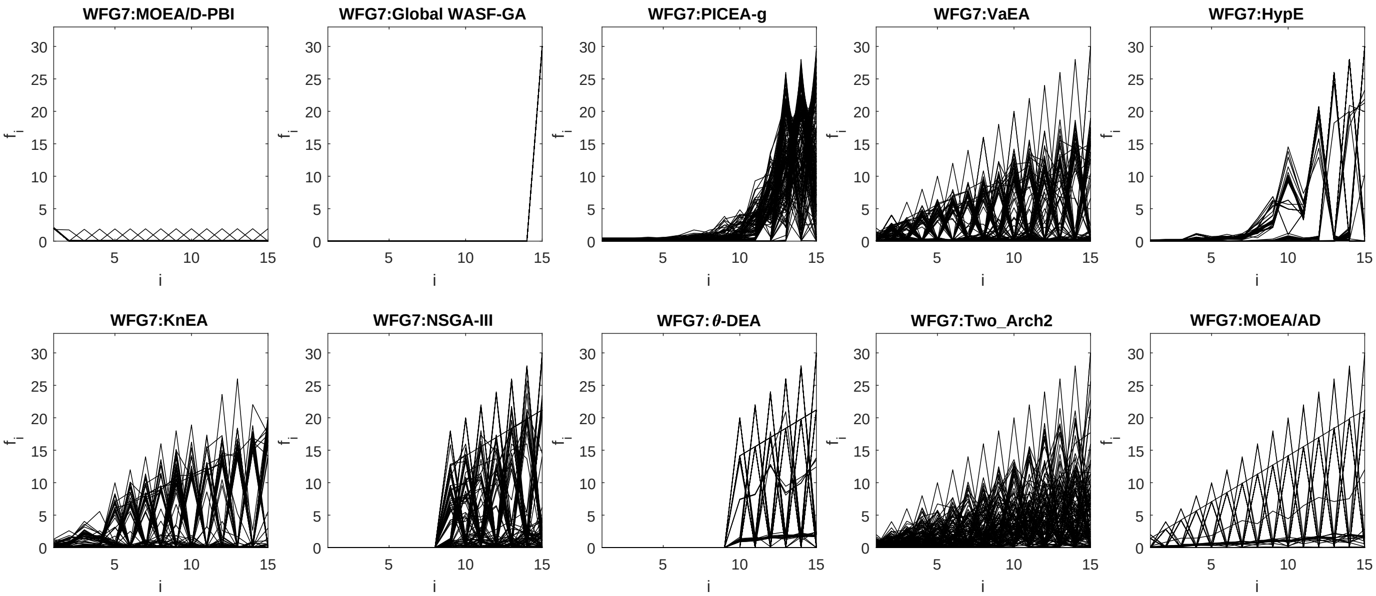

Fig. 125: Final solution sets on 15-objective WFG7 test problem obtained by 10 algorithms in the run of median HV metric values with $\mathbf{z}^r = (2, \cdots, 2)^T$.

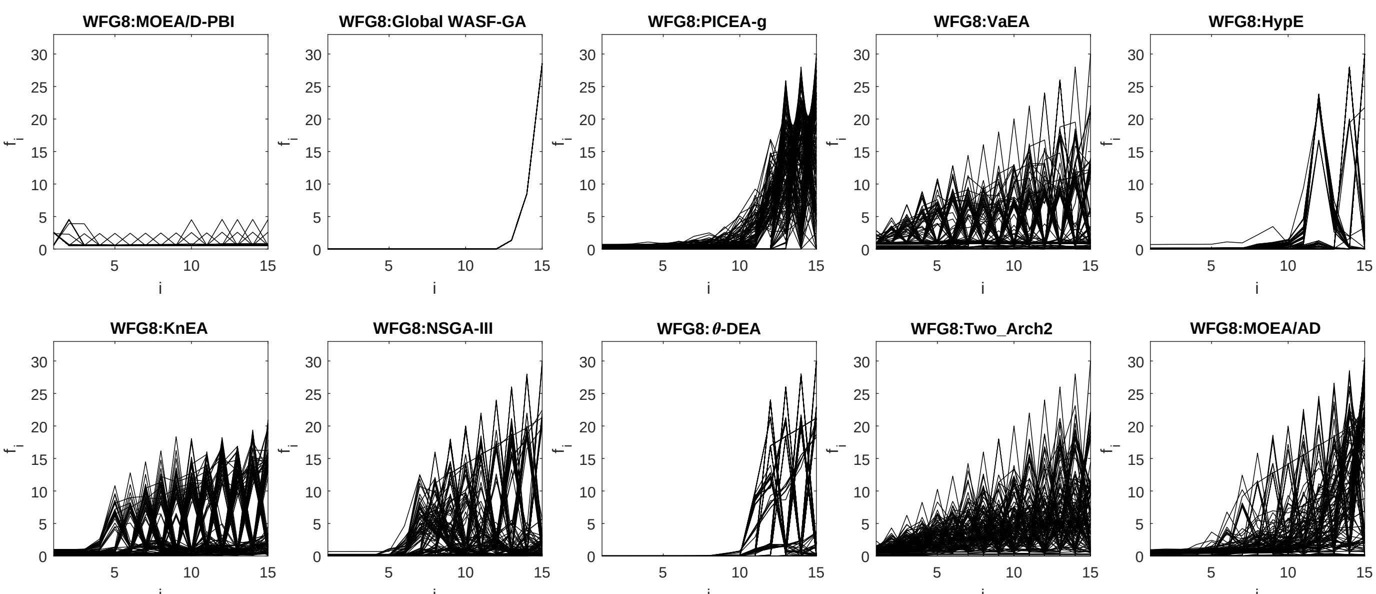

Fig. 126: Final solution sets on 15-objective WFG8 test problem obtained by 10 algorithms in the run of median HV metric values with $\mathbf{z}^r = (2, \cdots, 2)^T$.

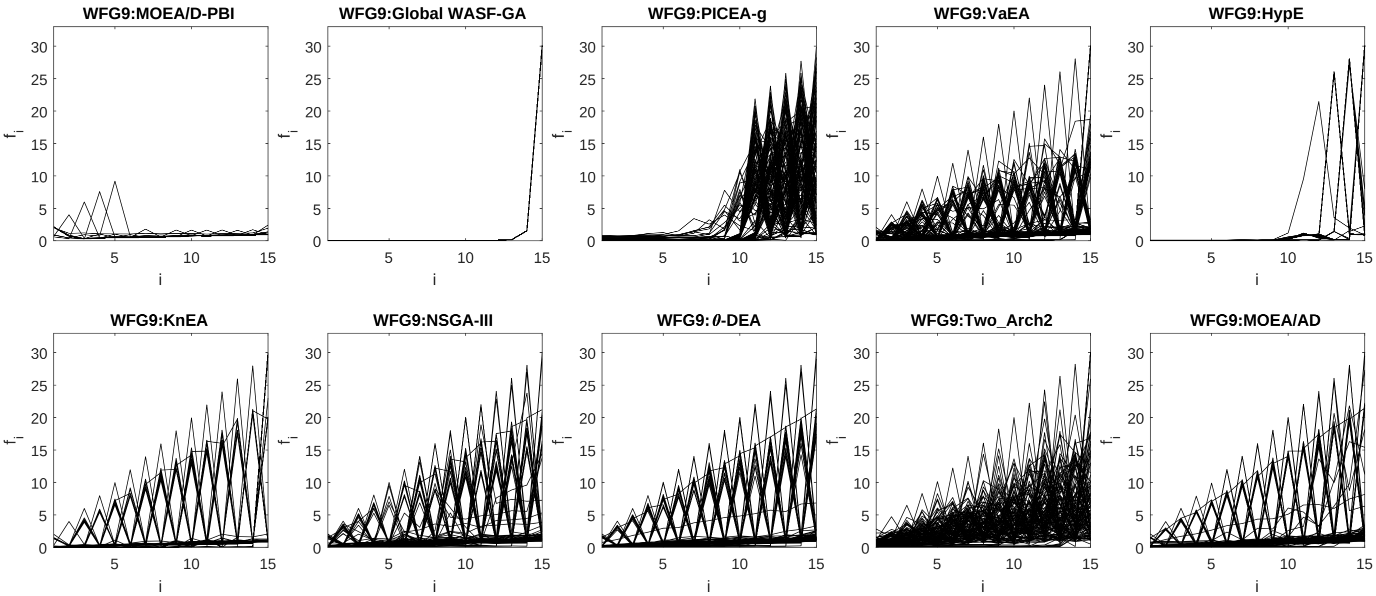

Fig. 127: Final solution sets on 15-objective WFG9 test problem obtained by 10 algorithms in the run of median HV metric values with $\mathbf{z}^r = (2, \cdots, 2)^T$.

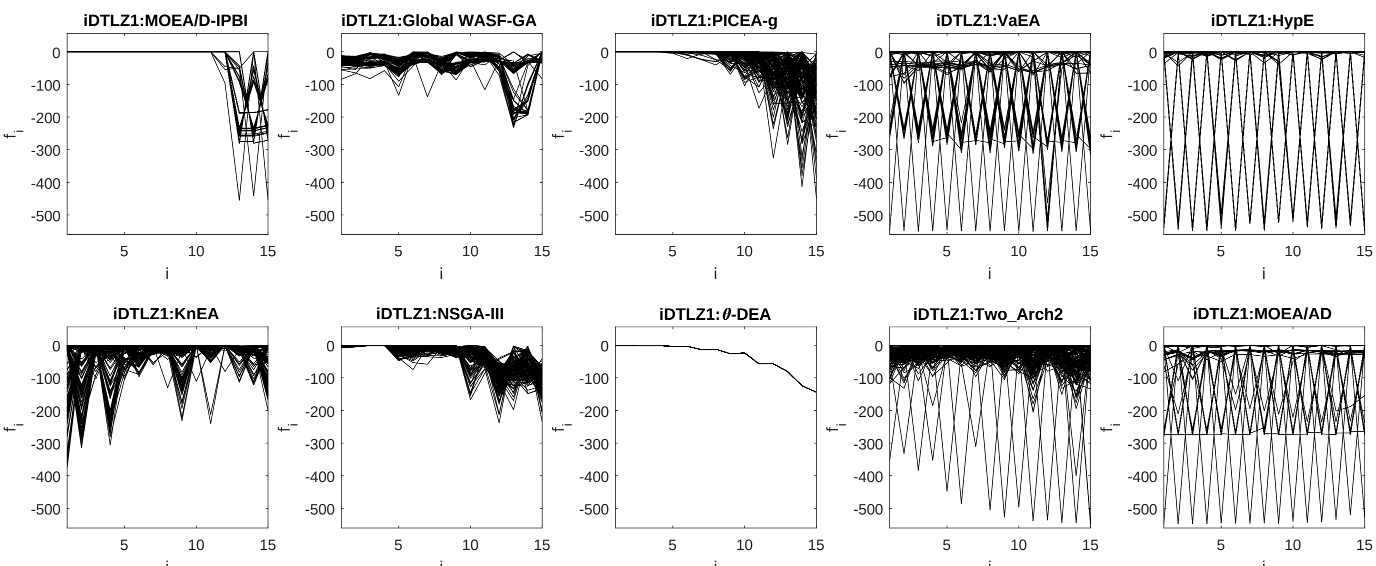

Fig. 128: Final solution sets on 15-objective DTLZ1^{-1} test problem obtained by 10 algorithms in the run of median HV metric values with $\mathbf{z}^r = (2, \cdots, 2)^T$.

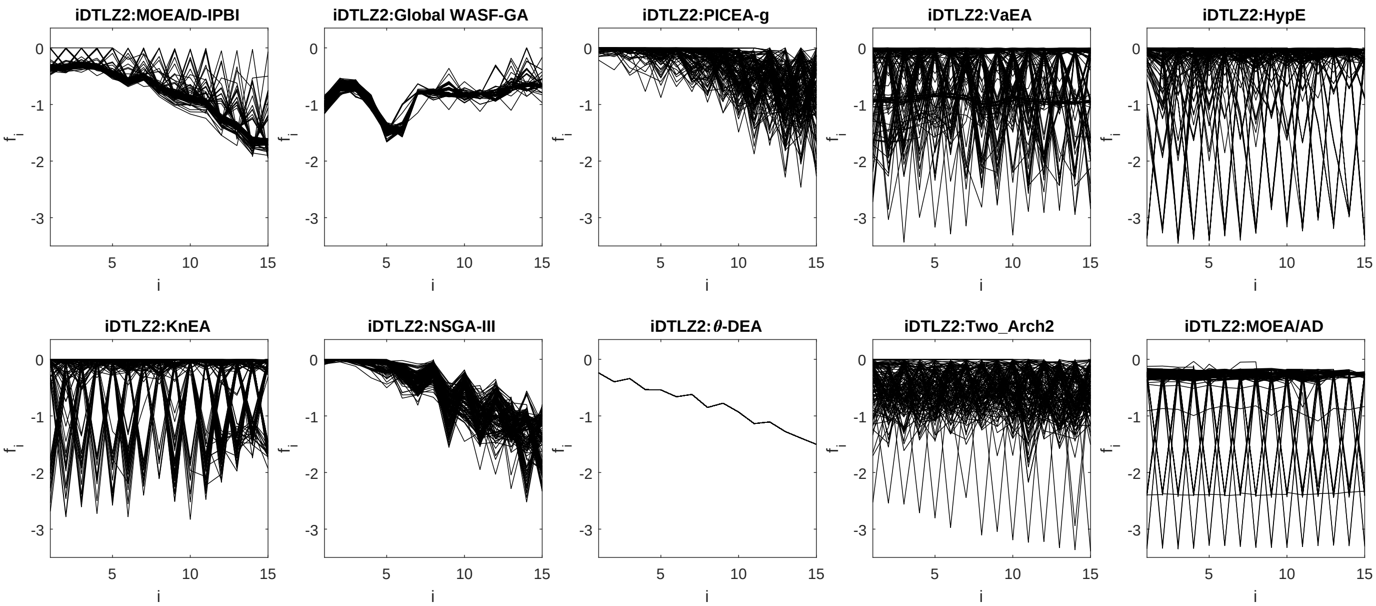

Fig. 129: Final solution sets on 15-objective DTLZ2^{-1} test problem obtained by 10 algorithms in the run of median HV metric values with $\mathbf{z}^r = (2, \cdots, 2)^T$.

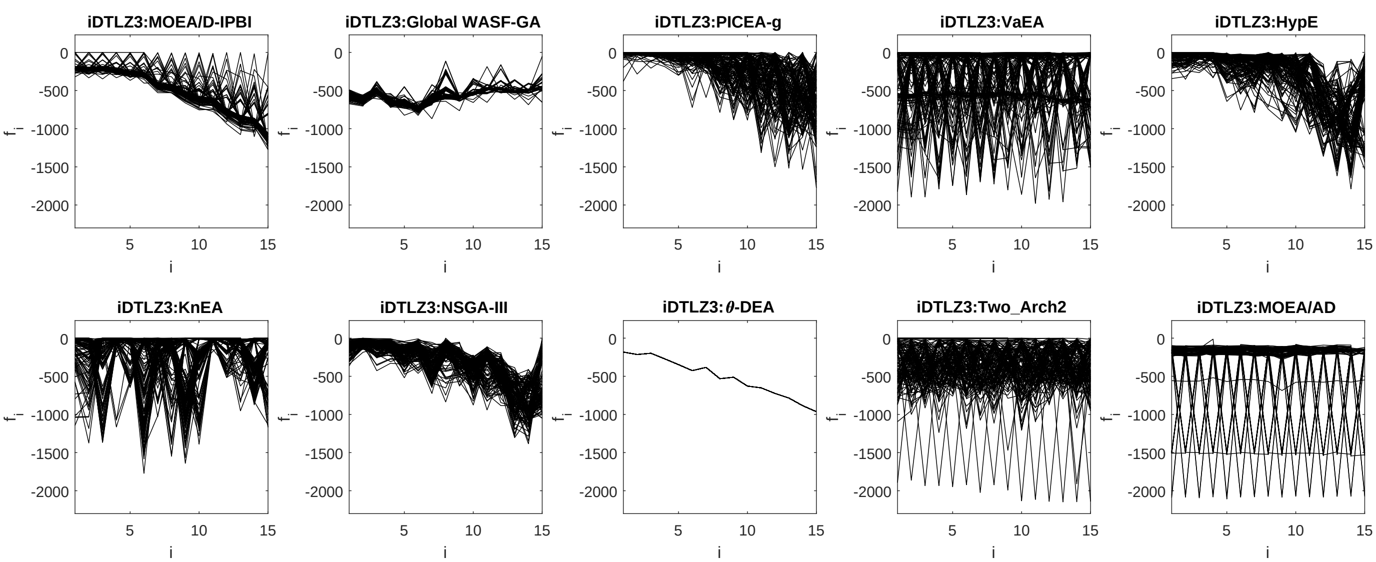

Fig. 130: Final solution sets on 15-objective DTLZ3^{-1} test problem obtained by 10 algorithms in the run of median HV metric values with $\mathbf{z}^r = (2, \cdots, 2)^T$.

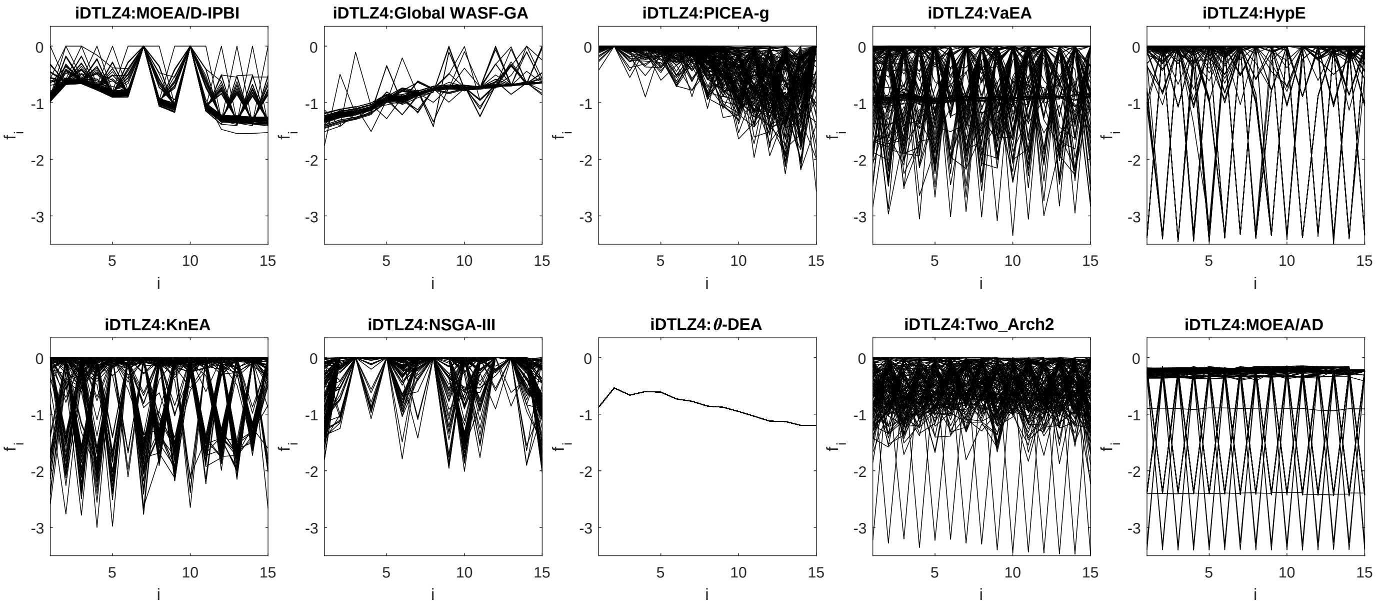

Fig. 131: Final solution sets on 15-objective DTLZ4^{-1} test problem obtained by 10 algorithms in the run of median HV metric values with $\mathbf{z}^r = (2, \cdots, 2)^T$.

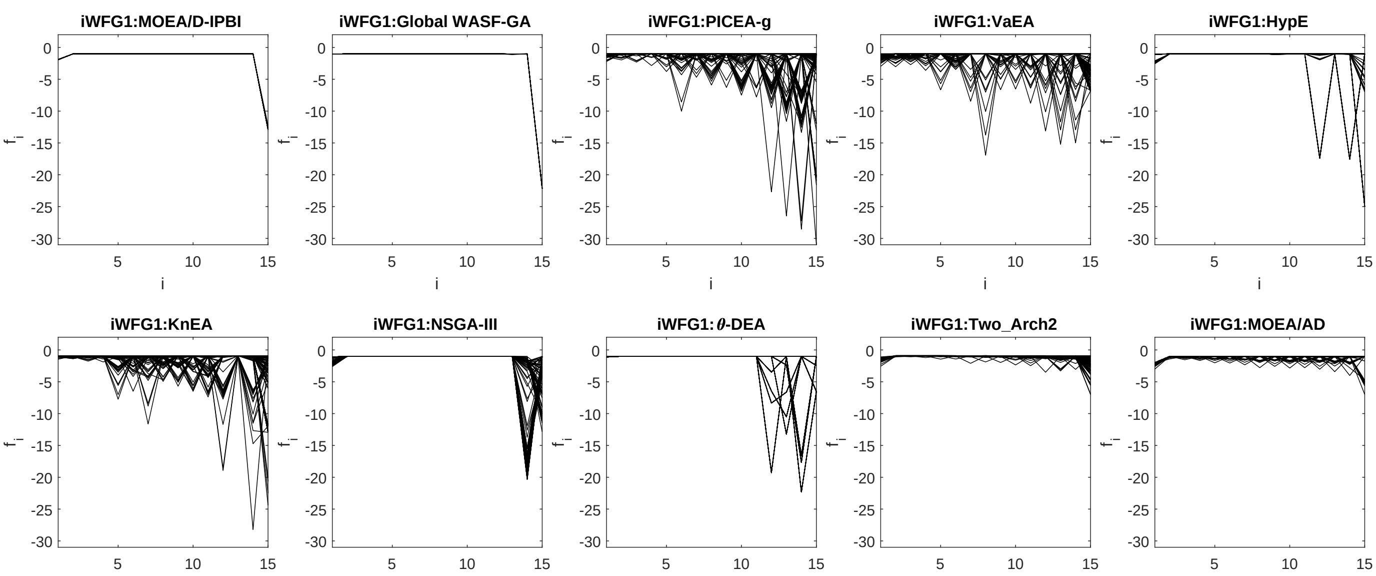

Fig. 132: Final solution sets on 15-objective WFG1^{-1} test problem obtained by 10 algorithms in the run of median HV metric values with $\mathbf{z}^r = (2, \cdots, 2)^T$.

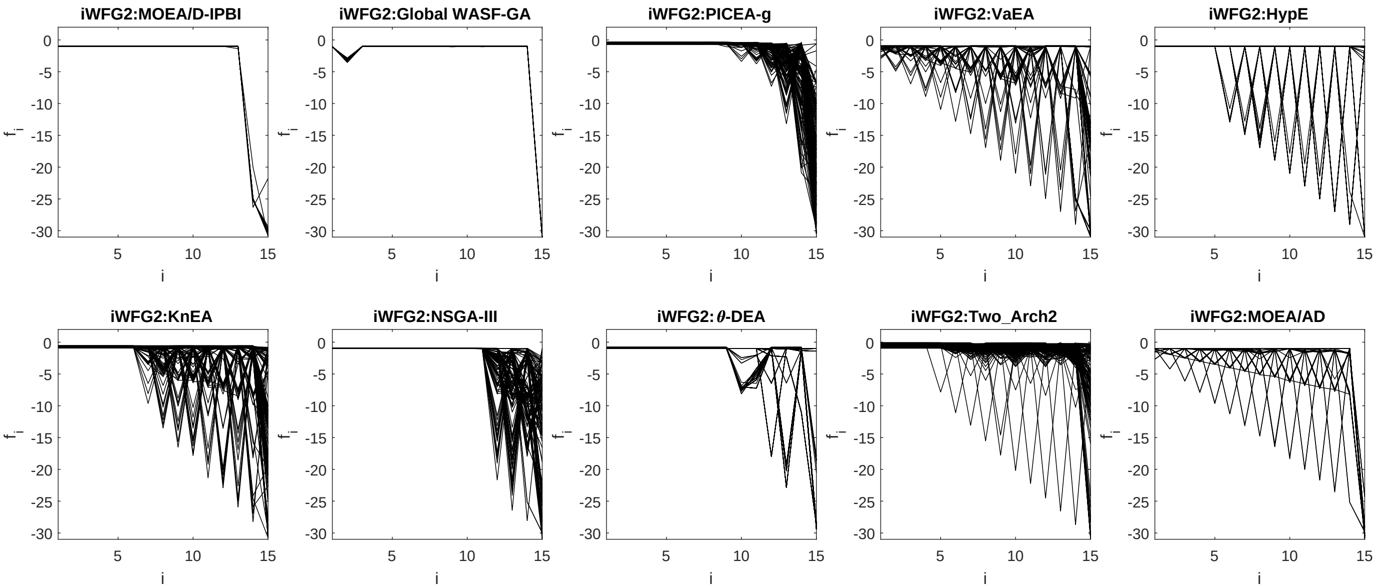

Fig. 133: Final solution sets on 15-objective WFG2^{-1} test problem obtained by 10 algorithms in the run of median HV metric values with $\mathbf{z}^r = (2, \cdots, 2)^T$.

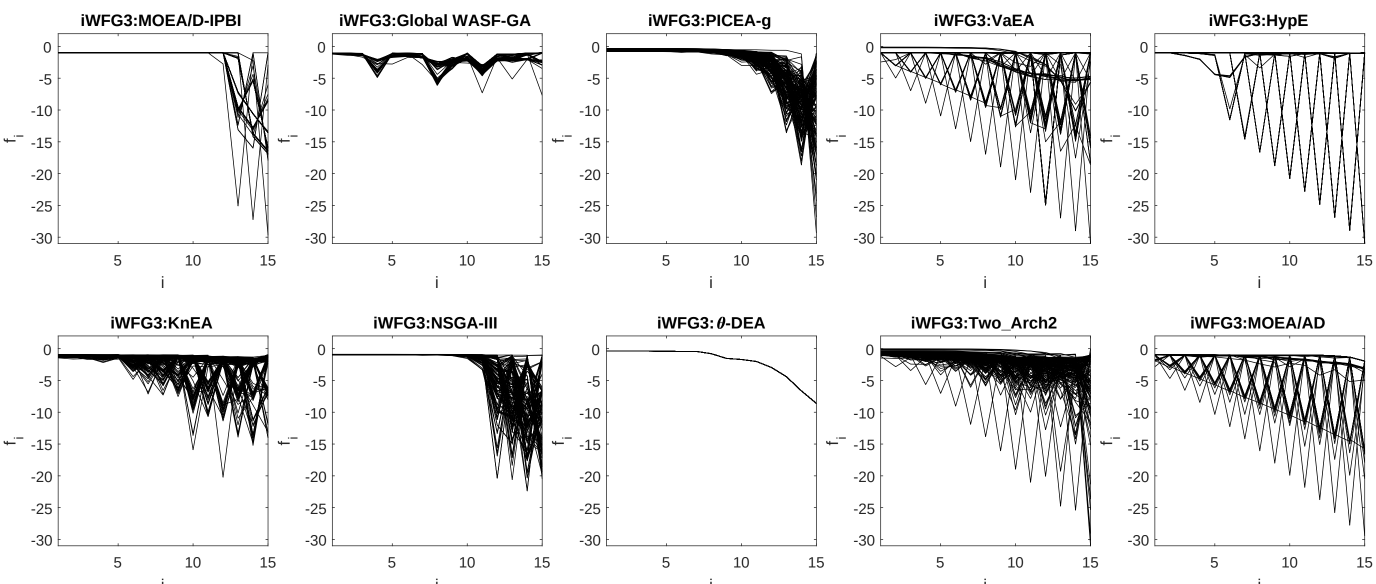

Fig. 134: Final solution sets on 15-objective WFG3^{-1} test problem obtained by 10 algorithms in the run of median HV metric values with $\mathbf{z}^r = (2, \cdots, 2)^T$.

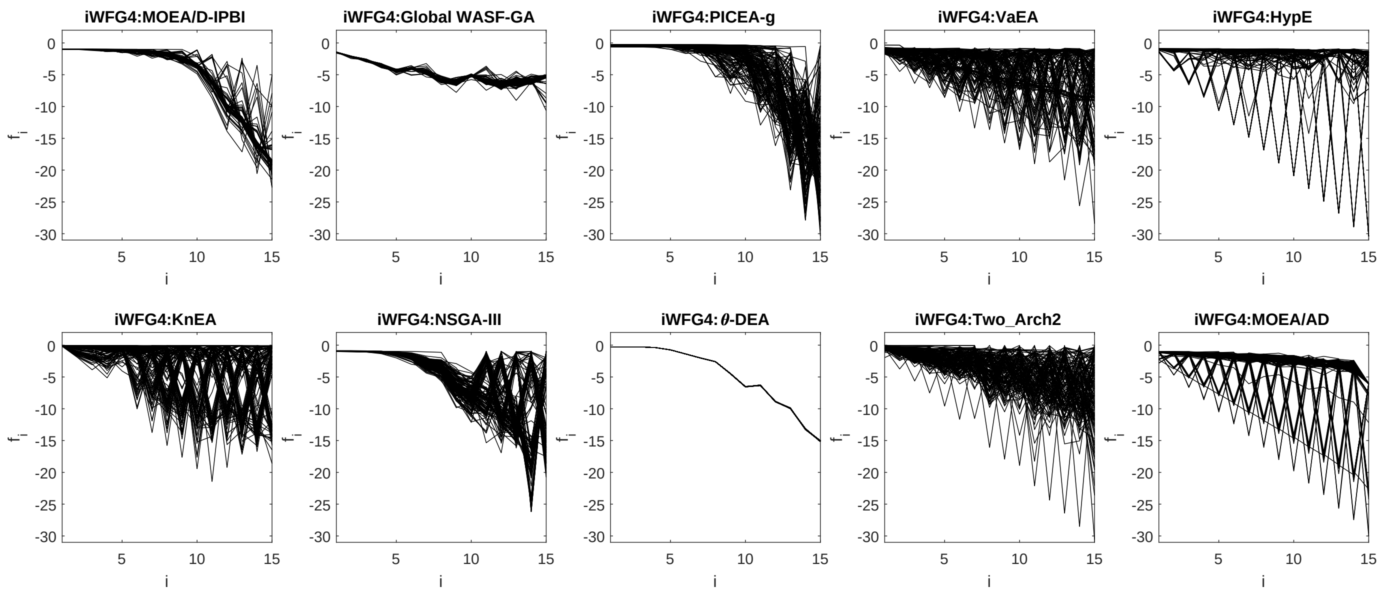

Fig. 135: Final solution sets on 15-objective WFG4^{-1} test problem obtained by 10 algorithms in the run of median HV metric values with $\mathbf{z}^r = (2, \cdots, 2)^T$.

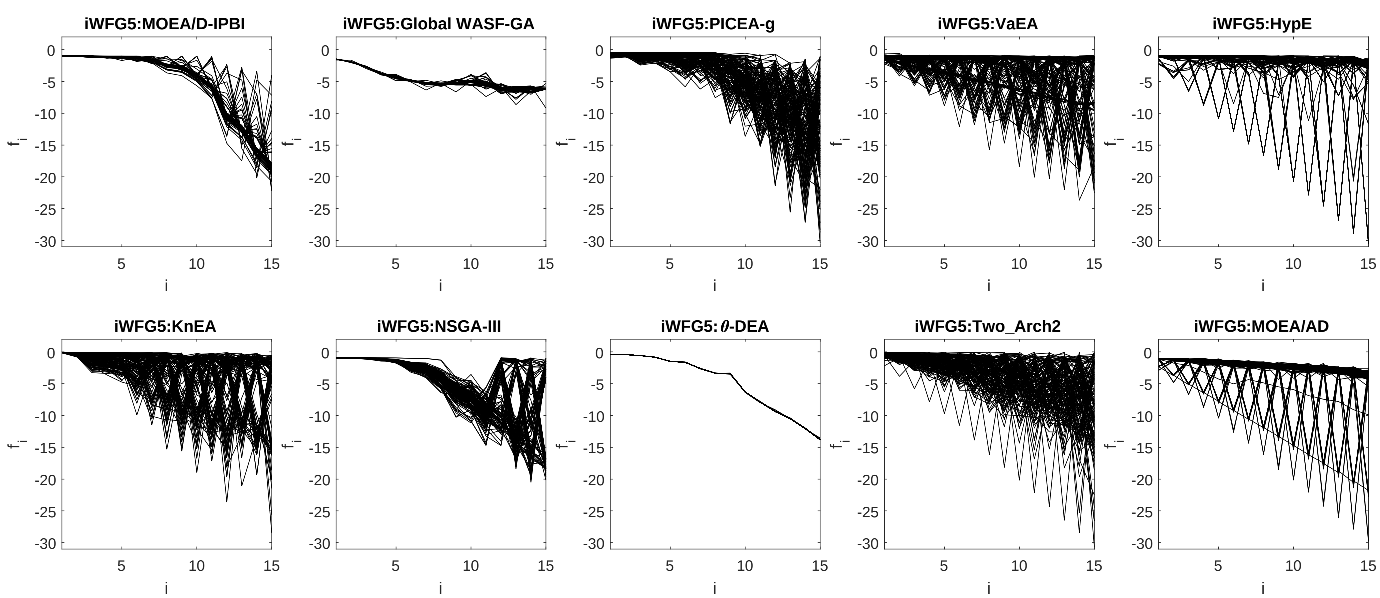

Fig. 136: Final solution sets on 15-objective WFG5^{-1} test problem obtained by 10 algorithms in the run of median HV metric values with $\mathbf{z}^r = (2, \cdots, 2)^T$.

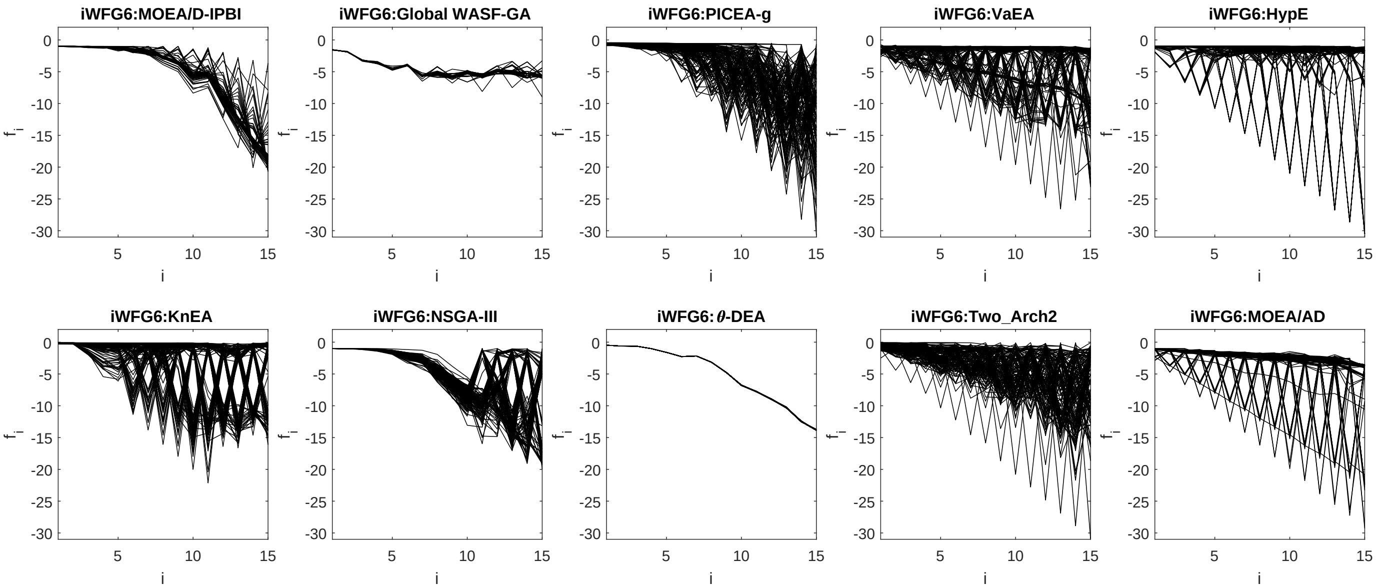

Fig. 137: Final solution sets on 15-objective WFG6^{-1} test problem obtained by 10 algorithms in the run of median HV metric values with $\mathbf{z}^r = (2, \cdots, 2)^T$.

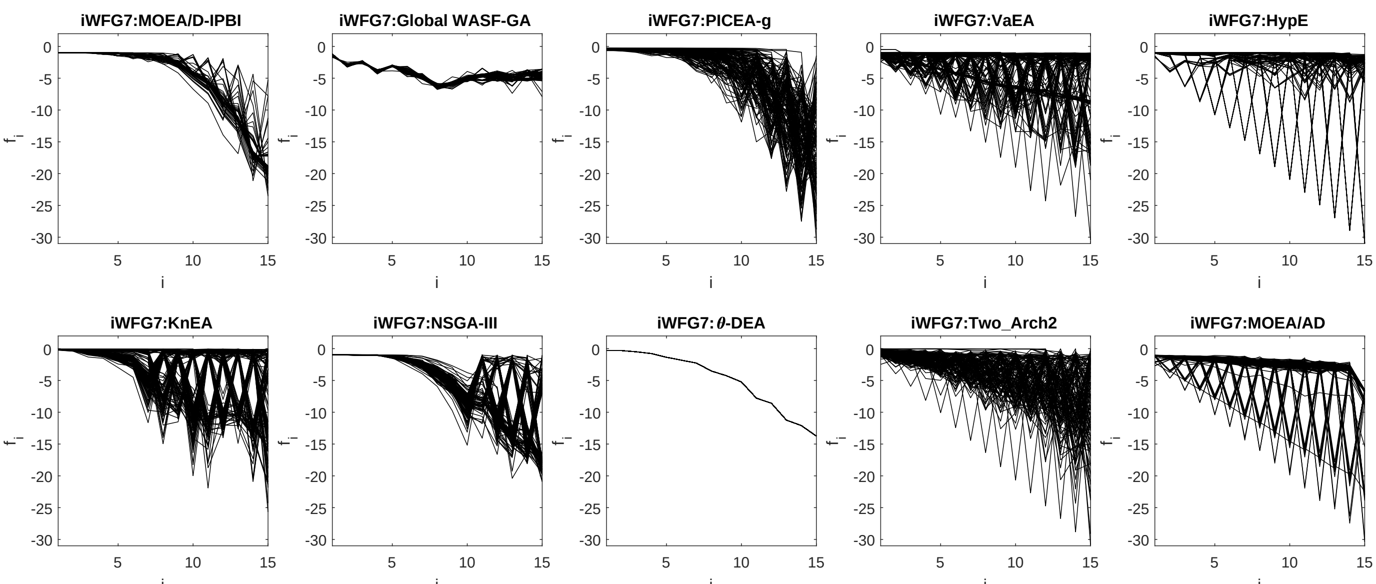

Fig. 138: Final solution sets on 15-objective WFG7^{-1} test problem obtained by 10 algorithms in the run of median HV metric values with $\mathbf{z}^r = (2, \cdots, 2)^T$.

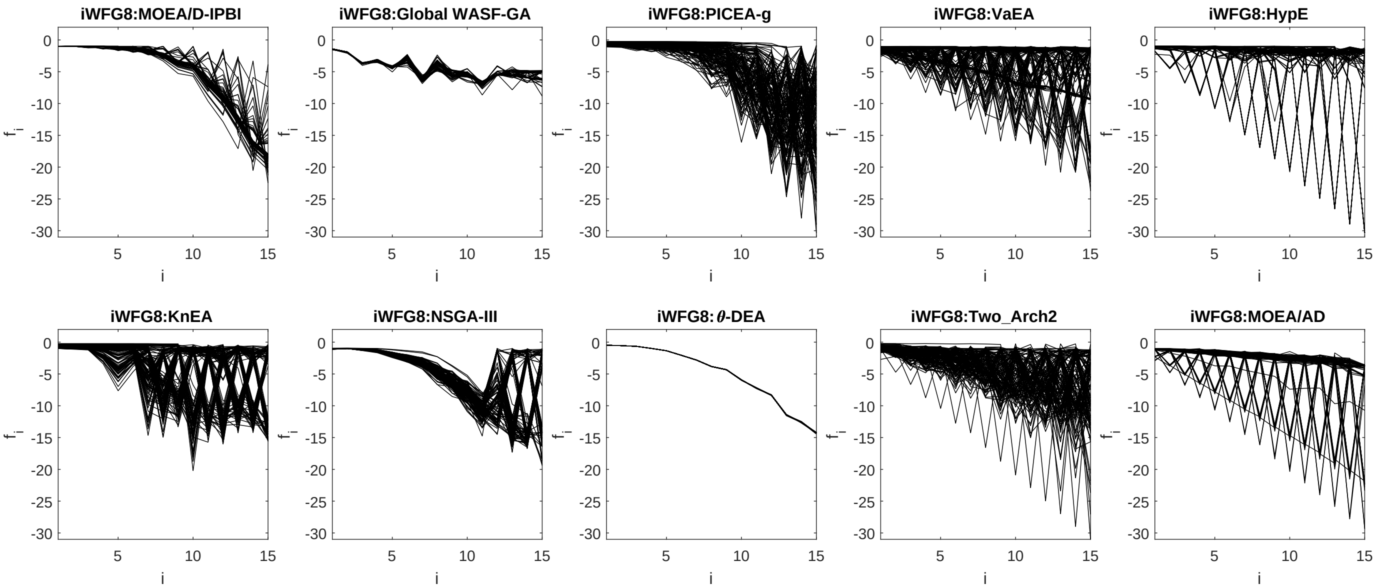

Fig. 139: Final solution sets on 15-objective WFG8^{-1} test problem obtained by 10 algorithms in the run of median HV metric values with $\mathbf{z}^r = (2, \cdots, 2)^T$.

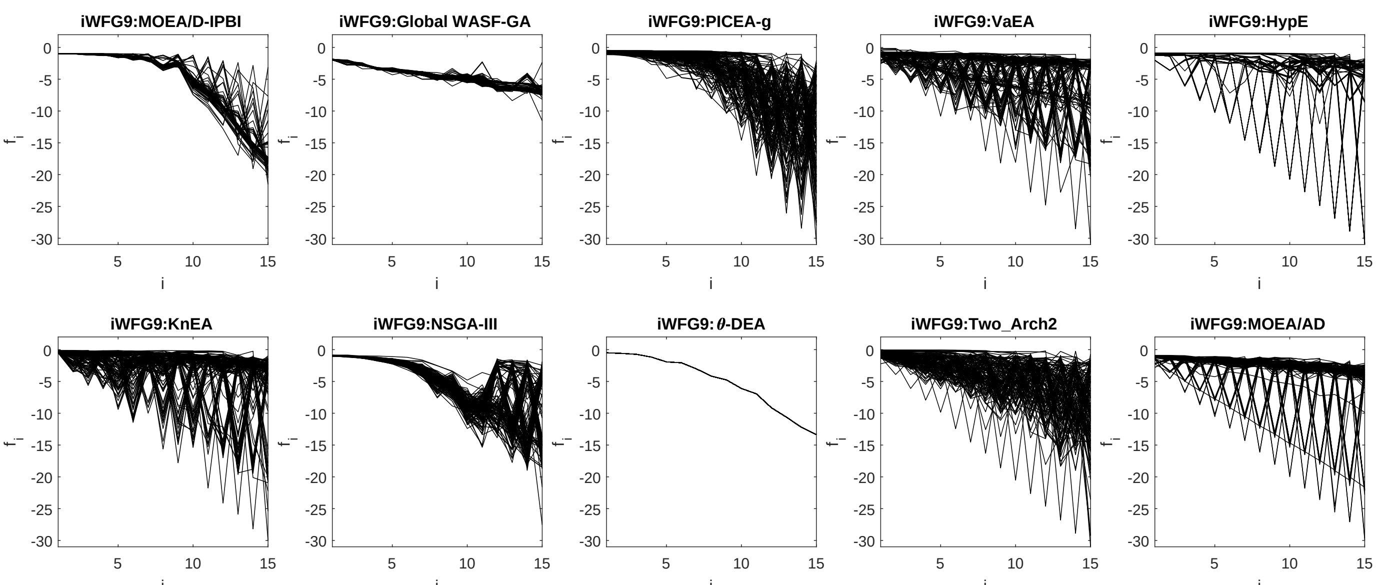

Fig. 140: Final solution sets on 15-objective WFG9^{-1} test problem obtained by 10 algorithms in the run of median HV metric values with $\mathbf{z}^r = (2, \cdots, 2)^T$.

REFERENCES

[1] Z. Wang, Q. Zhang, H. Li, H. Ishibuchi, and L. Jiao, "On the use of two reference points in decomposition based multiobjective evolutionary algorithms," *Swarm and Evol. Comput.*, vol. 34, pp. 89–102, 2017.

[2] K. S. Bhattacharjee, H. K. Singh, T. Ray, and Q. Zhang, "Decomposition based evolutionary algorithm with a dual set of reference vectors," in *2017 IEEE Congress on Evol. Comput., CEC 2017, Donostia, San Sebastián, Spain, June 5-8, 2017*, 2017, pp. 105–112.

[3] H. Ishibuchi, N. Akedo, H. Ohyanagi, and Y. Nojima, "Behavior of EMO algorithms on many-objective optimization problems with correlated objectives," in *Proceedings of the IEEE Congress on Evol. Comput., CEC 2011, New Orleans, LA, USA, 5-8 June, 2011*. IEEE, 2011, pp. 1465–1472.

[4] D. K. Saxena, J. A. Duro, A. Tiwari, K. Deb, and Q. Zhang, "Objective reduction in many-objective optimization: Linear and nonlinear algorithms," *IEEE Trans. Evol. Comput.*, vol. 17, no. 1, pp. 77–99, 2013.

[5] M. Wu, K. Li, S. Kwong, Y. Zhou, and Q. Zhang, "Matching-based selection with incomplete lists for decomposition multiobjective optimization," *IEEE Trans. Evol. Comput.*, vol. 21, no. 4, pp. 554–568, 2017.